Kingston University London

Faculty of Health, Science, Social Care and Education

School of Life Sciences, Pharmacy and Chemistry

Development of Molecularly Imprinted Polymers (MIPs) - Assisted Sensitive Analytical Methodologies for Detection and Monitoring of Protein Biomarkers

Submitted by

Aya Mohamed

This thesis is being submitted in partial fulfilment of the

requirements of the university for the award of

Doctor of Philosophy

2024

بسم الله الرحمن الرحيم

In The Name of Allah The Most Merciful

وقل رب زدني علما

'And say O' Lord, increase my knowledge'

Acknowledgments

Abstract

Molecularly imprinted polymers (MIPs) are synthetic polymers with "structural memory", designed to bind target molecules with exceptional selectivity. Their unique properties make them valuable in medicine, chemistry, analysis, and sensing, particularly for recognising biomarkers which are measurable indicators of biological and pathological processes. This thesis explores MIPs for biomarker analysis, focusing on pepsin, a protein biomarker linked to gastroesophageal reflux disease (GERD).

This thesis includes a comprehensive investigation into various MIP types, synthesis methods, and applications. Practical work involved developing different MIP systems for pepsin enzyme analysis. The first approach entailed creating magnetic MIPs using magnetite nanoparticles, which facilitated easy separation and enhanced binding due to functionalisation with amino groups. This method achieved a binding capacity of 190 mg g^{-1} and an imprinting factor of 1.34 compared to non-imprinted polymers (NIPs). The magnetic MIPs demonstrated high selectivity in extracting pepsin from solutions and saliva samples. A new HPLC method was further employed for the determination of the extracted pepsin fragments using size exclusion chromatography technique.

A second approach involved developing fluorescent MIPs using fluorescein and rhodamine B dyes to create an integrated system for both extraction and analysis of pepsin. Rhodamine B MIPs (RMIPs) exhibited a superior binding capacity (256 mg g^{-1}), and sensitivity compared to fluorescein-dyed MIPs (FMIPs) which had a binding capacity of 217 mg g^{-1}. RMIPs achieved a linear detection range from 0.28 to 42.85 µmol L^{-1} and a limit of detection (LOD) of 0.11 µmol L^{-1}, whereas FMIPs had a range of 0.71 to 35.71 µmol L^{-1} with an LOD of 0.34 µmol L^{-1}. Both fluorescent MIPs were successfully applied in a separation-free system for quantifying pepsin in saliva.

A novel fluorescent molecularly imprinted membrane (FMIM) was also developed for the selective binding and qualitative detection of pepsin. This membrane integrated fluorescent carbon dots to enable immediate visual detection. Various combinations of functional monomers and cross-linkers were evaluated, with the optimal performance achieved using N-(hydroxymethyl)acrylamide and acrylamide with N,N-methylenebis(acrylamide) as the cross-linker. The FMIM showed a binding capacity of 21.56 mg g^{-1}, surpassing the fluorescent non-imprinted membrane (FNIM) at 8.49 mg g^{-1}. The FMIM effectively bound pepsin in both standard solutions and saliva samples, demonstrating its potential for optical sensing of pepsin.

Finally, an exploration into simplifying molecular imprinting by employing dopamine as both a functional monomer and cross-linker was undertaken. Dopamine's ability to auto-polymerise in alkaline conditions was used to create a polydopamine layer on silica nanoparticles or fluorescent carbon dots. While this approach faced challenges in optimisation, resulting in selectivity that was comparable to or slightly less than NIPs, the insights gained have paved the way for future improvements in the molecular imprinting process.

Keywords: Molecularly imprinted polymers, Biomarkers, Pepsin, HPLC, Fluorometric

analysis, Optical sensors, Polydopamine, Gastroesophageal Reflux Disease.

Disclaimer: This work has not been submitted for a qualification elsewhere or has been published, except in the following produced publications:

1- A.M. Mostafa, S.J. Barton, S.P. Wren, J. Barker, Design and preparation of a fluorescent molecularly imprinted membrane for the selective detection of pepsin enzyme as a biomarker for gastroesophageal reflux disease, Talanta open, August (2024), 100351. https://doi.org/10.1016/j.talo.2024.100351.

2- A.M. Mostafa, S.J. Barton, S.P. Wren, J. Barker, Development of highly sensitive fluorescent sensors for separation-free detection and quantitation systems of pepsin enzyme applying a structure-guided approach, Biosensors, 14 (2024), 151. https://doi.org/10.3390/bios14030151.

3- M. Mostafa, S.J. Barton, S.P. Wren, J. Barker, Development of magnetic molecularly imprinted polymers for the extraction of salivary pepsin prior to analysis by a novel HPLC-SEC method, Polymer (Guildf). 261 (2022). doi.org/10.1016/j.polymer.2022.125417.

4- A.M. Mostafa, S.J. Barton, S.P. Wren, J. Barker, Review on molecularly imprinted polymers with a focus on their application to the analysis of protein biomarkers, TrAC - Trends in Analytical Chemistry. 144 (2021). doi.org/10.1016/j.trac.2021.116431.

Table of Contents

Abbreviations

2-VP	2-vinyl-pyridine
4-VP	4-vinyl-pyridine.
AA	Acrylic acid.
ACN	Acetonitrile.
ADVN	2,2'-azobis(2,4-dimethylvaleronitrile).
AIBN	2,2'-azobis(isobutyronitrile).
Am	Acrylamide.
ANOVA	A one-way analysis of variance.
APS	Ammonium persulphate.
APTES	(3-Aminopropyl)triethoxysilane.
APTMS	(3-Aminopropyl)trimethoxysilane.
CDs	Carbon dots.
CRP	Controlled/living radical polymerisation.
CV	Cyclic voltammetry.
DES	Deep eutectic solvents.
DSC	Differential scanning calorimetry.
DVB	Divinylbenzene.
EDGMA	Ethylene glycol dimethacrylate.
EIS	Electro-impedance spectroscopy.
ELISA	Enzyme Linked Immunosorbent Assay.
EtOH	Ethyl alcohol.

FITC	Fluorescein isothiocyanate.
FMIM	Fluorescent molecularly imprinted membrane.
FMIPs	Fluorescein molecularly imprinted polymers.
FNIM	Fluorescent non-imprinted membrane.
FNIPs	Fluorescein non-imprinted polymers.
FTIR	Fourier transform infrared spectroscopy.
GERD	Gastroesophageal reflux disease.
HPLC-SEC	High-performance liquid chromatography - size exclusion chromatography.
IS	Internal standard
LC-MS	Liquid chromatography-mass spectrometry.
LLE	Liquid-liquid extraction.
LOD	Limit of detection.
LOQ	Limit of quantitation.
MAA	Methacrylic acid.
MBA	N,N'-methylenebis(acrylamide).
MeOH	Methyl alcohol.
MIMs	Molecularly imprinted membranes.
MIPs	Molecularly imprinted polymers.
NHMAm	N-(Hydroxymethyl)acrylamide.
NIMs	Non-imprinted membranes.
NIPAm	N-isopropylacrylamide.
NIPs	Non-imprinted polymers.
NMR	Nuclear magnetic resonance.

NPs	Nanoparticles.
PBS	phosphate buffered saline.
PDA	Polydopamine.
PSB	Polystyrene beads.
QCM	Quartz crystal microbalance.
QDs	Quantum dots.
RAFT	Reversible addition-fragmentation chain transfer.
RITC	Rhodamine b isothiocyanate.
RMIPs	Rhodamine b molecularly imprinted polymers.
RNIPs	Rhodamine b non-imprinted polymers.
SDS	Sodium dodecyl sulphate.
SEM	Scanning electron microscope.
SPE	Solid phase extraction.
SPR	Surface plasmon resonance.
TEM	Transmission electron microscopy.
TEMED	N,N,N',N'-tetramethylethylenediamine.
TEOS	Tetraethyl orthosilicate.
TGA	Thermogravimetric analysis.
THMMAm	N-[tris(hydroxymethyl)methyl]acrylamide.
XRD	X-ray diffraction.

List of Tables

List of Figures

Chapter 1

Introduction

Published along a critical review in

Trends in Analytical Chemistry:

Chapter 1. Introduction

Subchapter I. Molecular imprinting

1.1. Definition and history

Molecularly imprinted polymers (MIPs) represent a class of synthesised polymers designed for the selective identification of specific target molecules. The analogy of a "lock and key" model illustrates their functioning, where MIPs act as the lock, exhibiting complementarity in size, shape, and orientation of functional groups to the target molecule, analogous to the key (1).

The early concept of molecular imprinting was introduced by Polyakov in 1930s (2) who synthesised a type of silica gel that could imprint certain dyes. In 1940s Pauling (3) adopted the process of formation of antibodies in the presence of certain antigens as templates which carries the same idea of molecular imprinting. Until the 1970's molecular imprinting was a slowly explored field and was applied only to inorganic targets, however Wulff and his group were the first to expand the use of MIPs on organic targets. Wulff's major work was to develop biomimetic catalysts via molecular imprinting technique to be used in different chemical reactions (4–6). Another notable contribution came from Mosbach and his group in the 1980s, introducing non-covalent molecular imprinting based on weaker bonds between the monomers and the target, such as hydrogen bonds or hydrophobic interactions (7–9).

In consequence to the various efforts made in the field, different types of MIPs were developed depending on the starting materials used in their synthesis or the technique of synthesis itself which are explored further in detail in this section.

In addition, different characterisation methods can be used to identify the structure, shape, porosity, and functionality of MIPs, all of which are important parameters to determine their usefulness. However, the field faces challenges that necessitate exploration for potential solutions. This comprehensive review section delves into these aspects, exploring diverse methods and techniques employed in the production of MIPs, characterisation methods, applications, challenges, and solutions for imprinting protein targets.

1.2.　Principle of molecular imprinting

An MIPs is a type of biomimetic synthetic polymer that has a structural memory for specific target molecule. MIPs sometimes are referred to as synthetic antibodies since they can resemble antibodies in their structural recognition capabilities (1).

The synthesis of MIPs comprises four key components that come together to form the ultimate final structure. These components include the functional monomer, the cross-linker, the initiator, and the porogenic solvent.

The crucial step in the successful synthesis of MIPs involves establishing a robust interaction between the target molecule and the functional monomer. This interaction proves valuable not only during the MIP synthesis but also during the subsequent rebinding of MIPs with the target molecule in various samples. Therefore, selecting a functional monomer with complementary functional groups to those in the target molecule is of utmost importance. Following the formation of the template-monomer adduct, the cross-linking agent serves as a binding agent, bringing the adducts together into a cross-linked polymeric structure, as illustrated in **Figure 1**.

Initiating polymerisation requires the addition of an initiator to start a free radical reaction (in most cases). Ultimately, the porogenic solvent is employed to enhance the porosity, thereby increasing the surface area of the resulting polymer and facilitating easy access to the binding sites (1).
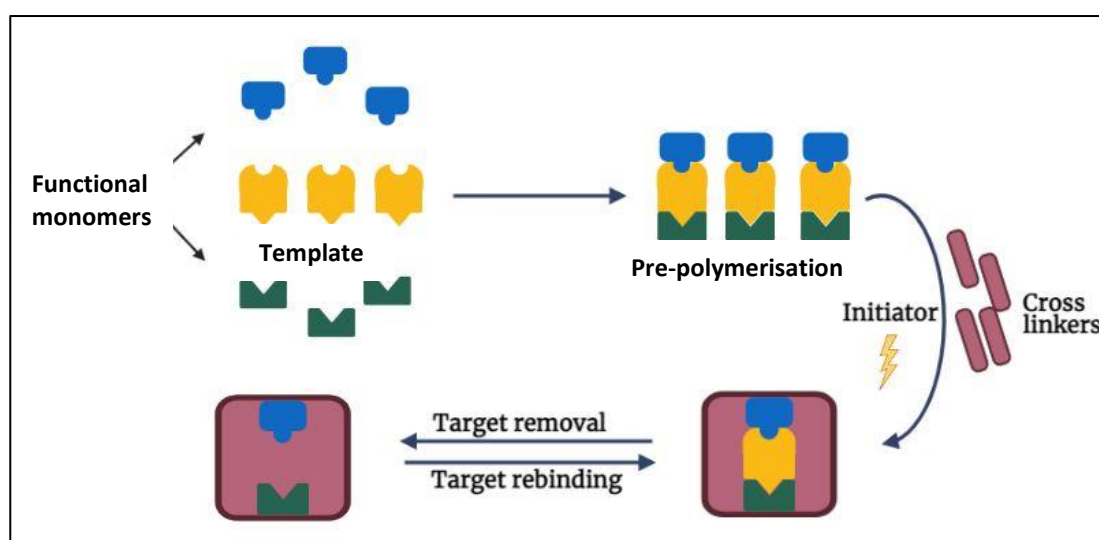
Figure 1. Schematic illustration of the process of molecular imprinting and target removal/rebinding.

Molecular imprinting involves three main bond types: covalent, non-covalent, and semi-covalent, determined by the nature of the adduct formed between the functional monomer and the target molecule. In covalent imprinting, a reversible covalent bond is established between the monomer and the target before adding them to the polymerisation reaction mixture. This bond is later broken after polymerisation to remove the template molecules, and upon rebinding, the covalent bond is re-established. While covalent imprinting offers high stability and allows the use of diverse reaction conditions, the slow formation of covalent linkages, results in extended times for template binding and release. Among the common covalent bonds that are used in this type of imprinting are Schiff base (10), acetals/ketals (11), or boronate esters (12).

On the other hand, non-covalent imprinting relies on weaker bonds like hydrophobic interactions, electrostatic forces, ionic bonds, and mainly hydrogen bonds. These adducts are formed *in situ* during the reaction, and template removal after polymerisation is facilitated by a suitable solvent. Non-covalent binding is easier to achieve, applicable to a broad range of targets, and allows relatively fast target binding and release. However, it requires careful optimisation of the reaction conditions to maximise interaction between the target and the monomer. Moreover, excess monomer usage can lead to non-specific binding sites formation, reducing the resulting MIPs' selectivity. The semi-covalent method is an intermediate approach, forming the template-monomer adduct with covalent bonds, while rebinding relies on non-covalent interactions. This method is less commonly used due to its challenging nature and optimisation process (13,14).

1.3. Pre-polymerisation and optimisation studies

The process of synthesis of MIPs is a rather challenging procedure, therefore the conditions of synthesis should be thoroughly investigated and optimised. Optimisation usually aims at various important goals, including: the formation of a stable template-monomer adduct, the formation of uniform size and porous polymer particles, easy and complete template removal and rebinding, reducing non-specific binding, and maintaining the structural and conformational integrity of the target molecules especially the bulky ones such as proteins (15).

Pre-polymerisation investigations involve experiments conducted before the polymerisation process to verify the stability of the template-monomer adduct and explore the impacts of different physicochemical parameters.

In the context of covalent imprinting, these studies aim to identify a suitable monomer capable of establishing a stable covalent bond with the template molecule, which can be conveniently broken post-polymerisation. Meanwhile, in the case of non-covalent imprinting, weaker bonds are involved such as ionic, van der Waals and hydrogen bonds which are easier to achieve with various monomers and targets. In both imprinting scenarios, diverse testing methods are employed on the pre-polymerisation mixture, comprising the template with the monomer and the solvent. These tests typically utilise spectroscopic techniques, including nuclear magnetic resonance (NMR), Fourier-transform infrared spectroscopy (FTIR), and ultraviolet (UV)-spectroscopy. Spectra are acquired for the template alone and the template-monomer adduct after reaching equilibrium. A comparative analysis of these spectra often reveals significant differences, providing valuable insights into the formation of bonds, their nature, and stability. A notable instance of applying UV-spectroscopy is exemplified by S. Scorrano et al., who investigated the interaction between their template amino acid, Fmoc-3-nitrotyrosine, and five different monomers (16). The spectra obtained from titrating Fmoc-3-nitrotyrosine in acetonitrile solutions of the monomers exhibited a stronger bond with the template, as evidenced by a hypochromic shift from the original spectrum of the template alone. Consequently, 4-vinylpyridine was selected in this study due to its robust interaction (16).

A more in-depth pre-polymerisation study is to compare different molar ratios of the template to the monomer in order to determine the most stable ratio. Using spectroscopic applications such as Job's method, binding isotherm and titration curves can reveal the nature of interaction, association constant (K_a) and coordination number of the complex (17).

The optimisation process in the synthesis of MIPs encompasses the systematic alteration of factors such as the type and the concentration of the functional monomer(s), cross-linker(s), initiator, and porogenic solvent, constituting classical optimisation. The efficiency of this optimisation is estimated through batch rebinding experiments, wherein the interaction between the template and the produced polymers serves as a metric for determining the optimum conditions. Theoretical chemical principles play an important role in this optimisation, providing insights into the nature of bonds and the mechanisms involved in the polymerisation reaction. Furthermore, some studies have introduced innovative approaches, including the utilisation of software techniques like artificial neural networks (18). These advanced methods aim to streamline the optimisation process by minimising the number of experiments required while enhancing precision and accuracy in achieving optimal synthesis conditions (18).

To elaborate on classical optimisation, the role of each element in polymerisation and the importance of optimisation must be explained regarding the type and the concentration.

1.3.1. The functional monomer

The selection of an appropriate monomer is primarily dependent on the nature of the template. The monomer should exhibit functional groups that are complementary to those present in the template molecule. In instances of covalent imprinting, derivatives of acrylic acid or methacrylic acid, such as amides or esters, are frequently employed. These derivatives facilitate the binding of templates to the vinyl moieties of the monomer.

Conversely, in non-covalent imprinting, the use of vinyl monomers is viable, provided they incorporate functional groups capable of engaging in hydrogen bonding with the template. Methacrylic acid (MAA) stands out as a widely favoured monomer due to its dual characteristics as both a hydrogen bond donor and acceptor, rendering it a versatile and popular choice. Additionally, other commonly utilised monomers include acrylic acid (AA), acrylamide (Am), and vinyl-pyridines (2-VP and 4-VP), each known for their ability to interact with a diverse array of templates. This diversity in monomer selection allows for tailored interactions with a wide variety of template molecules, enhancing the versatility of the molecular imprinting process (15). Structures of these monomers are illustrated in **Figure 2**.

N-isopropylacrylamide (NIPAm) (**Figure 2**) is a special type of functional monomer which has the advantage of thermo-sensitivity. Poly(NIPAm) polymers and hydrogels undergo a volume phase transition at lower critical temperature (~32°C). Therefore, polymers made using NIPAm possess reversible thermal transition response which is useful to control the capture and the release of the template (19). M. Fang et al. prepared fluorescent MIPs using NIPAm, and from their work it was found that the MIPs' binding capacity was significantly higher at 44°C compared to 28°C. The MIPs presented hydrophilic and swelling state at 44 °C which enabled easy access of the target molecules to the imprinted cavities (20). Nonetheless, polymer chains prepared with NIPAm fold randomly during the transition from an extended coil structure to a collapsed globule structure. Therefore, the conformation of the newly formed globules might differ from the original one, which in turn can affect the structural selectivity of the MIPs (21).
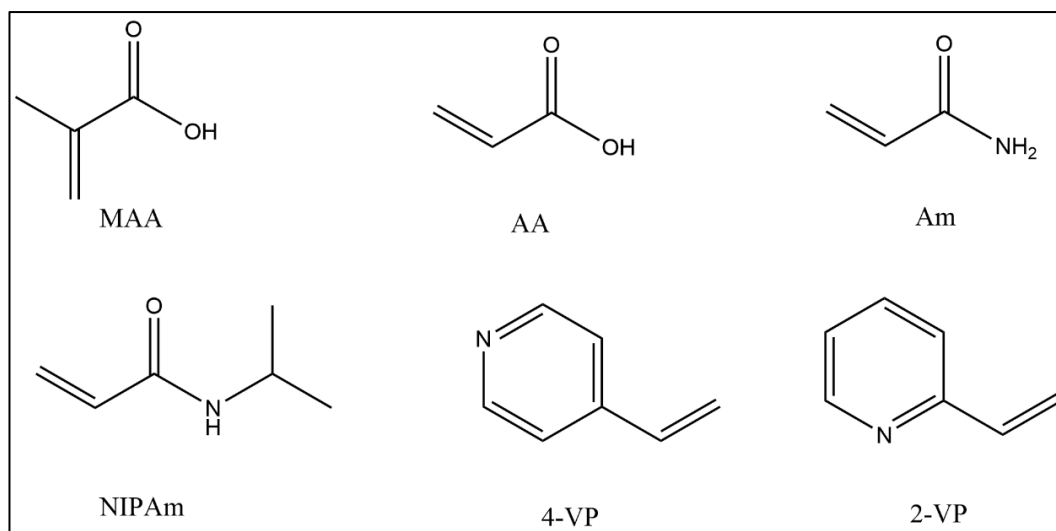
Figure 2. Chemical structures of common functional monomers.

Functional monomers can also be tailor-made to the studied template in order to achieve better binding. These monomers have a specific functionality to be used in MIPs. For example, W. Xu et al. reported synthesis of an imidazolium-based ionic liquid with vinyl groups that could provide multiple interactions with the template molecules and increase selectivity (22).

Deep eutectic solvents (DES) are a type of ionic liquid formed by the combination of a hydrogen bond donor, such as an ammonium or phosphonium salt, and a hydrogen bond acceptor, typically a metal chloride or other halide salt (23). Unlike traditional ionic liquids, which are composed of organic cations and large, asymmetric anions, DES consist of smaller, more symmetric ions. The resulting mixture exhibits a eutectic point, which is a temperature at which the mixture becomes a liquid with a lower melting point than the individual components. DES were first described by Abbot et al. (24), they resemble ionic liquids in some characteristics such as low melting point, high conductivity, electrochemical stability and excellent solubility for many substances.

However, DES surpass ionic liquids by offering the advantages of ease of preparation, low cost, biodegradability and low toxicity which make them ecofriendly (23). Recently, MIPs exploiting DES as functional monomers and/or cross-linkers were reported which had a significant positive impact on the selectivity, the affinity and the greenness of the resulting MIPs (25–28).

Balancing the concentration of the monomer is as crucial as selecting its type. The interaction between the monomer and the template follows an equilibrium. As a result, it preferable to introduce an excess of the functional monomer to encourage complex formation. Conducting pre-polymerisation studies aids in determining the most favourable template to monomer ratio, which can be further confirmed by assessing the binding capacity of the resultant MIPs. It is essential to note, however, that an excessive amount of monomer leads to the creation of multiple heterogeneous binding sites, diminishing selectivity. Hence, achieving the optimal molar ratio becomes essential, and this ratio varies depending on the nature of the template, making it challenging to provide a universal recommendation (29).

1.3.2. The cross-linker

The cross-linking agent plays a key role in creating the densely cross-linked structure encasing the template-monomer adduct. Utilising diverse cross-linkers can yield varying configurations of binding sites and different orientations of functional groups for binding. The cross-linker serves as the foundation for the structural stability, enabling MIPs to retain their structural memory of the template even after its removal (30).

Despite the simple role of the cross-linker, its optimal type and concentration require careful consideration. Initially, the chosen cross-linker must exhibit similar reactivity to the functional monomer, ensuring a balanced polymerisation process with a uniform distribution of functional residues. Moreover, the concentration of the cross-linker plays a critical role; if too low, it compromises the mechanical stability of the resulting polymers, leading to closely spaced binding sites that hinder efficient binding. Conversely, an excessive concentration of the cross-linker diminishes the number of binding sites per unit mass of MIPs. This can potentially disrupt the selectivity due to unintended non-covalent interactions between the cross-linker, template, or monomer. Achieving an optimal balance is essential to ensuring both mechanical stability and selective binding efficiency in the resulting MIPs (30).

Common cross-linkers employed in MIPs' synthesis are N,N'-methylenebisacrylamide (MBA), ethylene glycol dimethacrylate (EGDMA), and divinylbenzene (DVB) structures of which are illustrated in **Figure 3.**
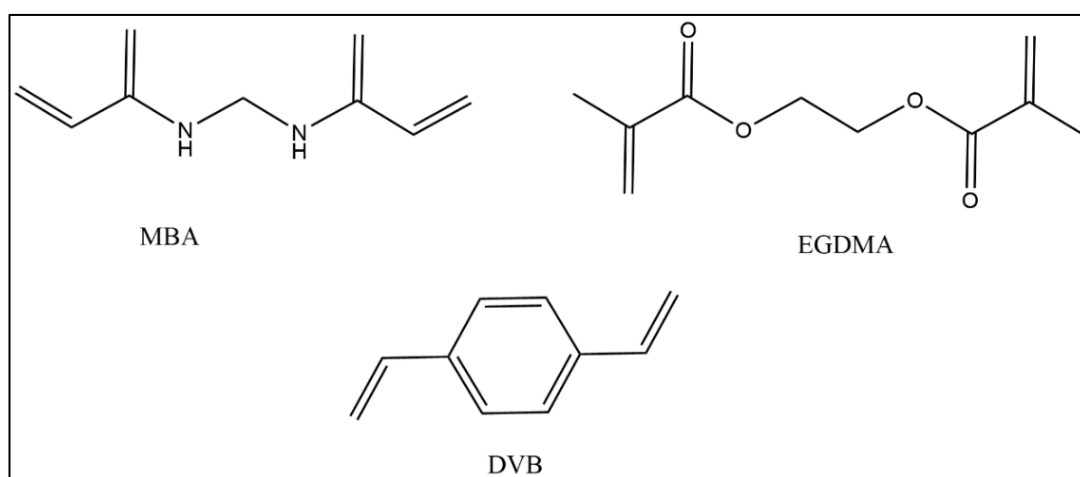
Figure 3. *Chemical structures of common cross-linkers.*

Cross-linkers may also be synthesised according to the required functional needs. R. Xu et al. (21) reported the synthesis of a new peptide cross-linker that exhibits a pH dependent helix-coil transition properties. Changing pH from 5.5 to 7.4 led to the expansion of the imprinted cavities and easy template removal, restoring pH to 5.5 returned the imprinted cavities to their original shape and size due to the precise peptide folding.

Another approach was introduced by Y. Sun et al. (31) where dopamine was utilised as both functional monomer and a cross-linker for synthesis of MIPs for detection of bovine serum albumin. The idea is based on the self-polymerisation of dopamine in weak alkaline medium (pH 8.5). In the presence of template protein in a weak alkaline medium, dopamine polymerises around the template creating cavities with high recognition without the need for a cross-linking agent (31).

1.3.3. The Initiator

Various polymerisation reactions, including cationic, anionic, and free radical methods, can be employed in the synthesis of MIPs. Among these, free radical polymerisation stands out as the most widely adopted due to its experimental simplicity and versatile applications. Azo-initiators such as 2,2'-azobis(isobutyronitrile) (AIBN) and 2,2'-azobis(2,4-dimethylvaleronitrile) (ADVN) are commonly utilised in free radical polymerisation processes (depicted in **Figure 4**). Typically, the reaction is thermally initiated at temperatures ranging from 50 to 70 °C. However, it's important to note that this temperature range can pose risks to the stability of the template-monomer adduct or to the template itself, especially when dealing with delicate structures like proteins.

In such cases, photochemical initiation using UV light can be a safer alternative (13). Some oxidising agents have been applied as initiators in different works, mostly a mixture of strong oxidising agent and an accelerator such as potassium persulfate and sodium bisulfite mixture (32) or ammonium persulfate (APS) and N,N,N',N'-tetramethyl ethylenediamine (TEMED) mixture (33,34). In all cases, dissolved oxygen in the reaction mixture must be removed prior to polymerisation simply by purging inert gas such as nitrogen or helium in the reaction mixture.
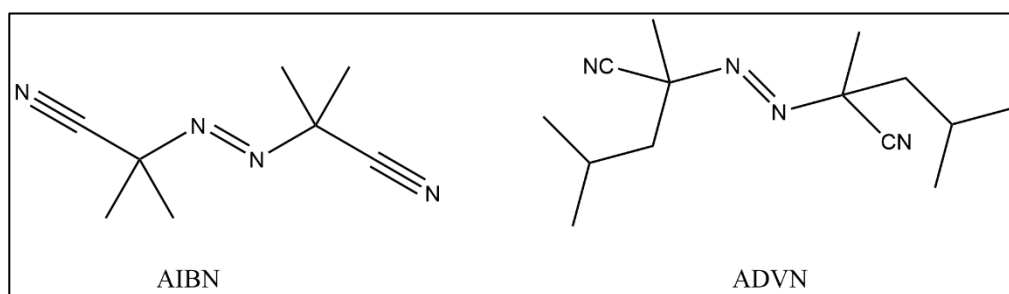
Figure 4. *Chemical structures of common azo initiators.*

1.3.4. The porogenic solvent

The prime roles of porogenic solvents are to solubilise all the starting materials of the reaction and act as a pore forming agent in the resulting MIPs. Solvent molecules are trapped in the polymer matrix and are removed after drying which leaves behind pores, and these pores are beneficial for easy access of the template to the binding sites. The polarity of the solvent is an important influential factor especially in non-covalent imprinting. Solvents should promote the formation of bonds between the template and the monomer; therefore, it is advisable to use non-polar aprotic solvents. Chloroform, acetonitrile, tetrahydrofuran and toluene are common porogenic solvents used for successful non-covalent imprinting. Water is a poor choice of solvent in non-covalent imprinting since it can disrupt the hydrogen bonds between the template and the monomer.

Nonetheless, numerous templates, particularly those of biological significance, exhibit solubility exclusively in water, posing a challenge for the non-covalent imprinting of such templates (35).

1.3.5. The template

The selection of a template is guided by its biological or chemical significance; however, a thorough examination of its chemical structure is required. It is crucial to verify the presence of accessible functional groups in the template capable of interacting with the functional monomer. However, these functional groups must not impede or interfere with the polymerisation reaction. Additionally, investigating the chemical stability of the template under the applied reaction conditions, including pH, temperature and other parameters, is essential to ensure the preservation of its structural integrity throughout the polymerisation process (36). Proteins specifically introduce the greatest challenge as templates due to their bulky structure, their insolubility in non-polar solvents and their sensitivity to different pHs and temperatures. Yet due to their high biological and medical significance, proteins have been applied as templates in many recent research articles despite the posed challenges (37–41).

1.4. Techniques of molecular imprinting

Over the course of their evolution, methodologies for synthesising MIPs have undergone significant advancements. Initially, bulk molecular imprinting emerged as the pioneering technique for MIPs. Nevertheless, given the numerous challenges associated with bulk imprinting, diverse alternative techniques have emerged, each possessing distinct advantages and applications.

It is noteworthy that across various molecular imprinting approaches, non-imprinted polymers (NIPs) are simultaneously synthesised in the absence of the template molecules. This parallel synthesis of NIPs serves the purpose of facilitating comparisons and eliminating potential errors in the evaluation of MIPs.

1.4.1.Bulk polymerisation

Bulk polymerisation represents the most straightforward and quickest approach to molecular imprinting. Herein, the template molecules are introduced into the reaction vessel alongside the monomer, cross-linker, initiator, and an appropriate solvent to initiate a free radical polymerisation. In this process, the template molecules are imprinted intact within the three-dimensional matrix of the polymer. These three-dimensional imprinted cavities afford high selectivity and easily accessible binding sites for the template. Following polymerisation, the resultant product is subjected to grinding and sieving to obtain fine particles. Ultimately, the imprinted template molecules are removed through the use of a suitable solvent (42).

Bulk imprinting is preferred for small template molecules, since they can be easily bound and released from the binding sites in a reversible and reproducible way. Moreover, bulk imprinting can also be beneficial for large molecules such as proteins since they are imprinted as whole molecules, which in turn increases recognition. However, drawbacks are inevitable in this type of imprinting especially with large molecules. First of all, the use of grinding results in irregular size distribution of the produced polymer particles which reduces their applicability especially for chromatographic purposes. Furthermore, grinding causes mechanical disintegration of

the intact particles which in turn produces heterogeneous binding sites and reduces sensitivity dramatically.

Second, the larger the template molecules, the more time they take to be released or bound to the binding sites, which makes the binding of proteins, microorganisms, and DNA highly time consuming. Third, during protein imprinting, problems such as maintaining conformational stability cannot be ignored. Finally, the large imprinted cavities can also attract smaller polypeptides in the sample resulting in cross-reactivity and reduced selectivity (43,44). Yet with the many drawbacks of bulk imprinting, it is still applied until today for imprinting of drugs (45,46), natural products (47,48), and proteins (49).

1.4.2. Suspension polymerisation

In this polymerisation technique, the polymerisation mixture undergoes mechanical agitation or ultrasonic treatment to form small droplets within a dispersion medium. Typically, water serves as the dispersion medium, but its usage is less favourable due to its disruptive impact on hydrogen bonds within the template-monomer adduct. Alternatively, mineral oils or perfluorocarbon liquids prove more advantageous. The outcome of suspension polymerisation generally yields spherical polymer beads of considerable size, ranging from micrometres to millimetres, making it particularly advantageous for large-scale MIP synthesis. However, a notable drawback lies in the potential interference of the dispersion medium with the recognition of the target molecules (43). By carefully selecting suitable dispersion media, suspension polymerisation becomes a versatile approach applicable to a broad spectrum of drugs, chemicals, and pollutants (50,51).

1.4.3. Emulsion polymerisation

Emulsion polymerisation involves the use of surfactants or cyclodextrins to form a water in oil or oil in water emulsion of the polymerisation mixture. Therefore, the monomer, cross-linker and initiator are dissolved in one phase mostly the organic one, and the template with a surfactant are dissolved in the opposite phase. The two solutions are then shaken vigorously. The formed emulsion results in fine mono dispersed polymer particles with very small particles size from tens to hundreds of nanometres. After polymerisation, organic solvent such as acetone is added to de-emulsify the mixture and template removal is carried out using a suitable solvent (44).

The obvious downside of this method is the use of water and surfactants since they can potentially disrupt the bonds between the template and the monomer. Moreover, surfactants may isolate the template in their interior core preventing it from being imprinted at all. Nonetheless, emulsion polymerisation is a popular technique that is still applied up to date for many templates (52–55).

1.4.4. Precipitation polymerisation

Precipitation polymerisation, while sharing similarities with bulk polymerisation, outperforms it in certain aspects. This polymerisation method is performed with a high concentration of the template and a large volume of the solvent. Consequently, monomer polymerisation takes place in a dilute solution, commencing with the growth of nanogel seed particles that progressively trap larger oligomers. As these polymer particles exceed a specific size threshold, they precipitate from the

solution. This process yields spherical particles with a consistently uniform size, typically less than one micrometre in diameter.

A notable drawback lies in the extensive use of solvent, diminishing the method's environmental sustainability, especially when organic solvents are employed. Additionally, the use of a higher concentration of template may prove uneconomical for rare and expensive templates (43,56).

Several factors demand careful consideration and optimisation during precipitation polymerisation to regulate the particle size, including the solvent's polarity, stirring speed, monomer's concentration, and reaction temperature. So far, precipitation polymerisation has been effective in imprinting many templates from small molecules (57–59) to large proteins (32). Moreover, due to the spherical shape and uniform size of the resulting MIPs, they are useful as potential stationary phase for chromatographic applications (60).

1.4.5. Multi-step swelling (seed) polymerisation

Multi-step swelling polymerisation is a complicated and time-consuming approach used to prepare uniform and spherical MIPs. Polymerisation takes place in gradual steps starting by the use of small polymeric seeds e.g.: polystyrene. Particle swelling grows in each step until MIPs of uniform size are obtained. Despite the prolonged procedure and the need to extensively optimise each step of polymerisation, multi-step polymerisation has few applications with different templates (61,62).

1.4.6. Surface imprinting

Due to the numerous limitations associated with the bulk imprinting technique, a more recent approach known as surface imprinting emerged in the 2000s. In surface imprinting, the binding sites of MIPs are created on the surface of a solid substrate or around nano/micro-sized solid particles. This technique offers a significant advantage that the binding sites are readily accessible since target molecules do not need to traverse the intricate structure of MIP particles formed by bulk imprinting. Consequently, the binding of the target is not diffusion-limited, facilitating rapid binding and release. As a result, surface imprinting has gained popularity, particularly for imprinting large molecules and proteins. However, this technique has its drawbacks, including a smaller number of available binding sites per unit area, which may reduce sensitivity. Additionally, the synthesis process is often time-consuming and involves multiple steps (63,64).

- Soft lithography

Soft lithography is probably among the first surface imprinting techniques to be applied for the synthesis of MIPs. In 1989, Bain and Whitesides (65) were the pioneers to introduce the chemistry and the physical procedure for surface imprinting on solid substrates. Later, this approach was adopted for surface imprinting of target molecules to produce MIPs films. In soft lithography, nano/micro scaled patterned MIPs films are formed on solid substrates using soft polymeric stamps. The procedure is quite simple; the pre-polymerisation mixture is spotted on the surface of a solid substrate usually a glass slide. The solution is then pressed between the glass slide and soft poly(dimethylsiloxane) mould.

Suitable pressure is applied, and reaction is initiated via UV light, as a result thin patterned polymeric films are designed and then dried. After the elimination of the template by suitable solvent, thin layered MIPs films with highly accessible and complementary binding sites are acquired. Moreover, the presence of the stamped patterned network on the MIPs film increases the exposed surface area and hence increases the binding capacity (66,67).

- Core-shell surface imprinting (grafting)

In this type of surface imprinting, MIPs are constructed around nano/micro sized solid particles. In contrast to soft lithography, MIPs are formed on the surface of many small particles instead of a planar solid surface which significantly increases the exposed surface area. Moreover, the use of solid particles enables accurate control of the MIPs particle size, morphology, and surface area (64). **Figure 5** illustrates a representation for the core shell imprinting procedure on nanoparticles (NPs).
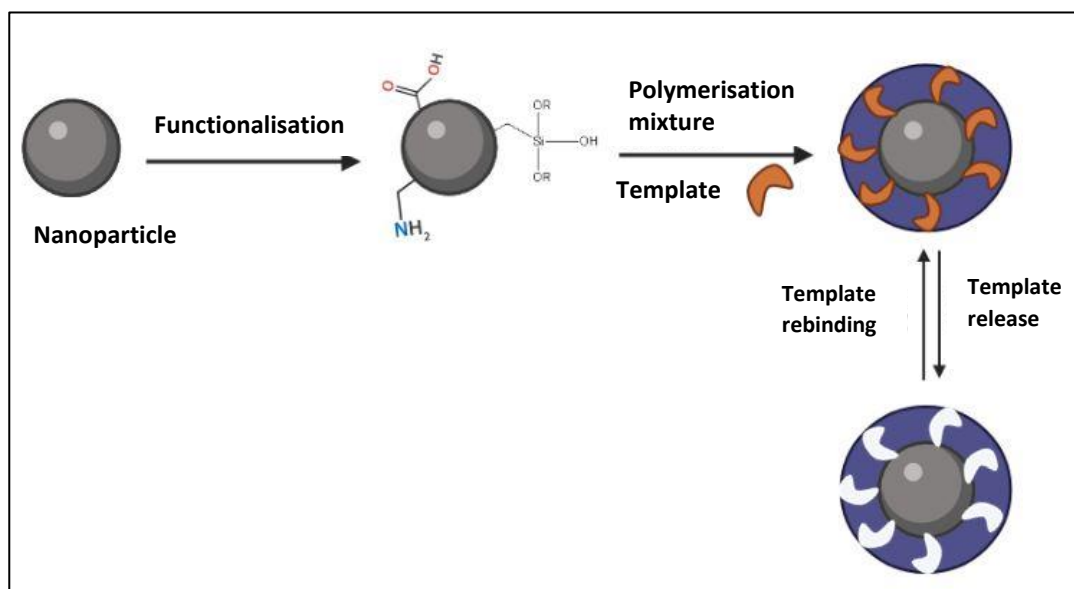
Figure 5. *Schematic illustration of the process of core shell imprinting on the surface of nanoparticles.*

Silica NPs are very common and widely used particles in the core shell imprinting. Due to their inertness, mechanical and chemical stability, and biocompatibility they have been useful substrates for MIPs proposed for sensitive biological applications. In addition, silica NPs possess many hydroxyl groups which enables easy polymerisation on their surface. Nevertheless, silica NPs can still be functionalised with vinyl, amino or cyanate groups to ensure better assembly of polymerisation mixture on its surface (68–70).

Other alternatives for core particles are introduced in some papers which include; metal organic frameworks (71), titanium dioxide NPs (72), attapulgite resin (73), and polystyrene beads (74).

A very attractive approach for core shell imprinting is the use of magnetite (Fe_3O_4) NPs as core particles. The use of functionalised magnetite particles in the core structure of MIPs imparts a magnetic quality which can be very beneficial to separate MIPs from complex matrices by simply using a magnet. Recently, this approach has been extensively applied to MIPs in different fields, a search on magnetic MIPs on the MIP database (75) gave almost 1000+ hits. This indicates a high volume of papers concerned with the application of this magnetic quality in different fields of analysis and extraction (64). Magnetic MIPs have their widest applications in the field of sample preparation and solid phase extraction (SPE). Their magnetic quality enables their use as stationary phase for chromatographic separations followed by their easy isolation using a magnet (76).

Another equally attractive approach for core shell imprinting is the incorporation of fluorescent NPs in the core of MIPs. Fluorescent quantum dots (QDs) impart fluorescent characteristics to MIPs that can be easily measured. In the event of target binding usually a noticeable quenching of fluorescence occurs which is detected and used to quantify the concentration of target. Recently, carbon dots (CDs) have been used as an eco-friendlier, less toxic, and more biocompatible option for the fluorescent MIPs (20,77–81). In addition, some metal organic frameworks prepared from lanthanide metals can also be used as a fluorescent core due to their natural fluorescent and less toxic properties (82–84). A search on the MIP database (75) for fluorescent MIPs gave about 290 hits which points out to the extensive use of fluorescent MIPs in recent research articles especially in the field of optical sensors (85).

Fluorescent core shell MIPs should not be confused with fluorescent bulk imprinted MIPs. The latter type utilises fluorescent co-monomers or fluorescent dyes such as fluorescein to impart the fluorescent quality. Therefore, the fluorescent element is part of the polymeric material itself and not incorporated in its core (86). In this type of MIPs, an increase in fluorescence intensity might be noticed in some cases upon binding to the target which is more analytically favourable than the quenching effect (87).

Some approaches combine both fluorescent and magnetic qualities in the structure of the developed MIPs. By incorporating both QDs or CDs and magnetite in the core of MIPs, they could acquire both characteristics for better extraction and detection of the target molecules (88,89).

- Surface imprinting after template immobilisation

Template immobilisation is considered a technique of surface imprinting in which the template molecules are immobilised to a solid support by chemical bonds. Therefore, after polymerisation, the solid support can be removed along with the immobilised template molecules leaving complementary binding sites on the MIPs surface. Thus, the immobilisation of template molecules gives some major advantages; first, the immobilisation of the template ensures that the binding sites are all on the surface and well oriented for rebinding of target. Second, this technique is useful for insoluble templates since they do not need to be incorporated in the solvent. Finally, the immobilisation of the template via chemical bonds enables complete and easy template removal after polymerisation without the need for excessive washing cycles (90,91).

Micro-contact imprinting is a procedure of template immobilisation that was introduced in 2005 that is quite simple and effective (92). Micro-contact imprinting depends on the immobilisation of target molecules on a glass cover slip via covalent bonds. The cover slip is then exposed to the functional monomer to form the pre-polymerisation mixture as in to orient the functional groups of the monomer towards the template molecules in a site-specific manner and create a strong template-monomer adduct. The cross-linker and initiator are dissolved in the porogenic solvent and spotted as a small drop on a glass slide. The imprinting process then starts by bringing the cover slip in contact with the glass slide and exposing them to UV radiation. After polymerisation, the cover slip is removed and unreacted monomers along with any template molecules that could have leaked into the surface are washed away.

Micro-contact imprinting provides an easy way for rapid and simultaneous polymerisation of many templates simultaneously. In addition, it is a very useful technique for expensive samples that are only available in scarce amounts since the procedure requires minimal amount of template molecules. Due to the previously mentioned advantages, micro-contact imprinting has been successfully applied to imprint different number of target molecules especially proteins (93–95).

Solid phase imprinting of MIPs is a very innovative and promising technique that relies on template immobilisation as well (96). In this imprinting method, the template is immobilised via covalent bonds on the surface of functionalised activated glass beads. The glass beads bearing the template are then brought in contact with the pre-polymerisation mixture to initiate the reaction. The polymerisation conditions are set to produce nano sized MIPs instead of films; conditions such as high dilution and short polymerisation times are favourable to produce nanoparticles. After polymerisation, the solid support plays another important role which is acting as an affinity medium (somehow like chromatographic stationary phase). The immobilisation of template on the solid support allows for the removal of unreacted monomers, and low affinity polymer particles from the high affinity nanoMIPs. This is achieved by washing the glass beads under specific conditions in which the nanoMIPs remain attached while the other unreacted components elute from the system. After successful washing, detachment of nanoMIPs from the glass beads is carried out by washing under different set of conditions (usually higher temperature and different solvent) after which nanoMIPs are eluted with complementary binding sites and complete template removal (97). **Figure 6** shows the process of solid phase imprinting and separation of nanoMIPs.

Although the yield from this imprinting method is usually small, their binding affinity is much higher than MIPs produced using other imprinting methods. In addition, yield can be increased by carrying out several cycles of synthesis using the same system which can be turned into an automated procedure. Solid phase imprinting has its biggest share of applications in the field of protein imprinting and sensor applications (41,98–100).
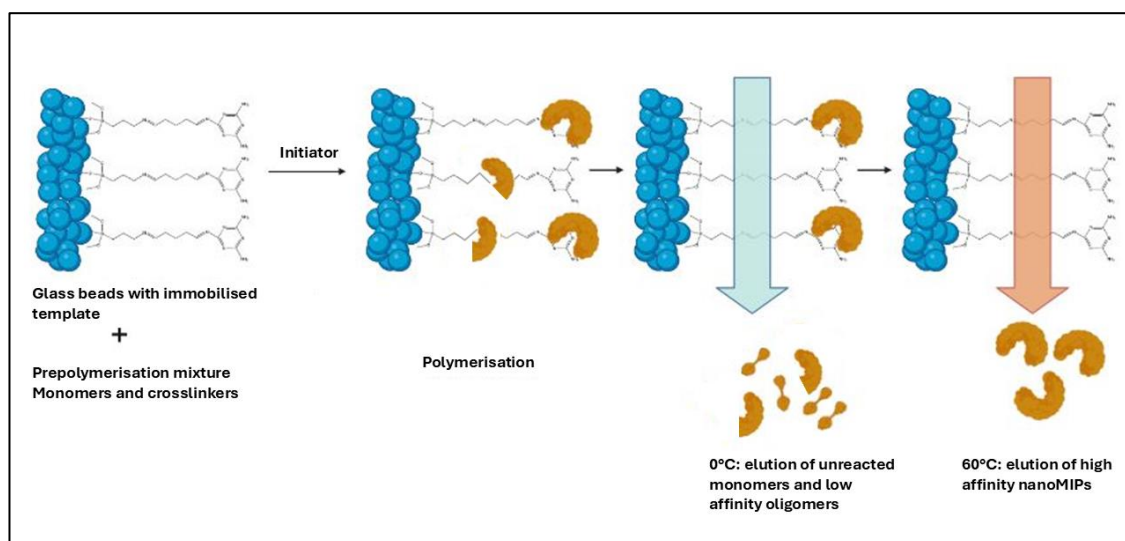
Figure 6. Schematic illustration of solid phase synthesis of nanoMIPs.

1.4.7. Controlled/living radical polymerisation

During the traditional free radical polymerisation, the high concentration of generated radicals leads to rapid chain propagation, resulting in uncontrollable premature chain termination. This phenomenon causes the production of polymer chains with varying lengths, contributing to the broad size distribution observed in MIPs produced using the free radical mechanism. Additionally, if the monomer exhibits different radical reactivity than the cross-linker, it will introduce variations in the distribution and the orientation of functional groups in MIPs.

To address these challenges, the controlled/living radical polymerisation (CRP) technique has been introduced in molecular imprinting. CRP relies on the use of temporary radical capping agents (dormant species) to protect radicals from premature termination. The employment of capping agents allows propagation chains to grow at the same rate and simultaneously until termination. This results in polymer chains with nearly uniform sizes and a very narrow size distribution range. Another advantage of CRP is the introduction of living functional groups to the polymer chain end, enabling further modification of the MIPs structure to reduce possible non-specific binding (101–103).

Various CRP chemistries, such as atom transfer radical precipitation polymerisation (104), reversible addition-fragmentation chain transfer (RAFT) (105), and nitroxide-mediated polymerisation (106), have been successfully applied to produce MIPs with small sizes and narrow size distributions. Among these, RAFT is considered the most versatile and suitable technique due to its applicability to a wide range of monomers, moderate reaction conditions, and easy control of the polymer structure through post-imprinting functionalisation (107). Despite these advantages, CRP techniques are less utilised compared to free radical polymerisation, mainly due to the requirement of expensive reagents and the relatively slow and time-consuming nature of the reactions.

1.4.1. Electro-polymerisation

Electro-polymerisation is a special class of molecular imprinting in which polymerisation occurs on the surface of a conducting electrode such as gold, platinum, glassy carbon electrode and others. A solution containing the target and suitable functional monomer(s) is subjected to electrochemical energy that initiates the polymerisation. As a result, a thin film of MIPs is formed on the surface of the electrode. Therefore, after the removal of template, this film contains gaps or cavities that are complementary to the analyte. Subsequently, upon rebinding to the target analyte in a sample, a signal is generated by the electrode, which is measured by a suitable electrochemical analytical device.

Pyrrole, scopoletin and o-phenylenediamine are among the most common functional monomers employed in electro-polymerisation due to their ease of polymerisation at low potential and their ability to form chemical bonds with a variety of targets. The choice of monomer usually depends on the planned electrochemical analytical method; pyrrole is most commonly used for direct voltametric assays (potentiometry, square wave voltammetry, cyclic voltammetry (CV), etc.). However, less conductive monomers, such as o-phenylenediamine are more commonly used in electrochemical impedance spectroscopy (EIS) assays (108).

Electro-polymerisation offers a group of advantages that makes it a very appealing technique, especially in the field of sensors. Compared to traditional bulk polymerisation, electro-polymerisation is much faster and easier. Moreover, it can be carried out *in situ* on the surface of the working electrode while the whole process is monitored on a computer screen.

In addition, the thickness of the produced film is manageable by variation of the applied charge, which makes the method more reproducible and reliable. Nonetheless, electro-polymerisation also suffers from some of the same drawbacks encountered by other types of polymerisations. Non-specific binding and incomplete template removal are two commonly encountered problems with electro-polymerisation, which require lengthy optimisation procedures to overcome and control. However, by overcoming these setbacks, electro-polymerisation is a very promising technique whose sensitivity can reach the picomolar levels with ease (109–111).

1.5. Characterisation of MIPs

1.5.1. Physical characterisation (morphological)

Physical characterisation provides valuable information about the morphology of the resulting MIPs as well as their size distribution, geometry and porosity. The size of MIPs is a crucial parameter, since the smaller the particle size the more surface area available for binding of target. Moreover, as mentioned before, different polymerisation techniques result in different particle sizes, therefore morphological testing can verify the anticipated particle characteristics using a particular polymerisation technique. It is also essential to identify the shape of the produced MIPs, especially if they are intended for chromatographic applications (112). Electron microscopy is a very popular technique to determine the shape, geometry and size of MIPs. Scanning electron microscopy (SEM) and transmission electron microscopy (TEM) are usually used to visualise the resulting MIPs and NIPs and to verify the surface imprinting on the surface of different nanoparticles (112,113).

Other particle size analysing methods include laser diffraction and dynamic light scattering. These techniques give more in-depth data such as mean size, mean surface area and size distribution. However, these methods are less popular than electron microscopy, since the later gives a visual approach to the shape of MIPs. In addition, it can reveal if aggregates of particles are formed, which can be misinterpreted as large particles while using laser diffraction (113).

To estimate MIPs porosity, two characterisation methods can be used: nitrogen gas adsorption and mercury intrusion porosimetry. These methods provide the ratio between the volume of pores to the total volume of polymer particles which can be used to investigate the volume and surface area of MIPs pores (113). Some studies utilising nitrogen adsorption have revealed that MIPs exhibit larger pore volumes than NIPs, affirming the role of the template in enhancing the surface area and porosity of MIPs (114).

1.5.2. Chemical characterisation

Fourier-Transform Infrared spectroscopy (FT-IR) is renowned for its efficacy in MIP characterisation. FT-IR serves as a practical method for analysing functional groups and ensuring the thorough polymerisation of MIPs. Through comparing spectra from initial monomers and templates to those obtained from MIPs, researchers can discern the absence of functional groups crucial to polymerisation, such as vinyl groups (C=C stretching), in the MIP spectra. In addition, it can be a useful tool to ensure complete functionalisation of magnetite or silica or other NPs intended for core shell imprinting (115).

UV-Vis spectroscopy proves influential in confirming the complete washing of MIPs, via analysing washing solution batches for the presence of the template. Additionally, it serves as the primary method in rebinding experiments, facilitating the detection and quantification of template or competitor molecules in supernatant solutions following rebinding (116).

X-ray diffraction (XRD) is a powerful analytical tool widely employed for the characterisation of MIPs. This method involves exposing a material to X-rays, and the resulting diffraction pattern provides insights into the crystallographic structure and arrangement of atoms within the material. In the context of MIPs, XRD is valuable for elucidating the structural characteristics of the polymer matrix. It can reveal information about the crystallinity, phase composition, and overall molecular arrangement of the imprinted polymers. The diffraction patterns obtained from XRD analyses contribute to understanding how the template molecules influence the polymer's internal structure. This technique plays a crucial role in advancing the knowledge of MIPs' morphology and can guide the optimisation of their synthesis for enhanced molecular recognition applications (117).

Nuclear Magnetic Resonance (NMR) is a spectroscopic technique also employed for chemical characterisation. Both solid-state and solution NMR play useful roles, particularly in pre-polymerisation studies. NMR facilitates an in-depth examination of the imprinting mechanism and the identification of bonds formed between the monomer and the template (118).

1.5.3. Thermal characterisation

Various thermal analytical techniques, such as thermogravimetric analysis (TGA) and differential scanning calorimetry (DSC), have found widespread application in numerous research endeavours focused on MIPs. TGA, a method monitoring mass loss at varying temperatures, proves advantageous for identifying the content of residual solvent, detection of unreacted monomers and cross-linkers, and determination of moisture content. Furthermore, TGA offers valuable insights into the thermal stability of MIPs, outlining the temperature range where they exhibit optimal stability (118– 120). On a parallel note, DSC involves subjecting materials to multiple cycles of heating and cooling, providing information about polymer crystallinity. Data from DSC also complements the data from TGA to give a complete picture about the melting behaviour and the thermal stability of the resulting MIPs. Thermal analysis becomes particularly relevant when considering applications like the immobilisation or deposition of MIPs on solid supports, as observed in the development of sensors or biosensors (113).

1.5.4. Functional characterisation

Functional characterisation, or alternatively referred to as binding studies, encompasses a series of experiments designed to explore the binding properties of the synthesised MIPs. These tests are conducted to quantify the binding affinity to the target using specific mathematical formulations. Additionally, evaluations extend to the binding interactions with competitive analytes, akin in structure to the target or coexisting within the same matrix.

Analytical techniques such as UV-Vis spectrometry or liquid chromatography are employed to monitor and analyse the results of these binding experiments (116).

1.5.4.1. Binding capacity

In order to estimate the binding capacity, a rebinding experiment is carried out. In this experiment, a certain weight of MIPs or NIPs is incubated with a specific volume of the target solution for a certain period of time until equilibrium is reached. Analytical methods such as UV spectrometry is used to determine the remaining concentration of the target in the solution after binding. The following equation is used to calculate the binding capacity for both MIPs and NIPs:

$$Q = \frac{C_i - C_t}{m} \cdot V \qquad \text{(eq.1)}$$

where, Q is the binding capacity in mg g^{-1}, where, C_i (mg mL^{-1}) is the initial concentration of the target, C_t (mg mL^{-1}) is the remaining concentration of the target after incubation time (t), V (mL) is the volume of solution, and m (g) is the mass of the polymers used in the experiment. It should be noted that V and m should be the same in both experiments for MIPs and NIPs.

The higher the value of Q, the greater the binding capacity. However, the value of Q for MIPs is expected to be higher than that of NIPs, due to the selectivity of MIPs for the target compared to the nonspecific binding of NIPs.

1.5.4.2. Binding selectivity

MIPs tend to have different non-specific binding sites (due to reasons that will be discussed further). Therefore, it is essential to estimate the selectivity of the developed MIPs to the target analyte to ensure that non-specific binding is not a problem.

One method to study binding selectivity is to compare the binding of MIPs against the binding of their respective NIPs. This comparison confirms the presence of specific binding sites in MIPs for the target that are absent in NIPs. Imprinting factor (IF) is a calculated parameter that is defined as the ratio between the binding capacity (Q) of MIPs to that of NIPs for a particular analyte under a specified set of conditions.

$$IF = \frac{Q_{MIPs}}{Q_{NIPs}} \qquad \text{(eq.2)}$$

From equation 2, the IF value should be higher than 1. The higher the value of IF, the greater the difference between MIPs and NIPs, which in turn proves the presence of selective binding sites in MIPs.

However, comparison to NIPs may not be the best way to ensure the selectivity of MIPs. This can be attributed to two main reasons. Firstly, the structure of NIPs tends to be more compact due to the absence of template during polymerisation, therefore the number of available free binding functional groups is by nature less than MIPs. Secondly, a published study has shown that during optimisation of MIPs' synthesis, the optimum composition of MIPs that has the highest binding capacity corresponds to NIPs that bind the target strongly as well (121).

A better way to estimate selectivity is to compare binding of MIPs to the target to binding with a competitive analyte under identical experimental conditions. Herein, a factor called selectivity factor (α) is computed for every competitor analyte tested in the binding experiments using the following equation.

$$\alpha = \frac{Q_{MIP.target}}{Q_{MIP.competitor}} \qquad \text{(eq. 3)}$$

The selectivity factor (α) should have a value higher than 1; the high values of α for different tested competitors are numerical proofs of selectivity of MIPs.

1.5.4.3. Binding kinetics and isotherm

When discussing binding kinetics, it is important to note that binding/release of target to MIPs is a diffusion limited process. In other words, molecules of the target need to undergo mass transfer from solution phase to solid phase of MIPs. This can be a slow process, since molecules need to cross the porous solid polymeric network to access the binding sites. In the case of surface imprinting, binding is usually faster, since the binding sites are located on the surface and readily accessible (122).

The best way to calculate the binding kinetics is to carry out a batch rebinding assay for both MIPs and NIPs. A batch rebinding experiment is conducted by incubating the exact same mass of MIPs and NIPs in the exact same concentration of target analyte solution, and then analysing aliquots of the solution over different time intervals. The graphical relationship between time and the free concentration can be used to determine equilibrium time and the order of binding kinetics.

On the other hand, determination of binding isotherm is another experiment in which the exact same mass (m) of MIPs or NIPs is incubated with different concentrations of the target analyte. After equilibrium is reached, aliquots of the supernatant solution are analysed to determine the concentration of the free target (F) in mol. L^{-1} and determine the bound concentration (B) in mol. L^{-1} using equation 4.

$$B = \frac{ntarget}{m} - \frac{V}{m} x\, F \qquad\qquad (eq.4)$$

Where n_{target} is the total number of target mols used in the experiment, and (v) is the volume of the solution. The binding isotherm is a graphical relationship between B and F. The isotherm for MIPs is usually not linear; it reaches a plateau at high F values indicating the saturation of the binding sites. However, the curve for NIPs is usually linear and indicates non-specific binding due to the randomly oriented functional groups on its surface. The difference between MIPs' and NIPs' curves is attributed to the specific binding of MIPs due to the presence of selective binding sites. Therefore, optimisation is carried out to maximise the difference between the two isotherms, which is reflected on the selectivity of MIPs.

Note that the word "isotherm" means constant temperature. Therefore, the binding experiments should be carried out under constant temperature, as well as constant solution conditions (pH, ionic strength, solvent, etc.) for all concentrations of the tested target.

Data from binding isotherms can be further fitted into theoretical models, such as Langmuir model or Freundlich model. The curve which fits the experimental data best can give us an estimate of the number of binding sites and their binding affinities (123).

1.5.5. Characterisation of MIP films

For MIPs imprinted as thin films or on the surface of a chip, a crystal or an electrode to be used as sensors, other characterisation methods are needed for the immobilised MIPs.

Atomic force microscopy, X-ray photoelectron spectroscopy, quartz crystal microbalance analysis (QCM), and surface plasmon resonance (SPR) are all useful techniques that can be used alone or in combination with electron microscopy to characterise on-surface MIPs. Such methods give us valuable information regarding surface homogeneity, roughness, and to ensure complete deposition of MIPs on the solid support. In addition, they can give an online monitoring of binding events as well as to ensure complete template removal (113).

1.6.   Advantages and challenges in the synthesis of MIPs

MIPs offer several notable merits, with one of the key strengths being their inherent stability, allowing for utilisation under diverse non-physiological conditions. Remarkably, MIPs exhibit prolonged storage capabilities at ambient temperatures without experiencing damage, degradation, or a decline in target recognition efficiency. The synthesis of MIPs is not only cost-effective but also time-efficient, presenting a favourable alternative to the production of antibodies. These attributes hold particular economic value, especially when considering large-scale industrial production. Additionally, the versatility of MIPs is highlighted by their amenability to functionalisation with fluorescent or magnetic labels, enabling customisation in various forms such as films, particles, or nanotubes tailored for specific applications. This flexibility surpasses the customisation possibilities of antibodies (124).

A recent study by K. Smolinska-Kempisty et al. conducted a comparative analysis of nanoMIPs and antibodies in an enzyme linked immunosorbent assay (ELISA) targeting a specific substance.

The study demonstrated that nanoMIPs are equally or even more effective than antibodies, positioning them as superior candidates for industrial diagnostic applications (125). Despite these remarkable qualities, the field of MIPs research faces several challenges, primarily associated with the intricate synthesis process and template-dependent variations. In this discussion, the prevalent challenges encountered in MIPs' synthesis are examined, presenting the most recent proposed solutions to address these issues.

1.6.1. Binding site heterogeneity

Binding site heterogeneity is considered an inevitable setback when developing MIPs. This problem usually results in MIPs that are "polyclonal" in nature, thus they might exhibit non-specific binding with other species in the target sample. Binding site heterogeneity is one of the main problems that limits the wide applications of MIPs and gives antibodies a significant leverage on MIPs, since antibodies are "monoclonal" and highly specific.

The drawback of binding site heterogeneity is caused by different factors and in almost all types of imprinting, yet it is more noticeable in non-covalent imprinting. One of the obvious reasons for this problem is that the monomer-template interaction is a process governed by equilibrium. Therefore, during equilibrium, the pre-polymerisation mixture contains many species of template-monomer interactions, different complex ratios, not just 1:1, in addition to free monomers.

Furthermore, some side interactions are likely to occur between the template and cross-linker, or between the monomer and the cross-linker or even between template molecules themselves forming clusters.

These random species occurring in the pre-polymerisation mixture are translated into the final polymer, forming many non-specific binding sites. Moreover, another array of factors also contributes to binding site heterogeneity after polymerisation, this includes grinding and sieving of the polymer, template removal process, and using different solvents during rebinding experiments. All these factors cause further heterogeneity by corrupting the binding sites, collapsing sites after template removal, and variable swelling/collapsing of the polymer upon exchange of the solvent (126). **Figure 7** is a schematic representation of how heterogenic binding sites can be generated during polymerisation and after.

Semi-covalent imprinting is considered a very promising imprinting method to reduce binding site heterogeneity to the minimum. Since this method combines the merit of covalent binding (control on the template-monomer interaction) and the merit of non-covalent release (reduced kinetic restriction), the method offers better control of the functional groups orientation on the binding sites and therefore reduces the resultant heterogeneity (13,14).

Stoichiometric non-covalent imprinting is another useful approach to reduce binding site heterogeneity. This approach was introduced first by Wulff et al. (127) and depends on reaching a high association constant between the template and the monomer, this is achieved by choosing a functional monomer that is capable of forming two or more hydrogen bonds with the template (128).
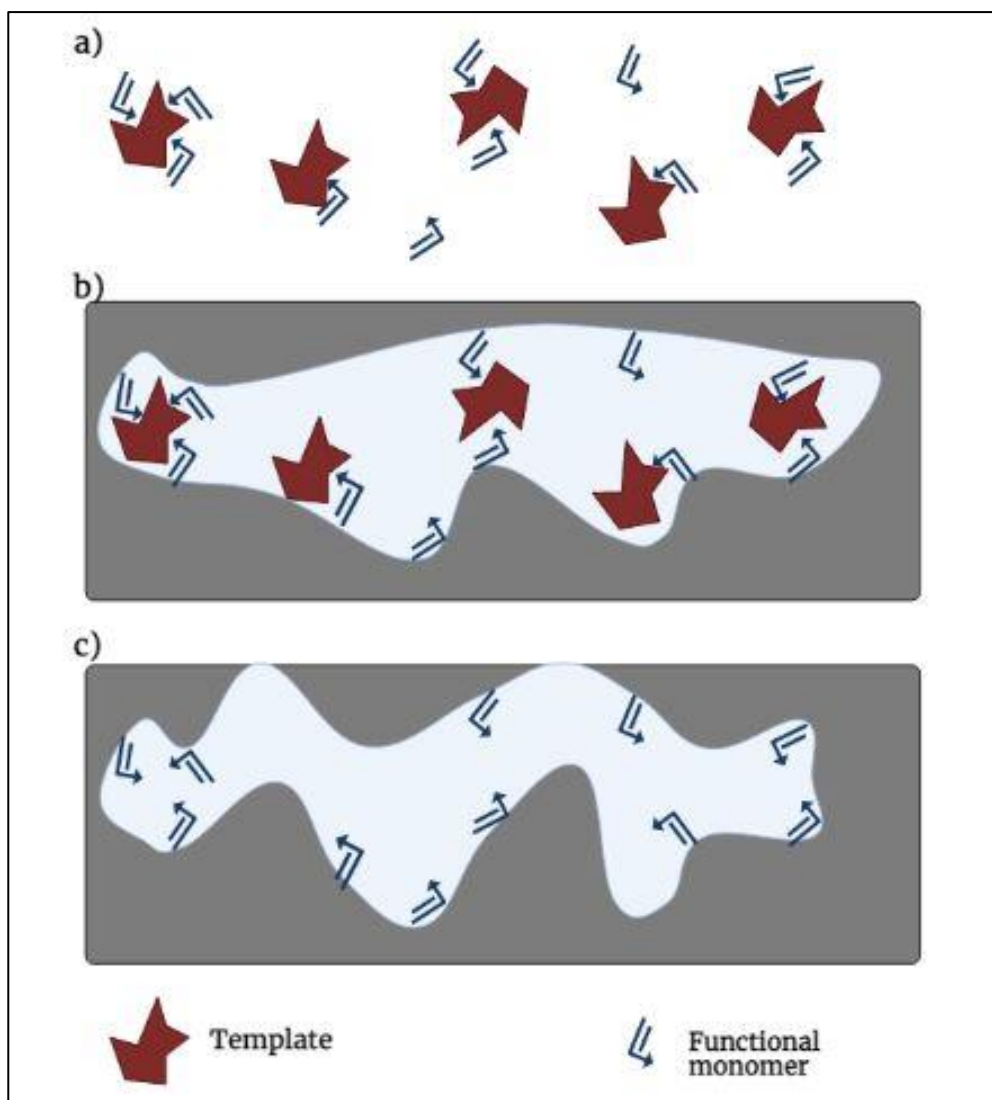
Figure 7. *Schematic representation of the possible origins of binding sites heterogeneity during molecular imprinting. a) Different species in pre-polymerisation mixture showing different possible complexes between the template and the monomer molecules including 1:1, 1:2 and 1:3 ratios in addition to free monomers. b) Structure after polymerisation showing heterogenous binding sites due to different binding sites accessibility and various polymer backbone conformations. c) Structure after polymer collapsing and fracturing due to template removal, solvent exchange and polymer swelling.*

Despite the use of the prior alternatives, semi-covalent, stoichiometric non-covalent or even covalent imprinting, MIPs still suffer from some binding site heterogeneity. This is attributed to the difference in the outer sphere structure in the final polymer; this essentially means a difference in the binding sites accessibility. Moreover, these methods do not eliminate the heterogeneity arising from grinding, sieving, and the collapse of binding sites on template removal and solvent exchange (116).

Surface imprinting is a more convenient method to reduce the binding site accessibility problem. Since the binding sites are all oriented on the surface, this can reduce the difference in the outer sphere nature of the binding sites (116).

1.6.2. Template bleeding

After successful molecular imprinting, template removal should be attempted using a suitable solvent or reagent. In the case of inefficient template removal, some of the template molecules remain stuck to the MIPs' binding sites. Under these circumstances, the entrapped template molecules can be released later during the application of MIPs to their intended purpose in a phenomenon known as template bleeding or "template leakage". Template bleeding is another setback that significantly hinders the applications of MIPs in the field of sensors and chromatographic separations. This is because if the held template molecules are released during the sensing process, a false positive result can be obtained. Moreover, in the case of chromatographic separations, template bleeding can cause a poor chromatographic performance and possible contamination of the fractionated sample components (126,129).

There are some proposed solutions for the problem of template bleeding including isotope molecular imprinting, microwave assisted extraction or carrying out a blank extraction (130). However, among the best and most widely used solutions for the template bleeding problem is the dummy imprinting approach.

Dummy imprinting is a process that refers to the imprinting of a compound that is structurally similar to the target compound instead of the target itself. There are two types of dummy imprinting: firstly, fragment imprinting, which utilises a part of the target molecules as the dummy (131). Secondly, interval immobilisation imprinting, which utilises an entirely different compound than the target, however this compound has the same distance between two identical functional groups to the target compound (132). Using either of the dummy imprinting approaches, if template leakage occurs, it will have no significant effect on the result or the accuracy of the testing method. In addition, dummy imprinting is a very suitable alternative if the template is expensive, dangerous or unstable. Nevertheless, dummy imprinting is not always a viable solution, since finding suitable dummies is not always simple.

Combining solid phase imprinting with a dummy imprinting technique can introduce an excellent solution for the problem of template bleeding. However, the template release process can still be slow and some researchers presume that complete template removal in the case of proteins is almost impossible (133).

1.6.3. Imprinting of hydrophilic templates and application to aqueous media

The imprinting of hydrophilic and polar compounds poses a significant challenge due to their limited solubility in organic solvents which are favoured for molecular imprinting. Over the years, researchers have devised several effective strategies to manoeuvre this issue. One early approach involves the structural modification of the hydrophilic template molecule by introducing a hydrophobic alkyl chain, aiming to enhance its solubility in organic solvents (134). However, this method is time-consuming and may alter essential functional groups required for imprinting. Another strategy employs the use of a hydrophobic dummy as an alternative to the original target, though finding a suitable dummy can be challenging (134). A more straightforward and effective approach for imprinting hydrophilic templates involves utilising ion-pairs. This technique relies on forming an ion pair between the hydrophilic template and a surfactant, which is subsequently extracted through liquid-liquid extraction (LLE) using an organic solvent, allowing molecular imprinting to proceed as usual (135).

Addressing the imprinting of polar templates does not guarantee applicability in aqueous media, as MIPs developed in organic solvents may exhibit weak recognition in water or polar samples due to the disrupted hydrogen bonds. Micro liquid-liquid extraction emerges as a useful method for extracting template molecules from aqueous samples using a minimal amount of organic solvent, followed by loading the extracted target onto solid MIPs (136). Another approach involves the use of hydrophilic monomers, such as (hydroxyethyl)methacrylate or β-cyclodextrins, for synthesising MIPs compatible with aqueous media by using water as a porogenic solvent (137,138).

Alternatively, hydrophilic properties can be imparted to MIPs through surface modification, as demonstrated by R. Song et al., who prepared hydrophilic MIPs with an ultrathin hydrophilic shell for the detection of glutathione in aqueous media (139). Surface modification proves to be a highly effective and relatively straightforward method for enhancing the hydrophilicity of developed MIPs, expanding their applicability. Moreover, a recent trend in MIPs' synthesis involves the utilisation of green and natural polymeric materials, such as polysaccharides or gelatine. Polymers derived from natural materials exhibit excellent applications in aqueous media due to their inherent hydrophilic nature, along with advantages like low toxicity, biocompatibility, cost-effectiveness, and biodegradability (140). Studies by L. Xu et al. and X. Zheng et al. exemplify the successful preparation of hydrophilic MIPs using chitosan and gelatine as monomers, demonstrating their applicability in aqueous media for the selective binding of specific targets (141). In addition, X. Zheng et al. prepared MIP membranes for L-tyrosine via the use of gelatine and chitosan as monomers in polyethylene glycol as a porogenic solvent. The resultant MIP membranes showed high selectivity and permeability for targets and were suitable for use in aqueous media (142).

A specialised class of MIPs, created through a metal coordination bond between the template and the functional monomer, proves effective as well in polar solvents. The strength of the metal coordination bond prevents disruption by water molecules, unlike hydrogen bonds. For instance, 8-hydroxy-2'-deoxyguanosine MIPs were prepared using a metal coordination bond with methacryloylamidohistidine-platinum(II) as the metal chelating monomer, enabling their incorporation into a sensor for the detection of 8-hydroxy-2'-deoxyguanosine in aqueous samples (143).

1.6.4. Protein imprinting

The challenges presented by proteins as targets exceed the normal challenges encountered with other hydrophilic templates. The large molecular weight of proteins ranging from a few Daltons to thousands of kilo Daltons is considered a big difficulty in protein imprinting. The bulkiness of proteins makes it difficult for protein molecules to diffuse through the highly cross-linked polymeric structure of MIPs resulting in very slow binding and release kinetics. Moreover, the large molecular weight may also impede the efficient template removal after MIPs' synthesis causing the phenomenon of template bleeding or reducing the number of available binding sites. Furthermore, proteins have poor solubility in organic solvents, which are commonly used in molecular imprinting. Proteins are also sensitive by nature to the extreme conditions required for radical polymerisation, such as elevated temperatures and different pHs. Therefore, protein imprinting needs to be carried out in conditions, which are similar to their natural physiological conditions, not only to prevent their degradation but also to maintain their conformational integrity (126). In addition to the aforementioned difficulties, protein molecules themselves have different recognition sites on their surface including charged amino acids and hydrophilic or hydrophobic regions, that can increase the chance of MIPs reduced selectivity and cross-reactivity with any other protein molecules containing similar regions or charges (144).

Bulk polymerisation is considered the least popular choice for protein imprinting. This is attributed to the fact that proteins in solution have multiple conformational variations that can result in a very broad range of binding sites and non-selective binding.

Moreover, the use of polar porogenic solvents favourable for proteins can reduce the strength of hydrogen bonds between the template and monomer resulting in reduced binding efficiency (129).

To date, surface imprinting techniques are the most satisfactory for protein imprinting because binding sites are all located on the surface. The presence of the binding sites on the surface of MIPs eliminates the need for protein molecules to diffuse through the polymer network. Specifically, template immobilisation techniques including solid phase synthesis and micro contact imprinting are among the most used approaches for protein imprinting (145).

In order to solve the problems associated with protein imprinting, an epitope approach has been introduced in 2001 by Rachkov and Minoura (146). In this approach, a small peptide segment is driven from the big structure of the template protein (usually the C-terminal sequence) and used in the imprinting procedure. In this way, the produced MIPs will be able to recognise this sequence in the whole protein molecule with higher degree of selectivity and minimal non-specific binding. A sequence of no less than 9 amino acids is chosen from the C-terminal of a template protein. The reason for choosing the C-terminal is that it is less prone to post-translational modifications, which increases the chance of its recognition in a sample by the developed MIPs (146). The epitope approach is an attractive alternative for imprinting of bulky protein templates (such as immunoglobulins) that provides the advantages of selectivity, high affinity and sensitivity. Moreover, this method is very cost effective, since it avoids the use of highly pure proteins that might be very expensive.

Nevertheless, finding the suitable epitope for protein imprinting is a complex procedure and requires knowledge of protein conformations to predict the exact structure of the produced peptide segment (147–149). Another recent approach in epitope imprinting is the use of hidden or internal epitopes. This approach was introduced first by Bossi et al. in which the protein template is exposed to enzymatic digestion or heat denaturation to expose the hidden peptide sequences in its structure (150). Those epitopes are usually hidden inside the folded structure of the protein and less exposed to the surface interactions. Imprinting on the hidden epitopes increase the recognition of MIPs immensely since after denaturation these peptide sequences become exposed and specifically bind with MIPs without interference from the steric hindrance. The choice of the peptide sequence is usually an *in silico* procedure and requires careful study of the protein structure (150).

As mentioned before, a metal coordination bond is an effective way for molecular imprinting in aqueous media since the metal coordination bond is much stronger than the hydrogen bond and less affected by water. Besides, relying on the metal coordination bond ensures highly specific binding to the target protein and efficient binding in aqueous matrices such as blood. However, the use of metal coordination bond is limited to protein targets that contain exposed histidine residues on the surface, which are capable of forming such bonds (143,151).

Hydrogel MIPs are a class of MIPs prepared using hydrophilic monomers and low concentration of hydrophilic cross-linkers such as polyethylene glycol. The resulting MIPs are in a gel form and have relatively small, cross-linked structure.

Hence, hydrogels are considered a good alternative for protein imprinting, since the template can easily diffuse through the low cross-linked mass to their specific binding sites due to the high permeability (152,153).

A novel method for protein imprinting is to combine the template immobilisation technique with the use of a sacrificial support. Template proteins are immobilised on the surface of nano structured polymeric material such as alumina membranes, nanotubes, nanorods, or nanofilaments. This method combines the advantages of template immobilisation with the huge surface area provided through the use of nano materials. The large surface area enables easy and rapid access of template protein molecules to their target sites and therefore, rapid detectability and response that can be beneficial for the application to sensors (154–156). A summative diagram for challenges and solutions for protein imprinting is shown in **Figure 8**.
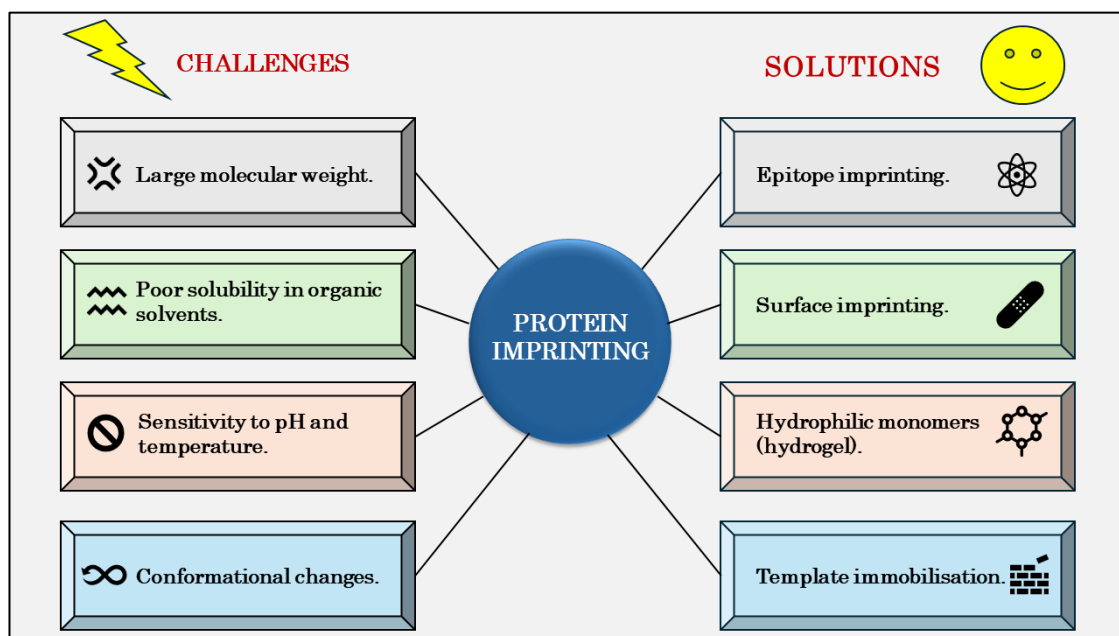
Figure 8. *Representative diagram of the challenges and the solutions for imprinting protein targets.*

1.7. Applications of molecularly imprinted polymers in different fields

1.7.1. Drug delivery (pharmaceutics)

Some researchers consider MIPs to be the future for a very selective and controlled drug delivery. The conventional polymer-based drug delivery systems suffer from some drawbacks the most famous of which is the bursting and sudden release of the drug due to the harsh surrounding conditions. MIPs can provide an alternative carrier system that excels the mundane polymeric materials in many aspects (157). Because of the high affinity of the designed MIPs to their target drug, they are able to provide a sustained and a slow drug release, which is highly desirable in the field of pharmacotherapy. Moreover, MIPs offer high drug loading capacity, increased stability against various harsh conditions, effective control over their cross-linked structure, and the ability to introduce magnetic or fluorescent labels to facilitate *in vitro* or *in vivo* testing and imaging (158).

To date, MIPs have been introduced in many pharmaceutical forms to overcome the problem of low bioavailability or to provide a controlled drug release. Soft contact lenses made of MIPs hydrogel were designed and introduced as an ophthalmic route of administration for glaucoma medications (159), as well as their applications in dermal and transdermal delivery of drugs such as propranolol (160). Furthermore, magnetic nanoMIPs were introduced as a smart intravenous route of administration of the anticancer drug 5-fluorouracil for breast cancer patients (161). MIPs are also useful in the oral route of administration since their high stability can prove effective against the different pHs encountered in the gastrointestinal tract.

For instance, MIPs were developed for the oral administration of the drug doxorubicin through the use of the biocompatible chitosan monomer (162).

However, the application of MIPs as drug delivery systems has some hurdles, such as the toxicity and biocompatibility issues encountered with some monomeric materials. In addition to the difficulty to ensure reproducible industrial scale synthesis and the need for complete pharmacokinetic and pharmacodynamics studies. However, these setbacks should be easily overcome by the continuous development and research (163).

1.7.2. MIPs as catalysts

There is an uncanny resemblance between the structure of MIPs and natural enzymes. It was that similarity that led researchers to investigate the potential use of MIPs as catalysts in variety of chemical or biochemical reactions. Catalytic MIPs can be imprinted on template analogues of the transition state of a specific reaction. Consequently, when these MIPs are introduced into the reaction, they can selectively bind to the transition state and stabilise it, and therefore decrease the activation energy required for the reaction (164). Alternatively, MIPs can be designed to selectively bind to the reactants or the products to be able to steer the reaction forwards or backwards. Another approach is to develop MIPs as selective carriers for metal NPs required to catalyse any reaction and that in turn facilitates their easy removal after completion (165). Collectively, the recent advances and applications of MIPs in the field of catalysis are illustrated in the review by S. Muratsugu et al. (166).

1.7.3. MIPs in chromatography and sample pre-treatment

In the realm of analytical chemistry, MIPs play an influential role, particularly in the domains of separation and sample extraction. Leveraging their remarkable selectivity and other advantageous properties, MIPs emerge as highly promising candidates for application as stationary phases in various chromatographic methods. The integration of MIPs' high affinity with the sophisticated technology of high-performance liquid chromatography (HPLC) represents a significant advancement in separation science. Diverse forms of MIPs, including NPs, monoliths, and spherical beads, have been harnessed as packing materials for columns employed in HPLC separations. A noteworthy example is the work of H. Xiao et al., who engineered surface-imprinted MIPs on silica microspheres utilising myricetin flavonoid as a template. These MIPs were then employed to pack a stainless-steel column, demonstrating exceptional efficiency and selectivity in the HPLC separation of myricetin from a mixture containing three other flavonoids (167).

MIPs are useful as well in racemic separations employing HPLC. Through tailoring and optimisation of MIPs' synthesis, scientists could create MIPs that are capable of separating different enantiomers of the same compound and apply them for HPLC separations. Enantioselective separation of phenylalanine enantiomers was achieved using MIPs developed via bulk polymerisation for the separation of L-phenylalanine in its racemic mixture (168). Another attempt for successful separation of racemic antihistaminic drugs using enantioselective MIPs beads was developed by suspension polymerisation method in aqueous media (169).

Through the high selectivity of the developed MIPs, two antihistaminic drugs: d-chlorpheniramine and d-brompheniramine were separated from their racemates. This is particularly important in the field of medicine due to the drastic difference in therapeutic efficacy between the two enantiomers of the same drug. More insights into the applications of MIPs in the field of chiral separations were introduced in some useful reviews (170,171). The sole cautionary note concerning the utilisation of MIPs in chromatography relates to the potential occurrence of peak tailing attributable to binding site heterogeneity. Hence, meticulous attention and caution are imperative during the synthesis and optimisation processes of MIPs designed for chromatographic purposes to mitigate this issue.

Sample extraction and purification is one of the most important steps required in almost all analytical procedures. SPE is a very common extraction technique used for complex samples such as blood and urine samples. It provides various advantages, some of which are high efficiency, rapid separation, reproducibility, and readiness for automation, especially in comparison with other extraction methods such as LLE. The application of MIPs as stationary phases inside the SPE cartridge added even more appealing qualities to SPE. The stability of MIPs made SPE suitable for samples with extreme pH values or those samples separated at elevated temperatures. In addition, MIPs are highly effective in the presence of organic solvents usually used to elute the samples. Furthermore, the cost effectiveness and easy procedure of MIPs' synthesis can contribute to reducing the cost of SPE cartridges (172).

An extensive literature search revealed over 350 publications utilising MIPs in the field of SPE, which emphasises the great role played by MIPs in the field of analytes' extraction. Regarding medical applications, one of many examples includes application of a MIPs SPE cartridge to extract and detect cotinine alkaloid. Cotinine can be used as a biomarker of nicotine exposure in both active and passive smokers. Researchers in this work were able to develop a SPE cartridge specific for cotinine that was easy to use, quick and reusable to extract cotinine from saliva of smokers (173). MIPs SPE is also very helpful in the field of food analysis; a group of researchers were able to combine a core shell imprinting technique with a dummy imprinting approach to create magnetic MIPs SPE specific for aminopyralid herbicide (174). Picloram was used as a dummy and molecular imprinting was carried out on the surface of carboxyl and amino functionalised magnetite particles. The developed MIPs SPE cartridge was able to extract aminopyralid in milk samples to be further analysed by liquid chromatography – mass spectrometry (LC-MS). In the scope of forensic analysis, MIPs also left a fingerprint. T. Murakami et al. developed MIPs SPE system for extraction of the addictive cathinones from blood and urine samples. The recovery of drugs using MIPs SPE was found to be higher than the conventional SPE and LLE, which is a solid proof for their efficacy in this field (174).

The offline SPE approach used in the aforementioned examples is relatively easy and flexible. However, it consumes a significant amount of solvent, and samples are prone to contamination prior to being analysed, therefore the online SPE systems are more favourable. In the online approach, analytes separated with SPE are automatically introduced into an analytical instrument such as HPLC or GC for further quantitative analysis.

A recent example is reported for the extraction and quantitation of the mycotoxin patulin (175). Herein, researchers developed surface imprinted MIPs for the extraction and pre-concentration of trace amounts of patulin in fruit derivatives via SPE. Following the extraction, samples were automatically loaded into HPLC column for analysis. The online approach here was very useful, since the concentration of target is very low. Moreover, no possible contamination of the analyte could have happened, since the samples were directly injected into the HPLC system with no need for an operator (175). More in-depth insights and critical review of the application of molecular imprinting into SPE is introduced in this review (96)

Collectively, MIPs find their widest applications in the area of analysis, however they are a more popular choice for sample pre-treatment to extract the target analytes prior to their quantitation.

1.7.4. MIPs in the field of sensors and biosensors

A sensor is defined as a device that measures a specific chemical or physical reaction and produces a certain signal that is corresponding to the concentration of the analyte involved in this reaction. In case the analyte is a biological molecule, the device is called a biosensor (176). There are three main elements in the structure of any sensor namely, the analyte, which is the target molecule that needs to be detected or quantified, the bioreceptor, which is responsible for selective binding of the target molecules in the sample and the production of a signal in different possible forms (light, pH change, or charge change, etc.).

Finally, there is the transducer, which is responsible for converting the resultant signal from the binding event into a measurable signal proportional to the concentration of target and can be displayed as readable units (176).

From this brief explanation about the nature of sensors and their structure, it can be clearly seen where MIPs can fit in. For the past decades, natural molecules such as antibodies or enzymes have been used as the bioreceptor as in the case with ELISA. However, due to the great advantages offered by MIPs over natural antibodies, MIPs are now leading the race in the field of sensing and biosensing.

The first type of MIPs that can be useful in the field of sensing is the fluorescent MIPs. Utilising this type of MIPs in a sensor device can translate the change in fluorescence that happens upon binding of the target to give a signal proportional to the analyte concentration. T. Zhou et al. developed a fluorescent nano-sensor for the detection and quantitation of the antibiotic tetracycline (177). Researchers prepared fluorescent core shell imprinted polymers on the surface of graphene QDs. The binding of these MIPs to tetracycline caused fluorescence quenching, which was proportional to tetracycline's concentration. Moreover, the authors applied the developed sensor to measure tetracycline in real milk samples and recovery percentages were promising, which in turn points out the great potential for MIPs in this field (177). The same sensor principle was also applied to larger targets including proteins such as lysozyme as a biomarker for cancer and the produced sensor revealed high efficacy and applicability in complex biological samples (178). Most of the recent applications of fluorescent MIPs in the field of sensing have been summarised in a review (179).

Electrochemical sensing is also a highly explored type of sensors in which the binding event translates into an electrochemical signal. MIPs labelled with a redox probe are utilised in electrochemical sensing of different analytes. The selective binding of the target causes conformational changes in the structure of MIPs, which are transformed into an electric current, thereby the concentration of target can be measured via different electrochemical methods (180). Nevertheless, the efficiency and accuracy of electrochemical MIPs based sensors are sometimes limited by the weak electrochemical conductivity of the cross-linked structure of MIPs. Consequently, Y. Li and his group prepared a smart type of MIPs imprinted on magnetite nanobeads and gold NPs to be deposited on a reduced graphene oxide electrode (181). The combination of reduced graphene oxide and metal nano particles was an excellent strategy to boost the response current and increase the sensor's efficiency. The developed sensor was used to detect ractopamine analyte in water samples with very high sensitivity using CV and EIS techniques (181). Progress and perspectives of MIPs in electrochemical sensing are discussed in detail in this review (182).

Capacitive sensors are a type of affinity sensors, which measures the change in dielectric properties (capacitance) upon binding of the target. N. V. Beloglazovaa et al. prepared a capacitive biosensor combined with MIPs for benzo(a)pyrene detection in water samples (183). MIPs were prepared using two different polymerisation techniques, the first produced MIPs beads, which were covalently coupled to the electrode, the other method involved *in situ* synthesis and deposition of MIPs on the electrode surface. The performance of the two types of MIPs as bioreceptors was compared to each other and to natural antibodies.

The results of the study showed that the latter approach of MIPs' synthesis provided better results compared to MIPs beads. In addition, sensors prepared using antibodies had a wider linear range, yet MIPs sensors showed higher stability and reusability (183). Another capacitive biosensor was prepared by electro-polymerisation of the naturally derived compound resorcinol to prepare polyresorcinol MIPs for the antibiotic sulphanilamide. The prepared sensor was applied to detect and quantify sulphanilamide in milk, tap water and drinking water with no need for pre-concentration steps (184).

A state-of-the-art technique for sensing that is increasingly applied nowadays is surface plasmon resonance (SPR). SPR is a type of optical sensor that depends on measuring the angle of reflection of a polarised light beam off an electrode surface separating two media. Usually, bioreceptors are immobilised on the other side of the electrode, which upon binding of the target analyte produces a change in the angle of reflection that can be directly correlated to the concentration of the analyte (185). Combining MIPs with a very sensitive technique such as SPR is very valuable in the field of analytical chemistry and microanalysis. A MIP SPR biosensor was prepared for detection and quantification of iron regulating hormone hepcidin. The sensitivity of the biosensor reached a remarkable picomolar range, which is very useful in testing real samples (186). Another SPR MIPs based sensor was developed for the analysis of amoxicillin antibiotic. The developed MIPs were coupled to two sensing techniques: SPR and QCM Although the SPR method showed a higher limit of quantitation, both methods were effectively applied to detect and quantify amoxicillin in real egg samples (187). This cited review discusses further data on MIPs coupled to SPR and other optical techniques in the field of biosensing (188).

Finally, an acoustic wave sensor is a type of mechanical sensor, which employs a piezoelectric material such as quartz to generate the acoustic wave by alternating current induced oscillation. These sensors are sensitive to mass changes occurring on its surface as well as the change in the physicochemical environment (189). Coupling of MIPs to surface acoustic sensors is very advantageous in the sensing field, especially after the recent application of acoustic sensors in liquid media. MIPs deposited as films on acoustic sensors such as QCM (190) or the higher frequency and higher sensitivity LOVE wave sensor have created a very useful and sensitive class of sensors for different target analytes (191).

Eventually, the future for MIPs' applications is coupling it to cutting edge sensing technologies. Sensors are needed now more than ever to provide rapid, sensitive, and onsite detection of different chemicals and biomolecules. Miniaturised sensors provide the basis for lab on chip or portable reactors that can be used anywhere to provide reliable results in the fields of medicine, forensics, food and environmental analysis.

Subchapter II. Biomarkers

1.1. Definition

The term "Biomarker" is short for a "biological marker", which can be defined as any substance found in the body (gene, protein, or polysaccharide etc.) that can be of medical or biological significance. This substance can be a part of a normal physiological process or a biochemical pathway or be a result of abnormal pathological condition (192). Pathological conditions can either generate whole new molecules into the body or cause a notable decrease or increase in naturally occurring molecules in which case their concentration itself is the biomarker. According to this description, biomarkers are like signals that give us insightful information about what is going on inside the body with minimal interference and less effort. These signals can also be warnings that a medical condition is evolving, which in turn provides us with a good diagnostic tool that enables early treatment of the condition, hence saving lives (193).

1.2. Classification of biomarkers

Biomarkers are categorised in various ways. The first classification distinguishes between imaging and non-imaging biomarkers. Imaging biomarkers are obtained through techniques like X-rays, positron emission tomography scans, and magnetic resonance imaging. While non-imaging biomarkers are measurable molecules with biophysical properties found in body fluids or tissues (192). Another classification is based on their nature, encompassing genetic biomarkers such as DNA, RNA, or specific gene mutations, as well as protein biomarkers with sizes ranging from a few Daltons to several thousand Daltons (e.g., immunoglobulins). Additionally, biomarkers can be specific entities like polysaccharides, glycans, or glycoproteins.

Further classification is according to their applications: diagnostic biomarkers which detect specific diseases, antecedent biomarkers which identify individuals at high risk of a particular disease, disease prognosis biomarkers which monitor the prognosis of conditions like cancers, and therapeutic drug monitoring biomarkers which determine the effectiveness of drugs or the need for dose adjustments based on the discovered biomarkers (194).

1.3.   Benefits of biomarkers in different fields

In addition, to their diagnostic role, biomarkers are very beneficial in the field of pharmacy and drug development. Analysing patients' and volunteers' biomarkers can predict who will respond better to a certain drug from efficacy and safety perspectives. This can determine the efficiency of newly discovered drugs, and help reduce the expenses and time of clinical trials (195).

Biomarkers also play an important role in studying the effects of environmental pollution. Pollution biomarkers are defined as quantitative measure of the alterations that happen to a biological system compared to its normal status after exposure to a specific pollutant (196). Exposure to different environmental pollutants such as heavy metals and toxic gases can result in significant changes in certain physiological processes in the body. The early detection of these variations is useful as sensitive warnings of environmental hazards, before they become on a population scale (196).

Pollution biomarkers vary in specificity; some processes are very specific such as aminolevulinic acid dehydratase mediated inhibition that is triggered by exposure to lead, and some are not so specific such as DNA damage or mutations, which indicate exposure to many pollutants. In this case, analysing biomarkers can give us an idea of what kind of pollutant is involved (196).

1.4. Pros and cons of biomarker analysis

The analysis of biomarkers has many advantages that makes it one of the most important topics of research nowadays. The biomarker research services market size is expected to reach 18.2 billion dollars globally by 2026, which proves that biomarker research is a promising field of study (197).

Versatility of biomarkers is also a very good advantage; as more than one biomarker may be found per one medical condition, which can give more confidence about the diagnosis. Another advantage is the high selectivity, as most of the biomarkers usually signal a specific condition with a high degree of precision. Other beneficial merits include reproducibility and their presence in different body fluids and tissues, which enables easy extraction with no need for invasive procedures (192). On the other hand, there are some challenges associated with the analysis of biomarkers, where the most common problem is cross-reaction. Cross-reaction happens when the applied analytical method gives a false positive result for a structurally or physically similar molecule. This problem mainly happens due to the poor selectivity of the analytical method. Another challenge is that some of these biomarkers exist in very low concentration in body fluids that makes their extraction and analysis extremely difficult.

This problem urges the development of very sensitive extraction and analytical methods for their detection. Moreover, a common challenge faced in biomarkers discovery is the low number of case studies involved in the early stages of a particular disease, since the early stages are mostly asymptomatic resulting in delayed diagnosis (198,199).

1.5. Common methods for the analysis of biomarkers

Various analytical tools are employed to analyse and quantify molecular biomarkers in the body. Each analytical method offers specific advantages and disadvantages depending on the biomarker and its concentration in the sample. The widely used ELISA has been the most popular analytical technique, yet it has its limitations. ELISA may yield false positive results in the presence of ineffective blocking solutions or false negatives when the target concentration is too low. Moreover, the multistep sample preparation, dilution, and washing processes in ELISA introduce a potential for errors and require skilled personnel. Antibody instability and the need for low storage temperatures further complicate its application. While sandwich and competitive ELISA types provide high sensitivity, they tend to be costly (200,201).

Other methods for biomarker analysis include various chromatographic techniques like LC-MS (202), thin layer chromatography (203), gas chromatography (204), and gel electrophoresis (204). However, many chromatographic assays face limitations when applied directly to complex sample matrices like blood or urine. To overcome this challenge, the target biomarker needs to be extracted first before quantification using the chromatographic method (205).

Promisingly, MIPs have emerged as effective sorbent materials for selective biomarker extraction. MIPs can be customised to target a specific biomarker, offering high selectivity in extracting it from complex matrices. This innovative approach holds potential for enhancing the precision and reliability of biomarker analysis (206).

1.6.   Medically useful biomarkers

Protein molecules by far are the most common biomarkers since they are found in a plethora of locations in the human body. Different protein molecules, peptides, or single amino acids can signal a variety of diseases or cancer types. Protein biomarkers are also present mostly in relatively high concentration, which makes their extraction and detection more convenient (207). For example, oestrogen receptor, progesterone receptor and human epidermal growth factor receptor 2 are types of tissue-based protein biomarkers (208). These tissue biomarkers have been used for years to monitor the course of treatment of breast cancer. DX 21-gene panel is also a useful biomarker to predict the risk of breast cancer recurrence and the potential benefit of chemotherapy (208). The intracellular coenzymes NAD(P)H and FAD are involved in all intracellular metabolic pathways by oxidation and reduction reactions. Therefore, they are useful biomarkers for detection of metabolic dysfunctions that happen on the intracellular level and are main causes for many diseases such as diabetes. In addition, these coenzymes are fluorescent by nature, therefore they can be easily scanned without the need for sample pretreatment procedures (209).

The identification of specific mutations in certain proteins such as receptors or enzymes can also help to detect or understand the cause of certain disorders or to target therapy to these specific proteins.

For example, according to P. Villalobos et al., epidermal growth factor receptor mutations and anaplastic lymphoma kinase enzyme translocations are promising and novel biomarkers for targeted molecular level therapies in a group of patients suffering from lung cancer (210).

1.6.1. Pepsin as a medically useful biomarker for gastroesophageal reflux disease

Pepsin, an enzyme originating from the stomach, plays a pivotal role in protein digestion by catalysing the hydrolysis of larger protein molecules into smaller peptides (211). Its importance extends beyond the area of digestion, particularly in the context of gastroesophageal reflux disease (GERD). GERD is a prevalent gastrointestinal disorder characterised by the regurgitation of stomach contents into the oesophagus, leading to irritation and, in severe cases, potential damage to the oesophageal lining. GERD is also a very common disorder occurring in over 20% of the world's population (212). Pepsin, being an intrinsic component of gastric juice, becomes a notable biomarker in the context of GERD. When reflux occurs, pepsin may travel beyond its typical anatomical confines, presenting itself in the saliva (211).

Elevated levels of pepsin in the saliva were significantly associated with GERD, where it serves as a reliable biomarker. Monitoring and quantifying pepsin levels in these samples provide clinicians with a valuable diagnostic tool for assessing the extent and severity of GERD. This diagnostic approach aids in the early identification and management of GERD, allowing healthcare professionals to tailor appropriate interventions and treatments to mitigate the impact of this prevalent gastrointestinal condition (213,214). To date, the main method of measuring the level of pepsin and diagnosis of GERD is the Peptest® which is an ELISA method utilising antibodies (215).

Pepsin possesses a molecular weight of approximately 34,000 Da and belongs to the aspartic protease family. It is biosynthesised in an inactive precursor form known as pepsinogen, which undergoes activation in the acidic environment of the stomach to form the active pepsin enzyme as illustrated in **Figure 9** (211). The mature pepsin enzyme exhibits a unique structure with two symmetrical lobes connected by a hinge region.
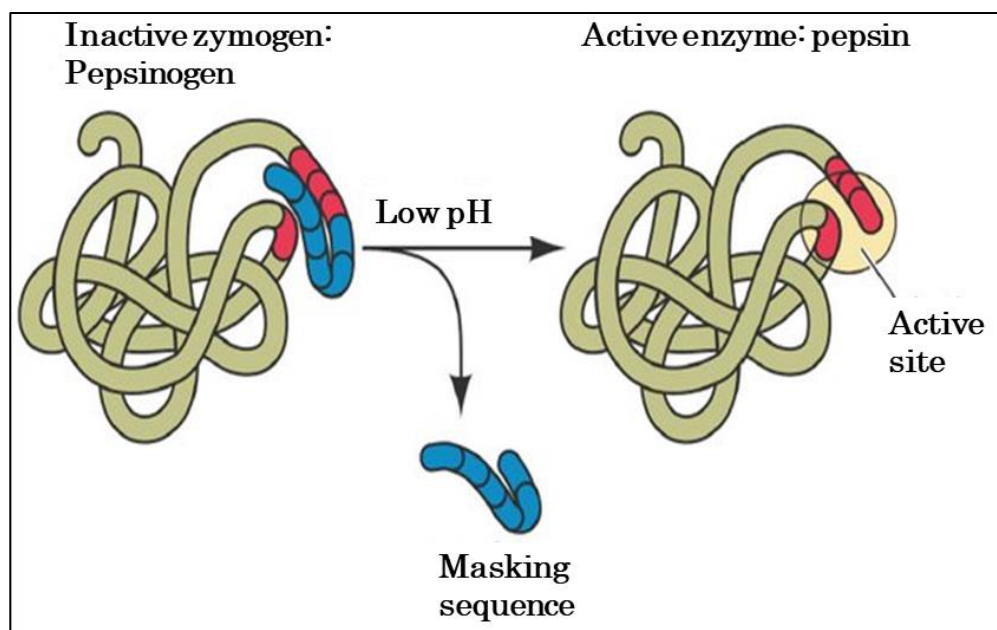
Figure 9. Activation of pepsinogen to pepsin at low pH in the stomach (211).

Pepsin's physicochemical parameters play a crucial role in its functionality, with an isoelectric point around pH 1.3, highlighting its optimal activity in the highly acidic conditions of the gastric environment. Pepsin demonstrates specificity for hydrolysing peptide bonds in proteins, particularly favouring aromatic and hydrophobic amino acids.

Understanding these molecular features, including molecular weight, isoelectric point, and pK$_a$ values, contributes to a comprehensive grasp of pepsin's role in digestion and its significance as a biomarker in various physiological and pathological conditions (216).

1.6.1.2. Analytical methods for detection and quantitation of pepsin

A review of the literature reveals very few methods for the analysis of pepsin. In comparison, pepsin is mainly utilised as an enzyme to digest other protein samples prior to analysis especially by LC-MS (217,218). One online immunoaffinity LC-MS method for the analysis of pepsin was found that goes back to 2010 (219). In this method, pepsin enzyme is cleaved using another digestive enzyme called endoproteinase AspN which can cleave proteins at aspartic acid residues that are frequent in the pepsin molecule. This cleavage would generate more target peptides for selective reaction monitoring mode in LC-MS analysis. The authors used immunoaffinity column for the enrichment of pepsin fragments before detection. Despite the complexity of the method and the multiple preparation steps, the detection limit reached picomolar range (219).

Another method for detection and quantitation of pepsin employs a molecular imprinting technique, more specifically magnetic MIPs in an ELISA format while applying fluorescent polystyrene beads (PSB) as labels (220). The principle of the method depended on immobilisation of the developed magnetic MIPs to the walls of the wells of a microtitre plate via magnetic inserts. The sample solution containing pepsin was mixed with PSB and subsequently pepsin was adsorbed onto their surface by hydrophobic interactions.

Afterwards, this solution was added to the wells and pepsin with the adsorbed PSB bound with the magnetic MIPs resulting in a corresponding decrease in central fluorescence of the solution in the wells. The advantages of this method included the use of MIPs instead of the conventional antibodies and the use of PSB instead of the enzyme label (220). Moreover, there was no need for a washing step after the addition of sample solution. Nonetheless, this method suffered from various drawbacks that needed to be addressed. Firstly, the authors mentioned that a very high concentration of target protein could saturate MIPs' binding sites as well as PSB leading to a reduced amount of PSB drawn to the magnetic inserts. Therefore, it was necessary to carry out a binding isotherm study to determine the maximum concentration of pepsin that MIPs could bind to, to avoid such an issue, yet this study was not presented. Secondly, MIPs' synthesis utilised three different functional monomers, which can increase non-specific interactions and binding sites heterogeneity through side reactions. However, the rationale for using three different monomers was not mentioned, nor why they were used in these ratios. Thirdly, an elucidation of the functional groups of pepsin involved in the binding with MIPs or PSB should have been included to verify that the hydrophobic binding with PSB did not adversely affect binding with MIPs. In addition, if PSB caused conformational changes to the structure of pepsin, this might result in total loss of binding selectivity. Finally, the authors mentioned they switched blue PSB to red PSB when applying the method to synthetic gastric fluid due to the effect of hydrochloric acid on binding with blue PSB and reduced sensitivity. However, the question is why did they not use red PSB from the start, especially given that all the optimisation studies were carried out using blue PSB?

Despite the promising approach used in this method, it lacked some fundamental elucidations and experiments to verify its usefulness (220).

A very recent method that adopted the same principle of an ELISA format was found. This method also adopted the use of microtiter plate modified with magnetic inserts which were used to immobilise pepsin that was covalently bound to magnetic iron (II, III) oxide nanoparticles. However, instead of using PSB, fluorescent MIPs for pepsin were used as labels. Herein, upon the addition of free pepsin in sample solution followed by addition of fluorescent MIPs a competitive binding between magnetic pepsin and free pepsin on the MIPs' binding sites occurs. As a result, fluorescence in the centre of the well is noticed which is used for detection of pepsin. This method opens the door for more abiotic detection methods which are cheap, stable and can be used more than once without the need for experience and with minimal errors. However, there was no application in this work for the detection of pepsin in saliva or gastric fluid and no detailed optimisation profile (221).

In 2013, MIPs were developed by the mini emulsion imprinting technique for binding of pepsin. The authors in this paper claimed the application of surface imprinting technique to make all the binding sites on the surface (222). However, surface imprinting technique necessitates the use of solid support, either nanoparticles, glass slides, or monoliths (223). In this paper, there was no use of any solid support, that makes this method only a mini emulsion imprinting technique which depends on the use of surfactant and ultrasonic waves to disperse the polymerisation mixture into fine droplets into the continuous phase.

The application of this type of polymerisation resulted in a very small particle size as illustrated by the authors (400 – 600 nm) and increased surface area available for binding (30 – 65 m^2). Nonetheless, this paper lacked a complete optimisation profile for all the elements involved in the synthesis procedure, where the authors only tested four monomers to choose the optimum one.

There was no optimisation for the cross-linkers, initiators, porogens and other factors that can affect imprinting (222). Later in 2015, the same authors published another paper showing some in-depth binding assays to highlight the binding performance of their developed polymers, yet still, an optimisation profile was missing. Moreover, there was no application to biological samples to indicate their suitability and applicability as extraction media (224). A summary of the key features of the molecular imprinting methods for pepsin is presented in **Table 1**.

Table 1. *Summary of the MIPs prepared for pepsin from the literature search.*

Technique of polymerisation	Composition of MIPs monomer, cross-linker, initiator, porogenic solvent	LOD	Applications	Ref. and year
-Solid phase synthesis on glass beads with magnetic element.	N-tert-butylacrylamide & NIPAm & N-(3-aminopropyl) methacrylamide hydrochloride & AA, MBA, TEMED & APS, water.	Not mentioned.	Microplate-based assay equipped with magnetic inserts and polystyrene beads used as fluorescent coloured label for detection of pepsin with application to synthetic gastric juice samples.	(220) 2018.
-Solid phase synthesis on glass beads with a fluorescent monomer. -Post-imprinting modification with fluorescent dye.	-NIPAm, AA & N-tert-butylacrylamide, MBA, TEMED & APS, water & EtOH. -same composition followed by modification with Fluor® 647 NHS ester.	1 µmol L^{-1}.	MINA abiotic assay for the detection and measurement of pepsin with no application in biological fluids.	(221) 2022.
-Mini-emulsion polymerisation.	2-Aminoethyl methacry- late hydrochloride, (3-acrylamidopropyl)trimethy- lammonium chloride & EGDMA, Lutensol AT50 (surfactant) & AIBN.	Not mentioned.	Binding of pepsin. No quantitation or application to biological fluid.	(222)(224) 2013.

Subchapter III. Hypothesis and thesis rationale

Protein biomarkers are the most common biomarkers in the human body, and they signal multiple types of disorders including cancer, infections, inflammations and others. During the literature search, the majority of research was found to be focused on cancer biomarkers due to their significance and contribution to a non-invasive diagnosis to patients who are suffering from this terrible disease. However, much less research was oriented in other biomarkers which are also important to help other groups of patients. Pepsin enzyme was one of those biomarkers that had very little research focused on its analysis as a biomarker for GERD.

Pepsin is normally present in the stomach as a digestive enzyme for proteins, nevertheless, due to the reflux in patients with GERD, some of the pepsin is regurgitated to the mouth resulting in significant increase in its salivary concentration. However, due to the complex nature of the human saliva and the presence of other salivary enzymes, it was necessary to come up with a highly selective extraction method to ensure complete and selective extraction of pepsin prior to its analysis.

Based on the previous, pepsin enzyme was chosen as the target of this project to achieve the following aims:

- Develop, optimise, and characterise new magnetic MIPs for the selective binding, extraction, and the following release of pepsin in solutions and in human saliva samples (Chapter 2, subchapter I).

- Devise, optimise, and validate a highly sensitive, simple, and novel HPLC method for the detection and quantitation of the pepsin fractions extracted via the magnetic MIPs to build an integrated diagnostic system (Chapter2, subchapter II).

- Develop new fluorescent MIPs for the simultaneous extraction and quantitation of pepsin enzyme. Therein, the highly selective binding sites would capture pepsin enzyme followed by quenching of some of the fluorescence in a concentration dependent fashion (Chapter 3).

- Compare the utilisation of both fluorescein isothiocyanate and rhodamine isothiocyanate as fluorescent dyes in the development of the fluorescent MIPs in terms of binding efficiency, selectivity, and sensitivity and introduction of a possible structure-based explanation to the difference in their binding to pepsin enzyme (Chapter 3).

- Manufacture a new fluorescent membrane for the selective binding and detection of pepsin enzyme using fluorescent carbon dots integrated in its matrix. Furthermore, exploration of the effect of binding of pepsin enzyme to the fluorescent membrane as an indicator switch for the simple and rapid detection of pepsin in any specimen (Chapter 4).

- Utilise dopamine as a self-polymerising monomer for the development of surface imprinted MIPs on silica nanoparticles for pepsin enzyme. In addition, exploration of the possible hurdles, challenges, and literature-based explanations to the alleged high selectivity of dopamine MIPs (Chapter 5).

- Provide general conclusions on the work done in this thesis, showcasing advantages, challenges, potential applications, recommendations, and future plans (Chapter 6).

Finally, it was a challenge, involving exhaustive effort to develop, optimise, characterise, and test all the developed MIPs. Therefore, a specified workflow was followed to achieve the desired aims smoothly, as shown in **Figure 10**.

Figure 10. Workflow of the thesis project.

Chapter 2

Development of Magnetic MIPs for

The Extraction of Pepsin Enzyme Prior

to HPLC-SEC Analysis

Chapter 2 was published in Polymer journal.

Chapter 2. Development of magnetic MIPs for the extraction of pepsin enzyme prior to HPLC-SEC analysis
Subchapter I. Development of magnetic MIPs

2.1. Background

Magnetic MIPs represent a specialised class of materials that combines the advantages of molecular imprinting technology with the magnetic properties of iron oxide nanoparticles. The incorporation of magnetic nanoparticles into MIPs enhances their separation and retrieval capabilities using only a strong magnet, eliminating the need for centrifuge or filters. Therefore, they are ideal candidates for targets that normally exist in complex matrices such as blood, urine, or saliva. As a result, magnetic MIPs simplify the sample preparation process in analytical applications (225).

Magnetic MIPs are prepared utilising the surface imprinting technique that was mentioned earlier in chapter 1, under section 1.4.6, where the polymerisation is conducted on the surface of iron oxide nanoparticles (magnetite). This in turn creates a thin layer of polymer that contains multiple binding sites for the target molecule (225,226).

In the context of protein targets recognition, magnetic MIPs offer distinct appealing features. Due to the application of surface imprinting technique, all the binding sites are localised on the surface of the particles allowing easy binding and release. The rapid binding and release kinetics in addition to the high selectivity are important in many fields including bio separation, biosensing, and targeted drug delivery (227).

Protein-imprinted magnetic MIPs find applications in sample preparation and purification, where they can selectively extract and isolate target proteins from complex biological samples. This is particularly valuable in proteomic studies and diagnostic applications. Moreover, they can serve as the recognition element in biosensors, contributing to the development of highly selective and sensitive protein detection platforms (228).

In recent years, research efforts have been directed toward optimising magnetic MIPs for various proteins, including antibodies and biomolecules and herein, it is taken to the world of enzymes, more specifically pepsin enzyme.

2.2. Advantages offered by magnetic MIPs for the extraction of protein targets

MIPs have risen as an alternative tool to classical antibody testing commonly used for diagnostic purposes. Magnetic MIPs specifically have offered extra benefits making them ideal for protein targets. Among the many advantages offered by magnetic MIPs the most important are:

- Enhanced Sample Preparation.

The incorporation of magnetic nanoparticles enables the easy separation of magnetic MIPs from the sample matrix using an external magnetic field. This not only streamlines the sample preparation workflow but also enhances the overall efficiency of protein analysis (225).

- Reusable and Cost-Effective.

The magnetic nature facilitates their easy recovery and reuse. After capturing the target proteins, magnetic MIPs can be quickly separated from the sample matrix using a magnet, allowing for multiple uses without significant loss of binding efficiency. This reusability not only makes magnetic MIPs cost-effective but also reduces waste, contributing to environmentally friendly analytical practices (229).

- Biocompatibility and Biomedical Applications.

Magnetic MIPs exhibit excellent biocompatibility, making them suitable for applications in the biomedical field. They can be employed in targeted drug delivery systems, where the selective recognition of specific proteins ensures the efficient delivery of therapeutic agents (230).

2.3. Methods applied for the synthesis of magnetic nanoparticles employed in the synthesis of magnetic MIPs

2.3.1. Co-precipitation method

Co-precipitation method involves introducing an alkaline substance into an aqueous solution containing Fe^{2+}/Fe^{3+} salts under an inert atmosphere, resulting in the formation of iron oxide nanoparticles through a precipitation reaction. This method offers a well-controlled preparation process with advantages such as low production costs, a brief production cycle, and minimal environmental impact (231). The adjustment of key experimental parameters, including the ratio of iron (II) and iron (III) salts, pH, temperature, reaction time, and ionic strength, plays a crucial role in synthesising iron oxide nanoparticles with controllable shape, size, and morphology.

Higher concentrations of the iron (II) precursor can lead to the formation of numerous seeds, thereby increasing the yield of smaller nanoparticles. Increasing ionic strength in the system slows down growth and nucleation rates, favouring the production of smaller nanoparticles. Additionally, the incorporation of stabilising agents, such as chelating organic anions (citrate, glucose, oleic acid) and polymer surface complexing agents (chitosan, carboxylated chitosan, starch, polyethylene glycol), helps prevent agglomeration (232,233).

2.3.2. Solvothermal method

The Solvothermal method involves sealing the reaction media in a special reactor (autoclaves) to create a high-temperature and high-pressure environment for the synthesis of magnetite nanoparticles. This method, categorised as hydrothermal or organic solvothermal synthesis based on the solvent type, promotes rapid convection of the solvent and active diffusion of solutes. These conditions enhance the formation of nanoparticles with a narrow size distribution, uniform morphology, and improved dispersion properties. Careful consideration of the reaction factors, such as the type and amount of iron source, solvent, temperature, and time, is crucial for achieving a high-quality final product (234).

2.3.3. Microemulsion method

The microemulsion route involves obtaining magnetite nanoparticles through reactions confined to a water-in-oil or oil-in-water microemulsion stabilising system. This system is created by mixing a surfactant, an oil phase, a water phase, and a co-solvent in correct proportions which prevents aggregation due to surfactant coating.

The nucleation process can be controlled by adjusting the microemulsion volume. Despite its applicability in preparing various magnetite nanoparticles, the resulting material from microemulsion approaches may have drawbacks like poor crystal quality, low magnetisation, and small output due to the low reaction temperature, limiting its range of applications (235).

2.3.4. Sol-gel synthesis

The sol-gel method is a vital technique for producing materials such as inorganic nanoparticles at room temperature through a wet chemical process. In this procedure, a chelator and other solvents are added to an aqueous solution or alkoxide containing Fe^{3+}; subsequently, stable, and uniform sol (nucleation) of metal oxides or metal hydroxides occurs through hydrolysis reaction and condensation polymerisation. As the reaction progresses, the particles gradually grow, forming a three-dimensional network gel (aging) in the liquid phase. Further heating and drying treatments are necessary to obtain monodisperse magnetite nanoparticles (236).

2.4. Aims and Objectives of this work

For the past decades, antibodies have been the main method used for the diagnosis and binding of different biological targets. This is mainly due to the high selectivity of antibodies and lack of synthetic alternatives. However, multiple misdiagnosis incidents have occurred over the years due to the interference from cross-reactors or false readings in addition to their high cost of production (237).

Over the literature survey, only two studies have been found describing the synthesis of magnetic MIPs for pepsin which were covered in chapter 1, subchapter II, section 1.6.1.2.

The multiple drawbacks of these methods were discussed which included the lack of optimisation profiles and actual applications on biological samples. Therefore, the aims of this work were:

- Development of new magnetic MIPs for pepsin enzyme using cheap, green, and affordable starting materials.

- Optimisation of all the reagents involved in the synthesis procedure to achieve the highest possible selectivity.

- Characterisation of the resulting magnetic MIPs on all aspects including morphology, functionality, thermal stability and binding characteristics.

- Assessment of the reproducibility and reusability of the developed magnetic MIPs to verify their cost effectiveness.

- Application of the resulting magnetic MIPs for the extraction of pepsin from solutions and saliva samples.

2.5. Anticipated challenges

As mentioned before in the introduction, imprinting of protein presents its own set of problems. Pepsin is a 34.5 kDa protein that is only soluble in water and aqueous buffers. Therefore, the imprinting, binding and analysis had to be conducted in aqueous media. Moreover, the pH of the solution had to be maintained at the pH range of the human saliva (6.2-7.6) with 6.7 being the average (238). This is crucial to avoid any change in the conformation of the protein and hence a weakened binding to the developed MIPs. Imprinting in water is difficult due to the predicted competition between water molecules and the target on the hydrogen bonds with the monomer.

Therefore, meticulous optimisation was necessary to minimise this problem as much as possible. The cost effectiveness was one of the main concerns in developing the magnetic MIPs. Therefore, it was important to choose affordable yet effective starting materials for the polymerisation in order to make the resulting MIPs more economic than antibodies.

Finally, due to the large size of the protein molecule, there was a concern about the efficient template removal and rebinding within an acceptable time frame to make the developed MIPs user friendly and time efficient. As a result, the washing step for the resulting MIPs was carefully optimised to achieve the best possible template removal and the conditions for rebinding were prudently studied as well.

2.6. Experimental

2.6.1. Materials and Instrumentation

Methacrylic acid 99% (MAA), acrylamide 99% (Am), acrylic acid 99% (AA), N-isopropylacrylamide (NIPAm) 99%, N,N'-methylenebisacrylamide 99% (MBA), ethylene glycol dimethacrylate 98% (EGDMA), phosphate-buffered saline tablets (PBS), glacial acetic acid 99%, hydrochloric acid 36%, ammonium persulphate 98% (APS), N,N,N',N'-tetramethylethylenediamine 99.5% (TEMED), phosphate buffered saline tablets (PBS), N,N-dimethylformamide 99.8%, maleic anhydride, and tetraethyl orthosilicate for synthesis (TEOS) were all purchased from Sigma-Aldrich, UK.

Deionised water, methanol 99%, ethanol 99%, sodium dodecyl sulphate 99% (SDS), oxalic acid 98%, sodium chloride 99.5%, sodium bisulphite 95%, potassium persulphate 99%, 2-aminoethylmethacrylate hydrochloride 90%, dimethylaminoethyl acrylate 99%, human pepsin, human amylase, human lipase, iron (II) chloride 98%, iron (III) chloride 98%, 4-dimethylaminopyridine, and (3-aminopropyl)trimethoxysilane 98% (APTMS) were all purchased from ThermoFisher Scientific, UK. FindMag™ strong Neodymium magnets were purchased from Amazon, UK. All reagents were used as received, without further purification.

UV spectra were collected using a Cary UV-Vis Compact, running on a Cary UV Workstation™, software version 1.0.1284 (Agilent, UK). IR spectra were collected using a ThermoScientific Nicolet iS5 Fourier transform infrared spectrometer running on OMNIC™ software. For thermogravimetric characterisation, a Mettler Toledo TGA/DSC 1 Series – running on STARe™ software Version 10.00 – was used. DSC was performed on TA Instruments DSC25 Series, running on Trios™ software, v5.4.0.300. Visualisation of the developed polymers was carried out via scanning electron microscopy (SEM) using a Zeiss Evo-50 electron microscope, operating on Smart SEM™ software. Weighing of chemicals was performed using Sartorius handy balance-H51 (Hannover, Germany). Data analysis and calculations were performed using Origin™ 8.5 software (OriginLab Corporation, North Hampton, USA).

2.6.2. Pre-polymerisation study

The aim of a pre-polymerisation study was to find a functional monomer capable of forming stable non-covalent bonds with the pepsin either through hydrogen bonds, van der Waals, or hydrophobic interactions. To be able to choose the appropriate monomer for the synthesis of highly selective magnetic MIPs, especially in water as a solvent, the stability of the template-monomer adduct had to be estimated. UV spectrometry was applied in a reported method to estimate possible interactions between the template and the suggested functional monomers (239).

Therefore, UV spectrometry was applied in this work to measure any interactions between pepsin and a number of monomers through measuring the change on the original UV spectrum of pepsin. Pepsin solution (0.5 mg mL^{-1}) in water was titrated with 10 mmol L^{-1} solutions of different monomers including MAA, Am, AA, 2-aminoethylmethacrylate hydrochloride, dimethylaminoethyl acrylate, and NIPAm. Those monomers were chosen due to their theoretical ability to form hydrogen bonds with either the amino or the carboxylic groups in the structure of pepsin. The collected UV spectra were compared to determine the monomer with the strongest interaction, identified by a noticeable shift from the original spectrum of pepsin.

2.6.3. Synthesis of functionalised iron oxide nanoparticles

2.6.3.1.   Synthesis of iron oxide (magnetite) nanoparticles

Among the previously discussed methods for the synthesis of magnetite under section 2.3, the chemical coprecipitation method was chosen due to its simplicity, greenness, and high yield.

Synthesis of magnetite (Fe_3O_4) was achieved according to a previously reported method with some modifications (231). Briefly, in 100 mL deionised water, 1.5 g of iron (II) chloride and 3.0 g of iron (III) chloride were dissolved and heated in a water bath under a continuous nitrogen stream with vigorous stirring at 1200 rpm. After reaching a temperature of 80 °C, 10 ml of 25% w/v ammonium hydroxide was added dropwise until reaching a pH of 10 to initiate the precipitation of the black iron oxide nanoparticles. After the complete precipitation, the obtained nanoparticles were collected using a neodymium magnet and washed with deionised water multiple times to remove excess ammonium and chloride ions.

Factors including the ratio of iron (II) to iron (III) species, pH, and stirring speed were optimised to control the size and dispersibility of the produced nanoparticles.

2.6.3.2. Functionalisation of magnetite

In order to direct the polymer chains to gather around the surface of magnetite nanoparticles, they had to be surface modified with specific functional groups that would draw the polymerisation mixture to their surface. The first step was the process of silanisation which introduced a thin layer of silicon dioxide (SiO_2) around the surface of magnetite. Silanisation was carried out via TEOS, according to a reported method, with some modifications (240). Briefly, the resulting magnetite nano particles from the previous coprecipitation reaction were redispersed after washing into a mixture of 380 mL of ethanol, 80 mL of deionised water, and 5 mL of 25% w/v ammonium hydroxide via ultrasonication. The mixture was heated to 30°C and 4 mL of TEOS were added dropwise. The mixture was left to react for 6 hours with continuous vigorous stirring.

The resulting silanised magnetite nanoparticles (Fe_3O_4-SiO_2) were collected via a neodymium magnet and washed with ethanol and deionised water 4 times, then dried under vacuum at 70°C.

The next step was the further functionalisation of Fe_3O_4-SiO_2 to introduce amino groups on the surface via APTMS (240). Silanised magnetite (2.5 g) nanoparticles were dispersed in 200 mL of ethanol via ultrasonication followed by heating the solution to 70°C. APTMS (4 mL) was then added dropwise over a period of 15 minutes. The mixture was allowed to react under a nitrogen gas atmosphere for 12 hours. The resulting magnetite nanoparticles (Fe_3O_4-SiO_2-NH_2) were collected with a neodymium magnet and washed with ethanol and deionised water 4 times, then dried under vacuum at 70°C.

The last step of functionalisation was the introduction of carboxylic groups via maleic anhydride (240). Fe_3O_4-SiO_2-NH_2 nanoparticles (1.2 g) were dispersed in 50 mL of N,N-dimethylformamide containing 400 mg of 4-dimethylaminopyridine and 5 g of maleic anhydride. The reaction was left overnight at 60°C and with continuous stirring. The product was collected with a neodymium magnet and washed with deionised water and ethanol four times and then freeze dried.

2.6.4. Preparation of magnetic MIPs and NIPs

The functional monomers that were assessed in the pre-polymerisation studies were tested in a series of prepared MIPs either alone or in a combination of two monomers. Moreover, different cross-linkers, initiators, and porogens were tested as well, in order to optimise the synthesis procedure to reach the MIPs with the highest possible selectivity.

It was a long procedure of testing different combination of monomers and cross-linkers and applying different previously reported methods on similar targets. The outcomes would vary between no reaction at all to the formation of a solid bulk. Therefore, a wise approach and calculation of the ratios of monomer to cross-linkers to target was a necessity to reach the desired goal of selectivity. **Table 2** summarises some of the trials conducted on the way to the optimum procedure which reflects the systematic approach followed during this course of development.

Table 2. *Different combinations of monomers, cross-linkers, initiators, and solvents to synthesise magnetic MIPs and their outcome.*

Functional monomer	Cross-linker	Solvent	Initiator	Result
MAA (0.9 mL)	600 mg (MBA)	30 mL water.	50 mg persulphate + 100 mg bisulphite.	Polymerisation was fast with distinct particulates of polymer, however, after solvent evaporation the yield was very low, and product was flaky.
MAA (1.2 mL)	600 mg	30 mL water.	50 mg persulphate + 100 mg bisulphite.	Polymerisation was in 15 min. and particulates of black polymer were produced.
MAA (1.4 mL)	600 mg	50 mL water.	50 mg persulphate + 100 mg bisulphite.	Polymerisation was in 15 min and a bulky black polymer was produced with the excess water (20 mL) on top.
MAA (1.4 mL)	600 mg	20 mL water + 10 mL MeOH (protic solvent).	50 mg persulphate + 100 mg bisulphite.	No polymerisation occurred over 48 hours.
MAA (1.4 mL)	600 mg	20 mL water + 10 mL acetonitrile (aprotic solvent).	50 mg persulphate + 100 mg bisulphite.	Polymerisation occurred overnight with a transparent gel like polymer.
MAA (1.4 mL)	200 mg	30 mL water	50 mg persulphate + 100 mg bisulphite.	No polymerisation occurred over 48 hours.
MAA (1.4 mL)	1 g	30 mL water	50 mg persulphate + 100 mg bisulphite.	Big particulate brittle black polymers were produced with high yield.
AA (1.2 mL)	600 mg	30 mL water.	50 mg persulphate + 100 mg bisulphite.	Polymerisation occurred in half an hour with very fine particles difficult to collect.
MAA + AA (0.9 + 0.3 mL)	600 mg	30 mL water.	50 mg persulphate + 100 mg bisulphite.	Polymerisation occurred in half an hour with very fine particles difficult to collect.

Functional monomer	Cross-linker	Solvent	Initiator	Result
MAA (1.4 mL)	600 mg	30 mL water.	10 mg persulphate + 20 mg bisulphite.	No polymerisation occurred over 48 hours, only turbidity appeared.
MAA (1.4 mL)	600 mg	30 mL water	50 mg persulphate + 25 mg bisulphite.	No polymerisation occurred over 48 hours, only turbidity appeared.
MAA (0.7 mL)	300 mg	15 mL water.	25 mg persulphate + 50 mg bisulphite.	Polymerisation to a bulky black polymer after an hour.
MAA (1.4 mL)	600 mg	30 mL water.	60 mg AIBN (UV initiation).	No polymerisation occurred over 48 hours.
MAA (1.4 mL)	600 mg	30 mL PBS.	2 mL (1.5%) APS + 1mL (3.75%) TEMED.	Polymerisation occurred overnight to black polymer particles.
MAA (1.4 mL)	600 mg	30 mL water.	2 mL (1.5%) APS + 0.5 mL (3.75%) TEMED.	Polymerisation occurred overnight to black polymer particles in MIPs' flask only.
MAA (1.2 mL)	EGDMA (0.65 mL)	30 mL water.	50 mg persulphate + 100 mg bisulphite.	Fast polymerisation occurred producing black polymer particles, after drying it was brittle amorphous powder and easily ground.

All tests were performed with 200 mg bare magnetite.

Overall, the optimal procedure was as follows: amino functionalised magnetite (250 mg) was dispersed in 30 mL of deionised water via ultrasonication followed by the addition of 14 mmol of MAA (1.2 mL), 8 mmol of EGDMA (0.6 mL) and 50 mg of pepsin. The solution was stirred for 1 hour to allow for pre-assembly with continuous nitrogen sparging to remove dissolved oxygen. Finally, 25 mg of potassium persulphate and 50 mg of sodium bisulphite were added to initiate a free radical polymerisation reaction. After the complete formation of the brown polymer particles, they were collected by a neodymium magnet and washed with water four times to remove unreacted monomers and oligomers.

To remove pepsin from the imprinted binding sites, MIPs were washed with a mixture of 1% w/v SDS/ and 10% v/v acetic acid. MIPs were stirred with this solution for 4 hours to ensure complete template removal followed by washing with deionised water 5 times. UV spectrometry was used to detect pepsin in fractions of the washing solution to confirm complete washing.

In order to compare the performance of MIPs and ensure their selectivity, control non-imprinted polymers (NIPs) were prepared using the same procedure without the addition of pepsin. Both MIPs and NIPs were dried under vacuum overnight at 70°C. **Figure 11** illustrates the functionalisation of magnetite and the core shell imprinting process that was carried out on the surface of the functionalised magnetite nanoparticles in the presence of pepsin as a template.
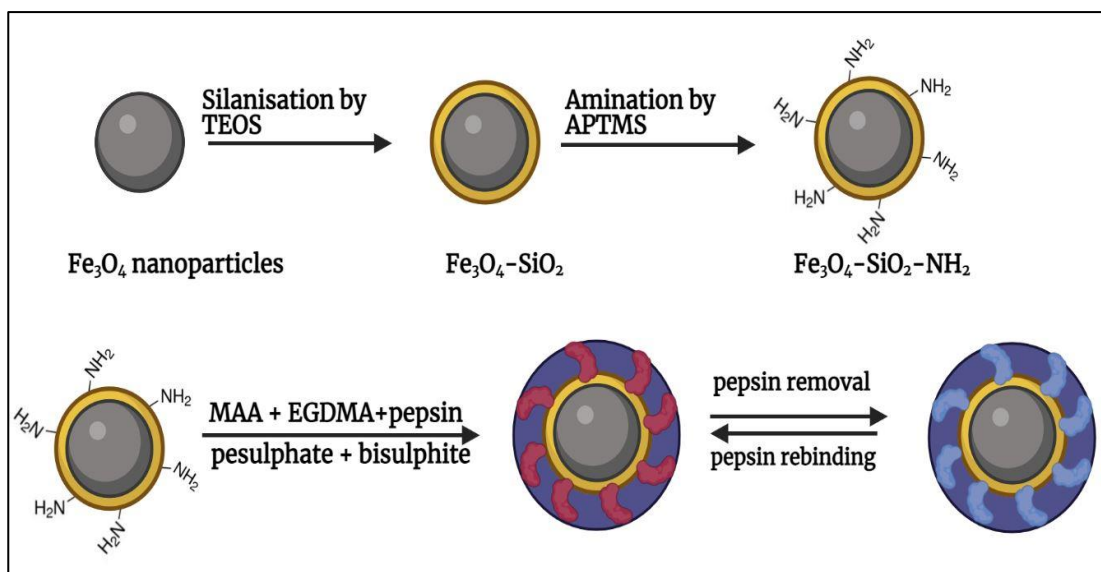
Figure 11. *Functionalisation of magnetite and synthesis of magnetic MIPs.*

2.6.5. Protein adsorption experiments

A batch adsorption method at the room temperature (25°C ± 2°C) was used to assess the binding capacity of all the developed polymers. Briefly, 50 mg of the magnetic MIPs or NIPs were incubated with 20 mL of 0.5 mg mL^{-1} pepsin solution in water for 2 hours on a mechanical shaker. Afterwards, polymers were collected by a neodymium magnet and the concentration of pepsin remaining in the solution was determined by UV spectrometry to calculate the amount in milligrams bound per gram of polymer (Q).

In the case of incomplete template removal upon washing of MIPs, the problem of template bleeding can occur, in which case the template is released upon using the developed MIPs resulting in erroneously high results (241). To reduce the probability of template bleeding, a blank rebinding experiment was conducted simultaneously in which 50 mg of MIPs or NIPs were incubated with 20 mL of deionised water for 2 hours and the supernatant after magnetic separation was used as a blank for the UV measurements of pepsin.

Q (mg g^{-1}) was calculated using equation 5:

$$Q = (Ci - Ct).V/m \hspace{3cm} \text{(eq. 5)}$$

where, C_i (mg mL^{-1}) is the initial concentration of pepsin, C_t (mg mL^{-1}) is the remaining concentration of pepsin after incubation time (t), V (mL) is the volume of solution, and m (g) is the mass of the polymers used in the experiment. All the tests were conducted in triplicate to ensure precision of the results.

2.6.6. *Calibration curve of pepsin via UV spectrometry*

In order to determine the concentration of pepsin in the supernatant of the solution after binding to MIPs or NIPs, it was essential to use a simple, fast, and reliable analytical method. UV spectrometry is a simple and useful analytical tool that was chosen for this purpose. Different concentrations of pepsin enzyme were prepared in water in the concentration range of 0.05 to 1.2 mg mL^{-1}. Spectra of each standard were collected and stacked as shown in **Figure 12**. A calibration curve was constructed between the concentration in mg mL^{-1} and the absorbances at 270 nm, the lambda max for pepsin, from which the linear regression equation was computed.

The linear regression equation was then used to calculate the concentration of pepsin in all the solutions from the subsequent protein binding experiments.
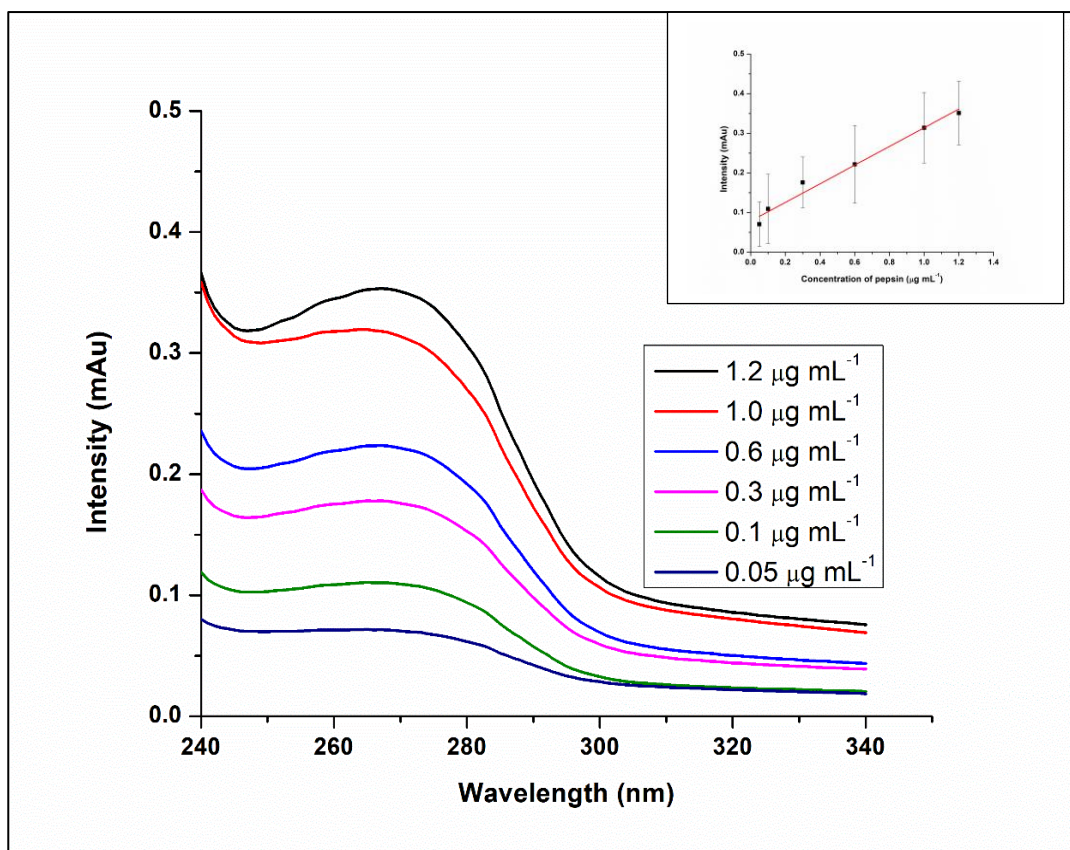
Figure 12. *Stacked UV calibration spectra of pepsin.* ***Inset****: calibration curve of pepsin via UV (triplicate measurements).*

2.6.7. Characterisation of magnetic MIPs

The morphology of the synthesised magnetite, amino functionalised magnetite, magnetic MIPs, and NIPs was investigated using SEM which enabled visual detection of the polymeric layers and an estimate of the particle size to confirm surface imprinting.

A batch rebinding assay at the room temperature (25°C ± 2°C) was performed to determine the binding kinetics order and the time of equilibrium for both magnetic MIPs and NIPs. The same mass of both polymers (50 mg) was incubated with 20 mL of 0.5 mg mL^{-1} of pepsin solution for different time intervals (t). The amount of pepsin bound per gram (Q) of magnetic MIPs or NIPs was computed for each time interval.

A similar batch adsorption experiment was conducted however using different concentrations of pepsin during a fixed time interval to determine the binding isotherm model for both magnetic MIPs and NIPs. 50 mg of MIPs or NIPs was incubated for 2 hours with different concentrations of pepsin and the amount of pepsin bound per gram (Q) of MIPs or NIPs was calculated for each concentration.

Binding selectivity was validated through comparing the binding of MIPs and NIPs to competitive analytes that can coexist with pepsin in human saliva. Amylase and lipase among other proteins were chosen for selectivity testing. A solution of each protein (20 mL of a 0.5 mg mL^{-1}) was incubated with 50 mg of magnetic MIPs or NIPs for 2 hours, and the amount bound per gram (Q) was computed for each analyte and compared to that of pepsin.

Thermal analysis was used to provide useful information about the relative mass ratio of the polymeric layer to the mass of magnetite in its core, the amount of adsorbed moisture, and the presence of any unreacted monomers or cross-linkers. The developed magnetic MIPs and NIPs along with functionalised magnetite were analysed using TGA with a temperature program set from 25 to 750 °C at a heating rate of 10 °C min^{-1} and a nitrogen gas flow rate of 50 mL min^{-1}. In addition, DSC was conducted at a temperature range from 25 to 350 °C at a heating rate of 10 °C min^{-1}.

2.6.8. Development of dispersive solid phase extraction of pepsin via magnetic MIPs

The developed magnetic MIPs were used as an adsorbent for the extraction of pepsin enzyme from aqueous solutions and saliva samples prior to quantitation. The eluting solvent and elution time were thoroughly optimised to achieve the utmost recovery of pepsin.

Herein, 50 mg of magnetic MIPs were incubated with different concentrations of pepsin standard solutions from 0.5 to 1.2 mg^{-1} mL on a mechanical shaker to extract the target. After two hours, the magnetic MIPs were collected by a neodymium magnet and eluted using PBS buffer (pH 7.2) for one hour, and the collected fractions were analysed by the newly developed HPLC-SEC method described in chapter 2, subchapter II.

2.7. Results and Discussion

2.7.1. Pre-polymerisation study

The results of the pre-polymerisation study are shown in **Figure 13** which reveals a reduction in absorption intensity on the spectrum of pepsin with all the tested monomers. However, the strongest shift was observed with MAA which indicated the formation of a strong and stable bond with pepsin. Nevertheless, since all the tested monomers caused a shift, they were further tested in the optimisation phase to verify the selectivity of their corresponding MIPs towards pepsin. Combinations of MAA and the other monomers were tested and compared to MAA derived MIPs as previously mentioned in **Table 1.**
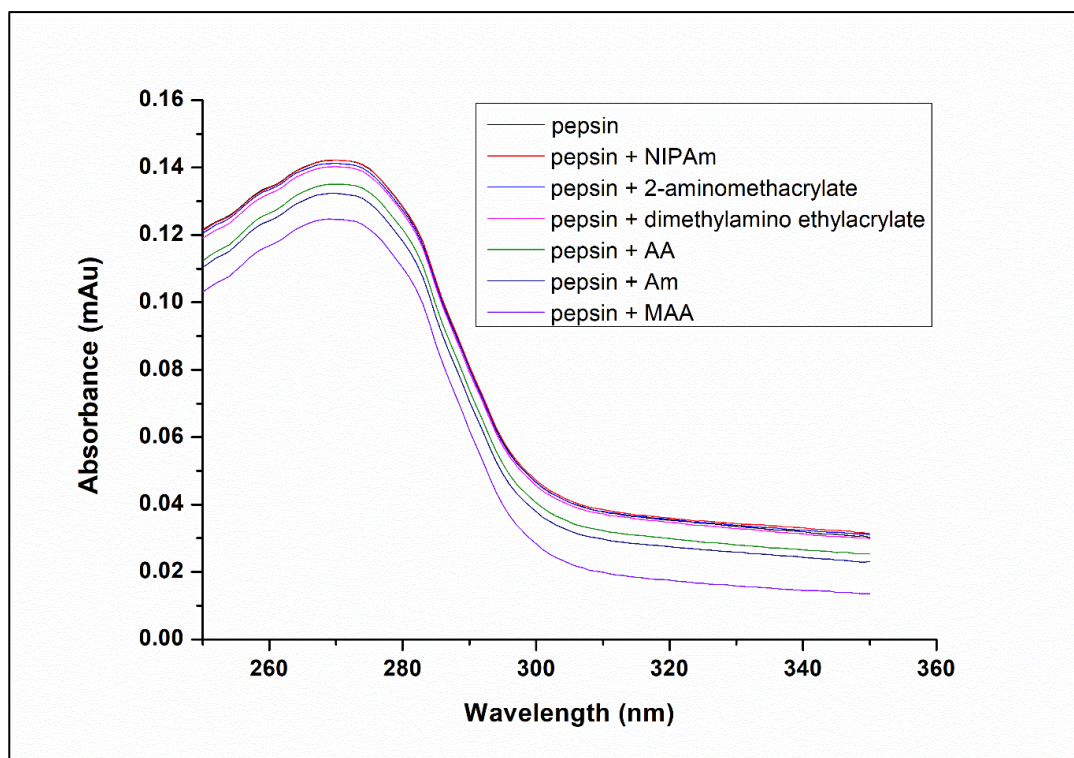
Figure 13. *UV spectra of pepsin solution titrated with potential monomers (average of triplicate measurements).*

2.7.2. Synthesis of functionalised magnetite

Synthesis and surface modification of magnetite were performed according to previously reported methods for chemical coprecipitation method (231,240). However, in the reported method for silanisation of magnetite, dry magnetite nano particles were weighed and dispersed in ethanol prior to the reaction with TEOS. Upon replicating the same procedure, it was noted that the magnetite nanoparticles were severely aggregated after drying which resulted in very poor dispersibility prior to silanisation even with prolonged sonication. This aggregation was attributed probably to the high surface charge due to their very small particle size. As a result, a modified *in situ* silanisation reaction was adopted in which silanisation followed the synthesis of magnetite nanoparticles without an intermediate drying step.

Using this approach, the resulting nanoparticles (Fe_3O_4-SiO_2) had a very good dispersibility and could be further modified with ease.

Functionalisation of magnetite was confirmed by FT-IR spectroscopy for bare magnetite, silica, and amino modified particles. **Figure 14** shows the IR spectrum of bare magnetite in which a band at 580 cm^{-1} corresponding to the vibration of the Fe-O bonds was prominent. In addition, two more peaks at 1633 cm^{-1} and 3400 cm^{-1} could be attributed to the stretching of the hydroxyl groups on the surface of magnetite. These results were in concordance with the IR spectrum for the reported method of synthesis (240). Further IR spectrum was collected for magnetite after silanisation in which an additional peak at ~ 1000 cm^{-1} corresponding to the stretching of the Si-O-Si bonds appeared. Moreover, the IR spectroscopic analysis of the amino functionalised magnetite showed a double peak at ~ 3600 cm^{-1} corresponding to the stretching of the N-H bond. The new peaks after silanisation and amination provided proof of successful surface modification of bare magnetite nanoparticles (242).
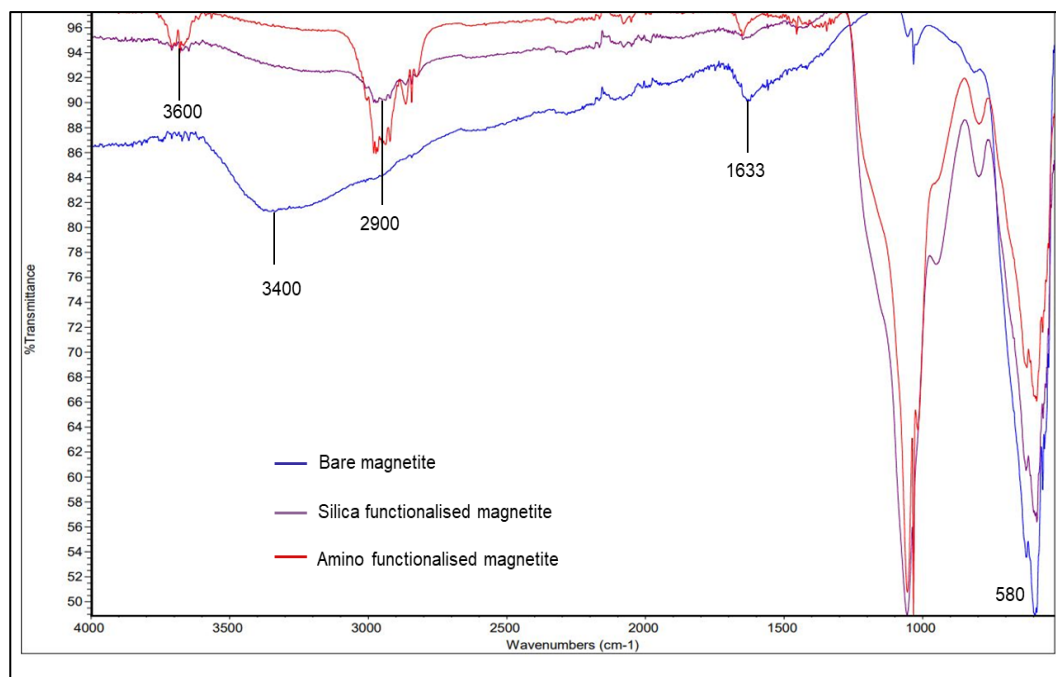
Figure 14. *Infrared spectra of bare magnetite, silica functionalised magnetite (Fe$_3$O$_4$-SiO$_2$), and amino functionalised magnetite (Fe$_3$O$_4$- SiO$_2$-NH$_2$).*

The surface modification of magnetite should ideally involve functional groups that attract the template-monomer adduct to its surface. Since the isoelectric point of pepsin is relatively low (3.24) (243), this means that at the working pH of the polymerisation solution (6 – 8), pepsin would be negatively charged. Therefore, amino functionalisation of magnetite would result in the presence of positively charged amino groups on the surface that would attract the negatively charged pepsin molecules resulting in electrostatic bond formation. Hence, amino functionalised magnetite nanoparticles were suitable for the synthesis of magnetic MIPs for pepsin since they provided more points of interaction. Meanwhile, carboxyl surface modification would result in negatively charged carboxylic groups that would repel pepsin molecules resulting in poor selectivity in the resulting MIPs. This hypothesis was further confirmed by comparing the binding performance of MIPs prepared using bare magnetite, amino functionalised magnetite, and carboxyl functionalised magnetite.

It was found that MIPs prepared with amino functionalised magnetite had the highest binding capacity indicated by the value of Q, as shown in **Figure 15**.
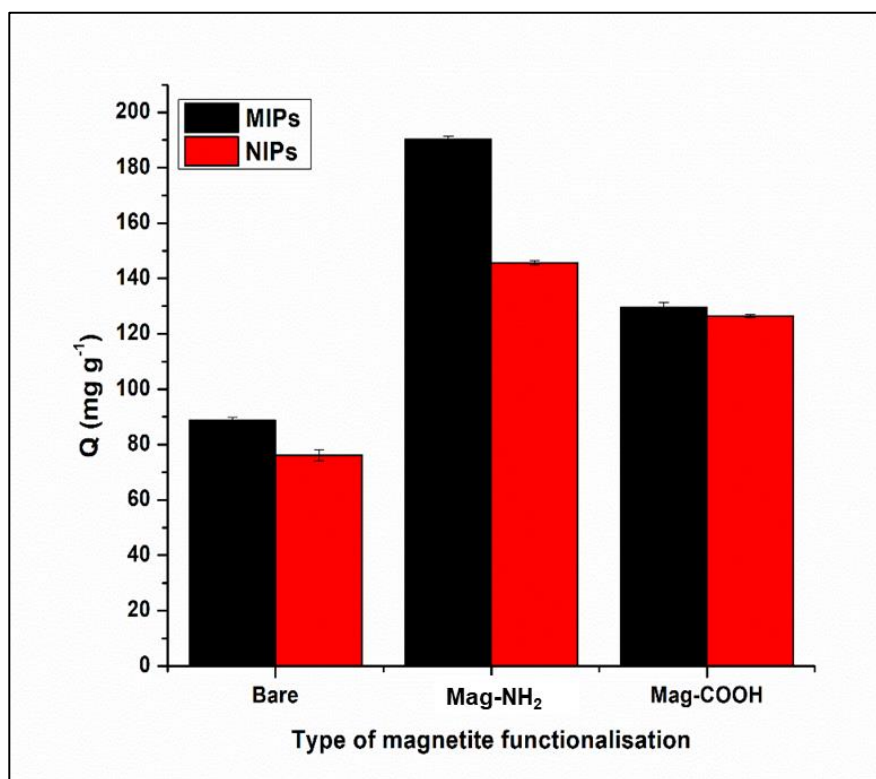
Figure 15. Optimisation of the type of magnetite functionalisation(average of triplicate measurements)..

2.7.3. Synthesis and optimisation of magnetic MIPs

Since MAA showed the strongest interaction in the pre-polymerisation studies, it was tested alone or in combination with other monomers as stated in the experimental section. MIPs and their corresponding NIPs were prepared from MAA, MAA with AA, MAA with Am, MAA with NIPAm, MAA with 2-aminoethyl methacrylate hydrochloride, and MAA with dimethylaminoethyl acrylate, using MBA as cross-linker and deionised water as porogen. The mixture of MAA with either 2-aminoethyl methacrylate hydrochloride or NIPAm did not polymerise under the specified polymerisation conditions.

The mixture of MAA with dimethylaminoethyl acrylate produced hydrophobic polymers that had very poor dispersibility in water which would compromise the application in aqueous media. Finally, **Figure 16** shows the difference in binding performance indicated by (Q) for the three magnetic MIPs prepared with MAA and their corresponding magnetic NIPs. It was concluded that the mixture of MAA with Am was the optimum combination of monomers.
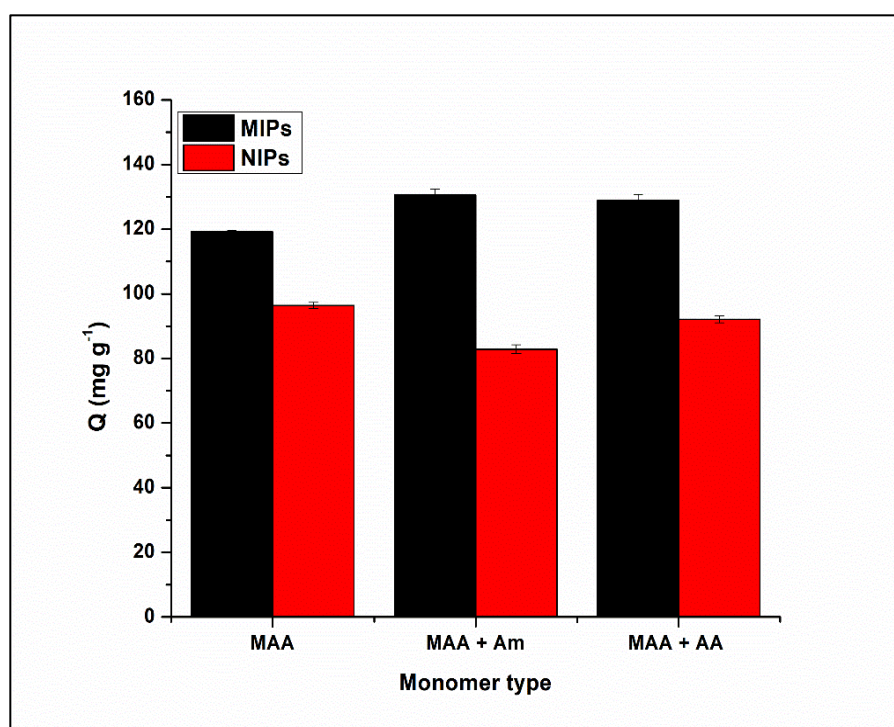
Figure 16 Optimisation of the type of monomer(average of triplicate measurements)..

Two cross-linkers were tested, namely, MBA and EGDMA in different concentrations. From **Figure 17**, it is obvious that EGDMA provides a better binding than MBA. Nonetheless, when EGDMA was tested with MAA and Am as functional monomers, the binding was significantly reduced. Therefore, MAA was used alone as functional monomer with EGDMA as cross-linker which gave an unprecedented binding capacity for magnetic MIPs. Moreover, the concentration of EGDMA was optimised as well, as shown in **Figure 18**.

The 4 mmol concentration gave a higher Q value for MIPs, however the 8 mmol concentration provided a better selectivity difference between magnetic MIPs and NIPs, therefore it was chosen as the optimum concentration.
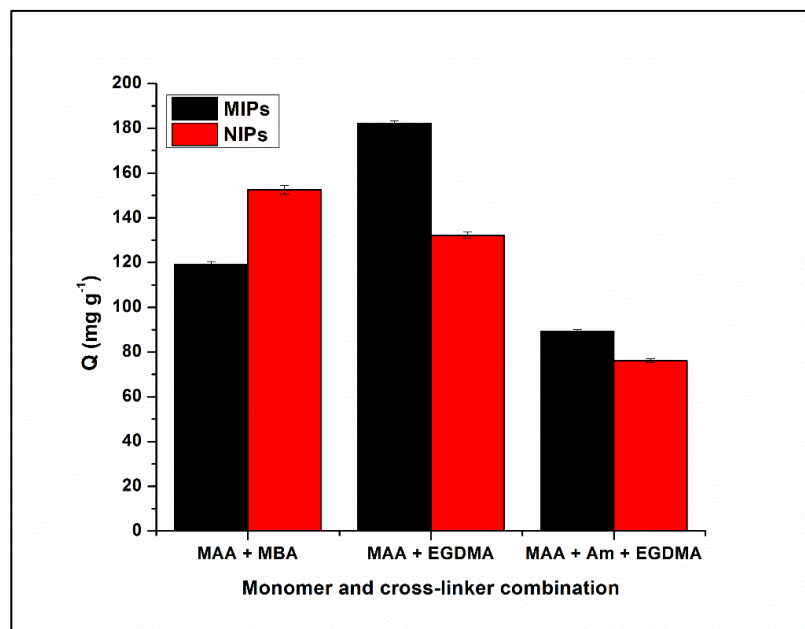
Figure 17. *Optimisation of the type of cross-linker(average of triplicate measurements).*
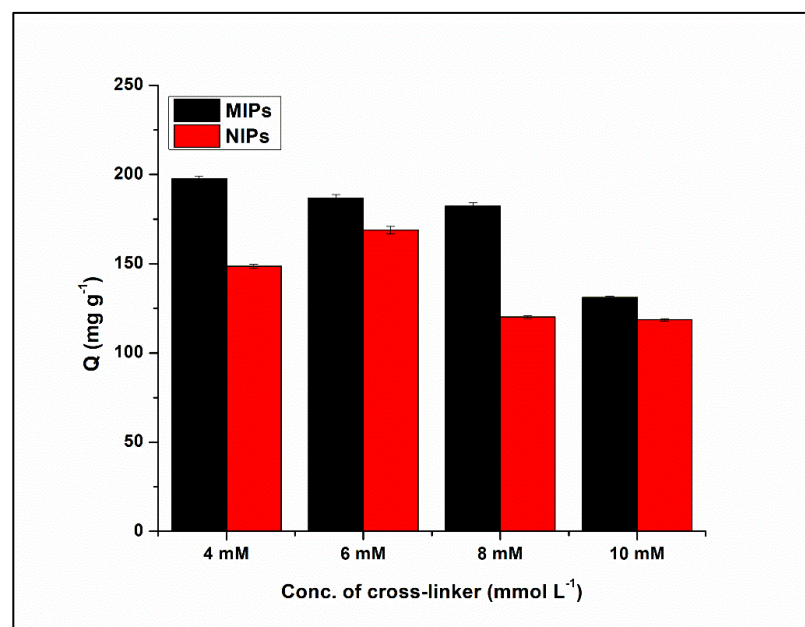
Figure 18. *Optimisation of the concentration of cross-linker(average of triplicate measurements).*

Due to the very poor solubility of pepsin in organic solvents, only water and aqueous buffers were tested as porogens. However, polymerisation in water is challenging as mentioned before since water molecules can disrupt the hydrogen bonds between the monomers and the template. Nevertheless, the careful choice of monomer, the presence of useful functional groups in both the monomer and the solid core, along with the appropriate pre-assembly time can help alleviate the problem. Upon testing deionised water and PBS buffer (pH 7.2) as porogens, deionised water gave slightly better rebinding results, so it was selected as the optimal solvent.

There are different types of initiators that can be used to start a free radical polymerisation, these include mainly azo initiators and oxidising agents (36). Since the application of heat (mostly required for azo initiators) can affect the conformation of pepsin, oxidising agents with low activation energy were chosen for initiation. Mixtures of APS and TEMED, and potassium persulphate and sodium bisulphite were tested in different ratios. APS and TEMED mixtures required a much longer time to initiate the reaction in comparison to a persulphate and bisulphite mixture, therefore the latter was used in this work. Different ratios of bisulphite to persulphate were tested including 1:1, 2:1, and 1:2. The optimum ratio was 2:1 which initiated the reaction at reasonable speed and produced magnetic MIPs with the strongest binding, as shown in **Figure 19**.
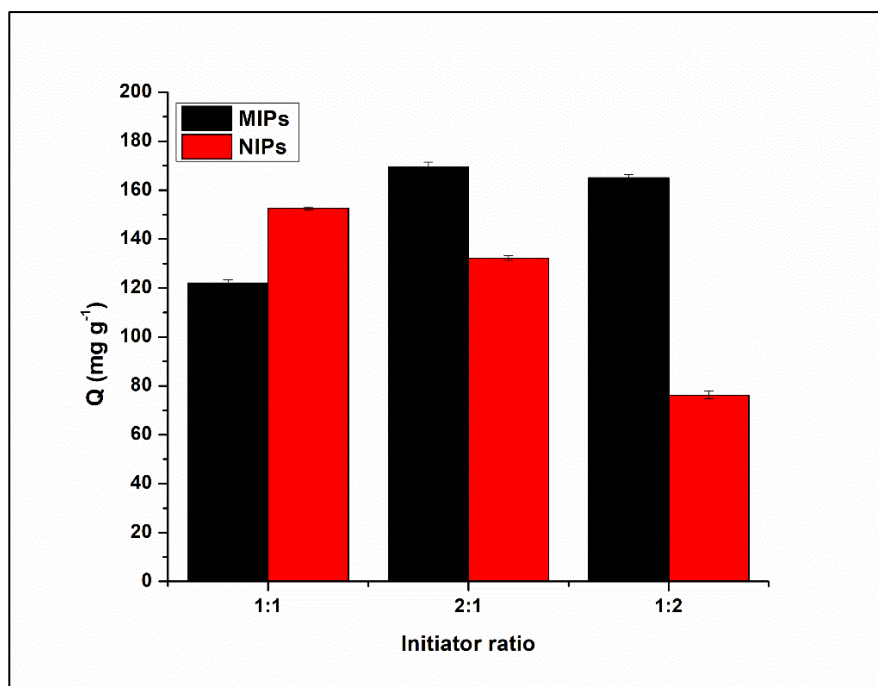
Figure 19. *Optimisation of the ratio of initiators(average of triplicate measurements).*

The amount of pepsin was also optimised as it was important to achieve an optimum ratio of monomer to target that would not compromise the selectivity. **Figure 20** shows that the optimum amount of added pepsin is 50 mg (~ 1.4 μmol).
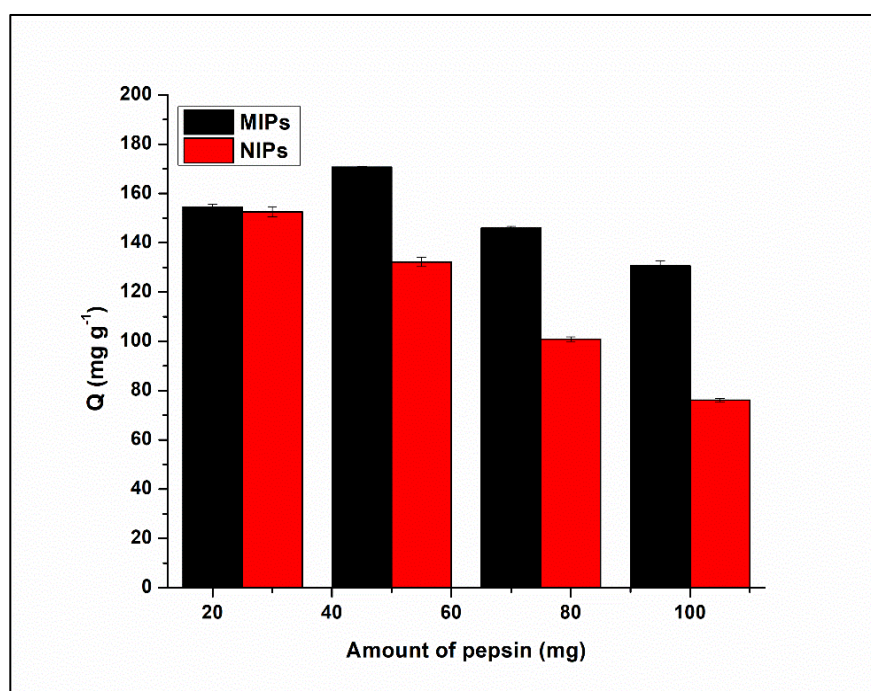
Figure 20. *Optimisation of the amount of pepsin(average of triplicate measurements).*

Moreover, the pre-assembly time between pepsin and the monomer is a critical factor that also needed to be optimised, especially applying water as a solvent. Experiments with 0, 1, 2, and 3 hours of pre-assembly, showed that 1 hour was sufficient to achieve the strongest assembly, which was reflected in the binding of the corresponding magnetic MIPs, as shown in **Figure 21.**
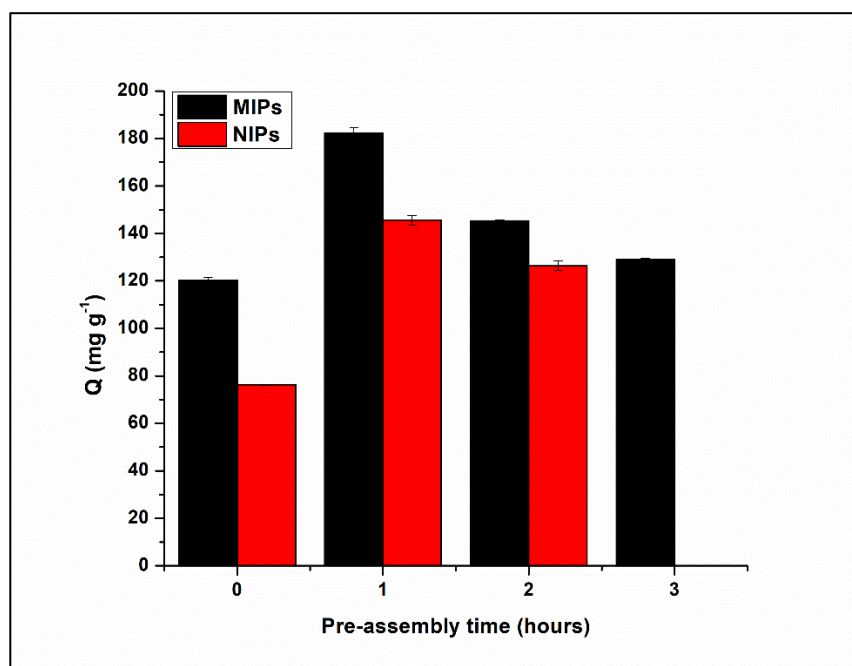
Figure 21. *Optimisation of the pre-assembly time(average of triplicate measurements).*

Removal of the template after polymerisation is a very important step to free the binding sites for further rebinding of target analyte in different samples. Incomplete template removal can result in reduced sensitivity of MIPs due to the limited availability of the binding sites. In addition, these trapped template molecules can cause template bleeding (126). Since pepsin is a huge target (34.5 KDa), its removal was a tricky step and needed to be considered thoroughly. Therefore, it was important to ensure complete template removal, through the selection of the best washing solvent, optimisation of the washing time and number of washing cycles.

Reported solutions for washing of protein targets in literature included solutions of oxalic acid (0.5 mol L^{-1}), PBS (0.02 mol L^{-1}, pH 7.2), sodium chloride (0.5 mol L^{-1}) and mixture of 1%w/v SDS and 10%v/v acetic acid (36). Therefore, all these solutions were assessed for complete pepsin enzyme removal. It was found that the mixture of SDS and acetic acid was the most successful in removing the template, as indicated by the UV measurements of the washing solutions. This was also verified by the high selectivity of the magnetic MIPs washed using this solution in comparison to the same magnetic MIPs washed with the other solutions. The optimal washing procedure involved the use of 75 ml of SDS/acetic acid solution with vigorous stirring for 4 hours followed by washing with deionised water 5 times to completely remove any traces of the SDS and acetic acid.

Due to the protein nature of pepsin enzyme, testing different reaction temperatures was restricted to temperatures around the average physiological temperature (37°C). Therefore, different temperatures in the range of 15 to 45°C in addition to the room temperature (25°C) were tested during the polymerisation reaction. However, it was found that temperature does not have any effect on the selectivity of the produced magnetic MIPs. Alternatively, higher temperatures only expedited the polymerisation reaction and lower temperatures made it slower.

Similarly, different pHs were tested during the polymerisation to study the effect of pH on the selectivity of the resulting magnetic MIPs. Yet again, due to the protein nature of pepsin, pH could significantly affect the conformation of pepsin in solution resulting in binding sites that do not match the actual pepsin in saliva samples.

Therefore, only pHs in the range of the pH of human saliva (6 to 8) were tested using PBS buffers in addition to deionised water (pH 6.8). Results showed that polymerisation in water produced magnetic MIPs with higher selectivity than all the other magnetic MIPs produced at different pHs.

2.7.4. Characterisation of magnetic MIPs and NIPs

2.7.4.1. Physical characterisation

SEM was used to determine the surface morphology and relative size range of the developed magnetite nanoparticles, magnetic MIPs and magnetic NIPs. From the images shown in **Figure 22**, the formation of the polymeric layer on the surface of magnetite nanoparticles could be visually detected in **Figures 22c and 22d**. This was further confirmed by the determination of particle size of magnetite, MIPs and NIPs. The measured diameter of amino functionalised magnetite was 75 nm, while that of NIPs and MIPs was 134 nm and 169 nm respectively. The increase in diameter of the polymer was consistent with the surface imprinting on magnetite nanoparticles. Furthermore, the slightly bigger diameter of MIPs could be attributed to the presence of wider imprinted cavities in MIPs compared to NIPs.
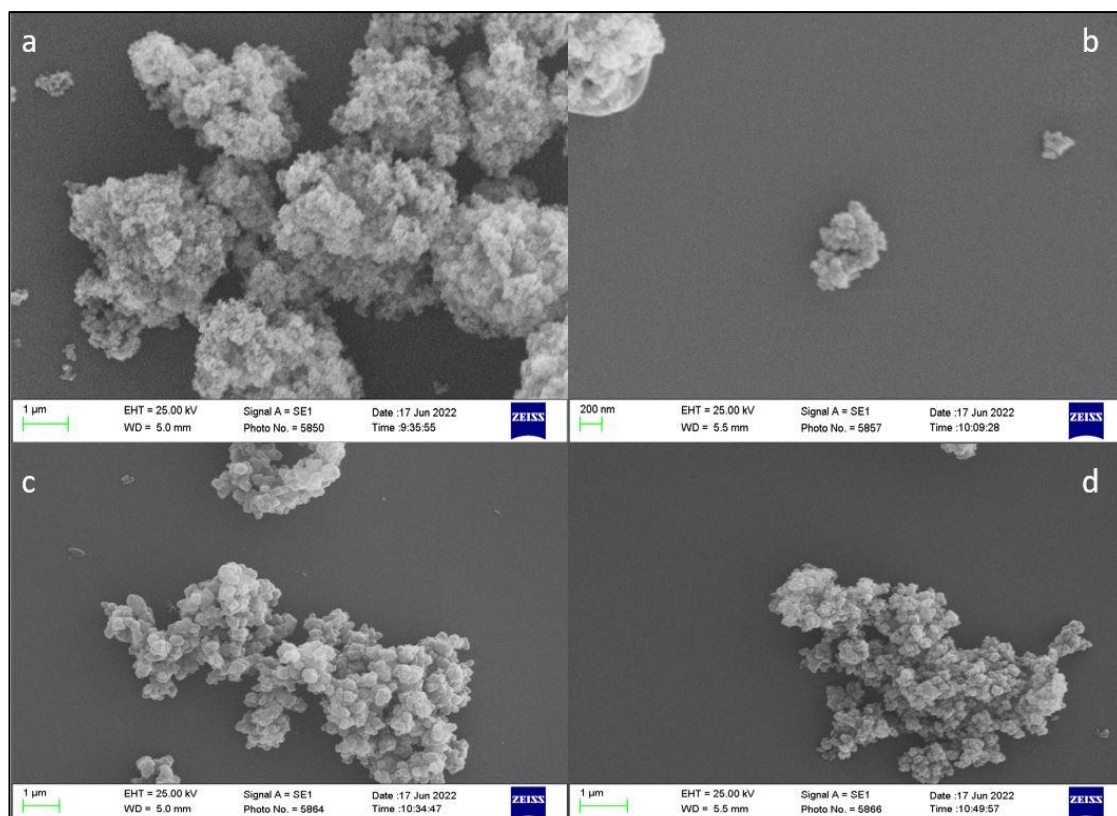
Figure 22. *SEM pictures of (a) bare magnetite (Fe$_3$O$_4$) 75nm, (b) amino functionalised magnetite (Fe$_3$O$_4$-SiO$_2$-NH$_2$), (c) magnetic MIPs 169 nm, (d) magnetic NIPs 134 nm.*

2.7.4.2. Functional characterisation

From the graphical representation of the binding kinetics study shown in **Figure 23**, it was estimated that the maximum binding for magnetic MIPs occurred after 2 hours which could also be considered as the equilibrium time. The fast-binding kinetics were due to the application of surface imprinting technique which confined all the binding sites on the surface to enable rapid binding and release. This provided an explanation to a problem that was encountered during the development phase. At the very early stages of development of the magnetic MIPs, the protein binding assays were performed for 4 hours according to a reported method for another similar target protein (240).

However, magnetic NIPs showed equivalent or even higher binding than the corresponding MIPs which was very confusing. Following this issue, a binding kinetics experiment was conducted which showed that the optimal binding time for magnetic MIPs was 2 hours and not 4 hours. Moreover, after 4 hours, pepsin started to be released again into the solution which accounted for the reduced binding in comparison to NIPs which had their maximum binding at 4 hours as reflected in **Figure 23**.
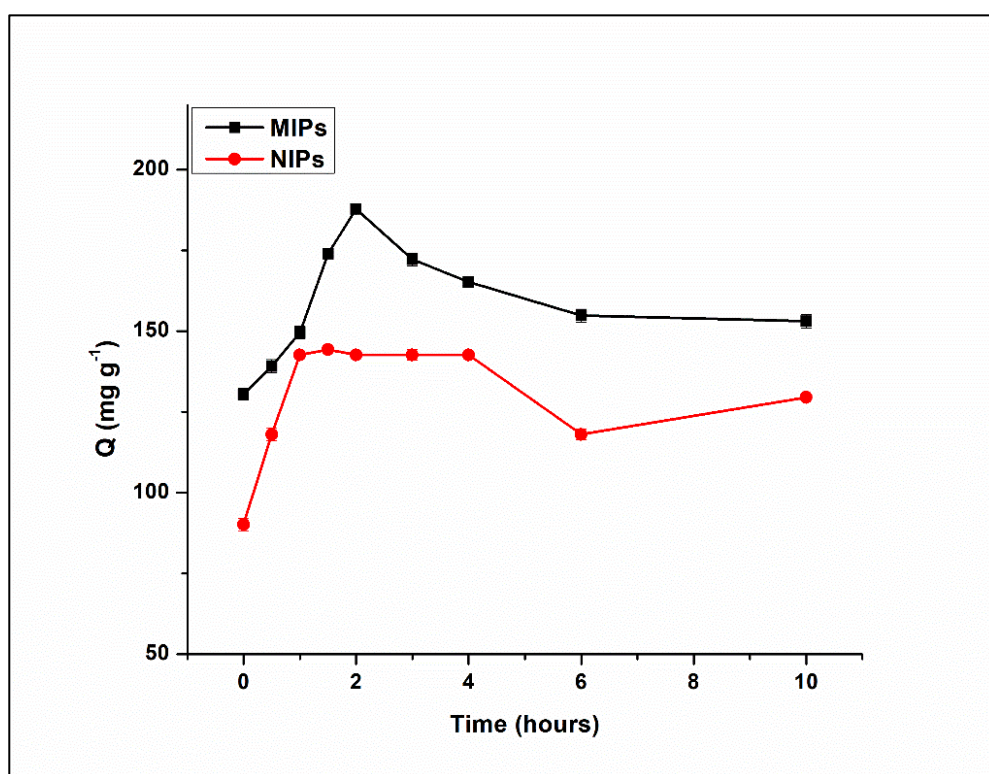
Figure 23. *Binding kinetics of magnetic MIPs and NIPs(average of triplicate measurements).*

To be able to understand the binding mechanism of pepsin to the imprinted polymers, both pseudo first order and pseudo second order kinetics' models were computed to fit the adsorption data. From **Table 3**, it was determined from the value of R^2 that pseudo second order is a much better fit for the experimental data, which suggests that binding is governed by a chemical adsorption mechanism.

Table 3. *Binding kinetics parameters for the adsorption of pepsin on magnetic MIPs and NIPs applying two binding orders.*

Pseudo first order parameters					
MIPs			**NIPs**		
K_1 (min $^{-1}$)	Qe (mg g^{-1})	R^2	K_1 (min $^{-1}$)	Qe (mg g^{-1})	R^2
0.00425	24.6	0.0426	0.00228	44.9	0.111
Pseudo second order parameters					
MIPs			**NIPs**		
K_2 (g mg^{-1} min^{-1})	Qe (mg g^{-1})	R^2	K_2 (g mg^{-1} min^{-1})	Qe (mg g^{-1})	R^2
0.0396	152	0.997	0.0520	127	0.992

K_1 and K_2 are the first and second order rate constants respectively, Qe is the amount of pepsin adsorbed per gram of polymer at equilibrium, and R^2 is the linearity coefficient.

The results of the binding isotherm experiment are shown in **Figure 24** in which a linear relationship between the concentration of pepsin and Q was observed. This linear relationship indicated that the adsorbed amount increased with increasing concentration until a maximum concentration was reached, after which all the binding sites would be saturated. However, higher concentrations of pepsin could not be actually tested via UV spectrometry due to the cloudy nature of their solutions.
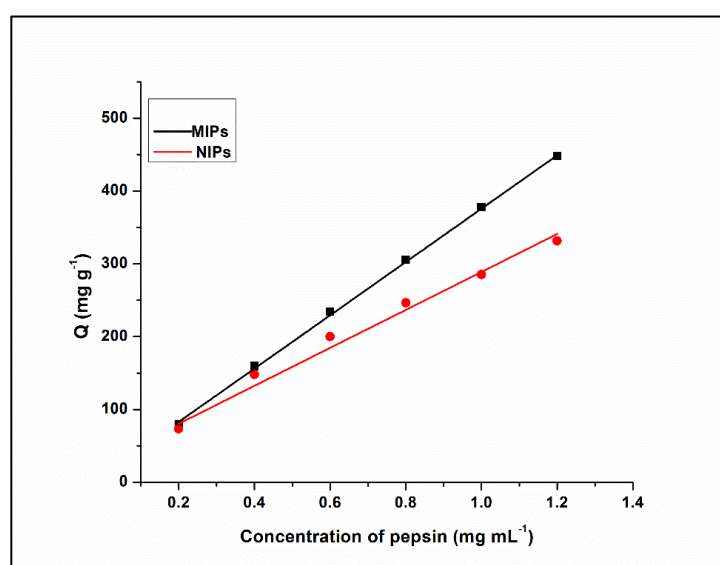
Figure 24. *Binding isotherm of magnetic MIPs and NIPs(average of triplicate measurements).*

The binding isotherm data was fitted into Langmuir and Freundlich isotherm models to determine if the adsorption of the target is in a monolayer or in multiple layers and if the binding sites are homogenous or heterogenous in nature. From **Table 4** the experimental data reflected a better fit with the Langmuir adsorption isotherm suggesting that the adsorption of pepsin on the surface of MIPs is in a monolayer form on homogenous binding sites.

Table 4. Adsorption isotherm parameters of magnetic MIPs and NIPs applying two models.

Langmuir isotherm							
MIPs				NIPs			
K_L (L mg^{-1})	Q_{max} (mg g^{-1})	RL	R^2	K_L (L mg^{-1})	Q_{max} (mg g^{-1})	RL	R^2
5.45	770	0.234	0.981	17.2	355	0.132	0.963
Freundlich isotherm							
MIPs				NIPs			
n	K_F		R^2	n	K_F		R^2
2.37	509		0.935	1.69	937		0.941

K_L and K_F are the Langmuir constant and Freundlich constant respectively, Q_{max} is the theoretical maximum adsorbed concentration, RL is the separation factor ($1/1+C_{eq}.KL$), n is the variation trend coefficient for the adsorption isotherm, and R^2 is the linearity coefficient.

In order to confirm the selectivity of the developed magnetic MIPs to pepsin, the binding of optimum MIPs was compared to the binding of the corresponding NIPs to calculate the imprinting factor (IF).

$$IF = \frac{Q_{MIPs}}{Q_{NIPs}}$$ (eq. 6)

The value of IF at the concentration of 0.5 mg mL^{-1} of pepsin was 1.34 indicating a significant difference in selectivity between magnetic MIPs and NIPs.

However, for a further confirmation of the selectivity of MIPs, it was better to compare the binding with the target (pepsin enzyme) to the binding with other competitive analytes. Amylase (58.4 kDa) and lipase (48 kDa) were chosen as competitive analytes as they are naturally occurring enzymes in the human saliva along with thrombin and ɣglobulin. The selectivity factor (α) for every competitor analyte was calculated using equation 7.

$$\alpha = \frac{Q_{MIP.target}}{Q_{MIP.competitor}} \qquad \text{(eq. 7)}$$

As demonstrated in **Figure 25**, The values of α were 3.17 and 9.52 for amylase and lipase respectively, indicating higher selectivity towards pepsin.
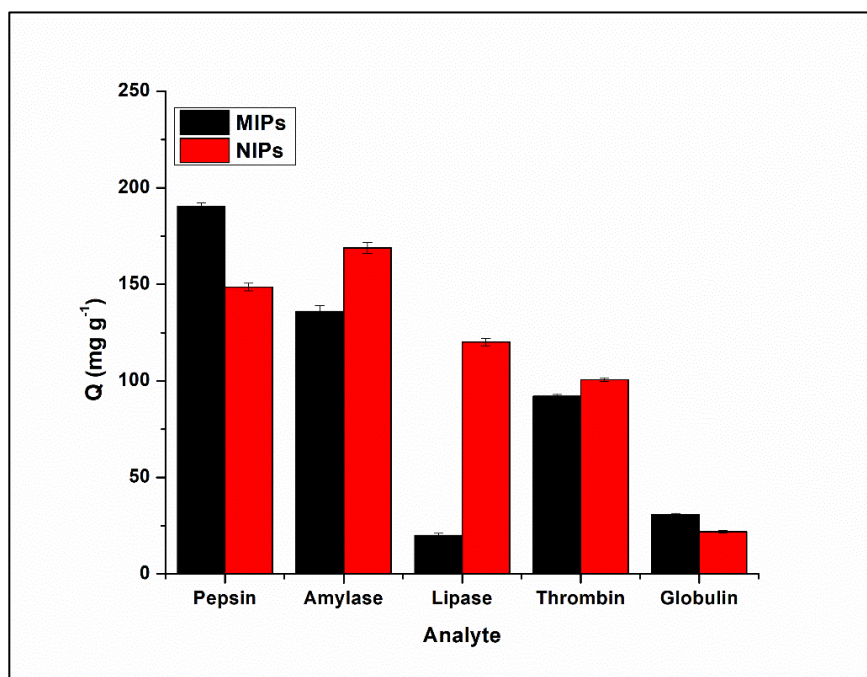
Figure 25. *Binding selectivity of magnetic MIPs and NIPs to pepsin compared to other proteins (average of triplicate measurements).*

The developed magnetic MIPs were tested for the number of times they could be used to adsorb and desorb pepsin with no loss in the binding capacity or selectivity as well as the magnetic quality.

From **Figure 26,** it could be observed that the binding of MIPs remained almost the same during the first three cycles of usage, however, it started to decline after the fourth cycle, reaching a much lower value on the fifth cycle. Moreover, the developed polymers did not show any reduction in the magnetic properties and could still be completely separated from solution using neodymium magnet. Therefore, the magnetic MIPs could be used safely for three consecutive cycles, which contributed to the economic value of the developed MIPs and made them suitable for commercial applications.
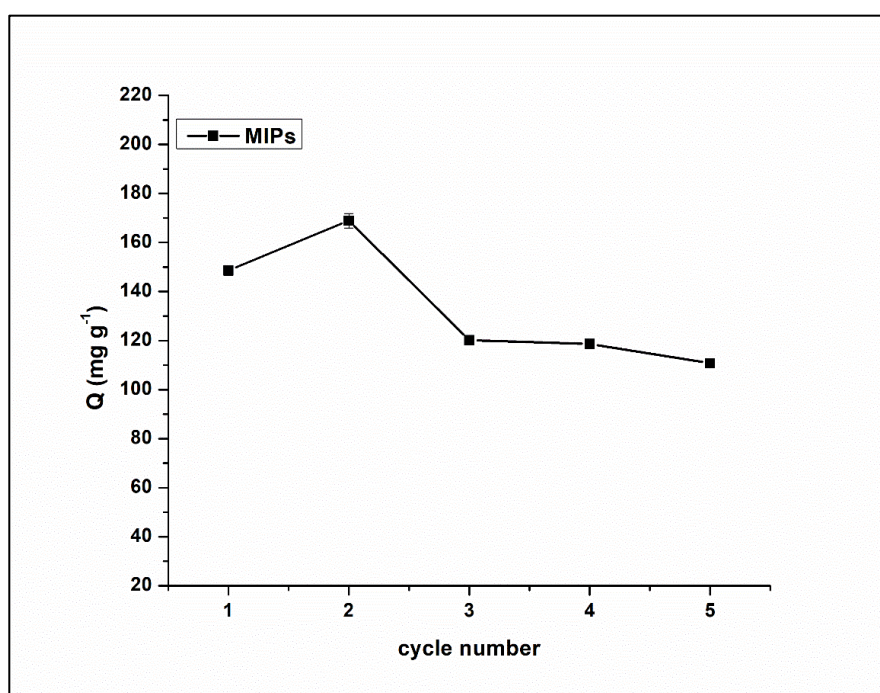
Figure 26. Reusability of the developed magnetic MIPs expressed as cycles of adsorption and desorption(average of triplicate measurements).

2.7.4.3. Thermal characterisation

TGA thermograms represented in **Figures 27a1 & 27a2** for both magnetic MIPs and NIPs, didn't not show any noticeable difference between both curves, which was expected as there is no chemical structural difference between the two materials. Decomposition occurred at almost 430 °C accompanied by almost 75% mass loss followed by a plateau corresponding to the mass of the residual magnetite.

As for DSC analysis, two endothermic peaks were observed for both MIPs and NIPs, again with no noticeable difference, as illustrated in **Figures 27b1, b2 & b3**. The first peak at ~ 100°C corresponded to evaporation of moisture, while the second peak corresponded to the melting of the polymeric layer at around 257°C. The curve for amino functionalised magnetite showed only one endothermic peak representing the evaporation of moisture similar to the peak observed for NIPs and MIPs.
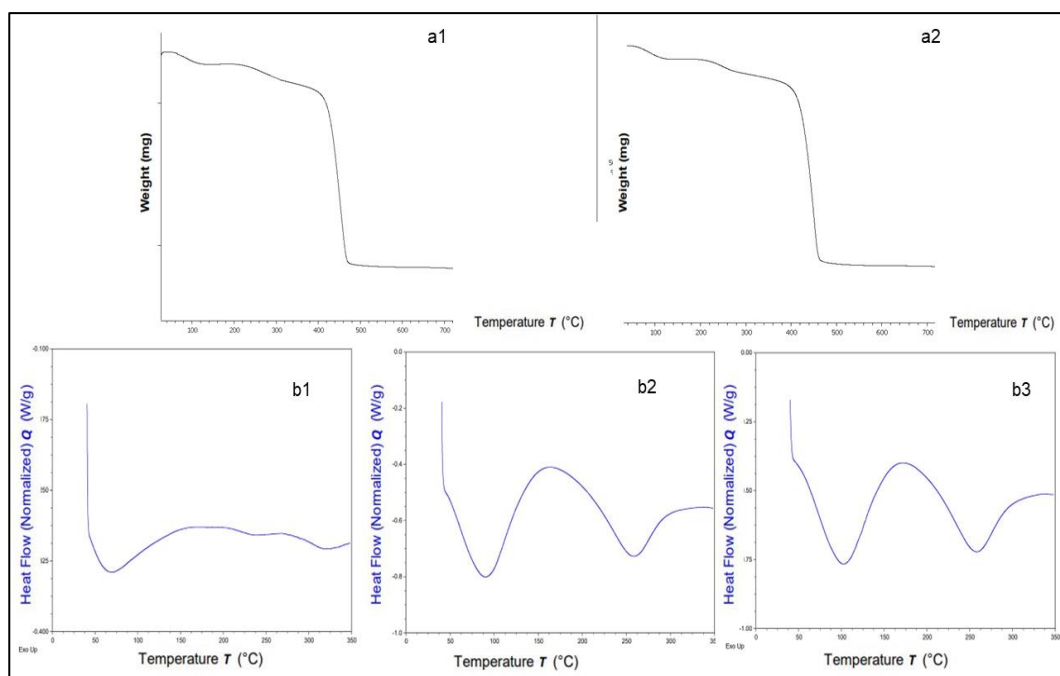
***Figure 27**. Thermal characterisation (a1) TGA thermograph of MIPs (a2) TGA thermograph of NIPs. (b1) DSC curve for (Fe$_3$O$_4$-SiO$_2$-NH$_2$), (b2) DSC curve for MIPs, (b3) DSC curve for NIPs.*

2.7.5. Dispersive solid phase extraction of pepsin from aqueous solutions

The conditions for extraction and elution of pepsin using the developed magnetic MIPs were studied wisely. Different eluting solvents were tested for their ability to completely elute pepsin adsorbed to the magnetic MIPs. Water was tested alone and with application of ultrasound waves, however in both cases the elution was not satisfactory. This can be attributed to the fact that it is very difficult to completely extract an analyte from water to water. Ultrasonic waves did improve the extraction, yet it was still not high enough and pepsin molecules were still trapped inside the MIPs' binding sites. 0.01 mol L^{-1} HCl (pH ~2.4) was tested as an eluting solvent, but the elution was worse than that obtained by water. Finally, PBS (0.02 mol L^{-1}, pH 7.2) buffer was tested and here the recovery of pepsin reached ~ 85%, which was greater than all the obtained values from the other tested solutions and hence it was selected as the eluting solvent. This percentage is among the highest recovery percentages from MIPs (38). In addition to trying different eluting solvents, different elution times (0.5, 1, 2 and 3 hours) were tested to select the time corresponding to the complete release. It was found that the optimal time corresponding to maximum release was 1 hour. As a result, the optimum elution process was to stir the magnetic MIPs with PBS buffer (0.02 mol L^{-1}, pH 7.2) for 1 hour, after which the bound pepsin was released. The short time of release was considered an advantage for the developed MIPs which again highlights the benefit of applying surface imprinting technique. The produced fractions of released pepsin were then quantified via the newly developed HPLC-SEC method mentioned in detail in chapter 2, subchapter II.

2.8. Potential application of magnetic MIPs in treatment of GERD and ulcers

As mentioned previously, pepsin contributes to the damage to the gastric mucosa in the cases of peptic ulcers (211). Therefore, denaturing excess pepsin can help with the symptoms, reduce the pain, and have a great therapeutic value.

Magnetic hyperthermia is a property that relies on the use of alternating magnetic field (AMF) to induce magnetic nanoparticles to release heat. Hence, due to the presence of magnetite in the core of MIPs, applying AMF after binding with pepsin can cause heat denaturation of excess pepsin in the stomach in a very simple, non-invasive and easily controlled process. This procedure has proven to be very effective before to denature green fluorescent protein (244). Therefore, the combined use of magnetic MIPs to selectively target pepsin, and magnetite in their core to inhibit it, can be a very promising tool to efficiently help patients with GERD after appropriate toxicity testing.

2.9. Conclusion

In the course of this work, novel magnetic MIPs were engineered specifically for the selective binding and extraction of the pepsin enzyme. These magnetic polymers exhibited a multitude of advantages, including selectivity, reproducibility, reusability, ease of synthesis, and cost-effectiveness. Rigorous optimisation of all synthesis parameters was meticulously undertaken to ensure not only maximum selectivity but also the highest efficiency in separation. A comprehensive characterisation of the magnetic MIPs was conducted using various methods, encompassing morphological, functional, and thermal analyses, thereby establishing their validity.

The magnetic MIPs were applied to selectively extract pepsin from both standard solutions and saliva samples using dispersive solid-phase extraction. The incorporation of a magnetic core facilitated swift and straightforward separation after extraction and the extracted pepsin was easily released within 1 hour.

Subchapter II. Development of a new high-performance liquid chromatography - size exclusion chromatography (HPLC-SEC) method for the determination of pepsin enzyme

2.1. Background

HPLC is one of the simplest and most common techniques of analysis for a wide range of analytes starting from small molecules reaching to huge macromolecules. However, the nature of the stationary phase and the mobile phase are completely dependent on the nature of the target analyte. Therefore, in developing a new HPLC method, careful consideration must be given to the properties of the target analyte or the mixture of analytes to be determined. Properties like molecular weight, pK_a, solubility, log P, chemical structure, and others can directly affect the separation, peak resolution, and quantitation of the analyte (245).

In the literature search for previously reported analytical methods for the determination of pepsin, a notable trend emerged, wherein pepsin was predominantly employed not as an analyte but as a crucial tool for analytical processes. Given its intrinsic digestive properties, pepsin finds extensive application in the enzymatic digestion of large protein analytes, effectively facilitating their subsequent analysis by simplifying their molecular structure (246,247). Another group of papers were focused on the determination of the enzymatic activity of pepsin and how it might be influenced by the presence of other molecules (248,249). However, very few papers were concerned with the analysis of pepsin itself as a biomarker for GERD. These papers were mentioned in detail in chapter 1, subchapter II, section 1.6.1.2 along with a critical review of their drawbacks (219–223).

The primary objective of this chapter extended beyond the development of an extraction method; it encompassed the quantification of pepsin concentrations to facilitate diagnostic outcomes. Consequently, the imperative arose to devise a novel analytical method for determining the concentrations of pepsin fragments extracted through the developed magnetic MIPs.

2.2. Advantages offered by HPLC analysis for proteins

HPLC stands out as a powerful analytical technique, particularly for the analysis of proteins, offering several advantages over traditional methods like UV spectroscopy. The advantages of HPLC in protein analysis are numerous and contribute to its common use in various scientific areas.

- HPLC provides excellent sensitivity, allowing the detection of proteins even at low concentrations.

- The technique offers high selectivity due to the ability to choose specific separation conditions, such as column type, mobile phase composition, and gradient profiles.

- Coupling HPLC with MS enhances the analytical capabilities for protein identification. This combination allows not only for separation, but also mass-based detection, improving specificity and facilitating structural elucidation. However, due to the limitations of the mass range of the MS detector on site at Kingston, it was resolved to employ UV detection.

- HPLC typically requires smaller sample volumes compared to UV spectroscopy, making it suitable for applications with limited sample availability or when dealing with precious biological samples. This is useful due to the small volume of saliva samples collected from GERD patients.

- Automation of HPLC processes ensures reproducibility, reducing the likelihood of human error and improving overall data quality.

Size Exclusion Chromatography (SEC), when integrated into HPLC, presents distinct advantages for protein analysis, particularly when compared to traditional C18-based methods. One particular merit lies in SEC's ability to separate proteins based on their size and molecular weight, offering insights into their structure and oligomeric state. Unlike C18, SEC enables the analysis of intact proteins without denaturation or modification, ensuring the preservation of their native conformation and functional characteristics. Additionally, SEC is non-destructive, allowing for the recovery of separated protein fractions for further analysis or downstream applications. In contrast to C18, SEC offers enhanced selectivity for large biomolecules, reducing interference from small molecules often observed in traditional reversed-phase chromatography. In essence, the incorporation of SEC into HPLC not only enhances the precision and reliability of protein analysis but also provides distinct advantages over C18 methodologies.

2.3. An attempt to replicate the reported LC-MS method for pepsin

The reported LC-MS method for the analysis of pepsin was initially tested to determine the concentration of pepsin extracted via the magnetic MIPs (219). The enzyme endoproteinase AspN was purchased from New England Biolabs (UK) and was freshly prepared in Tris buffer (10 mmol L^{-1}, pH 7.5) as instructed by the manufacturer to the final concentration of 2ng mL^{-1}. The prepared enzyme solution was then used according to a modified reported procedure to digest pepsin for a bottom-up LC-MS analysis (219).

The modified procedure was adopted from the reported paper despite its complexity. Herein, 450 µL of pepsin solution (200 ng mL^{-1}) were added to 300 µL of ammonium bicarbonate solution (pH 7.9) followed by 160 µL acetonitrile and finally 187.5 µL of AspN enzyme. The mixture was incubated for digestion at 37 °C for 16 hours.

Five microliters of the sample were injected into the analytical LC-MS system Agilent 1260 Infinity coupled with a 6430 Triple Quad LC/MS. The LC column used for the analytical method was a Synergy 4µm Fusion-RP 80 Å (150 x 2 mm) column from Phenomenex, UK. The mobile phase consisted of 0.1% formic acid solution in water (pH 3) running at a flow rate of 0.2 mL min^{-1}. The mass detection was operated at selected reaction monitoring (SRM) mode with a mass detection range from 500 to 2250 (which the maximum mass detected by the machine).

The reported method used the ions 662.85 $[M+2H]^{2+}$ to 1039.53 (b_{10}^{+}) for quantitation. However, the obtained chromatograms did not show any peaks even after increasing the concentration of pepsin.

Therefore, it was concluded that the masses of the resulting fragments of pepsin after digestion were too big for the detection range of the available machine. Additionally, the reported procedure was not accurate and needed further study and experience in proteomics which was not available at the time.

2.4. Aims and objectives of this work

- Development of a robust HPLC method for the analysis of pepsin enzyme, integrating SEC technique.

- Exploration of the suitability of SEC for enhanced separation of pepsin, optimising parameters such as column selection, mobile phase composition, flow rate, and detection wavelength.

- Validation of the developed method's performance in terms of sensitivity, selectivity, accuracy, and reproducibility through systematic experimentation and analysis.

- Assessment of the applicability of the method in the biological matrix in which pepsin exists; saliva.

- Evaluation of the method's selectivity by analysing the effects of potential interfering substances commonly found in saliva such as lipase and amylase.

- Integration of the developed magnetic MIPs to the developed HPLC method in order to devise a new diagnostic method for GERD.

2.5. Experimental

2.5.1. Materials and instrumentation

Phosphate-buffered saline (PBS) tablets (pH 7.2), sodium acetate 99%, glacial acetic acid 99%, Tris base 99.9%, hydrochloric acid 36%, phosphoric acid 85%, sodium hydroxide (98%) and arginine were all purchased from Sigma-Aldrich, UK. HPLC grade water, HPLC grade methanol (MeOH), HPLC grade acetonitrile (ACN) human pepsin, human amylase, human lipase, bovine thyroglobulin, myoglobin, immunoglobulin G, and sodium chloride were purchased from ThermoFisher Scientific (UK).

The HPLC-SEC method was performed on a LC Agilent 1260 Infinity ii (Agilent, UK) equipped with: 1260 Vial Sampler G7129A, Variable Wavelength Detector 1260 G7114A, Quat Pump VL 1260 G7111A, and a Biozen 1.8 µm dSEC-2, 200 Å LC column with the dimensions of 150 x 4.6 mm (Phenomenex, UK). The system control and data acquisition of the HPLC were performed by Chemstation™ C.01.10 software (UK). Filtration of buffer solutions and samples was carried out using 0.20 µm cellulose nitrate membrane filters (Whatman Laboratory Division, Maidstone, UK). Adjustment of the pH of the mobile phase was performed using a Jenway™ 3510 pH meter (UK). Weighing of chemicals was performed using Sartorius handy balance-H51 (Hannover, Germany). Data analysis and calculations was performed with Origin™ 8.5 software (OriginLab Corporation, North Hampton, USA).

2.5.2. Preparation of standard solutions

A stock solution of pepsin (0.5 mg mL^{-1}) was freshly prepared by transferring accurately weighed 25 mg of pepsin into a 50 mL volumetric flask containing 30 mL of PBS buffer (pH 7.2), the mixture was sonicated for 10 min., and completed to the mark with the same solvent. Stock solution of the internal standard (IS) (2.5 µg mL^{-1}) was prepared by dissolving 25 µg into 10 mL volumetric flask containing 5 mL of PBS buffer (pH 7.2), the mixture was sonicated for 10 min. and completed to the mark with the same solvent. The working solutions were prepared by appropriate dilutions from the stock solution with PBS buffer to obtain suitable concentrations within the desired linear range of pepsin (0.5 – 150 µg mL^{-1}). The stock and the working solutions of pepsin and IS were freshly prepared before analysis.

2.5.3. Preparation of spiked saliva samples

This study was conducted in agreement with the declaration of Helsinki principles and under the rules of UK Human Tissue Act (HTA) 2004 and received a full ethical approval from Kingston University Ethics Committee under Ethics Code 2895. Saliva samples were collected from one subject after rinsing the mouth three times with water, centrifuged at 4500 rpm for 30 minutes and then used immediately. Aliquots of saliva (150 µL) were then spiked with different volumes of standard pepsin solution and vortex mixed for 1 minute. To extract the spiked pepsin, 50 mg of the developed magnetic MIPs were added to the spiked saliva samples followed by addition of HPLC water to make a final volume of 10 mL. Samples were then incubated on a mechanical shaker for 2 hours. A neodymium magnet was used to separate the magnetic MIPs from solution and 5 mL of PBS buffer were used to elute pepsin from MIPs' binding sites for 1 hour.

After magnetic separation, triplicate injections of 20 µL of each of the extracted samples were injected into the HPLC-SEC system after filtration through a 0.20 µm cellulose nitrate membrane filter and the addition of the IS. Peak area ratios were plotted against the concentration in µg mL^{-1} to obtain a calibration curve and calculate the linear fit equation in saliva.

2.5.4. Optimisation of the developed HPLC method for pepsin

A working solution of 100 µg mL^{-1} was used throughout the entire optimisation procedure.

2.5.4.1. Choice of stationary phase (the column)

The analysis started using the conventional C18 column as a stationary phase for separation of pepsin. However, the peak became very distorted and split with significant tailing. Other columns including C8, C4, and phenyl columns were tested, yet similar results were obtained every time in which distorted peak or multiple peaks emerged despite using different mobile phases. In an attempt to understand the reason behind the shape of the resulting peak, a literature search was carried out for possible reasons and methods to mitigate this problem. It was found that in most cases, the use of conventional reversed phase columns for the analysis of proteins is not always a straightforward process (250). As a result, it was not useful for the analysis of pepsin as it caused denaturation and unfolding of the protein causing very irregular and unreproducible peak shape and sometimes many split peaks. Consequently, SEC was chosen for the analysis of pepsin enzyme due to its ability to separate large biomolecules. In which case, a SEC column would separate pepsin from other cross-reactors and the internal standard depending only on the size.

Therefore, pepsin molecules would pass between the pores of the column without any interaction that can cause unfolding or denaturation. In addition, the use of SEC would enable the determination of the efficiency of the extraction procedure and the presence of any other proteins in the extracted samples.

2.5.4.2. Choice of the mobile phase

In order to obtain a good peak shape, the method was meticulously optimised by testing different buffer compositions, pHs, ionic strengths, and concentrations. Since pepsin is only soluble in aqueous solutions, organic solvents were ruled out to avoid the precipitation of the protein in the column. Phosphate buffer, acetate buffer and Tris buffer covering a pH range from 2.5 to 7.5 were tested as mobile phases to give the best peak shape. In addition, different concentrations of the buffer solutions including 0.01, 0.02, 0.05 and 0.1 mol L^{-1} of the optimum buffer were applied to investigate their influence on the resulting peak. Moreover, sodium chloride solution (200 mmol L^{-1}) as ionic strength modifier was added to the optimum buffer to study its contribution in the separation efficiency.

2.5.4.3. Choice of internal standard

In order to ensure the reproducibility of the results and avoid any instrumental error, an internal standard had to be added. Since pepsin has a molecular weight of about 34.5 kDa and a hydrodynamic radius (Rh) of about 3 nm (30 Å) (251), any protein with an Rh value of 55 - 80 Å would be suitable to the linear range for the applied column, which is about 25 - 80 Å.

Different proteins were tested as internal standards such as bovine thyroglobulin (86 Å)(251), human ɣ-globulin (51 Å)(251), and myoglobin (18.4 Å)(251) to select a protein with a suitable retention time and a good separation from the peak of pepsin.

2.5.5. Validation of the developed HPLC-SEC method

The developed method was validated according to the ICH guidelines (252). Linearity was verified at eight different concentrations of pepsin with a fixed concentration of the internal standard (2.5 µg mL^{-1}) through triplicate injections of each concentration level and applying the linear regression equations to the resulting peak area ratios.

Accuracy and precision were evaluated across three different concentration levels of pepsin including high, medium, and low. Triplicate injections of each concentration were measured within the same day for accuracy and intraday precision and within three consecutive days for inter-day precision. Herein, accuracy was expressed as a percentage of recovery from the regression equation and precision was expressed as relative standard deviation percentage (%RSD).

To estimate the sensitivity of the developed HPLC-SEC method, the limit of detection (LOD) and the limit of quantitation (LOQ) were practically tested through injecting very low concentrations of pepsin (0.05 to 0.2 µg mL^{-1}) and calculating the signal to noise ratio (S/N). LOD and LOQ were then defined as the concentrations giving S/N value of 3 and 10 respectively.

In addition, to ensure the robustness of the developed method, minor changes in the chromatographic conditions such as flow rate, pH and concentration of buffer were applied to assess their influence on the peak area ratio and method performance.

Finally, the system suitability parameters were calculated for a representative chromatogram which included retention factor, separation factor, resolution, number of theoretical plates, height equivalent to theoretical plates and tailing factor.

2.5.6. Chromatographic conditions
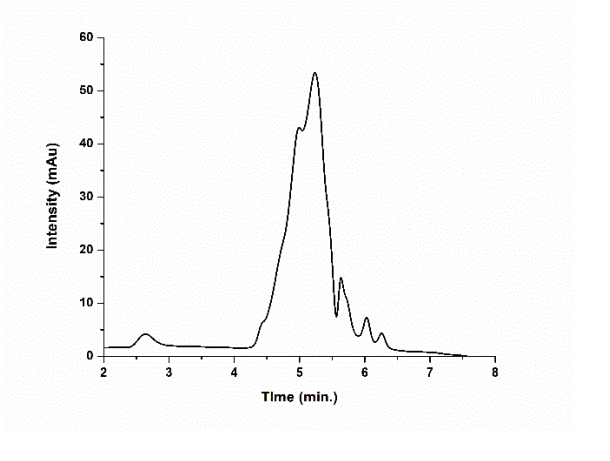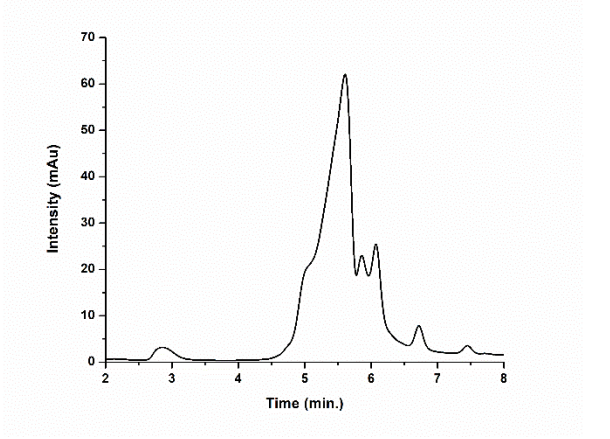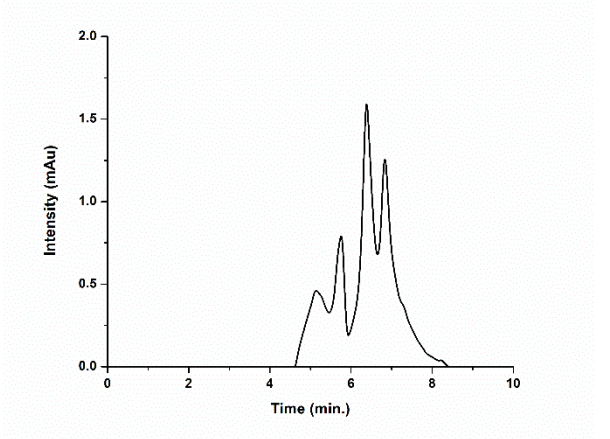
A mobile phase consisting of 0.02 mol L^{-1} phosphate buffer (adjusted to pH 3.0 with o-phosphoric acid (85%) and 1 mol L^{-1} sodium hydroxide solution) was used at a flow rate 0.35 mL min^{-1} to separate and quantify pepsin. Aliquots of 20 μL of each sample were injected into the system at ambient temperature. Detection was performed at wavelength of 270 nm for both pepsin and IS.
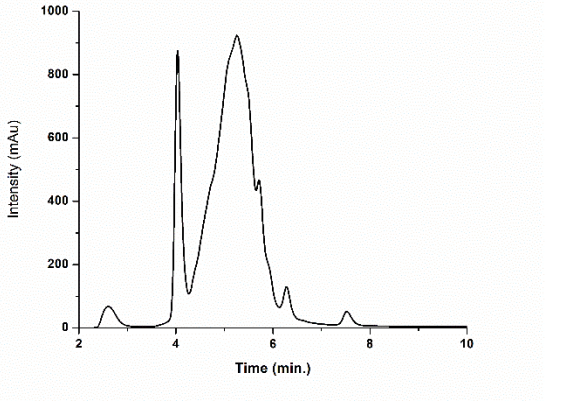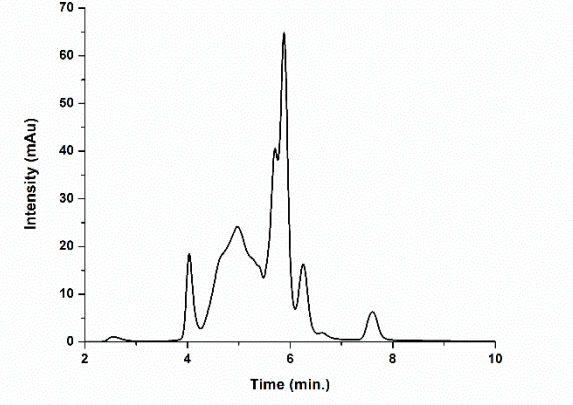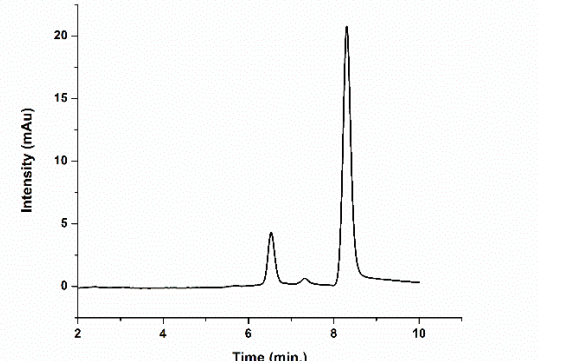
2.6. Results and Discussion

2.6.1. Optimisation of the HPLC-SEC method

Due to the use of SEC column for HPLC analysis of pepsin, the tested mobile phases were limited to aqueous solutions only. It was noted that the peak of pepsin became very distorted at high pH values in the range (5.0 to 7.5). However, the shape of the peak got significantly better at lower pH values (2.5 to 3.5) with pH 3.0 being the optimum value. This could be related to the unfolding of the protein structure at higher pH values compared to the lower pH in which it normally exists in the stomach (pH 2.0)(253). Summary of some of the optimisation trials for mobile phase and the resulting chromatograms are shown in **Table 5**.

Table 5. Summary of the optimisation of the mobile phase for the developed HPLC-SEC method for pepsin.

Mobile phase	Result	Chromatogram
Acetate buffer pH 3.75 (100%)	Peak shape was slightly distorted.	
Acetate buffer pH 3.75 (100%) + 0.02 mol L^{-1} NaCl solution.	The peak shape was more split.	
Acetate buffer pH 5.75 (100%).	Peak shape was split and distorted.	

Mobile phase	Result	Chromatogram
Phosphate buffer pH 6.0 (100%).	Peak was distorted significantly.	
Phosphate buffer pH 7.5 (100%).	Multiple peaks reflecting denaturation.	
Phosphate buffer pH (3.0) (100%).	Perfect peak.	

Addition of ionic strength modifiers such as 200 mmol L^{-1} sodium chloride to the buffer solution as well as the use of higher or lower concentrations of the buffer solution itself (0.01, 0.05 mol L^{-1} or 0.1 mol L^{-1}) did not contribute much to peak shape improvement. Myoglobin was chosen as internal standard since it eluted at a suitable retention time and with a good resolution from the peak of pepsin.

Therefore, after careful optimisation and testing, the optimum parameters for the HPLC-SEC were the use of 0.02 mol L^{-1} phosphate buffer (pH 3.0) at a flow rate 0.35 mL min^{-1}, injection volume was 20 μL, UV detection was performed at 270 nm, and the total run time was 11 minutes in which pepsin eluted at 6.9 minutes while the IS eluted at 9 minutes.

2.6.2. Validation of the HPLC-SEC method

The procedure was fully validated with some limitations to avoid damage to the packing of the column that can result from higher flow rates or the use of very low or very high pH values. Linearity, accuracy, precision and robustness were validated in accordance with ICH guidelines (252), and limits of detection and quantitation (LOD & LOQ) were validated according to USP guidelines (254). For the statistical analysis, Excel 2020 (Microsoft Office) was used at a 5 % significance level.

Linearity was determined by plotting the peak area ratio (peak area of pepsin to that of IS) versus the concentration of pepsin within the range of (0.5 – 150 μg mL^{-1}). Linearity of the peak area ratio response was verified at eight concentration levels by making triplicate measurements for each concentration. Calibration chromatograms overlay for seven different concentrations are shown in **Figure 28** and calibration curve and residuals are shown in **Figure 29**.

Linear regression equations were calculated, quantitative parameters and statistical data for determination of pepsin are given in **Table 6**.
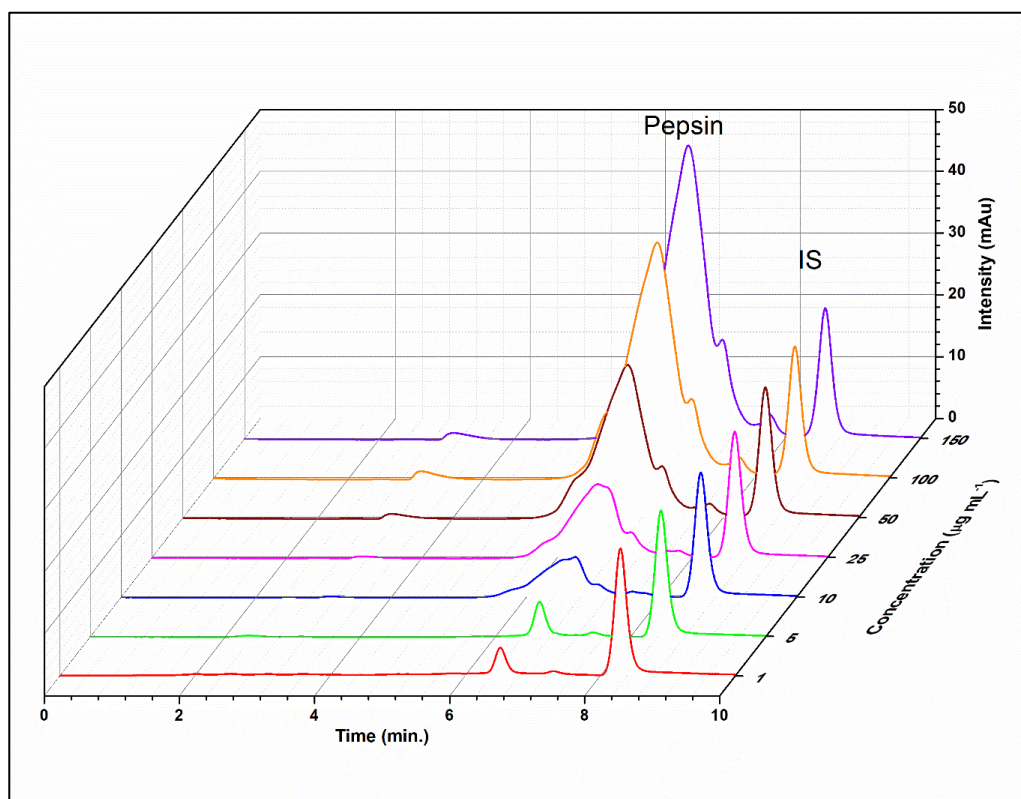
Figure 28. *Calibration chromatograms overlay for pepsin in concentration range from 1 to 150 μg mL^{-1}.*
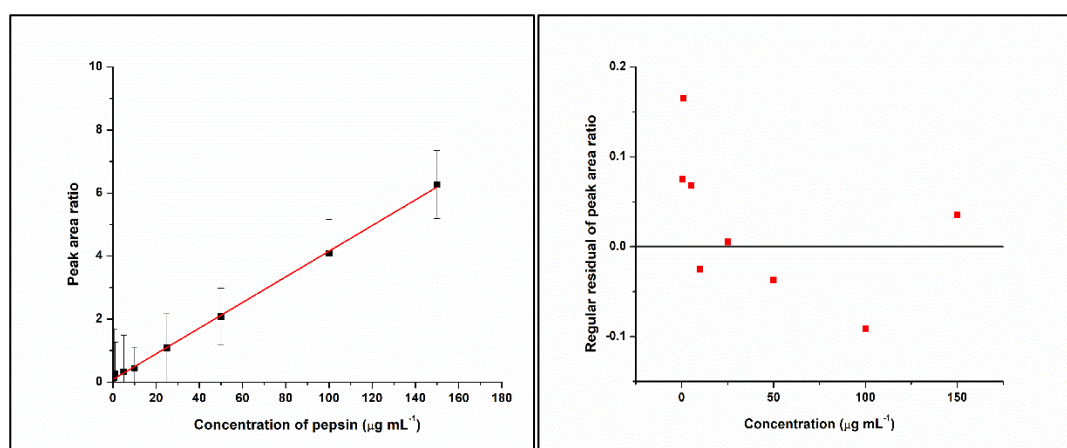
Figure 29. *Calibration curve and residuals for pepsin using the developed HPLC-SEC method(average of triplicate measurements)..*

Table 6. *Linearity parameters of the developed HPLC-SEC method.*

Linearity range (µg mL^{-1})	Intercept (a)± SD^a	Slope (b)± SD^b	$S_{yx}{}^c$	R^d	LOD (µg mL^{-1})^e	LOQ (µg mL^{-1})^f
0.5-150	0.103± 0.0350	0.0406± 0.001	0.0770	0.9989	0.10	0.25

^{a} Standard deviation of the intercept, ^{b} Standard deviation of slope, ^{c} Sum of square errors, ^{d} R is the correlation coefficient, ^{e} LOD is limit of detection, ^{f} LOQ is limit of quantitation.

Accuracy at three different concentrations along the calibration range with triplicates of each concentration was expressed as percent recovery of pepsin from the linear fit equation. Percentage RSD was used as indicative of precision along the same three concentration levels injected within the same day (intra-day) and within three different days (inter-day). Results are expressed in **Table 7**. For all concentration levels, the RSD did not exceed 2.20 %, indicating good reproducibility, and repeatability.

Table 7. *Accuracy and precision results for the developed HPLC-SEC method.*

Accuracy as percentage recovery of pepsin and precision as relative standard deviation (RSD%)			
Concentration (µg mL^{-1})	%Recovery ± SD	Intra-day %RSD	Inter-day %RSD
5	100.22 ± 2.68	0.027	2.01
50	98.04 ± 1.21	1.26	0.88
100	99.95 ± 2.17	2.17	1.55

To study the robustness of the method, minor changes applied to the chromatographic conditions such as flow rate, pH and concentration of mobile phase were tested. It was found that these changes did not affect the method performance as indicated by calculating the percentage of recovery for each change from the linear fit equation as shown in **Table 8**.

Table 8. *Robustness results for the developed HPLC-SEC method.*

Robustness as percentage recovery of pepsin at 50 µg mL^{-1}

Experimental parameter	%Recovery ± SD
pH of buffer	
2.8	100.46 ± 1.61
3.2	99.51 ± 0.38
Conc. of phosphate buffer (mol L^{-1})	
0.01	102.27 ± 0.51
0.03	100.41 ± 1.97
Flow rate (mL min^{-1})	
0.30	99.82 ± 0.45

SD is the standard deviation of triplicate results.

The system suitability parameters including retention factor, selectivity factor, resolution, number of theoretical plates and tailing factor have been calculated for a representative chromatogram of pepsin. Results are given in **Table 9**.

Table 9. *System suitability parameters for the developed HPLC-SEC method.*

Analyte	K^g	α^h	Rs^i	N^j	HETP^k x 10^{-3} (cm)	T$_f$^{L}
pepsin	2.45			1009.9	14.853	1.755
IS	3.5	1.428	3.796	22898.979	0.655	0.160

^{g} *Retention factor, k = t_R- t_0/t_0,* ^{h} *Separation factor (α) between pepsin and IS peaks = t_{R2} - t_0/ t_{R1} - t_0,* ^{i} *Resolution factor (Rs) between pepsin and IS peaks = 2(t_{R2} – t_{R1})/ (w_1 + w_2),* ^{i} *Number of theoretical plates (N) = 16(t_R/w)^2,* ^{k} *Height equivalent to theoretical plates = length of column/ N and* ^{L} *Tailing or asymmetry factor, Tf = (a + b)/2a. Where t_0 is the dead time, t_{R1} and t_{R2} are the retention times and w_1 and w_2 the baseline peak width of successive peaks.*

2.9.3. Application to human saliva samples

The developed magnetic MIPs in chapter 1, subchapter I were successfully applied for the extraction of pepsin from the spiked saliva samples prior to quantitation via the developed HPLC-SEC method.

Figure 30 shows a representative chromatogram of pepsin (25 µg mL^{-1}) and the internal standard (2.5 µg mL^{-1}) in a saliva sample.
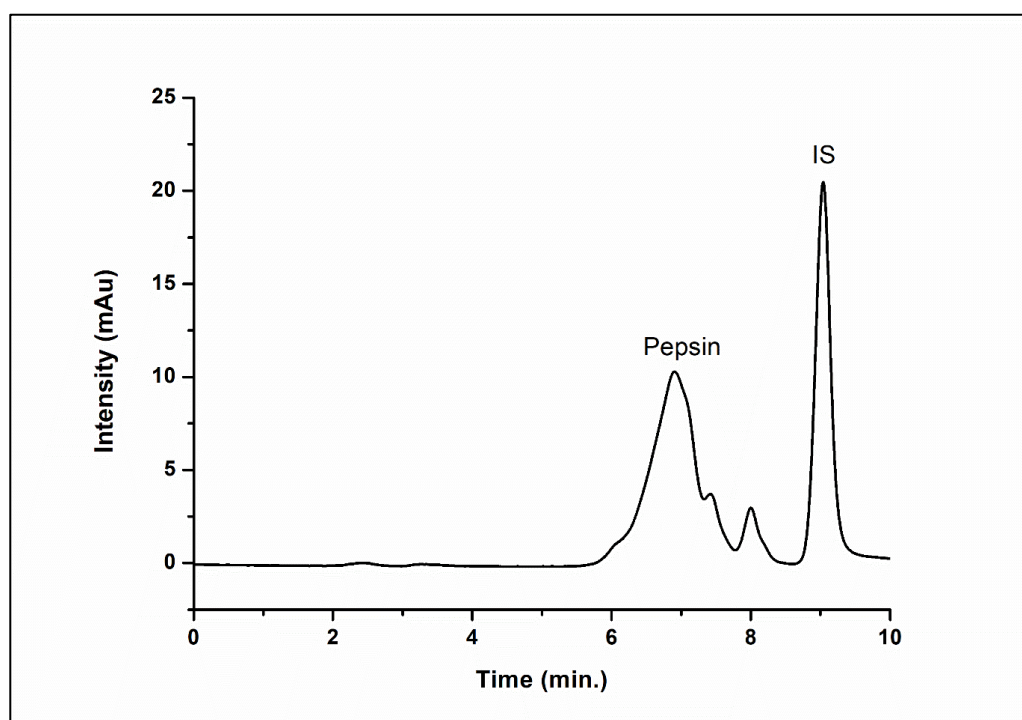
Figure 30. Representative chromatogram of pepsin in a spiked saliva sample using the developed HPLC-SEC method.

A calibration curve was constructed for the spiked pepsin in saliva after subtraction of blank saliva readings, and the linearity parameters were computed and presented in **Table 10**. Moreover, to verify the applicability, percentage of recovery for three different pepsin concentrations from spiked saliva were computed from the linear fit equation and presented as well in **Table 10**.

Table 10. *Linearity parameters of the proposed HPLC-SEC method and percentages of recovery of pepsin in saliva samples.*

Linearity range ($\mu g\ mL^{-1}$)	Intercept (a)± SD[a]	Slope (b)± SD[b]	S_{yx}[c]	R[d]	LOD ($\mu g\ mL^{-1}$)[e]	LOQ ($\mu g\ mL^{-1}$)[f]
5 - 150	3.940 ± 0.006	0.035 ± 0.001	0.068	0.9990	0.598	1.813

Recovery of spiked pepsin from saliva samples			
Concentration ($\mu g\ mL^{-1}$)	Average total amount found ($\mu g\ mL^{-1}$)	Average% recovery ± SD	RSD%
10	9.748	95.749 ± 0.673	0.703
50	49.330	98.661 ± 1.319	1.336
100	97.314	97.315 ± 0.188	0.194

[a] *Standard deviation of the intercept,* [b] *Standard deviation of slope,* [c] *Sum of square errors,* [d] *R is the correlation coefficient,* [e] *LOD is limit of detection,* [f] *LOQ is limit of quantitation.*

2.7. Conclusion

A novel, highly sensitive, HPLC method was developed for the quantitation of pepsin, which along with the application of size exclusion chromatography (SEC) allowed for clean and reproducible chromatograms. The developed HPLC-SEC method was optimised in terms of column, mobile phase, pH, and internal standard. Moreover, the method was validated according to ICH guidelines and USP guidelines regarding linearity, accuracy, precision, LOD, LOQ, robustness, and system suitability. Consequently, the method was applied successfully in conjunction with the produced magnetic MIPs to extract and quantify pepsin in solutions and saliva samples. Finally, it can be concluded that the combined use of the developed magnetic MIPs and the HPLC-SEC method could provide a highly promising and an effective diagnostic tool for patients with GERD through a very simple, non-invasive, and rapid procedure.

Chapter 3

Development of Highly Sensitive Fluorescent Sensors for Separation-Free Detection and Quantitation Systems of Pepsin Enzyme Applying a Structure Guided Approach

Chapter 3. Development of highly sensitive fluorescent sensors for separation-free detection and quantitation systems of pepsin enzyme applying a structure guided approach

3.1. Background

Fluorescent molecularly imprinted polymers are a class of advanced materials that combine the selective recognition capabilities of MIPs with the sensitive detection properties of fluorescent sensors (255).

The integration of fluorescence into MIPs began gaining attraction in the late 1990s and early 2000s, driven by the need for more sensitive and selective detection methods in analytical chemistry (256). Researchers started incorporating fluorescent co-monomers and fluorescent nanoparticles into the polymer matrices, leading to the first generation of fluorescent MIPs. These innovations allowed for the visual and quantitative detection of target molecules through fluorescence changes. Over the past two decades, advancements in polymer chemistry, nanotechnology, and fluorescence imaging have significantly improved the performance and application range of the fluorescent MIPs. Today, they are utilised in various fields, including environmental monitoring, food safety, and biomedical diagnostics, showcasing their versatility and the continuous innovation in this area (256).

3.2. Advantages offered by fluorescent MIPs

Fluorescent MIPs offer not only a means to detect binding events but also to quantify the concentration of the target molecules through changes in fluorescence. When the target binds to the fluorescent MIPs, there is a corresponding alteration in the fluorescence intensity, which can either increase or decrease.

This change in fluorescence is typically proportional to the concentration of the analyte, allowing for precise quantitation. Thus, fluorescent MIPs serve a dual purpose: they facilitate both the extraction and the detection of the target analyte and provide a highly sensitive and accurate quantification method. This dual functionality makes fluorescent MIPs a comprehensive and self-sufficient analytical technique, suitable for various applications where precise measurement and detection are crucial (126). In addition, fluorescent MIPs offer a range of other benefits including:

- High selectivity**:** fluorescent MIPs offer precise binding sites, ensuring selective binding to target proteins in complex samples. This specificity enhances accuracy in protein analysis and aids in accurate identification of target molecules (179).

- Sensitive detection: the sensitivity of fluorescent MIPs allows for the detection of low-abundance proteins in protein analysis. In analytical chemistry, this sensitivity aids in identifying trace amounts of analytes, improving detection of contaminants (257).

- Wide range of applications**:** fluorescent MIPs can be tailored to any target starting from small molecules up to huge molecules. This makes fluorescent MIPs useful in the fields of sensing, environmental analysis, and forensic sciences (179).

- Immediate readout: fluorescent MIPs provide quick and easy-to-read outputs, facilitating real-time monitoring in protein analysis (258).

3.3. Methods applied for synthesis of fluorescent MIPs

Labelling MIPs with a fluorescent reporter is a highly effective method for translating the binding event between MIPs and the target into a detectable signal. There are three main approaches to create fluorescent MIPs:

- Incorporating fluorescent particles, such as carbon dots (20,259), quantum dots (34,260–262), metal organic frameworks (84,257) or gold nanoparticles (263) in the core of the polymer, which lies within the surface imprinting technique.

- Using a fluorescent functional co-monomer in the polymerisation mixture (264–266).

- Post imprinting modification of the resulting MIPs with a fluorescent dye (267).

The first two methods are more commonly used and pose less risk of altering the binding properties of the developed MIPs (86).

3.4. Aims and Objectives of this work

The aim of this work was to develop new fluorescent MIPs for the extraction, detection, and quantitation of pepsin enzyme as a salivary biomarker for GERD. For this purpose, the method of incorporating a fluorescent co-monomer in the structure of the developed MIPs was chosen to translate the binding event into readable signal.

In the review of the literature, only one paper described the development of fluorescent MIPs for the detection of pepsin in an ELISA-like format (221). In this study, the analysis of pepsin relied on the interaction between fluorescent pepsin-specific MIPs and magnetic pepsin nanoparticles, which were immobilised on magnetic inserts within the wells of a microtiter plate.

Here, free pepsin in the sample competed with the immobilised pepsin, resulting in a reduction in the binding of fluorescent MIPs to the magnetic inserts and subsequently increasing the central fluorescence of the well. The synthesis of fluorescent MIPs in this study was intricate, involving multiple steps, and lacked certain crucial optimisation and characterisation tests. Therefore, the aims of this work were:

- The development of two new types of fluorescent MIPs for pepsin enzyme using cheap, green, and affordable starting materials.

- Utilisation of fluorescein and rhodamine B as two available and affordable organic fluorescent dyes for the synthesis of the fluorescent MIPs.

- Studying the possibility of a better selectivity and binding capacity that could be offered by rhodamine B in comparison to fluorescein in the resulting MIPs based on the structural merits of the first.

- Optimisation of all the starting materials involved in the synthesis procedure to achieve the highest possible binding capacity.

- Characterisation of the resulting fluorescent MIPs on all aspects including morphology, functionality, thermal stability, and binding performance.

- Comparing fluorescein MIPs and rhodamine B MIPs based on the binding capacity, binding kinetics, selectivity, and other criteria to determine the validity of the theory.

- Application of the resulting fluorescent MIPs for the extraction and quantitation of pepsin from solutions and saliva samples.

3.5. Fluorescein and rhodamine B

Fluorescein is a widely known fluorescent dye that belongs to the xanthene class of dyes which has been used for decades in fluorescent labelling. The incorporation of fluorescein into the structure of MIPs has been successfully reported multiple times to determine different targets, owing to its strong fluorescence and market availability (179). In the paper reported by F. Wang *et al*, fluorescein was applied in the development of fluorescent MIPs for the detection of naproxen, a common non-steroidal anti-inflammatory drug through a simple and catalyst free sol-gel polymerisation method (268). The authors acknowledged that the achieved limit of detection for the developed MIPs was not satisfactory in comparison to other methods reported for naproxen and the use of a more sensitive dye was recommended. Therefore, rhodamine B was suggested as an alternative to fluorescein. Rhodamine B is a fluorescent dye widely used in various applications, ranging from microscopy and flow cytometry to chemical tracing and biological labelling (269). This organic compound belongs also to the xanthene family and is known for its intense pink to red fluorescence under visible light excitation. Rhodamine B's versatility stems from its high quantum yield, photostability, and compatibility with numerous solvents and materials. Rhodamine B was incorporated before in the structure of MIPs as a strong fluorescent dye to bind and detect proteins in water (270).

The structures of fluorescein and rhodamine B shown in **Figure 31** reveal the main differences between the two. The main interesting difference between both dyes is the presence of two diethylamino groups in the structure of rhodamine B.

Since the working pH of synthesis and application ranges from 6 to 8, these two diethylamino groups were assumed to carry a positive charge. Therefore, it was predicted that rhodamine B can provide more interaction with the negatively charged target; pepsin enzyme.
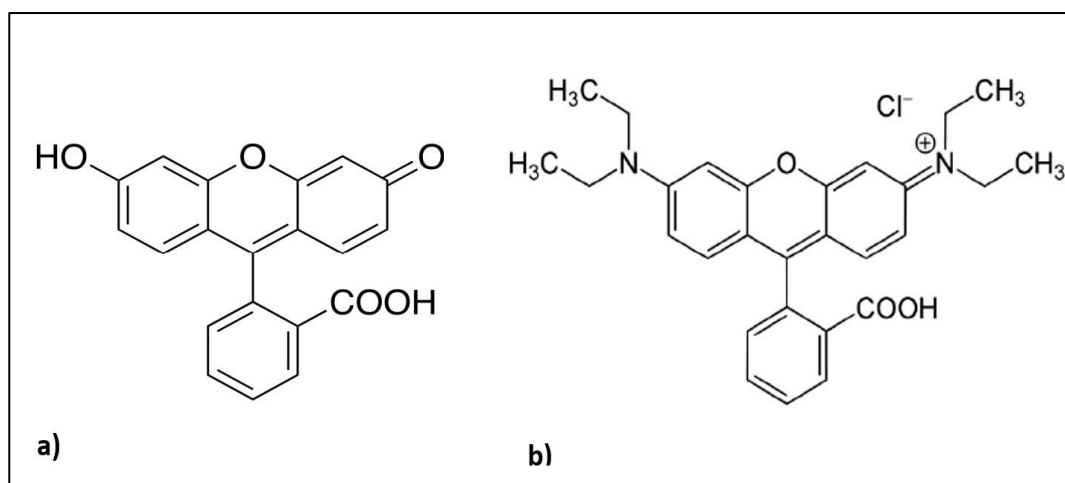
Figure 31. *Chemical structures of a) fluorescein and b) rhodamine B organic dyes.*

3.6. Experimental

3.6.1. Materials and instrumentation

Tetraethyl orthosilicate for synthesis (TEOS), sodium dodecyl sulphate 99% (SDS), (3-aminopropyl)triethoxysilane 98% (APTES), deionised water, absolute ethanol, sodium chloride 99.5%, phosphate buffered saline (PBS) tablets (pH 7.2), human pepsin, human lipase, human amylase, thrombin, and lysozyme were all procured from ThermoFisher Scientific, UK. Fluorescein-5-isothiocyanate 98% (FITC) and rhodamine B isothiocyanate 98% (RITC) were purchased from Fluorochem, UK.

Fluorescence measurements were carried out using a Cary Eclipse fluorescence spectrometer (Agilent, UK), running on a Cary Eclipse software version 1.1(132). UV measurements were conducted using a Cary UV-Vis Compact, operating on a Cary UV Workstation™, software version 1.0.1284 (Agilent, UK). Fluorescence detection was carried out with a UV lamp (UVitec, UK) at a wavelength of 365 nm. Thermal characterisation including thermogravimetric experiments was performed on a Mettler Toledo TGA/DSC 1 Series (UK) – running on STARe™ software Version 10.00, and DSC was performed on a TA Instruments DSC25 Series, running on Trios™ software, v5.4.0.300. Infra-red analysis was done using a ThermoFisher (UK) Scientific Nicolet iS5 Fourier transform infrared spectrometer running on OMNIC™ software. ^{13}C Nuclear magnetic resonance (NMR) analysis was carried out using a Bruker Avance III 600 two channel FTNMR spectrometer operating at 600 MHz and utilising TopSpin™ software for data analysis. SEM was used to visualise the resulting polymers using a Zeiss Evo-50 electron microscope, operating on Smart SEM™ software. Weighing of chemicals was performed using Sartorius handy balance-H51 (Hannover, Germany). Data processing and graph plotting were executed using Origin™ 8.5 software (Origin Lab Corporation, North Hampton, USA).

3.6.2. Synthesis of fluorescent co-monomers (FITC-APTES, RITC-APTES)

Two fluorescent co-monomers were prepared independently from a simple coupling reaction between APTES and FITC or RITC according to a previously reported method (271). Each dye (0.04 mmol) was dissolved in 8 mL absolute ethanol and 0.04 mmol of APTES was added to the solution and continuously stirred for 24 h.

The obtained products were used without further purification. The chemical reactions for both coupling reactions are shown in **Scheme 1**.
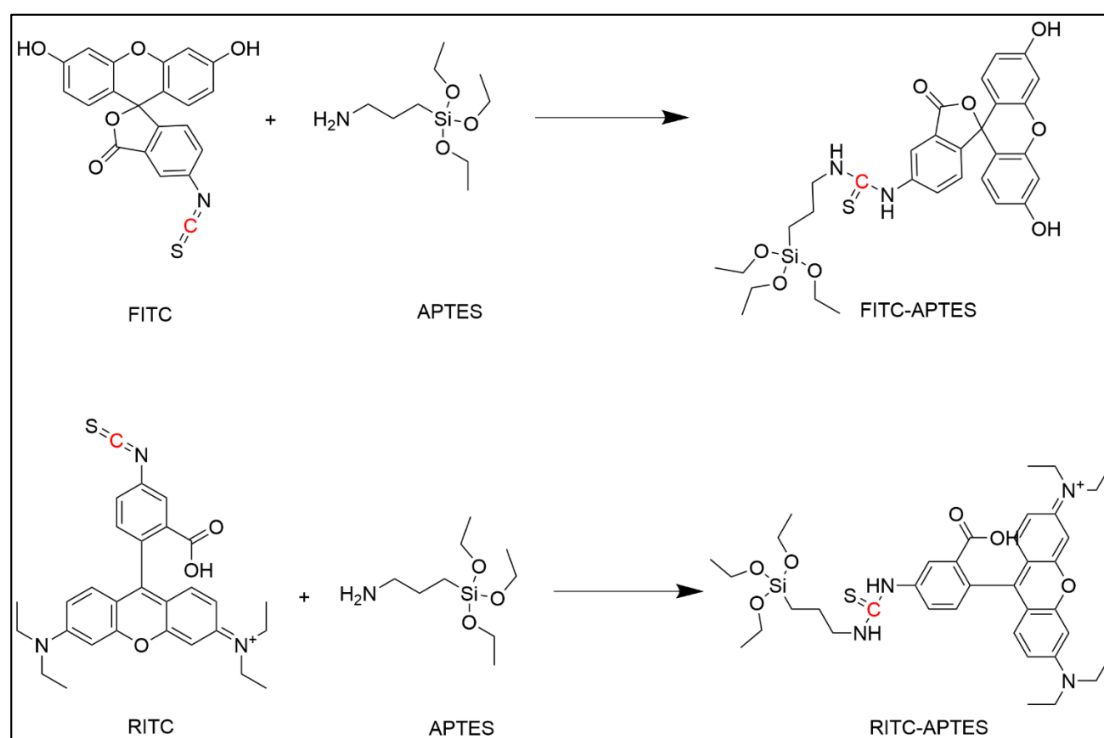
Scheme 1 . The reaction between FITC or RITC and APTES to form the fluorescent co-monomers.

3.6.3. Preparation of fluorescent MIPs

The synthesis of fluorescent MIPs was conducted via a straightforward sol-gel polymerisation, utilising APTES as the functional monomer and TEOS as the cross-linker. The quantities and volumes of the reagents were meticulously optimised to achieve optimal binding. The optimised procedure for fluorescein-dyed MIPs (FMIPs) manufacture was as follows: the target analyte pepsin (15 mg) was dissolved in 8 mL of PBS buffer (pH 7.2), followed by the addition of 0.50 mL of APTES. This mixture was stirred for 30 minutes for pre-assembly. Next, 9 mL of the fluorescent co-monomer (FITC-APTES) was added, and the mixture was stirred for another 30 minutes.

Finally, 0.9 mL of TEOS, dissolved in 3.5 mL of absolute ethanol, was added dropwise. The reaction mixture was then sealed under a nitrogen atmosphere and continuously stirred for 48 hours.

For rhodamine B-dyed MIPs (RMIPs), a similar procedure was followed with slight variations in reagent volumes. Specifically, 15 mg of pepsin was dissolved in 8 mL of PBS buffer (pH 7.2), followed by the addition of 0.75 mL of APTES and stirred for 30 minutes. Then, 8 mL of the fluorescent co-monomer (RITC-APTES) was added, and the mixture was stirred for another 30 minutes. Finally, 0.9 mL of TEOS, dissolved in 3.5 mL of absolute ethanol, was added dropwise. The reaction mixture was sealed under nitrogen and stirred continuously for 48 hours.

Fluorescent NIPs were also prepared for both FMIPs and RMIPs by omitting the addition of pepsin for comparison purposes. The resulting MIPs and NIPs were rinsed twice with deionised water and ethanol to remove any remnants of the starting materials and oligomers. To eliminate the target from the imprinted cavities, both fluorescent MIPs were washed with a 1% w/v sodium dodecyl sulphate (SDS)/10% v/v acetic acid solution for 4 hours, followed by multiple washes with deionised water to remove traces of the washing solution. UV spectrometry was employed to ensure complete washing by testing fragments of the washing solution. The final polymers were dried under vacuum at 60°C, finely ground, and stored in dark containers to prevent photobleaching.

3.6.4. Protein adsorption experiments

To assess the success of the imprinting process, binding assays were conducted for all the developed polymers using a known concentration of pepsin. The binding experiments involved incubating 50 mg of the polymers with 20 mL of a 1 mg mL^{-1} pepsin solution for 2 hours (for fluorescein-dyed polymers) and 1 hour (for rhodamine B-dyed polymers). After the optimal binding time, the solutions were centrifuged at 4500 rpm for 10 minutes. The pepsin concentration in the supernatant was measured by UV spectrometry against a blank of deionised water incubated with MIPs or NIPs for the same amount of time. To determine the binding capacity of MIPs and NIPs, the amount of pepsin adsorbed per gram of polymer was calculated using equation 8:

$$Q = (Ci - Ct).V/m \qquad \text{(eq. 8)}$$

where, Q (mg g^{-1}) is the quantity of pepsin in milligrams adsorbed per gram of polymer, Ci (mg mL^{-1}) is the starting concentration of pepsin, Ct (mg mL^{-1}) is the remaining concentration of pepsin after incubation time (t), V (mL) is the volume of pepsin solution, and m (g) is the mass of MIPs or NIPs applied in the experiment. Overall, the experiments were performed in triplicate to validate the precision of the results.

3.6.5. Characterisation of the fluorescent MIPs

Characterisation of the developed fluorescent polymers was essential to compare the properties of FMIPs and RMIPs, particularly their different binding parameters. The morphology of the polymers was assessed using SEM imaging, which also provided an estimation of the particle size. ^{13}C NMR was conducted on FITC, RITC, FITC-APTES, and RITC-APTES in deuterated DMSO to verify the formation of the thiourea linkage between FITC or RITC and APTES in the fluorescent co-monomers.

FT-IR spectra (4000 – 500 cm^{-1}) were collected for FITC, RITC, FMIPs, FNIPs, RMIPs, and RNIPs to compare the prominent bands, ensure template removal, and confirm the absence of any residual starting materials.

TGA and DSC were performed on FITC, RITC, FMIPs, FNIPs, RMIPs, and RNIPs. Data from TGA and DSC can confirm complete polymerisation, detect any unreacted starting materials, and determine the content of adsorbed moisture. TGA was conducted over a temperature range from 25 to 650°C at a heating rate of 10°C min^{-1} with a nitrogen gas flow rate of 50 mL min^{-1}. DSC was performed over a temperature range from 25 to 350°C at a heating rate of 10°C min^{-1}.

To determine the order of the binding kinetics, rebinding experiments were performed on the developed polymers at increasing time intervals. Specifically, 50 mg of the fluorescent polymers were incubated with 20 mL of a 1 mg mL^{-1} pepsin solution for 0, 1, 2, 4, 6, and 8 hours. The amount of pepsin adsorbed per gram (Q) for each time interval was plotted against time to determine the order of the binding kinetics.

Additionally, rebinding experiments were conducted by applying different concentrations of pepsin to determine the binding isotherm model. Thus, 50 mg of the fluorescent polymers were incubated with 20 mL of pepsin solutions in the concentration range of 0.2 to 1.5 mg mL^{-1} for 1 hour (for RMIPs and RNIPs) and 2 hours (for FMIPs and FNIPs). The amount of pepsin adsorbed per gram (Q) for each concentration was plotted against concentration to depict the binding isotherm model.

To verify the binding selectivity of FMIPs and RMIPs, their binding was compared to that of their corresponding FNIPs and RNIPs.

The imprinting factor (IF) was calculated by dividing the value of Q for MIPs by that of NIPs. Since the target analyte in this work is salivary pepsin, it was also necessary to test the selectivity of the developed fluorescent polymers against other proteins that may be present with pepsin in human saliva. Amylase and lipase, along with other proteins, were selected due to their abundance in saliva and potential cross-reactivity. Therefore, a similar binding assay as for pepsin was performed on the competitor enzymes. Herein, 20 mL of a 1 mg mL^{-1} solution of each enzyme was incubated with 50 mg of the fluorescent polymers for 1 hour (for RMIPs and RNIPs) and 2 hours (for FMIPs and FNIPs). The amount bound per gram (Q) was calculated for each enzyme and compared to that of pepsin.

3.6.6. Stability testing

The developed FMIPs and RMIPs were tested for stability and shelf life to verify their suitability for long-term use. The FMIPs and RMIPs were stored in dark containers for periods of 0, 1, 3, and 6 months. Additionally, other batches of FMIPs and RMIPs were stored at temperatures of 10, 25, 35, and 45°C for 1 month to assess stability against varying storage temperatures. After these storage periods, the binding capacity for pepsin was tested using the previously mentioned protein binding assay procedure.

3.6.7. Fluorescence measurements

The procedure for measuring the fluorescence intensity of the developed fluorescent polymers was carefully optimised to get the highest possible sensitivity for FMIPs and RMIPs.

Consequently, a (3 mg mL^{-1}) suspension of the fluorescent polymers was prepared in PBS buffer (pH 7.2), centrifuged to remove coagulated particles, and measured at an excitation wavelength (λ_{exc}) of 471 nm for FMIPs and 546 nm for RMIPs, and an emission wavelength (λ_{em}) of 515 nm for FMIPs and 585 nm for RMIPs, at PMT voltage of 600 V and slit width of 10 nm for both excitation and emission. Different concentrations of pepsin were added to the suspension of polymers for the optimal binding time of 2 hours or 1 hour for FMIPs and RMIPs respectively, with continuous shaking. Fluorescence intensity was measured for each sample and plotted against the concentration of pepsin to establish the linear range and calculate the regression equation.

3.6.8. Application to measuring pepsin in human saliva

This study received ethical approval from the Kingston University Ethics Committee (Ethics Code 2895) and was conducted in accordance with the UK Human Tissue Act (HTA) 2004. Saliva samples were collected from one participant, centrifuged at 4500 rpm for 30 minutes, and used immediately. Consequently, saliva samples (100 µL) were spiked with increasing concentrations of pepsin in the range of 0 to 42.85 µmol L^{-1}. One mL of the FMIP or RMIP suspension (3 mg mL^{-1}) was added to each sample and incubated for the optimal binding time. Each sample was measured in triplicate using a spectrofluorometer to ensure the precision of the results.

3.7.   Results and Discussion

3.7.1. Preparation of the fluorescent MIPs

A neutral pH was chosen as the working pH since pepsin is detected in saliva which has a neutral pH range (6.2-7.6) (238). As pictured in **Figure 32**, rhodamine B has two diethylamino groups in its structure which at the working pH (7.2) were predicted to be positively charged. On the other hand, pepsin has a relatively low isoelectric point of 3.24 (243), which means that it would be negatively charged at pH 7.2. Therefore, a strong electrostatic interaction was expected between rhodamine B based co-monomer and pepsin, unlike fluorescein which can only interact with pepsin through hydrogen bonds through its carboxylic group.
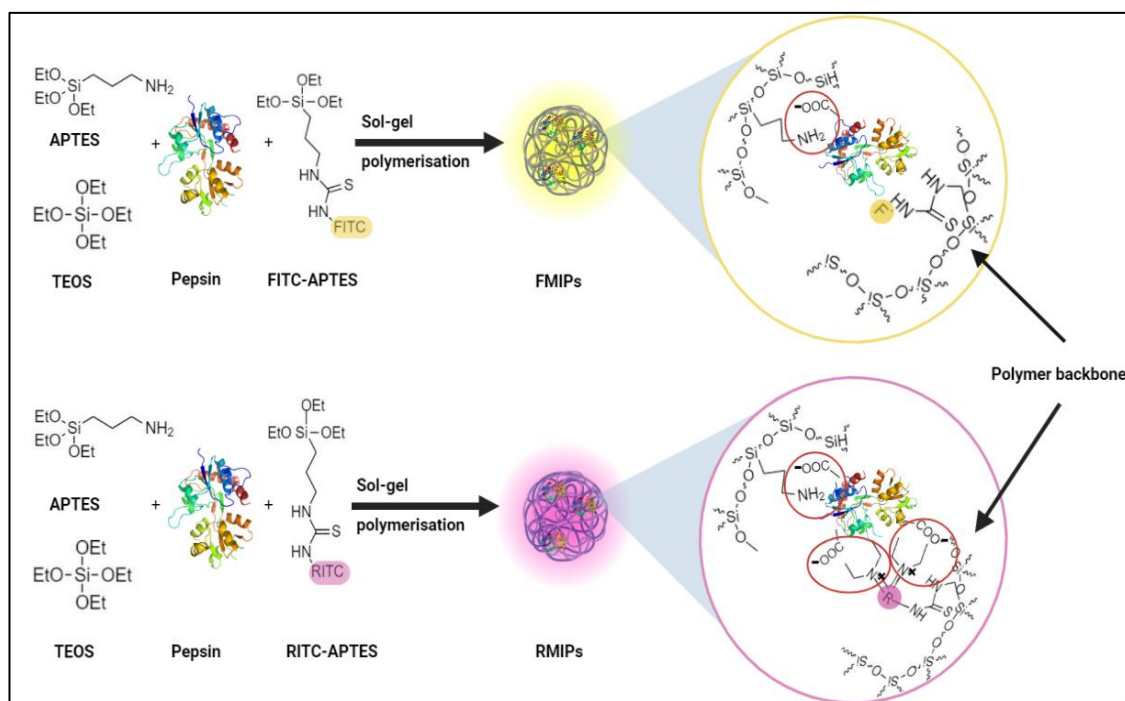
Figure 32. *Schematic presentation of the polymerisation and interaction points between pepsin and fluorescein or rhodamine B in the polymer backbone.*

APTES was selected as a functional monomer due to its capability to interact with the amino and carboxylic groups in the backbone of the pepsin molecule through hydrogen bonds. Additionally, APTES was coupled with FITC or RITC to produce the fluorescent co-monomers, which can also form hydrogen bonds with the pepsin. Consequently, after washing the developed FMIPs or RMIPs and removing the target, numerous binding sites complementary to pepsin would be generated. Furthermore, fluorescein or rhodamine B molecules would be distributed within the polymer matrix, with a high prevalence in the binding sites due to the pre-existing hydrogen and/or electrostatic bonds formed with the target during polymerisation. As a result, the binding and the release of pepsin to the binding sites would cause a significant change in fluorescence intensity, which could be recorded to detect the presence of pepsin and determine its concentration. Additionally, a slight colour difference between MIPs and their corresponding NIPs was observed, with MIPs appearing consistently darker than NIPs, as shown in **Figure 33**. This can be attributed to the higher concentration of the fluorescent co-monomer in the polymeric matrix of MIPs compared to NIPs, consistent with previous observations for fluorescein imprinted polymers prepared for naproxen (268). Since the pepsin molecule can form multiple bonds with the fluorescent co-monomer, it was anticipated that the presence of pepsin resulted in higher polymerisation efficiency of FITC-APTES or RITC-APTES into MIPs, leading to a darker colour.
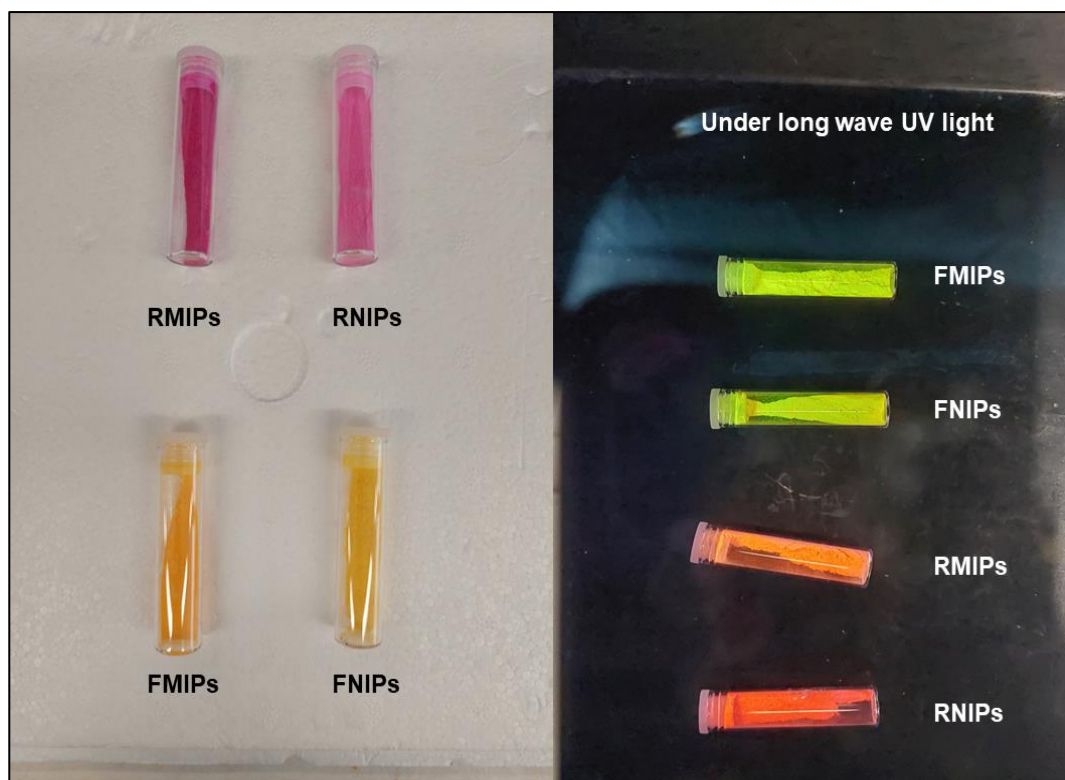
Figure 33. Pictures of the developed FMIPs, FNIPs, RMIPs, and RNIPs on the bench and under long wave UV light (365 nm).

All the reagents used in the synthesis procedure were thoroughly investigated to study their effect on the binding capacity (Q). Various volumes of APTES, FITC-APTES, or RITC-APTES, and TEOS were tested, along with different pre-assembly times and varying amounts of pepsin, to fully optimise the procedure. **Figures 34** and **35** display the optimum values obtained from the various optimisation experiments for both fluorescein-dyed polymers and rhodamine B-dyed polymers, respectively. Additionally, testing different washing solutions such as sodium chloride (0.5 mol L^{-1}), phosphate buffer (0.05 mol L^{-1}, pH 7.2), and a solution of 1% w/v SDS/10% v/v acetic acid was necessary to identify the solution that removes all traces of the template. This was crucial because incomplete template removal results in template bleeding, which can cause significant errors in the anticipated results and/or blockage of the available binding sites, leading to a reduction in sensitivity.

Therefore, after meticulous testing of various washing solutions and washing times, a solution of 1% w/v SDS/10% v/v acetic acid was found to be the most effective in removing the template within 4 hours.
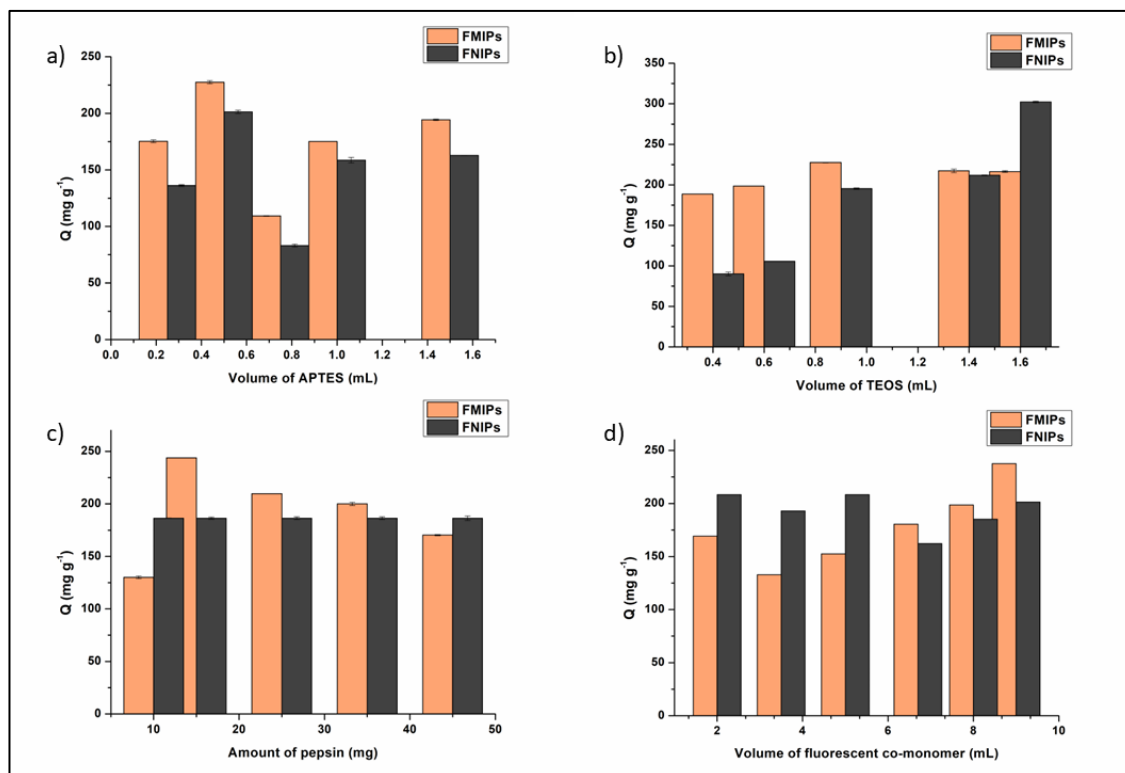
Figure 34. *Results of the different optimisation experiments for FMIPs and their corresponding FNIPs a) volume of APTES, b) volume of TEOS, c) amount of pepsin, and d) volume of fluorescent co-monomer (average of triplicate measurements).*
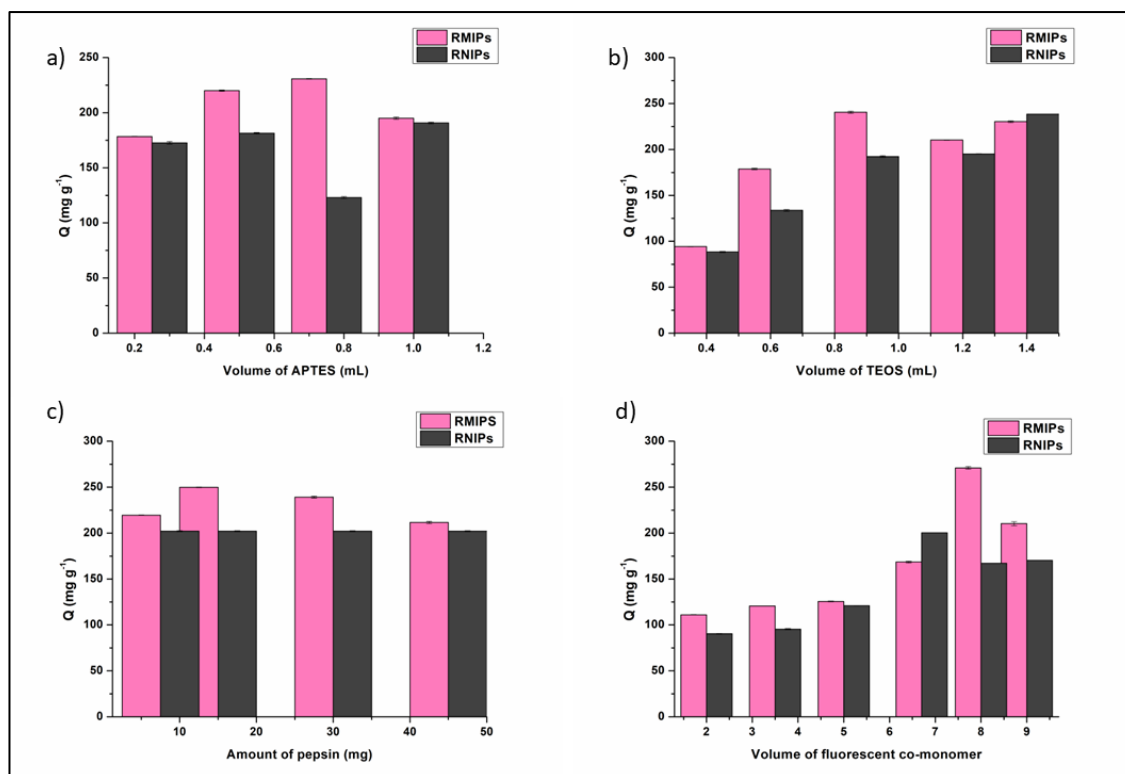
Figure 35. Results of the different optimisation experiments for RMIPs and their corresponding RNIPs a) volume of APTES, b) volume of TEOS, c) amount of pepsin, and d) volume of fluorescent co-monomer (average of triplicate measurements).

3.7.2. Characterisation of the fluorescent MIPs

3.7.2.1. Morphological characterisation

SEM images were obtained for FMIPs, FNIPs, RMIPs, and RNIPs and are presented in **Figure 36**. As shown in the images, the produced polymers are not perfectly spherical, exhibiting a rough surface with some scattered, coagulated areas. This is a result of using the bulk polymerisation technique, which does not allow for precise control over the size or the morphology of the synthesised polymers. An approximate estimation of the particle size from the SEM images indicated that the particles ranged from 0.5 to 2.0 microns, which is typical for bulk polymerisation.
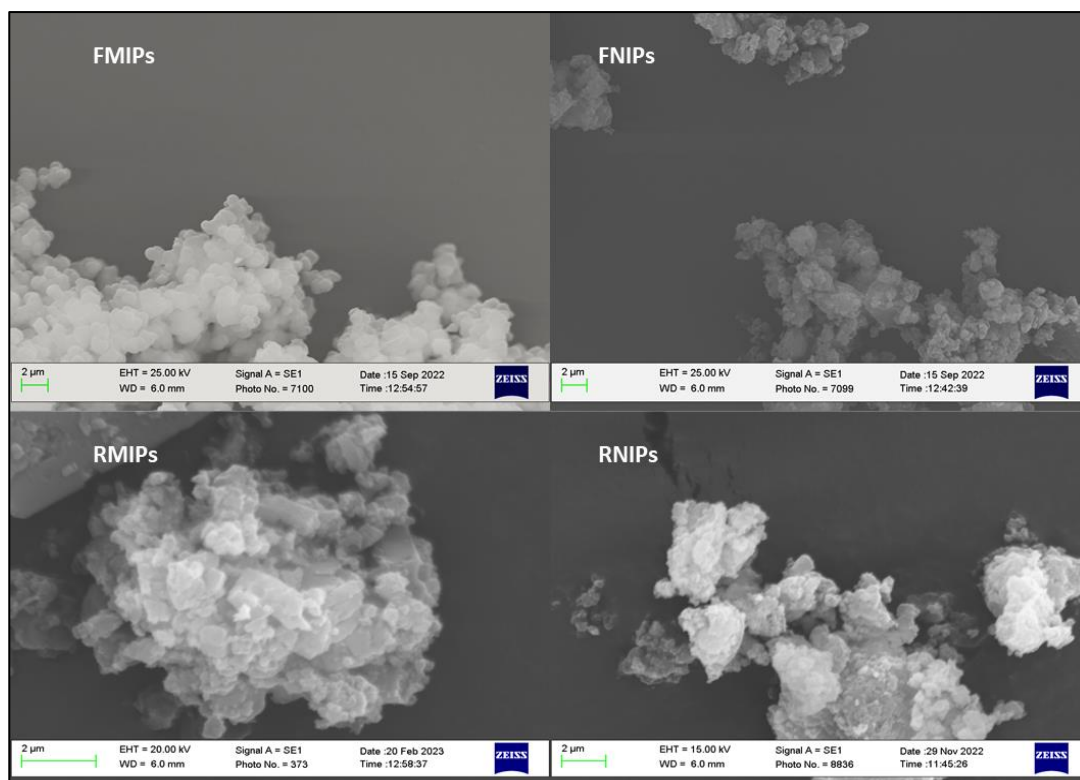
Figure 36. *SEM pictures of FMIPs, FNIPs, RMIPs, and RNIPs (average diameter 1 micron).*

To assess the impact of particle size variability on the fluorescence signal reproducibility, a one-way analysis of variance (ANOVA) test was performed. A batch (3 mg mL^{-1}) of each of the FMIPs, FNIPs, RMIPs, and RNIPs was prepared, and the fluorescence signal was measured three times for each solution. This experiment was repeated daily over a week. The data collected over the seven days (seven groups) for each polymer type were analysed using ANOVA, with the results displayed in **Table 11**. Since the F-statistic values were lower than the critical values, the differences between the group means were not statistically significant. This suggested that there was insufficient evidence to reject the null hypothesis, indicating that there were no meaningful differences between the group means across all polymers. In other words, the observed variation was likely due to random chance rather than actual differences between the groups.

Table 11. ANOVA parameters for testing the effect of particle size variability on the reproducibility of the fluorescence signal for FMIPs, FNIPs, RMIPs, and RNIPs.

Polymer	SSB	SSW	SST	F calculated	F critical (α= 0.05)
FMIPs	47.195	180.125	227.321	0.611	2.847
FNIPs	3.619	13.163	16.782	0.6415	2.847
RMIPs	7.272	24.678	31.950	0.687	2.847
RNIPs	6.404	60.741	67.146	0.246	2.847

SSB: sum of squares between groups, SSW: sum of squares within groups, SST: sum of squares for total data, F calculated: is the ratio of the mean square between groups to the mean square within groups, F critical: s the critical value of the F-distribution for the chosen significance level (α=0.05).

3.7.2.2. Chemical characterisation

To verify the formation of a thiourea linkage between FITC or RITC and APTES, ^{13}C NMR was conducted on both the reactants and the products. The analysis focused on the chemical shift of the carbon atom in the isothiocyanate group, which converted to a thiourea bond after reacting with the amino group of APTES. In **Figure 37**, it was observed that the chemical shift of the carbon atom in the isothiocyanate group of FITC changed from (δ=138.2, s) to (δ=180.7, s) due to the formation of a new single bond with the amino group of APTES. Similar changes were seen for RITC in **Figure 38**, where the chemical shift of the carbon atom in the isothiocyanate group changed from (δ=137.9, s) to (δ=179.3, s).
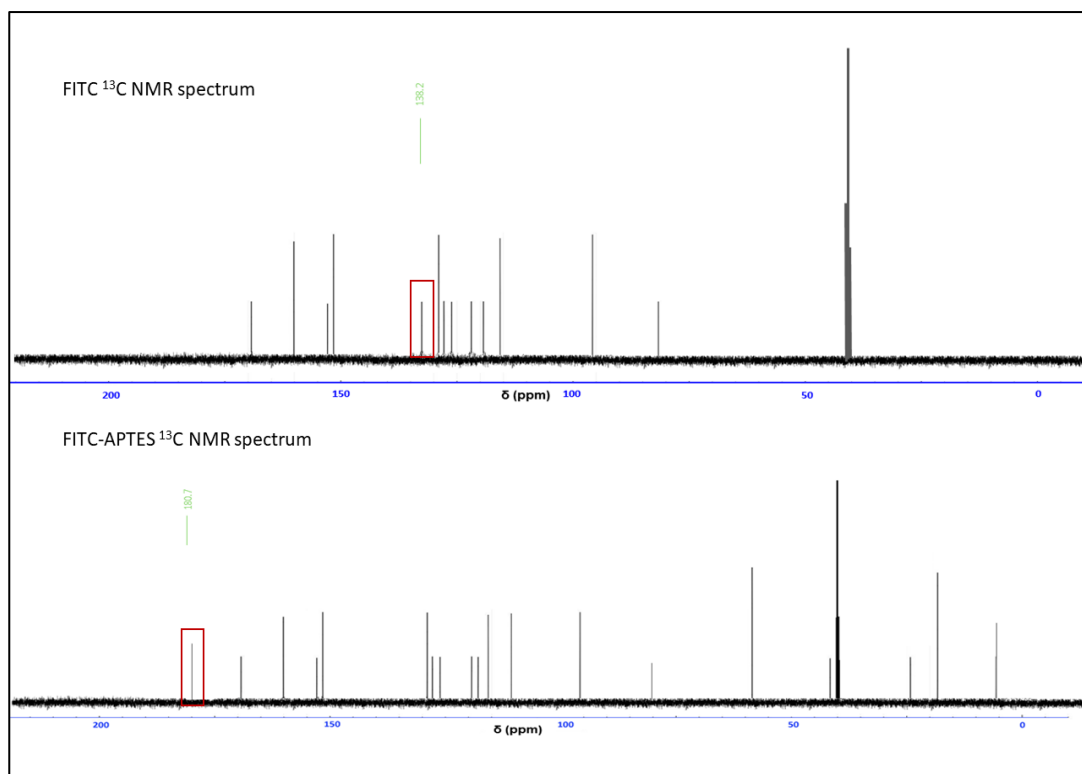
Figure 37. *^{13}C NMR spectra of FITC and FITC-APTES.*
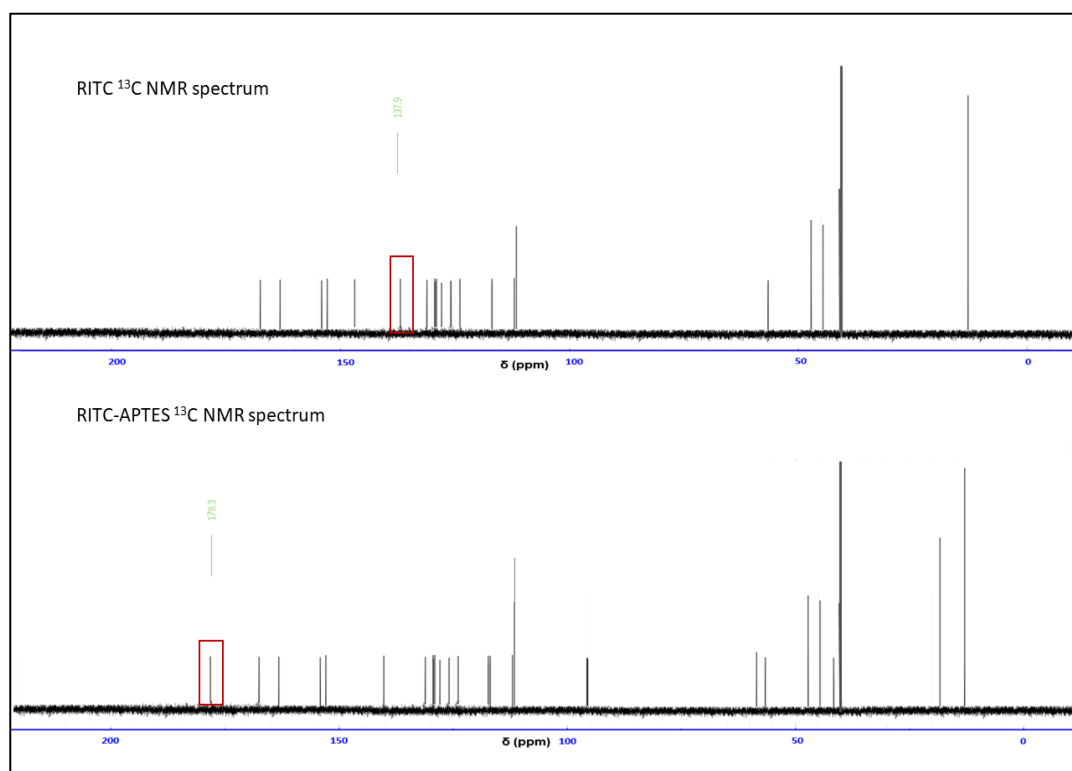
Figure 38. *^{13}C NMR spectra of RITC and RITC-APTES.*

The synthesised polymers and the organic dyes were characterised using IR spectroscopy to confirm the complete incorporation of the fluorescent dyes into the developed polymers. The spectra are shown in **Figure 39**. Both FITC and RITC displayed a distinct peak at approximately 2010 cm^{-1}, characteristic of the isothiocyanate group. This peak was not present in the spectra of the resulting polymers, verifying the incorporation of the dye into the polymeric structure. Additionally, the spectra of FMIPs and FNIPs, as well as RMIPs and RNIPs, were nearly identical, indicating no structural difference between them. Two peaks at 2922 cm^{-1} and 2852 cm^{-1} could be assigned to the C − H bonds asymmetric and symmetric stretching, respectively. The absence of peaks in the range of 3000 to 3300 cm^{-1}, characteristic of amino and carboxylic groups, confirmed the complete removal of pepsin from the binding sites of both MIPs (272).
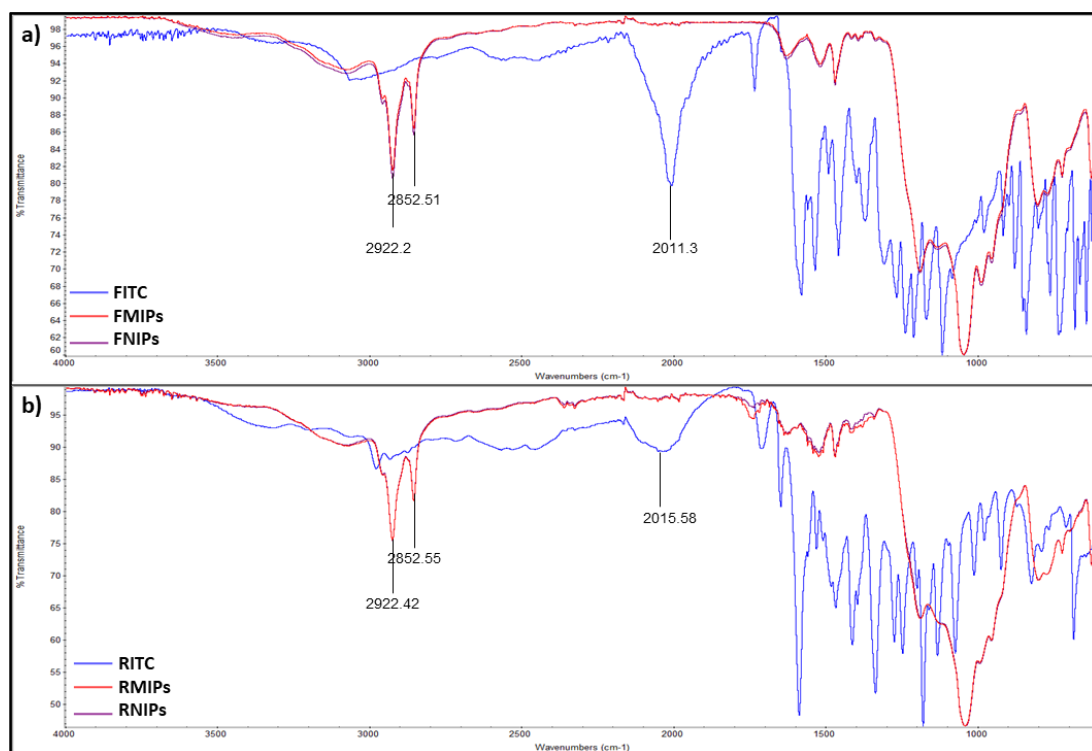
Figure 39. *FT-IR spectra for a) FITC, FMIPs, & FNIPs and b) RITC, RMIPs, & RNIPs.*

3.7.2.3. Thermal characterisation

DSC thermograms (**Figures 40a1 & 40a2**) collected for the organic dyes and their polymers confirmed the incorporation of the dyes in the structure of the produced polymers. The DSC thermogram of FITC showed only an exothermic peak around 290°C, yet DSC curves of both FMIPs and FNIPs showed only one melting peak at around 320°C, indicating the absence of any remaining FITC. Similarly, the DSC thermogram for RITC showed a melting peak of 210°C, however, the DSC graphs of both RMIPs and RNIPs showed only one endothermic melting peak at 320°C, which ascertained the absence of any residual fluorescent dye. This data was further verified with TGA (**Figures 40b1 & 40b2**), which showed no notable differences in the decomposition pattern between FMIPs and FNIPs and RMIPs and RNIPs, due to their structural similarity. Nonetheless, their decomposition models are obviously different from that of the fluorescent dyes.
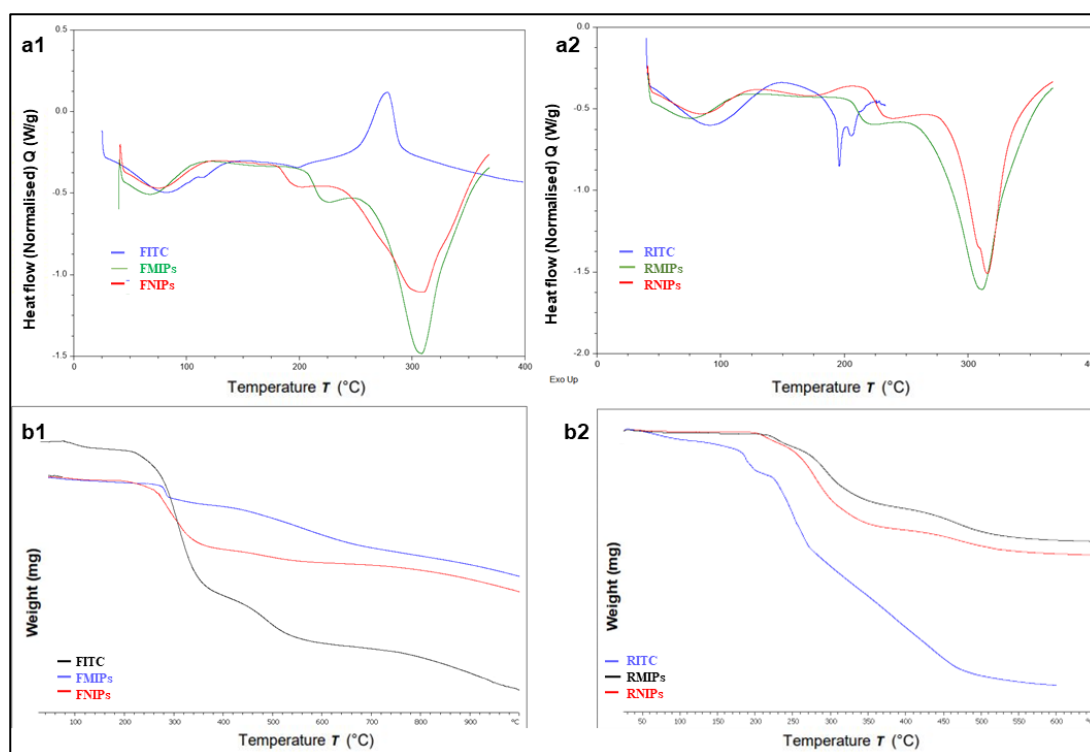
Figure 40. *DSC thermograms for a1) FITC, FMIPs, & FNIPs, a2) RITC, RMIPs, & RNIPs and TGA graphs for b1) FITC, FMIPs, & FNIPs, b2) RITC, RMIPs, & RNIPs.*

3.7.2.4. Functional characterisation

The results of the binding kinetics experiments are graphically represented in **Figures 41a and 41b**. A notable difference was observed between fluorescein-dyed polymers and rhodamine B-dyed polymers. The peak binding for FMIPs occurred after 2 hours, whereas RMIPs achieved maximum binding after just 1 hour. The faster binding kinetics of RMIPs could be attributed to the presence of two diethylamino groups in the structure of rhodamine B, whose positive charge interacted significantly with the negatively charged pepsin molecule, resulting in quicker binding kinetics. Additionally, the Q value (mg g^{-1}) at the maximum binding time for RMIPs (256 mg g^{-1}) was higher than the corresponding Q value for FMIPs (217 mg g^{-1}), further verifying the role of the diethylamino groups in enhancing pepsin binding. To understand the mechanism of pepsin binding to the developed polymers, pseudo-first order and pseudo-second order kinetics parameters were used to fit the adsorption data. As shown in **Table 12**, both rhodamine B and fluorescein imprinted polymers followed a pseudo-second-order model, confirming that the binding followed a chemical adsorption mechanism.
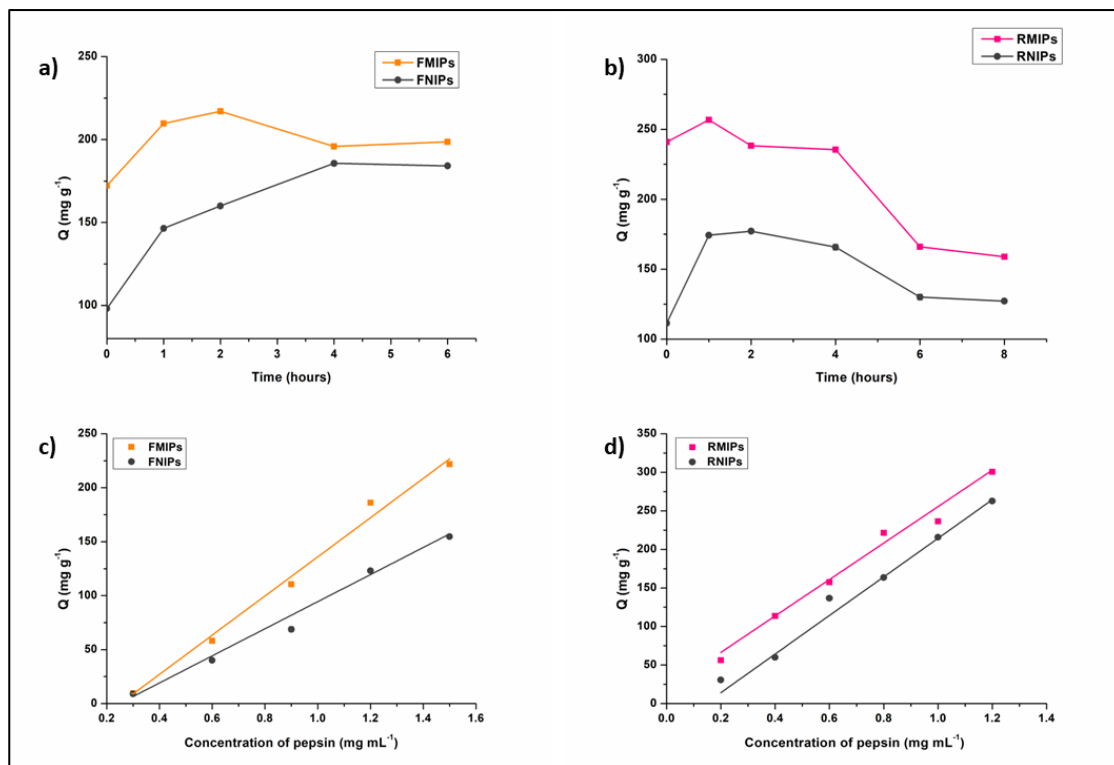
Figure 41. *Binding kinetics for a) FMIPs & FNIPs, and b) RMIPs & RNIPs, and binding isotherm for c) FMIPs & FNIPs, and d) RMIPs & RNIPs (average of triplicate measurements each).*

Table 12. *Binding kinetics parameters for the fluorescent MIPs and NIPs applying two binding orders.*

Pseudo first order parameters

FMIPs			FNIPs		
K_1 (min^{-1})	Qe (mg g^{-1})	R^2	K_1 (min^{-1})	Qe (mg g^{-1})	R^2
0.00077	25.432	0.0009	0.0309	81.183	0.872
RMIPs			**RNIPs**		
K_1 (min^{-1})	Qe (mg g^{-1})	R^2	K_1 (min^{-1})	Qe (mg g^{-1})	R^2
0.033	8.11	0.66	0.0173	10.175	0.163

Pseudo second order parameters

FMIPs			FNIPs		
K_2 (g mg^{-1} min^{-1})	Qe (mg g^{-1})	R^2	K_2 (g mg^{-1} min^{-1})	Qe (mg g^{-1})	R^2
0.0867	196.09	0.9989	0.02809	188.68	0.9961
RMIPs			**RNIPs**		
K_2 (g mg^{-1} min^{-1})	Qe (mg g^{-1})	R^2	K_2 (g mg^{-1} min^{-1})	Qe (mg g^{-1})	R^2
0.0136	156.25	0.9866	0.022	125	0.9759

K1 and K2 are the first and second order rate constants respectively, Qe is the quantity of pepsin adsorbed per gram of polymer at equilibrium, and R^2 is the linearity coefficient.

The graphical representation of the binding isotherm for both fluorescein and rhodamine B polymers (**Figures 41c** and **41d**) demonstrated a linear relationship between the binding capacity (Q) and the concentration of pepsin. The Freundlich isotherm, and the Langmuir isotherm models were applied to the binding isotherm data and results are shown in **Table 13**. From the computed R^2 values, the Freundlich binding isotherm model was a good fit for fluorescein dyed polymers, which suggested that the binding was in multiple layers on a heterogeneous surface. On the contrary, the Langmuir binding model was a better fit for rhodamine B dyed polymers, which indicated that binding occurred in a monolayer over a homogenous surface, which again proved the better performance of RMIPs.

Table 13. *Adsorption isotherm parameters of the fluorescent MIPs and NIPs applying two models.*

Langmuir isotherm

FMIPs				FNIPs			
K_L (L mg^{-1})	Q_{max} (mg g^{-1})	RL	R^2	K_L (L mg^{-1})	Q_{max} (mg g^{-1})	RL	R^2
0.002	19.45	1.002	0.9055	0.00158	25.22	1.001	0.9460
RMIPs				**RNIPs**			
K_L (L mg^{-1})	Q_{max} (mg g^{-1})	RL	R^2	K_L (L mg^{-1})	Q_{max} (mg g^{-1})	RL	R^2
1.241	830.67	0.573	0.9887	1.226	174.093	3.782	0.9360

Freundlich isotherm

FMIPs			FNIPs		
n	K_F	R^2	n	K_F	R^2
0.381	349.869	0.9599	0.470	156.50	0.9428
RMIPs			**RNIPs**		
n	K_F	R^2	n	K_F	R^2
1.285	553.384	0.9615	0.683	658.99	0.9117

KL and KF are the Langmuir constant and Freundlich constant respectively, Q_{max} is the theoretical maximum adsorbed concentration, RL is the separation factor (1/1+C$_{eq}$.KL), n is the variation trend coefficient for the adsorption isotherm, and R^2 is the linearity coefficient.

A binding selectivity assay towards pepsin was conducted for both FMIPs versus FNIPs, and for RMIPs versus RNIPs, and the imprinting factor (IF) was deducted using the equation.

$$IF = \frac{Q_{MIPs}}{Q_{NIPs}} \qquad \text{(eq.9)}$$

At a concentration of 1 mg mL^{-1} of pepsin, the IF values were 1.13 for fluorescein dyed polymers and 1.89 for rhodamine B dyed polymers, which further proved the higher selectivity of RMIPs compared to FMIPs.

Furthermore, selectivity was assessed against lipase and amylase due to their coexistence with pepsin in human saliva along with lysozyme and thrombin as other proteins. The results shown in **Figure 42** demonstrated remarkable selectivity towards pepsin in comparison to other proteins for both fluorescein and rhodamine B dyed polymers, while again RMIPs showed greater selectivity, indicated by the values of the separation factor (α) calculated using the formula.

$$\alpha = \frac{Q_{MIP.target}}{Q_{MIP.competitor}} \qquad \text{(eq.10)}$$

Herein, the values of α for FMIPs were 1.94 and 2.87 for amylase and lipase respectively. As for RMIPs, the values of α were 2.09 and 2.21 for amylase and lipase respectively.
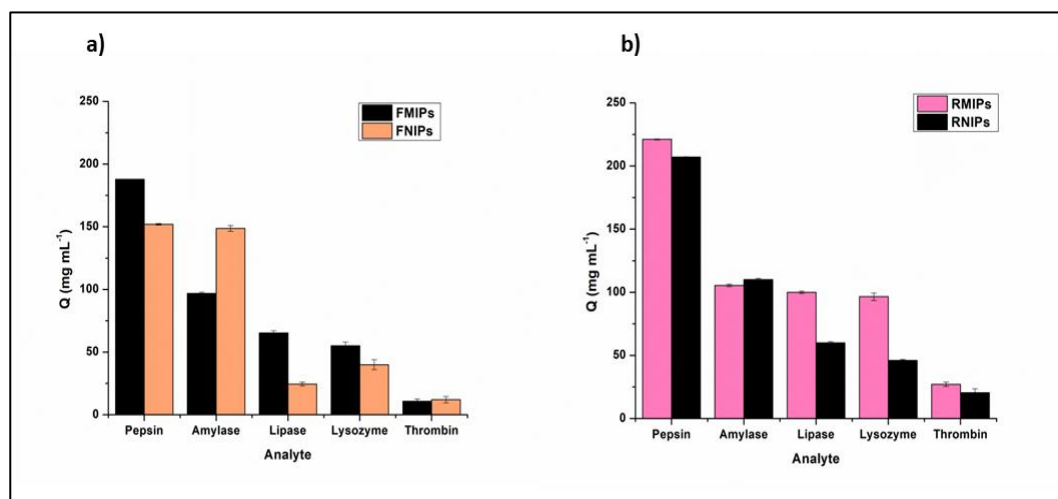
Figure 42. Selectivity studies of a) FMIPs & FNIPs, and b) RMIPs & RNIPs for pepsin against other proteins(average of triplicate measurements).

3.7.3. Stability testing

The results of the stability testing conducted over periods of 0, 1, 3, and 6 months showed a very slight decline in the binding capacity over time for both FMIPs and RMIPs. Similar outcomes were observed when testing at low and high temperatures, with the binding capacity for both FMIPs and RMIPs remaining nearly constant across all temperatures. These findings are collectively depicted in **Figure 43**. The results demonstrated the higher physical stability of MIPs compared to conventional antibodies.
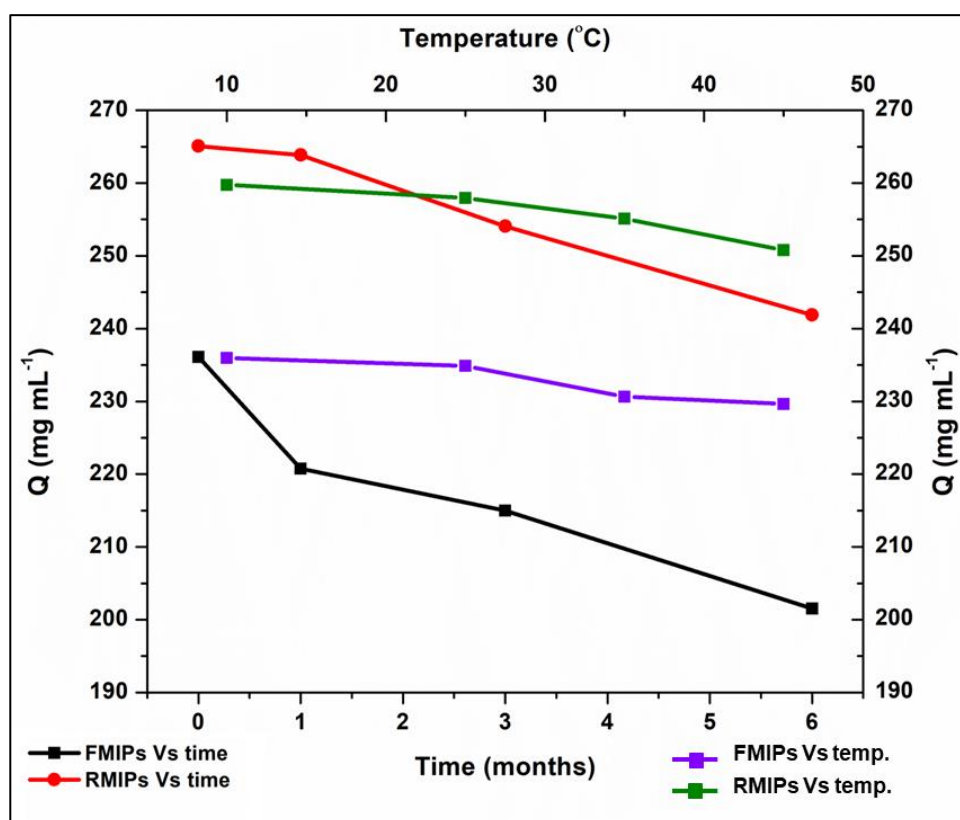
Figure 43. *Stability of FMIPs and RMIPs against time and temperature (average of triplicate measurements).*

3.7.4. Mechanism of fluorescence quenching

To study the mechanism of fluorescence quenching observed for FMIPs and RMIPs in the presence of pepsin, Stern-Volmer equation was used.

$$\frac{F0}{F} = 1 + Ksv[Q] \qquad \text{(eq. 11)}$$

In which F0 is the fluorescence intensity of the fluorophore without the quencher, F is the fluorescence intensity after quenching, Ksv is the Stern-Volmer constant, and Q is the quencher concentration. Ideally, a linear relationship observed in the Stern-Volmer plot (F0/F) versus the quencher concentration ([Q]) indicates the dominance of a single quenching process (dynamic quenching). Deviations from linearity in Stern-Volmer plots normally indicate the involvement of dual quenching mechanisms simultaneously, where dynamic quenching and static quenching play roles (273,274). As observed in **Figure 44**, a linear relationship between F0/ F and the concentration of pepsin (the quencher) was observed for both FMIPs (**figure 44a**) and RMIPs (**figure 44b**). This linear relationship reflected a dynamic quenching of fluorescence in which the quencher interacted with the fluorophore at the excited state via collisions leading to return to the ground state through non-radiative pathways.
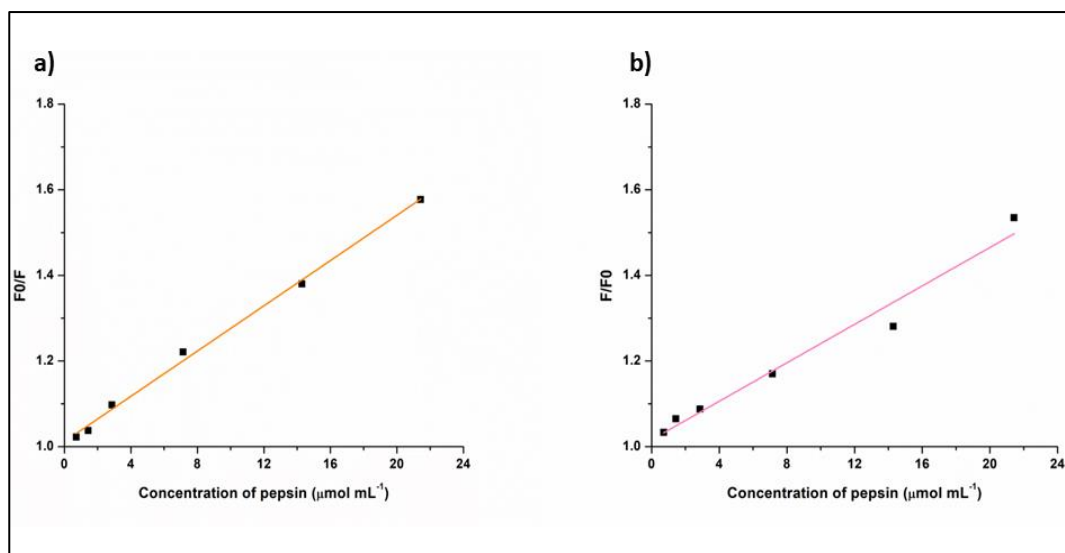
Figure 44. *Graphical representation of Stern Volmer relationship between the concentration of pepsin and the fluorescence quenching for a) FMIPs and b) RMIPs (average of triplicate measurements).*

3.8. Quantitative detection of pepsin

The fluorescence intensities of both FMIP and RMIP solutions in PBS buffer (pH 7.2) were measured in triplicate at their respective excitation wavelengths (λ_{exc}) after adding increasing concentrations of pepsin, ranging from 0 (blank) to 42.85 µmol L^{-1}. It was observed that the addition of pepsin caused a concentration-dependent quenching of the fluorescence intensity, as shown in **Figure 45**. However, at higher concentrations, the fluorescence response began to plateau, indicating the complete saturation of the binding sites for both FMIPs and RMIPs.
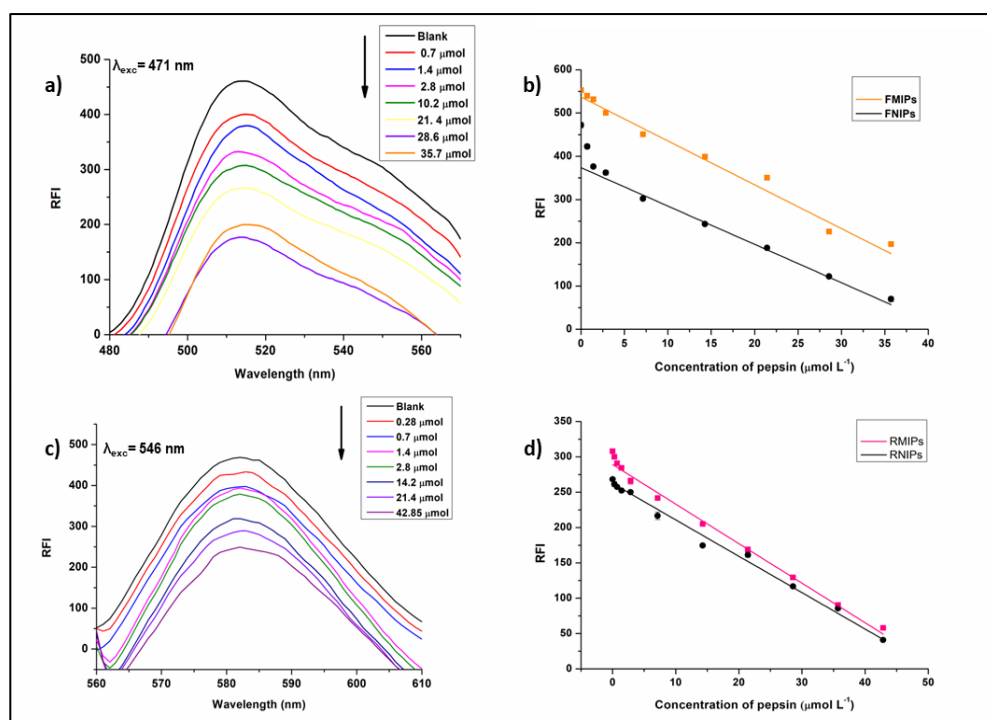
Figure 45 a) Stacked emission spectra for FMIPs, b) calibration curve for FMIPs & FNIPs, c) Stacked emission spectra for RMIPs, and d) calibration curve for RMIPs & RNIPs(average of triplicate measurements each).

The calculated linearity parameters for both MIPs are presented in **Table 14**. Notably, RMIPs exhibited a wider linear range, extending from a lower concentration limit of 0.28 µmol L^{-1} to an upper limit of 42.85 µmol L^{-1}, compared to FMIPs, which had a lower limit starting at 0.71 µmol L^{-1} and an upper limit reaching 35.71 µmol L^{-1}. This underscored the influence of the fluorescent dye's structure on target binding and the resulting MIPs' sensitivity. Consequently, RMIPs demonstrated a greater capacity to bind pepsin even at lower concentrations, resulting in significant sensitivity. Additionally, the limit of detection value was calculated for both FMIPs and RMIPs using equation 12:

$$LOD = \frac{3.3.\delta}{slope} \qquad \text{(eq. 12)}$$

where δ is the standard error of the intercept of the regression equation.

The computed LOD values further confirmed the hypothesis that RMIPs are more sensitive than FMIPs, where LOD for FMIPs was 0.36 µmol L^{-1}, while the value reached 0.12 µmol L^{-1} for RMIPs.

Table 14. Linearity parameters for quantitation of pepsin in standard solutions using FMIPs and RMIPs.

Parameter	Linearity range (µmol L^{-1})	Intercept ± SD[a]	Slope ± SD[b]	S_{yx}[c]	R^{2} [d]	LOD (µmol L^{-1})[e]
FMIPs	0.71 – 35.71	551.94 ±1.61	-0.42 ± 0.050	1.769	0.9842	0.36 ± 0.051
RMIPs	0.28 – 42.85	307.53 ± 0.85	-0.67 ± 0.055	0.973	0.9916	0.12 ± 0.048

[a] *Standard deviation of the intercept,* [b] *Standard deviation of slope,* [c] *Sum of square errors,* [d] *R the correlation coefficient,* [e] *LOD limit of detection.*

3.9. Development of a separation-free quantitation system for pepsin in human saliva samples.

The fluorescent MIPs were successfully utilised to quantify pepsin in human saliva samples. Due to the high selectivity of the developed FMIPs and RMIPs, there was no need for a prior extraction step, eliminating an extra step in sample preparation and enabling a sensitive, simple, one-step assay. Linearity in saliva ranged from 1.42 to 42.85 µmol L^{-1} for RMIPs and from 2.8 to 35.71 µmol L^{-1} for FMIPs. Additionally, the lower concentrations measured by both developed MIPs were well-suited for detecting the very low concentrations of pepsin present in the saliva of real GERD patients. The percentage of recovery was also calculated for pepsin from three different spiked samples, each containing three different concentrations along the calibration range. Recovery percentages ranged from 94.8% to 101.2% for FMIPs and from 96.29% to 100.21% for RMIPs, as demonstrated in **Table 15**.

Table 15. *Recovery of spiked pepsin from saliva samples using the fluorescent MIPs and NIPs.*

Concentration (µmol mL^{-1})	Average total the amount found (µmol mL^{-1})		Average% recovery ± SD		RSD %	
	FMIPs	RMIPs	FMIPs	RMIPs	FMIPs	RMIPs
2.8	2.65	2.69	94.84 ± 3.39	96.07 ± 3.07	3.57	3.19
14.28	14.24	14.31	99.76 ± 1.51	100.21 ± 2.08	1.52	2.08
35.71	36.14	35.50	101.22 ± 0.312	99.42 ± 0.99	0.31	1.00

Where SD is the standard deviation and RSD is the relative standard deviation.

3.10. Conclusion

In this study, the impact of the fluorescent dye's structure on the selectivity and the sensitivity of fluorescent MIPs was examined. Two fluorescent MIPs were prepared for the pepsin enzyme using two different fluorescent dyes: fluorescein and rhodamine B. Comparing the performance of both MIPs in terms of binding capacity, binding selectivity, and quantitation range of pepsin confirmed the hypothesis that rhodamine B would offer superior results due to establishing two additional electrostatic bonds with pepsin compared to fluorescein. Thus, rhodamine B was assumed to provide three points of interaction with the pepsin molecule, whereas fluorescein provided only one. This underscores the importance of a structure-based approach in selecting fluorescent dyes and monomers for preparing fluorescent MIPs. Additionally, both FMIPs and RMIPs were successfully applied for the detection and quantitation of pepsin in solutions and saliva samples, with RMIPs achieving higher sensitivity, indicated by an LOD value of 0.12 µmol L^{-1} compared to FMIPs with an LOD value of 0.36 µmol L^{-1}.

Therefore, both fluorescent MIPs offered the advantage of an integrated extraction and analysis tool compared to the magnetic MIPs developed in the previous chapter, which served only as extraction tools.

Chapter 4

Design and Preparation of a Fluorescent Molecularly Imprinted Membrane for The Selective Detection of Pepsin Enzyme as a Biomarker for GERD

Chapter 4. Design and preparation of a fluorescent molecularly imprinted membrane for the selective detection of pepsin enzyme as a biomarker for GERD.

4.1. Background

4.1.1. Molecularly imprinted membranes

Molecularly imprinted membranes (MIMs) are a class of MIPs that offers distinctive advantages over traditional bulk MIPs. Unlike bulk MIPs, which are usually in powder form, MIMs are thin, film-like structures with evenly distributed binding sites across their surface. This unique morphology provides several benefits, most notably increased accessibility to the binding sites and improved mass transfer kinetics. MIMs are particularly advantageous for binding larger analytes such as proteins due to their thin and porous structure. This increased binding capacity enhances the ability of MIMs to capture larger analytes efficiently, resulting in improved sensitivity and lower detection limits in analytical applications (275). Additionally, MIMs provide several other benefits, such as low preparation costs and ease of operation. Their straightforward synthesis and scalability make them a cost-effective option for large-scale applications. Moreover, their user-friendly nature and durability make MIMs practical choices for a wide range of analytical and separation tasks (276,277).

Fluorescent molecularly imprinted membranes (FMIMs) introduce an innovative method in sensor technology by embedding fluorescent elements such as QDs or CDs into their matrices. This integration enhances the selectivity of the MIMs and enables fluorescent detection of the target analyte (85,258).

4.1.2. Carbon dots

Carbon dots (CDs) are an emerging class of carbon-based nanomaterials celebrated for their distinct fluorescence properties, positioning them as promising candidates for various applications. Their fluorescence is derived from the quantum confinement effect and surface state emissions, allowing for adjustable emission wavelengths (278). CDs offer several advantages, including low toxicity, biocompatibility, and environmentally friendly synthesis routes using variable carbon sources. Their facile synthesis methods, often involving one-step processes, make them cost-effective and suitable for a large-scale production (279,280). A promising application of CDs is their integration with MIPs, where CDs function as visual detectors when they bind with target analytes. This combination enhances the selectivity and sensitivity of MIP-based sensors, providing a versatile platform for the rapid and visual detection of various targets in complex matrices (281).

4.2. Aims and Objectives of this work

The objective of this work was to create a new FMIM for the binding and detection of pepsin enzyme. To impart the fluorescent response, CDs would be incorporated in the matrix of FMIMs during the synthesis procedure. As a result, the binding event between pepsin and the FMIM could be detected. Furthermore, the fluorescence signal could be employed to measure the concentration of pepsin in different samples.

In the literature survey for fluorescent MIPs developed for the target, no FMIMs were previously reported for pepsin, which encouraged the idea of this work. Therefore, the aims of this work were:

- The development of FMIM capable of effectively binding pepsin enzyme.

- The careful optimisation of all components involved in the synthesis procedure to reach the highest possible binding and the best mechanical stability.

- Chemical, thermal, morphological, and functional characterisation of the developed membranes to verify their functionality.

- The application of the developed FMIM for the qualitative detection of pepsin in standard solutions and in saliva.

4.3. Experimental

4.3.1. Materials and instrumentation

N-(Hydroxymethyl)acrylamide (NHMAm) 98%, acrylamide (Am) 99%, acrylic acid (AA) (99%), N-isopropylacrylamide (NIPAm) 99%, N,N'-methylenebis(acrylamide) (MBA) 99%, ammonium persulphate (APS) 98%, N,N,N',N'-tetramethylethylenediamine (TEMED) 99.5%, phosphate buffered saline (PBS) tablets (pH 7.0), deionised water, sodium chloride 99.5%, human pepsin, human lipase, human amylase, ɣ-globulin, thrombin and Corning® microscope slides were all procured from Sigma Aldrich, UK. Folic acid (95%), N-[tris(hydroxymethyl)methyl]acrylamide (THMMAm) 99%, sulphuric acid AR, hydrogen peroxide 30%, and Parafilm™ laboratory wrapping film were all purchased from ThermoFisher, UK.

UV spectra were acquired using a Cary UV-Vis compact spectrophotometer with Cary UV Workstation™ software version 1.0.1284 (Agilent, UK). A UV lamp (UVitec, UK) was used for visual detection of fluorescence at wavelength 365 nm.

Thermogravimetric analysis was conducted using a TGA 550 instrument (TA Instruments, UK) with Trios™ software version 10.00 (UK), while differential scanning calorimetric assays were performed on a DSC25 series instrument (TA Instruments, UK) with Trios™ software version 5.4.0.300. Infrared analysis utilised a Nicolet iS5 Fourier transform infrared spectrometer (ThermoFisher Scientific, UK) instrument operated with OMNIC™ software (UK). Fluorescence detection was carried out with a UV lamp (UVitec, UK) at a wavelength of 365 nm. Images of the membrane surface were taken using an Olympus BX-51 light microscope with a Micropublisher 3.3 digital camera and Image-Pro Express capture software (Olympus, Tokyo Japan). Fluorescent images were taken via a Nikon 80i fluorescence microscope using mercury lamp illumination, Digital Sight DS-U1 camera and NIS elements capture software (Nikon labs, Toyo, Japan). Weighing of chemicals was performed using Sartorius handy balance-H51 (Hannover, Germany). Synthesis of CDs was performed using a UKFengHeng™ Teflon-lined stainless-steel autoclave. Data processing and graph plotting were carried out using Origin™ 8.5 software (Origin Lab Corporation, North Hampton, USA).

4.3.2. Synthesis of carbon dots

Ultra fluorescent CDs were synthesised according to a reported method from folic acid as a carbon source (282). Folic acid (50 mg) was dispersed in 7 mL of double-deionised water using ultrasonication. This solution was then transferred to a Teflon-lined stainless-steel autoclave and heated at 240°C for 6 hours. The resulting yellowish solution was filtered through a 0.45 μm filter to remove any undissolved particles and stored in amber-coloured containers to prevent any photobleaching.

4.3.3. Preparation of glass slides

Prior to spotting the FMIM mixture, the glass slides were immersed in a mixture of sulphuric acid and hydrogen peroxide for 24 hours to clean and activate their surfaces. Then, they were washed three times with double deionised water in an ultrasonic bath to get rid of any residual chemicals or impurities.

Subsequently, the slides were dried under nitrogen for 5 minutes to ensure a clean and dry surface, which was important for the smooth deposition of the FMIM mixture. This process was undertaken to enhance the adhesion and stability of the FMIM on the glass slides, thereby improving their performance for different applications (283).

4.3.4. Preparation of fluorescent molecularly imprinted membranes

Owing to the protein nature of the target pepsin enzyme, its limited solubility in water, and its prevalence in aqueous matrices (211), the synthesis of hydrophilic FMIMs was necessary. Various hydrophilic monomers were assessed to fabricate an optimal FMIM that could achieve the highest possible binding capacity while maintaining superior mechanical stability and reproducibility in aqueous environments (284). Achieving an ideal balance between optimal binding and robust mechanical stability posed a challenge. Various monomers, such as NHMAm, THMMAm, NIPAm, AA, and Am, were assessed individually and in combination to identify the most effective mixture for a superior binding capacity and a mechanical resilience. After thorough testing, the synthesis procedure was optimised using a combination of NHMAm (1.24 mmol) and Am (1.76 mmol) as functional monomers, with MBA (0.2 mmol) serving as the cross-linker.

These components were dissolved in 3 mL of phosphate buffer (0.02 mol L^{-1}, pH 7.0) containing 25 µL of CDs solution. Subsequently, 0.15 µmol of pepsin was introduced into the mixture, followed by sonication and stirring for 1 hour to facilitate pre-assembly between the target molecule and the monomers. After pre-assembly, 100 µL of (10% w/v) APS and 5 µL of TEMED were added, followed by immediate spotting of the mixture onto the activated glass slides.

The solution was carefully covered with 2 cm² square pieces of Parafilm™ and left to polymerise overnight. The same procedure was followed to prepare the fluorescent non-imprinted membrane (FNIM) without the addition of the target pepsin.

The resulting films were carefully cut into rectangles (2 x 1 cm), avoiding the dry edges, and washed with double-deionised water for 1 hour to remove residues of the starting materials. The membranes were then soaked overnight in a 0.5 mol L^{-1} sodium chloride solution to remove the target from the binding sites of FMIM, followed by two washes with double-deionised water.

4.3.5. Protein adsorption experiments

The binding capacity of the developed FMIMs was measured using a batch adsorption method at room temperature (25°C ± 2°C). Each FMIM and its corresponding FNIM were incubated with 10 mL of a 0.5 mg mL^{-1} pepsin solution in water for 4 hours with gentle stirring. After incubation, the membranes were removed, and the remaining pepsin concentration in solution was determined by UV spectrometry to calculate the amount of bound pepsin per gram of polymer (Q). To mitigate the risk of template bleeding, a blank rebinding experiment was conducted concurrently.

In this experiment, each FMIM and FNIM was incubated with 10 mL of double deionised water for the same duration, and the resulting solution was used as a blank for UV measurements of pepsin concentration. The binding capacity Q (mg g^{-1}) was calculated using equation 13:

$$Q = (Ci - Ct).V/m \qquad \text{(eq. 13)}$$

where, Ci (mg mL^{-1}) is the initial concentration of pepsin, Ct (mg mL^{-1}) is the concentration of pepsin after incubation time (t), V (mL) is the volume of pepsin solution, and m (g) is the mass of the membranes used in the experiment. The tests were performed three times to ascertain the precision of the results.

4.3.6. Characterisation of the developed FMIM and FNIM

To examine the surface of the developed membranes, a bright field light microscope was employed to check for any irregularities and to ensure that the surface was uniform. This was crucial because the surface quality could significantly impact the membrane's ability to bind the target. A fluorescent microscope was used to confirm that the CDs were evenly distributed throughout the membrane matrix. This step was important to ensure the proper incorporation of CDs. Additionally, images of the FMIM were captured both with and without pepsin under a UV lamp to observe the fluorescence changes resulting from the binding of the target.

For thermal analysis, TGA was conducted on the FMIMs and FNIMs to assess their thermal stability, decomposition temperature, moisture content, and to check for any residual starting materials. TGA was operated over a temperature range of 25 to 1000°C, with a heating rate of 10°C per minute and a nitrogen flow rate of 50 mL per minute.

To complement this data, DSC was used to provide additional information on moisture content and melting points, operating from 25 to 500°C at a heating rate of 10°C per minute under an inert atmosphere.

The synthesised CDs, FMIMs, and FNIMs were characterised using FTIR to confirm the synthesis of the CDs and their incorporation into the polymer matrices via comparing the prominent peaks.

To determine the binding kinetics, rebinding experiments were carried out with the FMIMs and FNIMs at various time intervals. Each membrane (approximately 150 mg) was incubated with 10 mL of 0.5 mg mL^{-1} pepsin solution for 0, 1, 2, 4, and 6 hours. The amount of pepsin adsorbed per gram (Q) was plotted against time to assess the kinetics of binding.

To establish the binding isotherm model, binding experiments were conducted by using different concentrations of pepsin. Each membrane (about 150 mg) was incubated with 10 mL of pepsin solutions with concentrations ranging from 0.2 to 1.2 mg mL^{-1} for 4 hours. The amount of pepsin adsorbed per gram (Q) was plotted against the concentration to illustrate the binding isotherm model.

To evaluate the binding selectivity of the FMIMs, their performance was compared to that of the FNIMs. The imprinting factor (IF) was calculated by dividing the Q value for the FMIMs by that for the FNIMs. The selectivity of the fluorescent membranes for pepsin was further assessed against other proteins commonly found in human saliva, such as amylase and lipase, to check for potential cross-reactivity.

Subsequently, a similar binding assay where 10 mL of 0.5 mg mL^{-1} solutions of each protein was incubated with the fluorescent membranes for 4 hours. The amount bound per gram (Q) for each enzyme was measured and compared to that of pepsin.

4.3.7. Application of the developed FMIM to spiked saliva samples

This study was conducted in agreement with the declaration of Helsinki principles and under the rules of UK Human Tissue Act (HTA) 2004 and received full ethical approval from Kingston University Ethics Committee under Ethics Code 2895. Saliva samples were collected from one subject after rinsing the mouth three times with water, centrifuged at 4500 rpm for 30 minutes and then used immediately. Aliquots of saliva samples (150 µL) were spiked with 350 µL of pepsin solution (1.5 mg mL^{-1}) and the final volume was made to 1mL using PBS buffer (pH 7.0). The FMIM was then added to the prepared samples and the enhanced fluorescence was visualised under UV light at 365nm.

4.4.   Results and Discussion

4.4.1. Synthesis of carbon dots

The CDs used in the synthesis of FMIM were chosen due to two influential factors. Firstly, the abundance of folic acid and amino group residuals on the surface of the produced CDs (282). This was an important parameter to ensure the formation of electrostatic interactions between pepsin enzyme and CDs. Since at the working pH of the solution (7.2), pepsin would carry a negative charge due to its low isoelectric point (3.24) (243), and the amino groups on the surface of CDs would carry a positive charge.

This guaranteed an electrostatic interaction between pepsin and CDs that would contribute to enhancing the binding capacity. Secondly, the ultra-high reported quantum yield (94%) of these CDs could contribute to the better visual detection of the binding event between the FMIM and pepsin that can be seen by the naked eye. **Figure 46** shows the excitation and emission spectra of the resulting CDs solution and their UV spectrum.
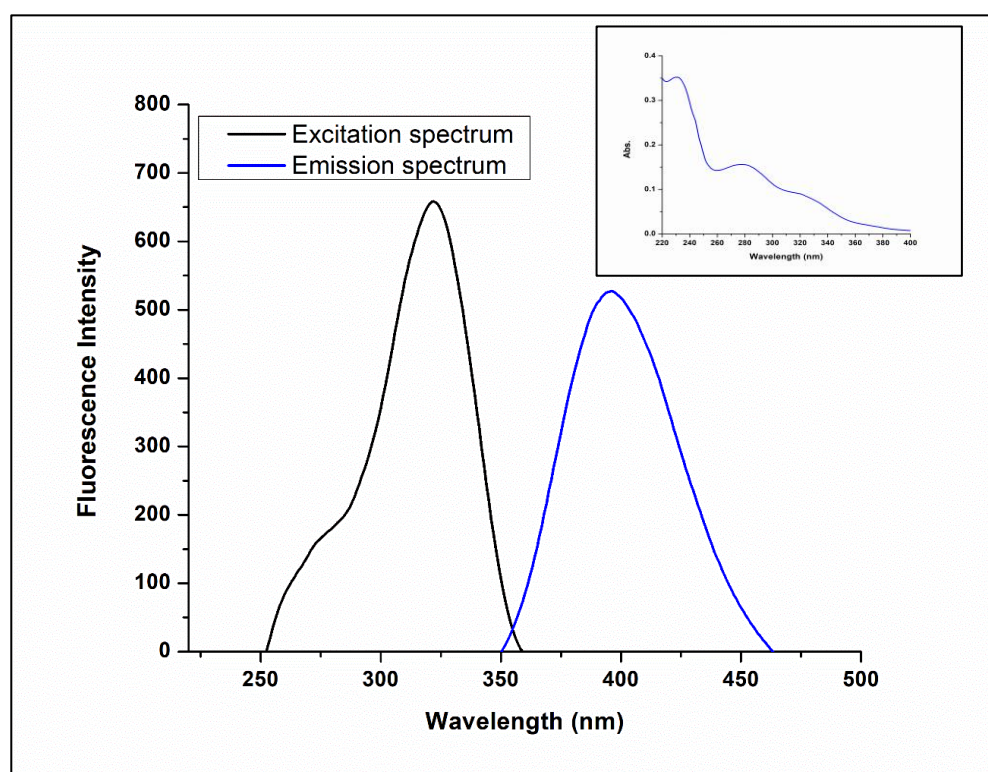
Figure 46. *Excitation and emission spectra of the developed CDs, **inset**: UV spectrum of CDs.*

4.4.2. Experimental determination of CDs' quantum yield

The quantum yield (Φ) of the synthesised CDs embedded in the FMIM was experimentally determined using quinine sulphate as a standard according to the reported method by Würth et al.(285).

For comparison, a solution of quinine sulphate 0.1 mol L^{-1} was prepared in sulphuric acid, which has a known quantum yield of 54% (Φ = 0.54) at excitation wavelength of 365 nm.

The absorbance spectra for both the CDs and the quinine sulphate solutions were recorded at the excitation wavelengths, ensuring that the absorbance values were below 0.1 to minimise the inner filter effects. The fluorescence emission spectra were then obtained under identical excitation conditions for both the sample and the standard.

The quantum yield of the CDs was calculated using equation 14:

$$\Phi u = \Phi s \times \frac{Fu}{Fs} \times As/Au \qquad \text{(eq. 14)}$$

Where, Φs and Φu are the quantum yields of quinine and CDs, respectively; Fs and Fu are the integrated fluorescence intensity after correction with the blank for quinine and the CDs, respectively; As and Au are the absorbances at the excitation wavelength of quinine and the CDs, respectively.

The obtained quantum yield value from this experiment was 92.8±0.2 % which is very comparable to the reported value in the applied method (282).

4.4.3. Preparation of FMIM and FNIM

Figure 47 illustrates the preparation process for the CDs and FMIM. Various hydrophilic functional monomers were tested at different concentrations, with MBA used as the cross-linker. Key considerations included binding capacity, selectivity, and the mechanical strength of the membranes, as well as their ability to retain CDs without leakage.
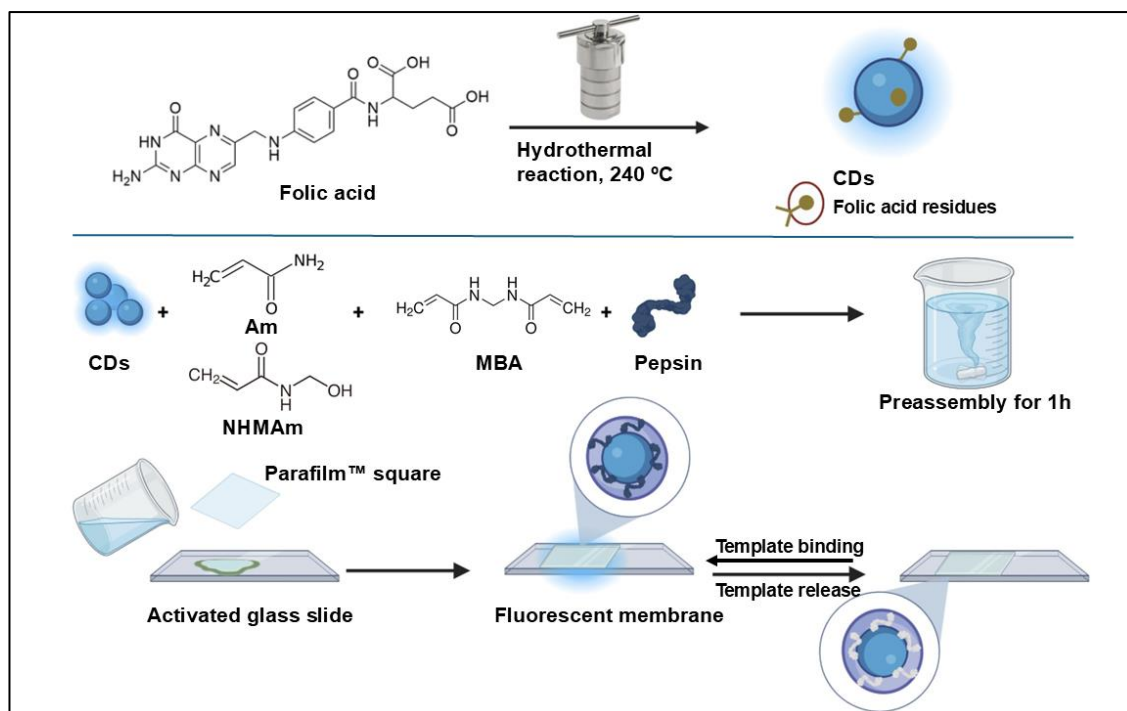
Figure 47. *Overview of the synthesis process for carbon dots (CDs) and the fluorescent molecularly imprinted membrane (FMIM).*

Table 16 details the different monomers, cross-linker concentrations, and amounts of CDs used in the optimisation trials, alongside the results. The data revealed that the combination 1.24 mmol NHMAm and 1.76 mmol Am as monomers, with 0.2 mmol MBA as cross-linker produced the most effective FMIM. This combination achieved the highest binding capacity and exhibited strong mechanical stability while preventing CD from leaching.

Table 16. *Different combinations of monomers and cross-linkers to synthesise FMIMs and their outcome.*

Composition	Binding	Mechanical stability
250 mg NHMAm + 20 mg MBA + 2mL CDs.	Poor.	Acceptable, however, leaching of CDs occurred.
250 mg NHMAm + 20 mg MBA + 0.5 mL CDs.	Poor.	Acceptable, however, leaching of CDs occurred.
250 mg NHMAm + 20 mg MBA + 25 µL CDs.	Poor.	Acceptable, No leaching of CDs.
125 mg NHMAm + 125 mg THMMAm+ 20 mg MBA + 25 µL CDs.	No polymerisation.	-----
250 mg Am +10 mg MBA + 25 µL CDs.	Poor.	Acceptable.
125 mg Am + 125 mL AA +20 mg MBA + 25 µL CDs.	Good.	Poor.
125 mg NHMAm + 125 mL AA + 20 mg MBA + 25 µL CDs.	Good	Acceptable.
125 mg NHMAm + 125 mg Am+ 20 mg MBA + 25 µL CDs.	Excellent.	Acceptable.
125 mg NHMAm + 125 mg Am+ 10 mg MBA + 25 µL CDs.	----	Hydrogel very weak membrane.
125 mg NHMAm + 125 mg Am+ 40 mg MBA + 25 µL CDs.	-----	Very solid, glass like membrane.
125 mg NHMAm + 125 mg Am+ 30 mg MBA + 25 µL CDs.	Excellent.	Excellent.

NHMAm and Am were effective monomers because they could form hydrogen bonds with both the amino and the carboxylic groups in the pepsin molecule, enhancing binding. Additionally, these monomers could interact with the folic acid residues on the CDs surface, preventing them from leaching out. The role of MBA was also crucial for mechanical stability. A lower concentration of MBA resulted in a liquid-like hydrogel that lacked strength and could not retain CDs effectively.

On the other hand, a higher MBA concentration produced a semi-solid, glass-like membrane with significantly reduced fluorescence due to the entrapment of CDs. Thus, optimising the MBA concentration was essential to achieving a balance between binding capacity and mechanical durability.

4.4.4. Characterisation of FMIM and FNIM

4.4.4.1.   Morphological characterisation

Figures 48a and **48b** show light microscope images of the FMIM and FNIM, revealing a consistently smooth, even, and wettable surface. This surface quality was crucial as it enhanced the membrane's binding capacity. A smooth and uniform surface allowed for efficient, swift, and dependable binding and release of the pepsin enzyme. The wettability of the surface further supported the FMIM's application in aqueous environments.

Figures 48c and **48d** display fluorescence microscopy images of the FMIM, highlighting the even distribution of CDs throughout the membrane. This uniform distribution was vital for ensuring that the CDs are well-positioned at the binding sites, enabling effective interaction with pepsin and a clear visual signal. It also helped to avoid inconsistencies in the fluorescence intensity, thereby ensuring reliable and uniform performance of the FMIM.
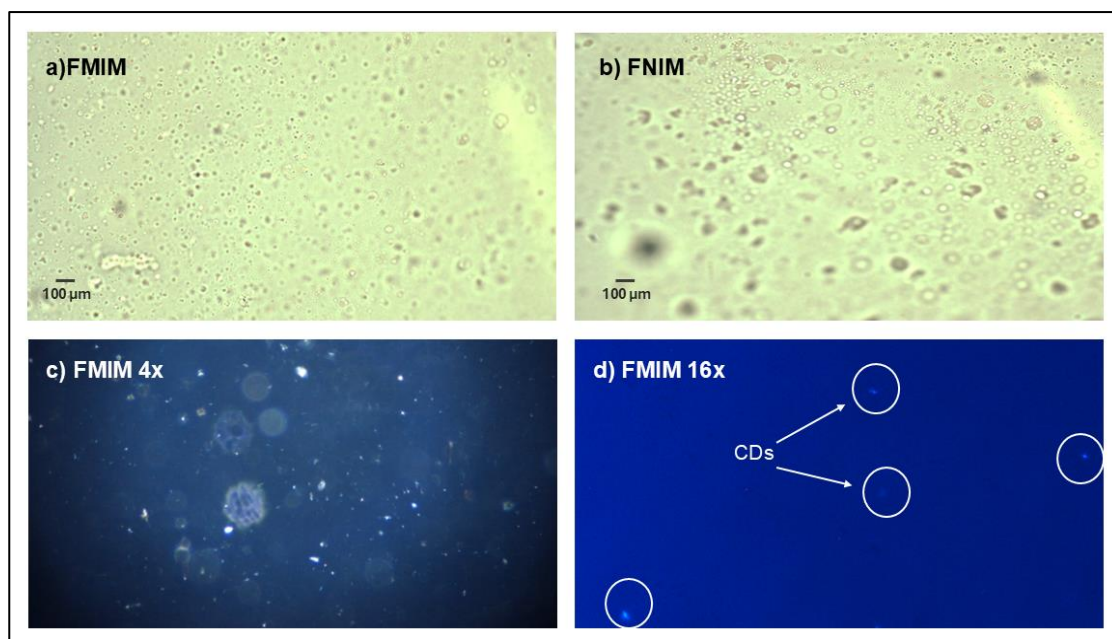
Figure 48. *The light microscope images of a) FMIM, b) FNIM, and the fluorescent microscope images of c) FMIM under 4x magnification, d) FMIM under 16x magnification.*

4.4.4.2. Chemical characterisation

Figure 49 displays the IR spectra collected for CDs, FMIM and FNIM. FTIR spectrum collected for CDs agreed with the reported FTIR spectrum for the CDs in the reported method (282). Herein, A prominent peak at 3274 cm^{-1} was observed, which corresponded to the N–H stretching vibration. Additionally, an asymmetric stretching peak at 1273 cm^{-1} was attributed to the C–N bond in the pterin ring of the folate residues. Peaks at 1644 cm^{-1} and 1447 cm^{-1} were linked to C=O stretching and C–O bending vibrations, respectively.

While the N–H stretching vibration peak of the CDs remained evident in the FTIR spectra of both FMIM and FNIM, this peak was shifted due to the presence of an OH group in the polymer structure. Moreover, its intensity was reduced because of the CDs' integration into the polymer matrix.

In the FTIR spectra of both FMIM and FNIM strong peaks were observed at 1705 cm^{-1} corresponding to the carbonyl group stretching within the polymer, and peaks at 1359 cm^{-1} were related to C–H bending. The IR spectra of both FMIM and FNIM were nearly identical, reflecting their similar chemical structures (272).
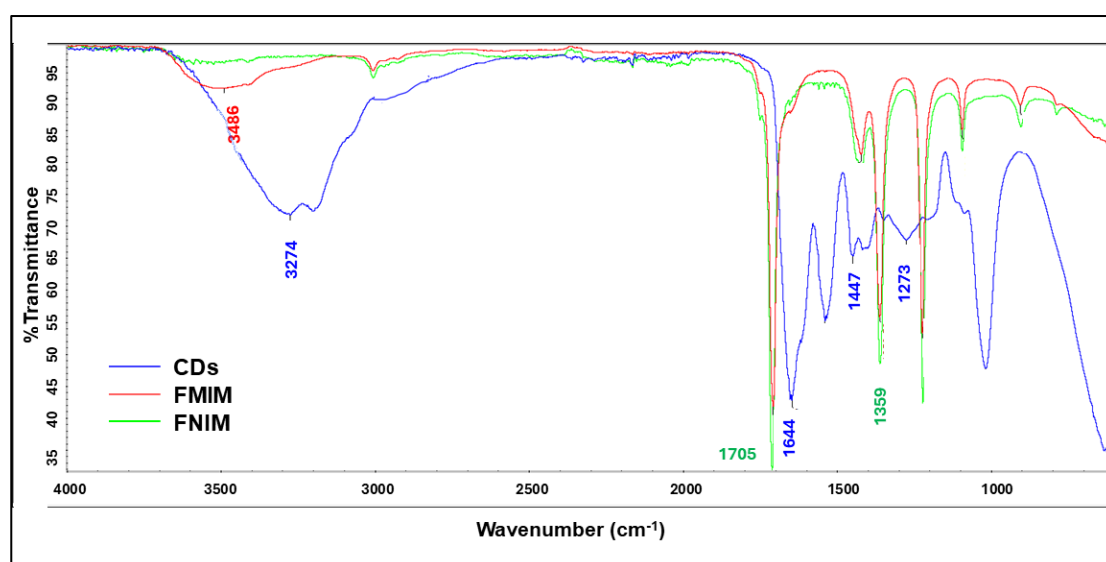
Figure 49. *FT-IR spectra comparing the chemical profiles of CDs, FMIM, and FNIM, illustrating the distinct functional groups.*

4.4.4.3. Thermal characterisation

The TGA curves depicted in **Figures 50a** and **50b** revealed two weight loss stages: the initial loss around 100°C, which was attributed to moisture evaporation, and the subsequent loss around 450°C, indicating membrane decomposition. The DSC thermograms for FMIM and FNIM, shown in **Figures 50c** and **50d**, displayed prominent endothermic peaks near 100°C, reflecting the high water content within the membrane. These results highlighted the excellent thermal stability of both FMIM and FNIM. The close alignment of the DSC and TGA curves for both types of membranes further supported their structural similarity and confirmed the absence of any residual target material in the FMIM.
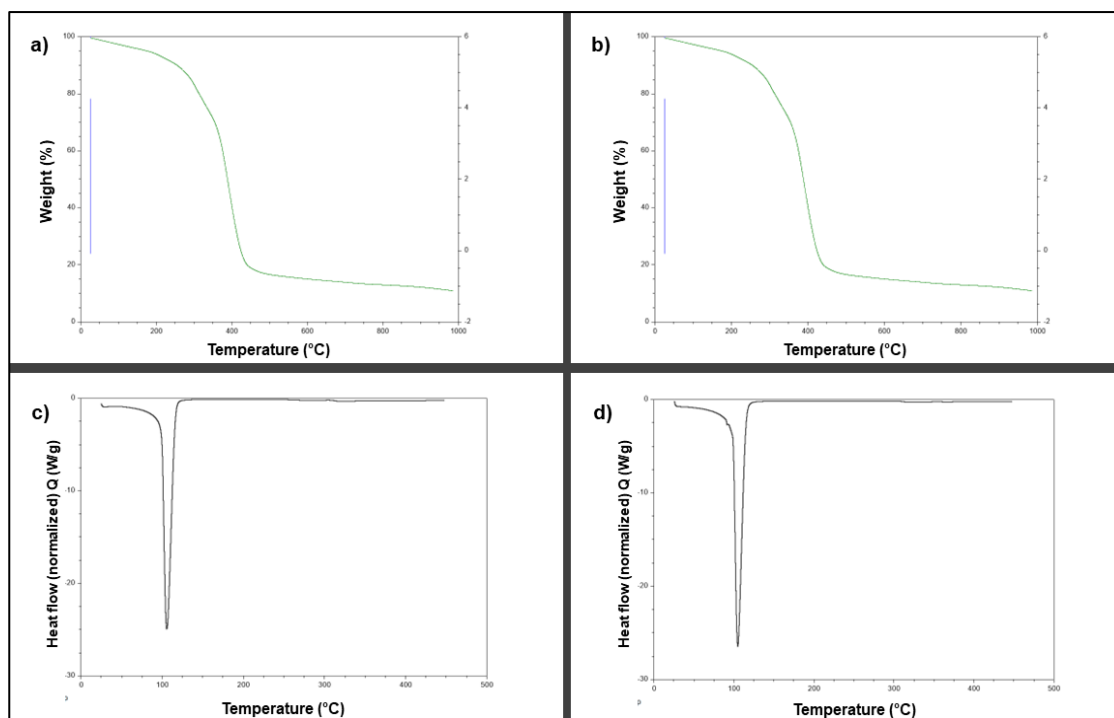
Figure 50. TGA thermograms of a) FMIM and b)FNIM and DSC thermograms for (c) FMIM and d) FNIM.

4.4.4.4. Functional characterisation

The results of the binding kinetics experiments conducted on FMIM and FNIM are graphically illustrated in **Figure 51**.
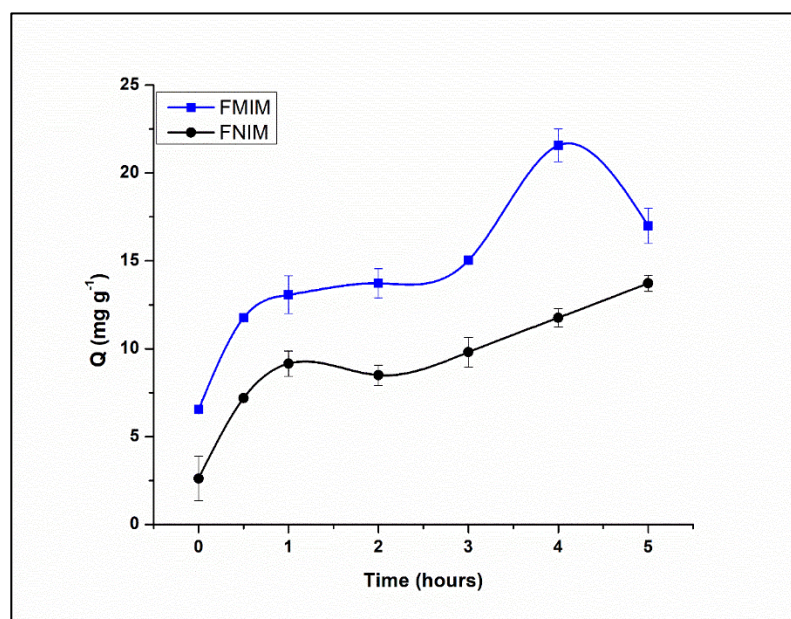
Figure 51. Binding kinetics of FMIM and FNIM (average of triplicate measurements).

The graph shows that FMIM exhibited a noticeably enhanced binding capacity compared to FNIM, with the highest binding capacity reached after 4 hours. Following this period, a slight reduction in binding capacity was observed, likely due to the release of pepsin from the binding sites as equilibrium was reached, which can be attributed to the bulky structure of the pepsin molecule. Pseudo-first and pseudo-second order kinetics parameters were computed for the experimental data of both FMIM and FNIM, as illustrated in **Table 17**. From the presented data, it was concluded that both FMIM and FNIM followed a pseudo-second order kinetics model, suggesting that binding followed a chemical absorption mechanism.

Table 17. *Binding kinetics parameters for FMIM and FNIM applying two binding orders.*

Pseudo first order parameters

FMIM			FNIM		
K_1 (min $^{-1}$)	Qe (mg g^{-1})	R^2	K_1 (min $^{-1}$)	Qe (mg g^{-1})	R^2
0.032	12.83	0.60	0.057	12.12	0.7700

Pseudo second order parameters

FMIM			FNIM		
K_2 (g mg^{-1} min^{-1})	Qe (mg g^{-1})	R^2	K_2 (g mg^{-1} min^{-1})	Qe (mg g^{-1})	R^2
20500.51	18.83	0.9447	4691.98	13.42	0.9359

K1 and K2 are the first and second order rate constants respectively, Qe is the quantity of pepsin adsorbed per gram of polymer at equilibrium, and R^2 is the linearity coefficient.

A linear correlation was found between the binding capacity (Q) and the concentration of pepsin (mg mL^{-1}) in the binding isotherm experiments performed on both FMIM and FNIM, as illustrated in **Figure 52**.
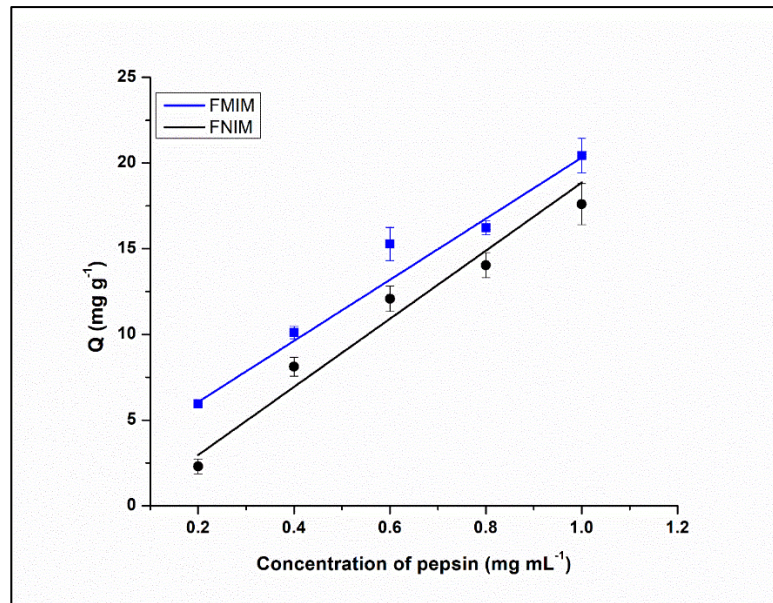
Figure 52. Binding isotherms of FMIM and FNIM (average of triplicate measurements).

To gain a deeper insight into the binding mechanisms, the experimental data were analysed using both Langmuir and Freundlich isotherm models. According to **Table 18**, the data for both FMIM and FNIM aligned more closely with the Langmuir model, indicating that the binding process occurred as a monolayer on a uniform surface.

Table 18. Adsorption isotherm parameters of FMIM and FNIM applying two models.

Langmuir isotherm

FMIM				FNIM			
K_L (L mg^{-1})	Q_{max} (mg g^{-1})	RL	R^2	K_L (L mg^{-1})	Q_{max} (mg g^{-1})	RL	R^2
0.79	45.97	0.68	0.9944	153.25	14.51	0.011	0.9570

Freundlich isotherm

FMIM			FNIM		
n	K_F	R^2	n	K_F	R^2
1.34	21.13	0.9846	0.79	21.15	0.9536

KL and KF are the Langmuir constant and Freundlich constant respectively, Q_{max} is the theoretical maximum adsorbed concentration, RL is the separation factor ($1/1+C_{eq}.KL$), n is the variation trend coefficient for the adsorption isotherm, and R^2 is the linearity coefficient.

The selectivity of FMIM was verified by comparing its binding capacity Q with that of the corresponding FNIM and calculating the imprinting factor (IF) using this formula.

$$IF = \frac{Q_{MIPs}}{Q_{NIPs}}$$ (eq. 15)

At a pepsin concentration of 0.5 mg mL^{-1}, the IF value was 1.83, giving a numerical proof of FMIM's selectivity.

The results of the selectivity tests conducted against other competitor enzymes, including amylase and lipase, are shown in **Figure 53**. These results demonstrated the superior selectivity of FMIM for pepsin compared to other enzymes that coexist with pepsin in saliva.
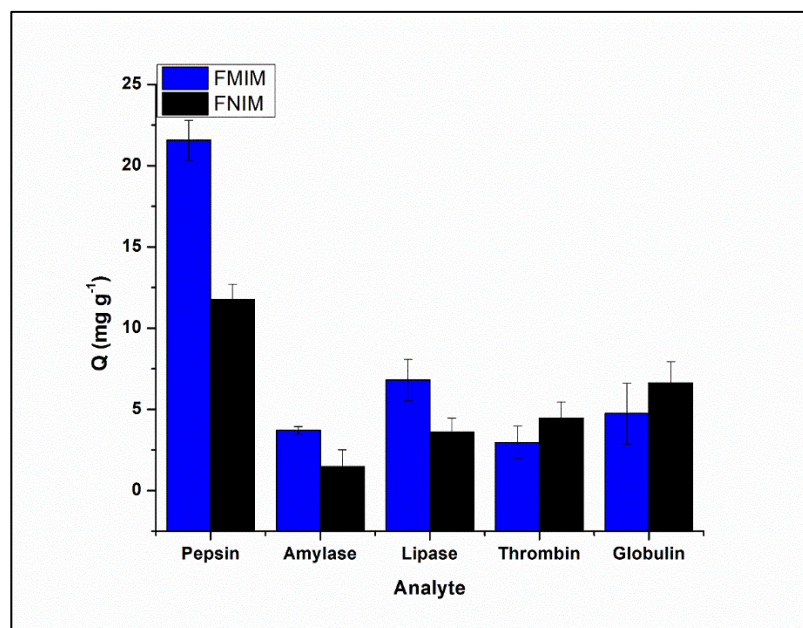
Figure 53*. Selectivity of FMIM and FNIM for pepsin against other proteins (average of triplicate measurements).*

The selectivity factor (α) was computed for each competitor enzyme using this formula.

$$\alpha = \frac{Q_{MIP.target}}{Q_{MIP.competitor}} \qquad \text{(eq. 16)}$$

The values of α for FMIM were 5.8 for amylase, 3.17 for lipase, 7.26 for thrombin, and 4.5 for ɣ-globulin. These values confirmed that FMIM could bind selectively to pepsin in saliva without cross interference from other coexistent enzymes.

4.4.5. Effect of pH on the fluorescence response

The pH value is a crucial parameter that can impact the fluorescence intensity of CDs, thereby affecting the sensitivity of the developed FMIM. Additionally, pH can influence the protein adsorption process by controlling properties of the protein such as ionisation, charge, and conformational integrity. Therefore, the fluorescence intensity of FMIM before and after binding the target was studied at different pH values to assess this effect. The results, shown in **Figure 54**, revealed that the fluorescence intensity, before binding pepsin, was the highest from pH 5 to pH 7, with the peak at pH 5, consistent with the reported method for synthesising CDs (282). However, after binding pepsin, the fluorescence intensity was the highest at pH 7. This pattern could be explained by the ionisation states of the interacting groups. At a lower pH (below 4 – 5), the carboxylic groups (pk_a ~ 4) of pepsin were protonated, reducing the binding interaction between the CDs and pepsin, leading to lower fluorescence. As the pH rose towards neutrality, these groups deprotonated, enhancing electrostatic interactions and hydrogen bonding between the CDs and pepsin, resulting in a peak fluorescence at pH 7. An optimal interaction occurred between the deprotonated carboxylic groups on pepsin and the amino groups on the CDs, which were not yet fully ionised.

Beyond pH 7, the decrease in fluorescence happened due to potential changes in pepsin's conformation that weaken the interaction with the binding sites in FMIM. Moreover, FMIM synthesis was conducted at pH 7.0, making the binding sites complementary to the conformation of pepsin at this pH, which is also within the physiological pH range of saliva (6.2 – 7.6) (238), the target matrix. Therefore, to achieve the highest possible fluorescence and optimal pepsin binding, pH 7 was chosen as the optimum pH for all the binding experiments.
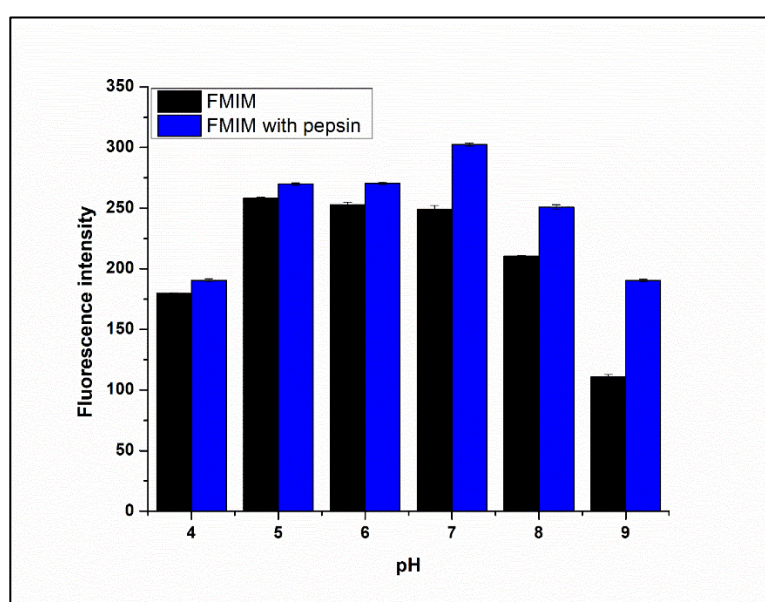
Figure 54. Influence of pH on the fluorescence intensity of FMIM in the presence and the absence of pepsin (average of triplicate measurements).

4.4.6. Mechanism of fluorescence enhancement

The enhancement of fluorescence of FMIM upon binding pepsin could be explained by several factors related to the interaction between pepsin and the CDs in the matrix of the FMIM. When pepsin bound to the binding sites containing CDs, it effectively passivated the non-radiative recombination sites on the CD surfaces. This reduction in non-radiative pathways led to an increase in fluorescence emission (286,287).

Additionally, the binding of pepsin to the folic acid residues on the surface of the CDs could cause conformational changes that stabilise the structure of the CDs, reducing quenching mechanisms and increasing fluorescence (288). Finally, the specific binding of pepsin to the imprinted sites could create a favourable environment for energy transfer mechanisms. Since pepsin binding could facilitate efficient energy transfer to the fluorescent centres of the CDs, it could lead to enhanced fluorescence (289).

4.4.7. Application to saliva samples

The FMIMs and FNIMs were tested to see how their fluorescence was enhanced when they bind with pepsin, both in solution and in spiked saliva samples. The FMIM was viewed under UV light in absence and the presence of pepsin both in solution and in spiked saliva samples. The samples were prepared in phosphate buffer (pH 7.0) and the visualisation was at room temperature. As depicted in **Figure 55**, there was a marked increase in fluorescence intensity of the FMIM and FNIM after binding with pepsin, indicating successful interaction. The tested concentration of pepsin in this qualitative experiment was 0.5 mg mL^{-1}, the FMIM, continued to show a visible fluorescent signal until the concentration of 0.1 mg mL^{-1}, after which the signal did not visibly change. While the visual fluorescence signal was apparent at higher pepsin concentrations, this sensitivity still supported the effectiveness of FMIMs as a biosensor. For lower concentrations or precise quantification, further measurements can be accurately performed using spectrofluorometers equipped with a membrane and film solid samples holder.

This dual capability highlights the potential of FMIMs for both qualitative and quantitative analysis of pepsin, making it a versatile tool for diagnostic applications.
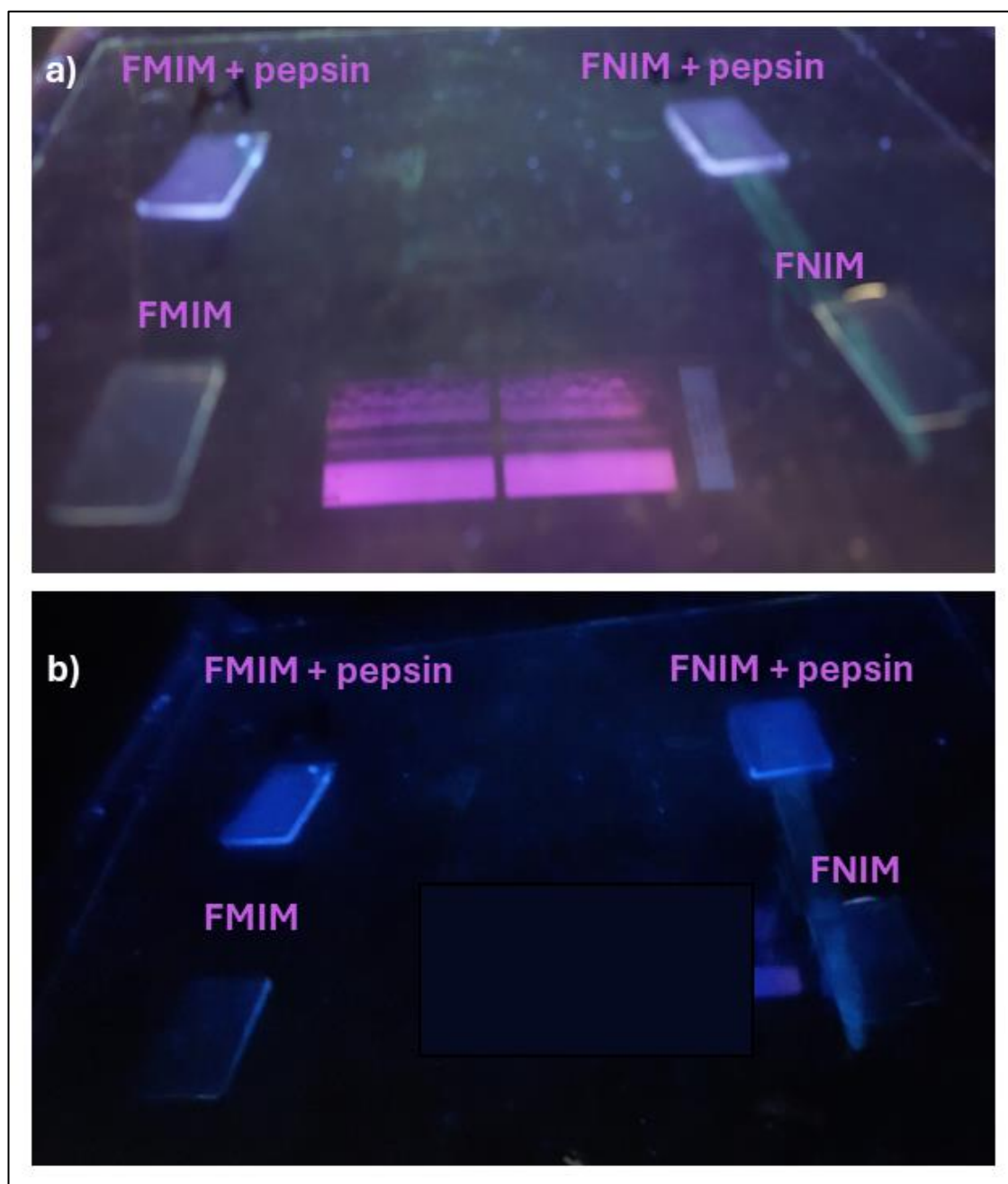
Figure 55. *Fluorescence images under UV light for (a) FMIM and FNIM in solution with and without pepsin; (b) FMIM and FNIM in saliva with and without pepsin.*

4.5. Conclusion

In this study, a new fluorescent molecularly imprinted membrane was developed to be both selective and cost-effective for binding pepsin enzyme. Various monomers were tested to optimise both binding performance and mechanical stability. The resulting FMIM demonstrated exceptional selectivity for pepsin compared to the fluorescent non-imprinted membrane and other competing enzymes. Carbon dots with high fluorescence intensity were incorporated into the membrane matrix, enhancing its ability to serve as a visual sensor for pepsin. As a result, pepsin binding to the FMIM led to a noticeable increase in fluorescence. Both the FMIM and FNIM were thoroughly characterised using various analytical techniques to assess their properties, stability, and binding behaviour. Ultimately, the FMIM and FNIM produced a clear visual response when pepsin was bound in both solution and spiked saliva samples.

Chapter 5. Investigating Polydopamine-Based Molecularly Imprinted Polymers for Pepsin Extraction and Detection

Chapter 5. Investigating Polydopamine-Based Molecularly Imprinted Polymers for Pepsin Extraction and Detection

5.1. Background

5.1.1. Dopamine as a neurotransmitter

Dopamine, a crucial neurotransmitter, plays a multifaceted role in both the central and peripheral nervous systems, making it a subject of extensive research in the field of neuroscience and beyond. In the brain, dopamine is involved in various vital functions, including reward and pleasure, motor control, mood regulation, and cognitive processes (290). Dysregulation of the dopaminergic system has been implicated in several neurological and neuropsychiatric disorders, such as Parkinson's disease, schizophrenia, and addiction. Additionally, recent research has expanded the understanding of dopamine's broader role in peripheral organs, contributing to functions like cardiovascular regulation, immune response modulation, and gastrointestinal motility. This versatile neurotransmitter continues to be a focal point of scientific investigation, with implications not only for neurological health but also for a broader understanding of physiology and behaviour (290).

5.1.2. Dopamine as a monomer

Dopamine is an interesting molecule with a chemical structure that intrigues research. It consists of a catechol structure, which comprises two hydroxyl groups (OH) attached to a benzene ring. In aqueous solutions, particularly at higher pH values, dopamine exhibits the intriguing ability to undergo auto-polymerisation, leading to the formation of a polymer known as polydopamine (PDA) as represented in **Figure 56**.

This unique property has caught significant attention in various fields, including materials science and bioengineering, as it allows for the development of surface coatings and functional materials with a wide range of applications, from drug delivery to biosensors (291). Therefore, dopamine has gone beyond its traditional role to become a pivotal monomer in the synthesis of polymers and materials. Its natural ability to undergo oxidative self-polymerisation allows for the facile formation of PDA coatings on diverse substrates, including nanoparticles and monoliths (292).
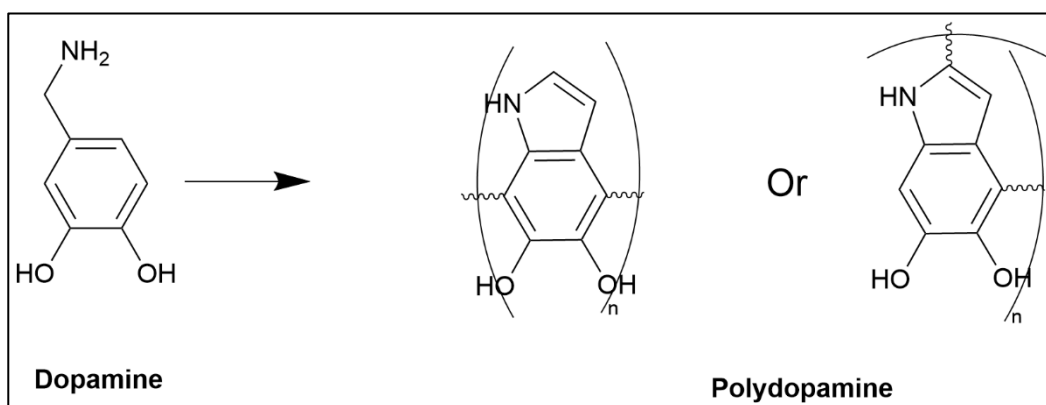
Figure 56. Polymerisation of dopamine into polydopamine.

This distinctive property has encouraged researchers to prepare MIPs with tailored binding cavities, providing a versatile foundation for molecular recognition. Herein, the PDA layer serves as a unique scaffold for imprinting target molecules, these scaffolds are capable of identifying and binding the target analyte in different matrices (293).

The integration of dopamine into the synthesis of MIPs provides several reported advantages. The simplicity of the PDA coating process accelerates MIP fabrication, facilitating reproducibility and large-scale production.

Furthermore, PDA MIPs also exhibit greenness, enabling utilisation across a spectrum of environmental applications. Their versatility, combined with the potential for tailor-made binding sites, grants good control over molecular recognition (293).

5.1.3. Applications of PDA MIPs

Dopamine has emerged as a versatile monomer in the development of MIPs with a wide range of applications spanning catalysis, analysis, drug delivery, and sensing. In catalysis, dopamine-imprinted polymers have been employed as molecularly selective catalysts, offering enhanced catalytic activity and selectivity for various chemical reactions. One example includes the development of PDA MIPs for *in situ* activation of peroxydisulfate without metal active sites for targeted pollutants removal (294). In analytical chemistry, PDA MIPs serve as very good sorbents for sample preparation, enabling efficient extraction and pre-concentration of analytes from complex matrices. These materials have found extensive use in solid-phase extraction and chromatographic techniques, facilitating accurate and sensitive analytical measurements (295). Applications of PDA MIPs in analytical chemistry are numerous and apply to many targets. This includes pharmaceutical drugs such as metronidazole (296), ecstasy (297), pregabalin (298) or drug metabolites (299), and different biomarkers (300–302). In drug delivery, PDA MIPs have showcased their potential for controlled release systems, allowing for precise and targeted drug delivery, reducing side effects, and improving therapeutic outcomes (303).

Additionally, PDA MIPs have been integrated into multiple sensor types, demonstrating remarkable selectivity and sensitivity in detecting specific analytes. PDA MIPs have been included in electrochemical sensors, in which PDA MIPs are fabricated on the surface of the electrode to increase its selectivity and sensitivity (297,298). In addition, PDA MIPs have been applied in optical sensors such as fluorescent sensors, in which case the binding of target causes an increase or decrease in the fluorescence (296,301) or through the integration with surface enhanced Raman scattering (304).

The development of PDA MIPs in protein biomarker analysis has been a recent trend due to its great convenience. By imprinting the three-dimensional architectures of specific protein targets, these synthetic materials offer the potential to selectively capture and quantify proteins of interest. This capability extends to the detection of elusive and low-concentration biomarkers, often encountered within complex biological matrices (300).

5.1.4. Challenges in the synthesis of PDA MIPs for protein targets

While PDA MIPs offer an appealing platform for protein biomarker analysis, challenges emerge. The inherent complexities of protein structures and conformations necessitate meticulous optimisation to achieve precise and selective recognition. Achieving optimal imprinting conditions, compatibility with complex biological matrices, and addressing potential non-specific interactions remain focal points of exploration (144).

PDA synthesis often involves the oxidation of dopamine in the presence of oxygen or oxidising agents at an alkaline pH. The reaction proceeds through the oxidative self-polymerisation of dopamine molecules, resulting in the formation of a brown-black precipitates (292). The specific pH required for dopamine polymerisation may vary depending on the reaction conditions and the intended application, but a pH above 8.0 is generally recommended for this process (292). However, imprinting proteins using dopamine as a monomer can be a challenging work due to the necessity of maintaining a relatively high pH (typically above 8) during the polymerisation process. This elevated pH can significantly impact the conformation of the protein molecules and alter them from their native forms, and therefore their identification by the developed MIPs in biological matrices would be compromised. Additionally, the alkaline conditions required for dopamine polymerisation can potentially lead to damaging effects on the protein itself, such as denaturation or aggregation (305). As a result, achieving precise molecular imprinting of proteins while preserving their structural integrity within PDA MIPs presents a challenge, requiring meticulous optimisation of reaction conditions.

5.2.   Aims and Objectives of this work

This study explored the synthesis of MIPs by employing dopamine as a monomer to create a PDA layer atop silica nanoparticles, aiming to capture pepsin enzyme, the diagnostic biomarker for GERD. In the literature survey, no PDA MIPs have been reported for the binding of pepsin.

Therefore, the aims of this work were:

- To develop new PDA MIPs for pepsin.

- To optimise the synthesis procedure to reach the best binding.

- To characterise the resulting PDA MIPs to verify their functionality.

- To apply the developed MIPs for the extraction of pepsin from different solutions and samples.

5.3. Experimental

5.3.1. Materials and Instrumentation

Dopamine 99%, Tris base 99.9%, citric acid 99%, ammonia solution 25%, sodium hydroxide 98%, tetraethyl orthosilicate for synthesis (TEOS), and 3-aminopropyl)triethoxysilane 98% (APTES) were purchased from ThermoFisher (UK). Absolute ethanol 99.5%, toluene 98%, acetone 99.5%, phosphate buffered saline (PBS) tablets (pH 7.2), sodium dodecyl sulphate 99% (SDS), glacial acetic acid 99%, and deionised water were all purchased from Sigma Aldrich (UK).

UV spectra were obtained using a Cary UV-Vis compact spectrophotometer, with data analysis performed using Cary UV Workstation™ software version 1.0.1284 (Agilent, UK). Fluorescence detection was carried out with a UV lamp (UVitec, UK) at a wavelength of 365 nm. Thermogravimetric analysis was performed using a TGA 550 instrument (TA Instruments, UK) with Trios™ software version 10.00 (UK), while differential scanning calorimetry was conducted on a DSC25 series instrument (TA Instruments, UK) using Trios™ software version 5.4.0.300. Infrared spectroscopy was carried out with a Nicolet iS5 Fourier transform infrared spectrometer (Thermo Fisher Scientific, UK), operated with OMNIC™ software (UK).

Synthesis of CDs was performed using a UKFengHeng™ Teflon-lined stainless-steel autoclave. Weighing of chemicals was performed using Sartorius handy balance-H51 (Hannover, Germany). Data processing and graph plotting were carried out using Origin™ 8.5 software (Origin Lab Corporation, North Hampton, USA).

5.3.2. Choice of core material

CDs were tested as core material to PDA MIPs in order to impart a fluorescent quality to the resulting MIPs. The utilisation of CDs in the development of MIPs offers a unique set of advantages. The use of CDs would enable real-time monitoring of the MIP binding process, making it particularly advantageous for sensing and biosensing applications. Additionally, CDs are renowned for their biocompatibility and low toxicity, rendering them suitable for imprinting biological macromolecules, including proteins and nucleic acids. Their small size and high surface area-to-volume ratio also contribute to the creation of highly porous MIP structures with enhanced binding capacities and rapid analyte recognition (306). The use of CDs as a core material for PDA MIPs has been reported several times (301,307), which encouraged testing them for pepsin.

Silica nanoparticles (NPs) were also tested as a solid support for the polymerisation of dopamine. Their high surface area and tuneable pore size make them ideal support for creating well-defined and highly specific binding sites within the polymer matrix. Moreover, silica NPs can be readily functionalised with a variety of functional groups, facilitating precise control over the interactions between the template molecule and the monomers during the imprinting process. This allows for enhanced selectivity and affinity of the resulting MIPs towards the target analyte.

Moreover, silica NPs provide mechanical stability to the MIPs, improving their durability and resistance to mechanical stress, which is especially valuable in practical applications. Additionally, their compatibility with a wide range of solvents simplifies the synthesis process (308). The application of silica NPs as solid support for PDA MIPs has been reported multiple times either as bare silica NPs or functionalised silica NPs (302,309–312). These appealing properties derived this study into developing PDA MIPs for pepsin using silica NPs.

5.3.3. Synthesis of carbon dots

Synthesis of CDs was adapted from a reported method which utilises citric acid as carbon source (313). Citric acid (2g) was mixed with 50 mL ultrapure water and stirred until a clear solution was obtained. Ammonia solution was gradually added to the mixture to reach pH 7.0 afterwards the solution was transferred to a Teflon lined stainless steel autoclave and heated to 200 °C for 6 hours. The resulting solution was filtered through a 0.45 µm filter and stored in a dark container to avoid photobleaching.

5.3.4. Synthesis of silica NPs

Silica NPs were prepared according to Stöber method via the hydrolysis of TEOS in alkaline medium (314). TEOS (13.5 mL) was dissolved in 136.5 absolute ethanol in a 500 mL round bottom flask. A mixture of 30 mL ammonia, 70.5 mL ultrapure water, and 48 mL absolute ethanol was added to the above solution gradually under vigorous stirring. After 2 hours, the cloudy white solution was collected and centrifuged to obtain the silica NPs. The product was washed twice with water and ethanol to remove traces of the starting materials.

5.3.5. Functionalisation of silica NPs

In order to improve the interaction of silica NPs with the monomer and the target protein, it was better to functionalise the surface with amino functional groups applying a modified reported method (315). The resulting silica NPs (1g) from the previous step were dispersed in 80 mL toluene via ultrasound sonication and then heated to 90 °C. Afterwards, 2 mL of APTES dissolved in 20 mL of toluene were added to the above solution dropwise with vigorous stirring. The solution was left to react for 12 hours under a N_2 atmosphere. The resulting NPs were centrifuged and washed with acetone and ethanol, and then dried at 70°C under vacuum.

5.3.6. Synthesis of fluorescent PDA MIPs

The fluorescent PDA MIPs were prepared via incorporating CDs in their structure using a reported method with slight modifications (316). The CDs solution (200 µL) was added to 25 mL of Tris buffer (pH 8.2) followed by the addition of 30 mg pepsin. The solution was stirred for pre-assembly for 1 hour followed by the addition of 200 mg dopamine. The solution was stirred at room temperature for 24 hours, then the black polymer precipitates were collected and centrifuged. Pepsin was removed from the binding sites via washing with 1% (w/v) SDS / 10% (v/v) acetic acid mixture for 4 hours followed by rinsing with distilled water twice and drying under vacuum to obtain the solid precipitates. PDA NIPs were prepared simultaneously without the addition of pepsin.

5.3.7. Synthesis of PDA MIPs on silica NPs

The amino functionalised silica NPs, prepared in the previous step, were used as a solid support in the core of PDA MIPs. The procedure was adopted from a reported method with some modifications (317). Silica-NH$_2$ NPs (200 mg) were dispersed in 25 mL of Tris buffer (pH 8.2) followed by the addition of 30 mg pepsin. The solution was stirred for pre-assembly for 1 hour followed by the addition of 200 mg dopamine. The solution was stirred at room temperature for 24 hours, then the black polymer precipitates were collected and centrifuged. Pepsin was removed from the binding sites via washing with 1% (w/v) SDS / 10% (v/v) acetic acid mixture for 4 hours followed by rinsing with distilled water twice and drying under vacuum to obtain the solid precipitates. PDA NIPs were prepared simultaneously without the addition of pepsin. The functionalisation and the synthesis procedures are illustrated in **Figure 57**.
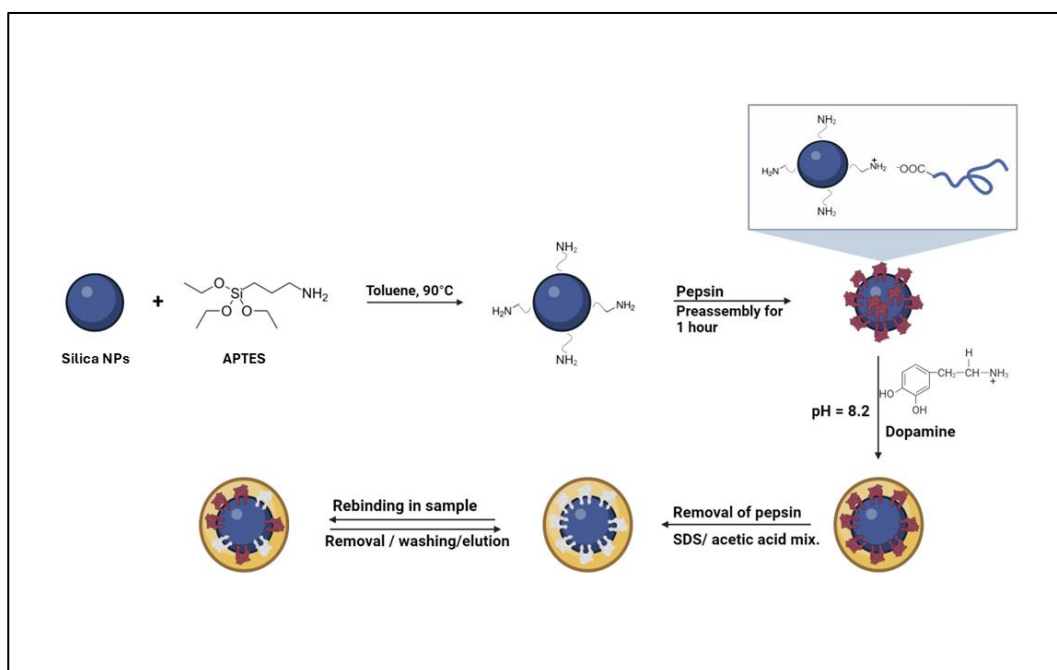
Figure 57. Functionalisation of silica NPs and the synthesis of PDA MIPs.

5.3.8. Protein binding experiments

To confirm the effectiveness of the molecular imprinting process, individual binding assays were conducted for each of the synthesised polymers using a known concentration of pepsin. These binding experiments involved incubating 20 mg of the prepared polymers with 5 mL of a 1 mg mL^{-1} pepsin solution for specific duration of time (2 hours). After the optimal binding duration was reached, the solutions underwent centrifugation at 4500 rpm for 10 minutes, and the concentration of pepsin in the supernatant was determined using UV spectrometry. A blank sample consisted of deionised water incubated with the same mass of either PDA MIPs or PDA NIPs for the same duration was used in all measurements. To estimate the binding capacity of the amount of pepsin adsorbed per gram of polymers was calculated using equation 17:

$$Q = (Ci - Ct).V/m \qquad \text{(eq. 17)}$$

where, Q (mg g^{-1}) is the quantity of pepsin in milligrams adsorbed per gram of polymer, Ci (mg mL^{-1}) is the starting concentration of pepsin, Ct (mg mL^{-1}) is the remaining concentration of pepsin after incubation time (t), V (mL) is the volume of pepsin solution, and m (g) is the mass of PDA MIPs or PDA NIPs applied in the experiment. All the experiments were done in triplicate to validate precision of the results.

5.3.9. Characterisation of PDA MIPs

Characterisation of the synthesised PDA MIPs constituted an important step in the assessment of their success, particularly in terms of their distinct binding properties. Therefore, the morphology of these polymers was evaluated using SEM, allowing for an estimation of particle size. Furthermore, FTIR spectra were acquired over the range of $4000 - 500$ cm^{-1} for pepsin, silica-NH$_2$ NPs, PDA MIPs, and PDA NIPs to identify key spectral features, ensure template removal, and confirm the absence of residual starting materials.

TGA and DSC were carried out on silica NPs, silica-NH$_2$ NPs, PDA MIPs, and PDA NIPs. Data obtained from TGA, and DSC analyses served to confirm the completeness of polymerisation, detect any unreacted starting materials, and quantify the moisture content. TGA was conducted over a temperature range of 40 to 800°C with a heating rate of 10°C min^{-1} under a nitrogen gas flow of 50 mL min^{-1}, while DSC measurements covered a temperature range of 25 to 400°C with a heating rate of 10°C min^{-1}.

To elucidate the order of binding kinetics, rebinding experiments were performed on the developed polymers at varying time intervals. Specifically, 25 mg of the PDA polymers were incubated with 5 mL of a 1 mg mL^{-1} pepsin solution for time periods ranging from 0 to 4 hours. The quantity of pepsin adsorbed per gram (Q) was plotted against time to deduce the binding kinetics order.

Binding isotherm characterisation was conducted as well on PDA MIPs and NIPs via incubating a certain mass of polymers (25 mg) with a specific volume of pepsin (5mL) of increasing concentrations from 0.2 to 1.2 mg mL^{-1} for 2 hours.

To evaluate the binding selectivity, the binding performance of PDA MIPs was compared to that of their respective PDA NIPs, with the imprinting factor (IF) calculated by dividing Q values for MIPs by those for their corresponding NIPs.

5.3.10. Fluorescence measurements for fluorescent PDA MIPs

The produced fluorescent PDA MIPs were initially examined under the UV light for visual detection of fluorescence. Furthermore, the produced CDs solution, a suspension of PDA MIPs and PDA NIPs (3mg mL^{-1}) in PBS buffer (pH 7.0) were measured using a spectrofluorometer at λ_{exc}= 320 nm and λ_{em}=410 nm.

5.4. Results and discussion

5.4.1. Synthesis of CDs

In the synthesis of CDs from citric acid, hydrothermal reactions at 200°C were sufficient to complete the carbonisation process, resulting in the production of fluorescent particles (313). In this process, ammonia reacted with citric acid in a pressurised environment, leading to the formation of citrazinic acid at temperatures exceeding 96°C. Because of the slow kinetics of this breakdown process and the relatively low nucleophilic strength of ammonia, the yield of citrazinic acid remained limited. Under these hydrothermal conditions, the carboxylic end of citric acid had the potential to react with terminal alcohols, resulting in the formation of networks held together by ester bonds (313) as shown in **Figure 58**.
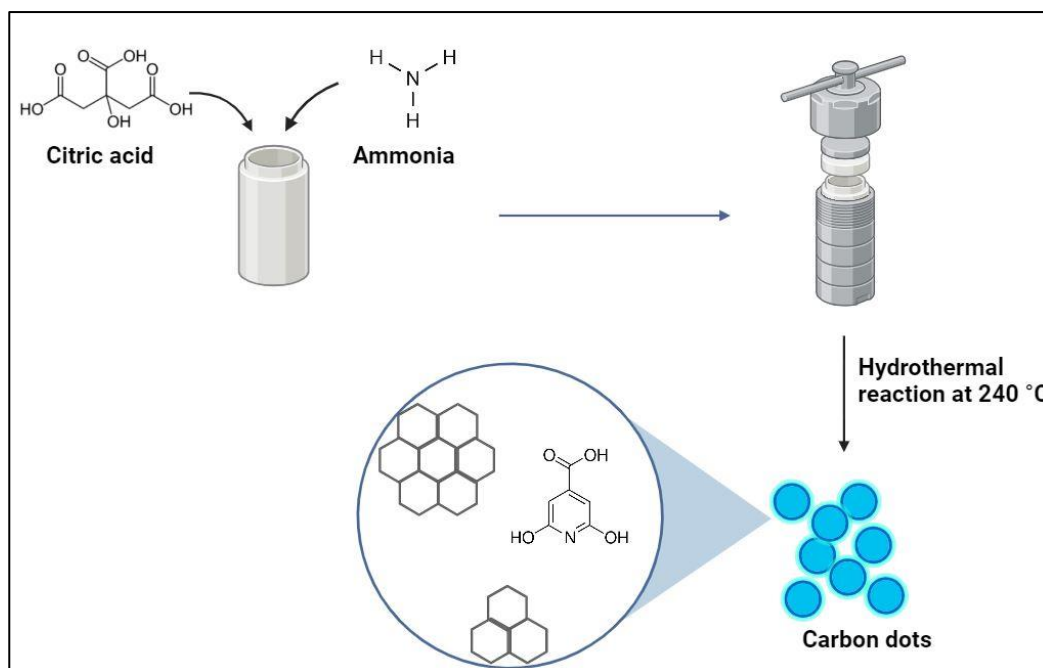
Figure 58. *Hydrothermal synthesis of CDs from citric acid.*

5.4.2. Synthesis and functionalisation of silica NPs

Uniform sized and well dispersed silica NPs were synthesised by the Stober method in which TEOS is used as silicon source in alkaline medium provided by ammonia (314). In order to maximise the interaction between silica NPs and pepsin, silica was further functionalised with amino groups using APTES to create (SiO_2-NH_2) (315). In this way, electrostatic interactions were predicted to be formed between the amino groups on silica NPs and the carboxylic groups in the protein backbone resulting in better binding. Silica NPs and amino functionalised silica NPs were characterised via FTIR to ensure complete functionalisation.

5.4.3. Synthesis of PDA MIPs on CDs

In an attempt to create fluorescent PDA MIPs, CDs prepared from citric acid via hydrothermal reaction were incorporated in their structure. The rationale behind this was that the further binding of pepsin to the binding sites in dopamine would result in quenching of fluorescence in a linear fashion which can be used to determine pepsin's concentration. However, after synthesis of PDA MIPs, there was a significant reduction in the native fluorescence of CDs observed both under UV light and quantitatively using the spectrofluorometer as shown in the **Figure 59**.
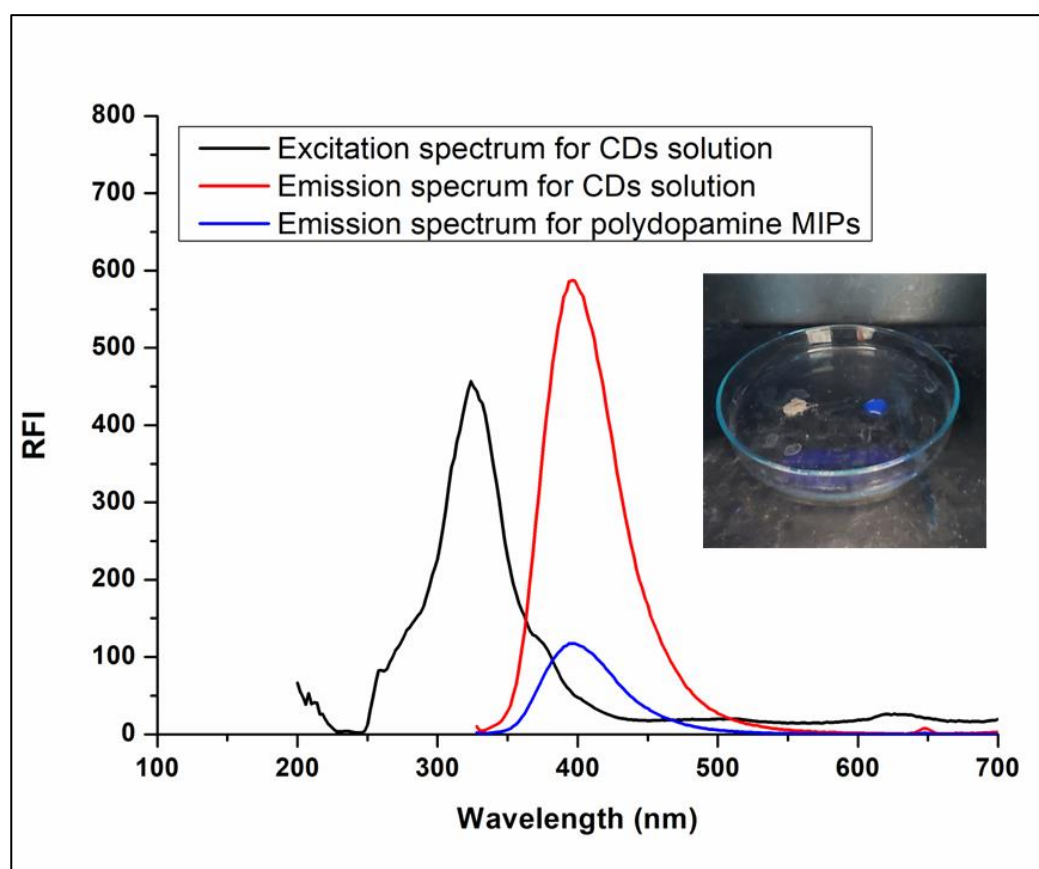
Figure 59. Excitation and emission spectra of CDs solution and the emission spectrum of PDA MIPs on CDs. Inset. Picture under UV for a drop of CD solution and PDA MIPs powder.

This could be attributed to many factors including mainly the black colour of PDA physically obscuring the fluorescence of CDs and the deep incorporation of CDs in the polymer matrix. This reduction in fluorescence was detrimental to their application. Therefore, the amount of dopamine in the reaction was reduced to 100, 50, and 25 mg however, the same outcome was observed for all the amounts of dopamine. As a result, this method came to an end and CDs were substituted with silica-NH_2 NPs as sacrificial support in PDA MIPs.

5.4.4. Synthesis of PDA MIPs on silica-NH_2 NPs

Silica NPs were used as a sacrificial support for PDA MIPs due to their wide variety of appealing properties including uniform size range, biocompatibility, and functionalisation ability. At the beginning, bare silica NPs were used as a support, however, binding to pepsin was very minor. Therefore, silica NPs were further functionalised with amino groups via APTES to enhance the interaction with pepsin. The initial results of the binding capacity showed very minor difference in binding between MIPs and NIPs. In an effort to enhance the binding capacity and increase the imprinting factor (IF), a complete optimisation of the reaction conditions and the starting materials was carried out. Variable amounts of dopamine, pepsin, and silica-NH_2 NPs were tested in addition to varying the pH in the alkaline range from (7.5 to 9.0). The results of optimisation are shown in **Figure 60**.
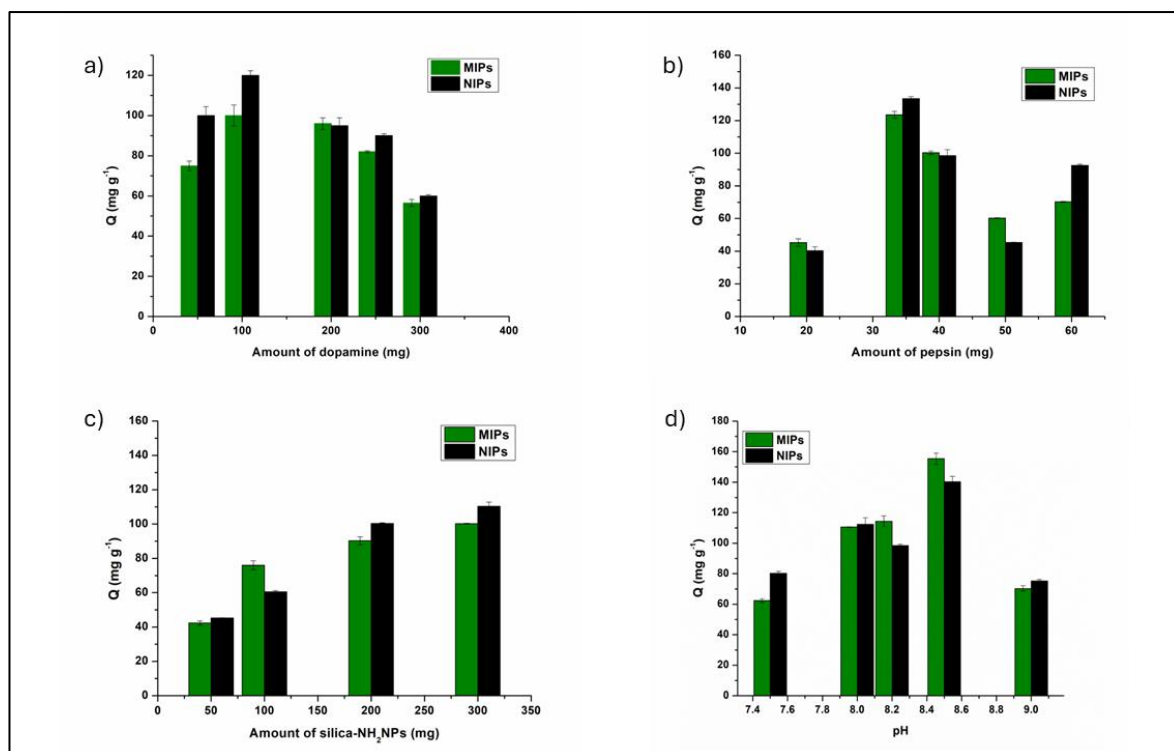
Figure 60. *Optimisation of different parameters for the synthesis of PDA MIPs, a) amount of dopamine, b) amount of pepsin, c) amount of silica NPs, d) pH (average of triplicate measurements each).*

The results of optimisation shown in the figure showed that the binding capacity reached higher values ~ 160 mg g^{-1}; however, NIPs exhibited very similar if not higher values resulting in very low imprinting factors. These results indicated that the binding of MIPs to pepsin is governed by non-specific binding. These findings come in contradiction with the huge volume of published work applying dopamine as monomer for MIPs for various targets.

5.4.5. Possible explanation of the poor binding behaviour of PDA MIPs

A thorough literature search was conducted to explore improved methods or modifications to enhance binding efficiency. During this process, a study highlighting the issue of non-specific adsorption in PDA MIPs following the template removal step

emerged (318). The researchers developed magnetic PDA MIPs and compared their binding efficiency with both unwashed and washed PDA NIPs.

They observed that, in most prior studies on PDA MIPs, only the MIPs were washed with a washing solution, while the NIPs were simply dried and tested without further treatment. To address this, they compared the binding of PDA MIPs to both washed and unwashed PDA NIPs. The findings revealed that both the PDA MIPs and the washed PDA NIPs showed similarly high binding capacities, significantly higher than those of the unwashed PDA NIPs (318). This suggested that the apparent superior binding capacity of PDA MIPs reported in the literature could primarily result from the non-specific binding, rather than the creation of specific binding sites in the polymer. Further analysis showed that the washing process likely disrupted the binding cavities in PDA MIPs and activated the PDA surface, increasing non-specific interactions. The authors also tested various washing solutions, including acetonitrile: acetic acid (20%:3%), sodium hydroxide (pH 11), methanol, and methanol: acetic acid (9:1 v/v), and found similar results, particularly with acetic acid, which notably increased the binding capacities of both PDA MIPs and PDA NIPs (318). When comparing the binding capacity of PDA MIPs washed with methanol: acetic acid (9:1 v/v) to PDA NIPs washed only with water, it was initially assumed that the superior binding observed in the MIPs was due to the imprinted cavities. However, this assumption proved incorrect. In fact, PDA NIPs that underwent the same washing procedure as the MIPs (using the same solvent and washing duration) exhibited similarly high binding capacities, comparable to those of the MIPs.

These results concorded with the findings of this work, since PDA NIPs were always washed simultaneously along PDA MIPs and therefore, providing a good explanation and insight into why the binding capacity of both PDA MIPs and PDA NIPs were very close even with thorough optimisation.

A binding selectivity assay towards pepsin was conducted for both PDA MIPs versus PDA NIPs and the imprinting factor (IF) was computed using the formula.

$$IF = \frac{Q_{MIPs}}{Q_{NIPs}} \hspace{3cm} \text{(eq. 18)}$$

Using a concentration of 1 mg mL^{-1} of pepsin, the IF value was 1.02, which proved the poor selectivity of PDA MIPs compared to PDA NIPs even after careful optimisation of the reaction parameters.

5.4.6. Characterisation of PDA MIPs and NIPs

5.4.6.1. Morphological characterisation

The produced PDA MIPs and NIPs were visually inspected under SEM to determine their shape, relative size and ensure the complete coating of the silica NPs with PDA. The SEM pictures shown in **Figure 61** revealed the formation of uniform sized silica NPs of an estimated size of ~ 210 nm. The further functionalised NPs did not show an increase in size. However, the pictures showing PDA MIPs and NIPs revealed a slight increase in the diameter to approximately 270 nm proving the grafting of the polymer on the surface causing PDA MIPs and NIPs to retain the same spherical shape.
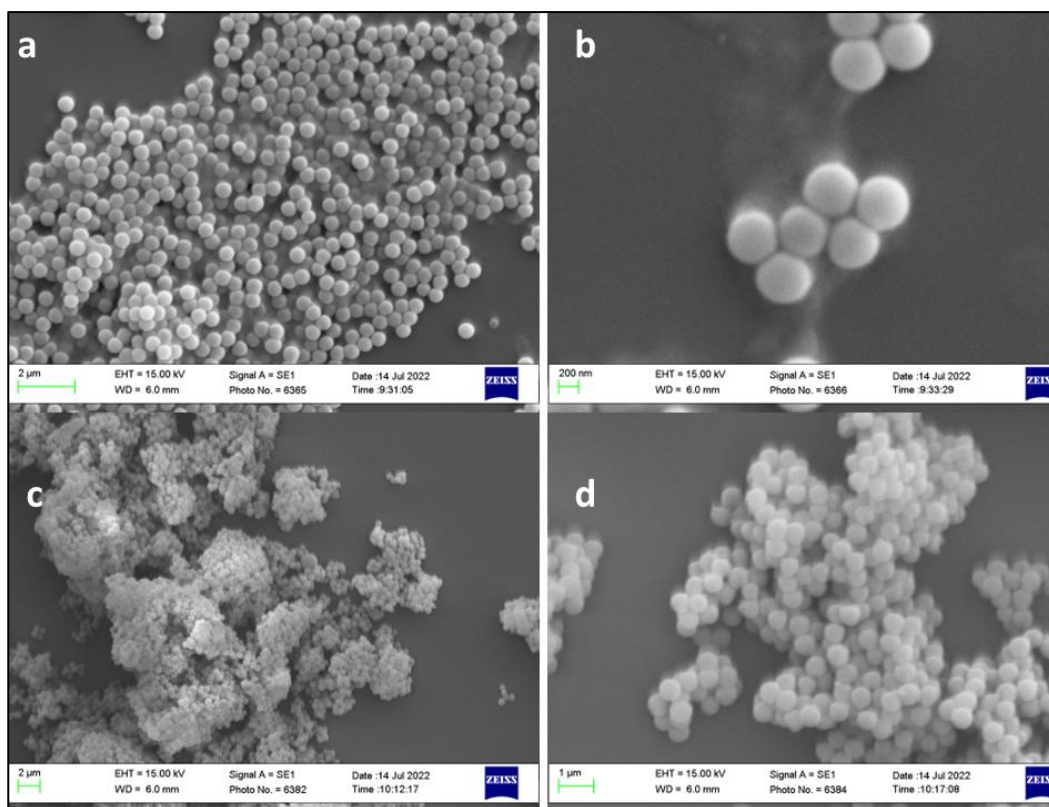
Figure 61. *SEM images of a) silica NPs 100 nm, b) silica-NH₂ NPs, c) PDA MIPs 120 nm, and d) PDA NIPs 120 nm.*

5.4.6.2. Chemical characterisation

The synthesised silica-NH$_2$ NPs, PDA MIPs and NIPs, as well as pepsin itself, were measured via IR spectroscopy to ensure complete grafting of PDA and absence of pepsin in the binding sites. **Figure 62** shows the IR spectra of all samples. The distinctive peaks for amino functionalised silica NPs at 3334, 3037, and 1500 cm^{-1} corresponding to the amino group, residual C-H stretching and bending, respectively, could be discerned. However, those peaks were completely absent in the IR spectra of PDA MIPs and NIPs indicating complete grafting of PDA on the surface. Moreover, the distinctive peaks of pepsin at 3236 cm^{-1} and 757 cm^{-1} were absent in the spectrum of PDA MIPs proving complete template removal.
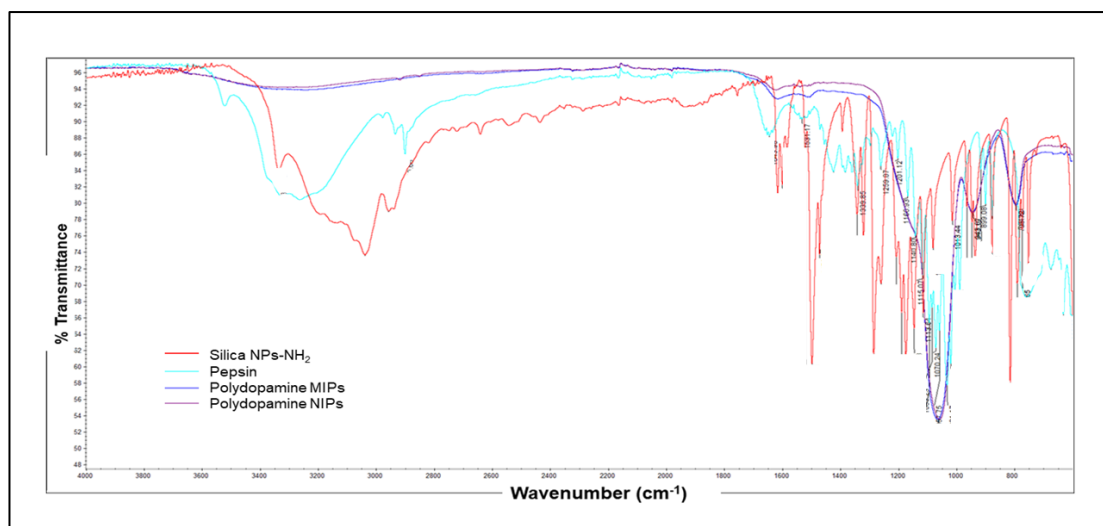
Figure 62. *FT-IR spectra of silica-NH$_2$ NPs, pepsin, PDA MIPs, and PDA NIPs.*

5.4.6.3. Thermal characterisation

DSC thermograms (**Figure 63**) were collected for silica NPs, silica-NH$_2$ NPs, PDA MIPs and NIPs. The DSC curves of silica NPs and silica-NH$_2$ NPs showed only an endothermic peak around 100°C corresponding to the evaporation of moisture, yet DSC curves of both PDA MIPs and NIPs showed two endothermic peaks at around 100°C and 310°C, indicating the melting of the grafted PDA layer on the surface of the thermally stable silica NPs.
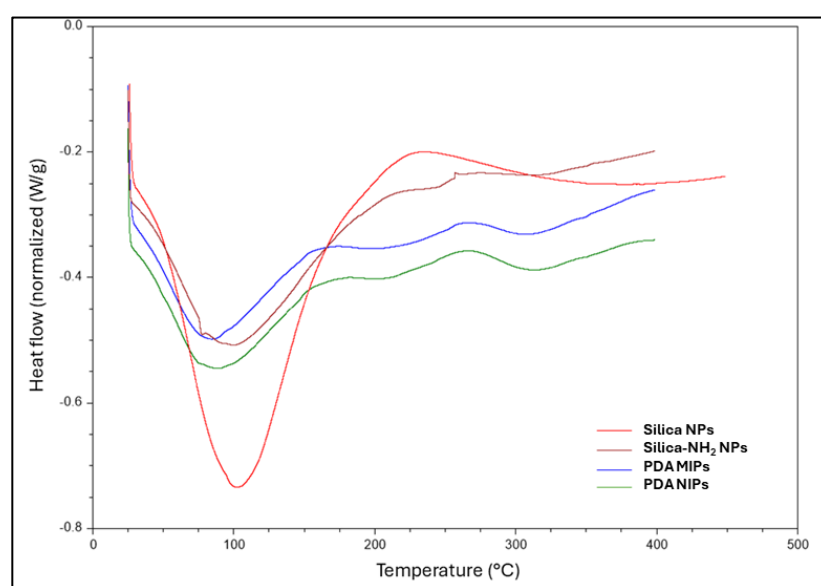
Figure 63. *DSC thermograms of silica-NH$_2$ NPs, PDA MIPs, and PDA MIPs*

217

This data was further verified with TGA (**Figure 64**), which showed no notable difference in the decomposition pattern between PDA MIPs and NIPs due to their structural similarity. However, there was an extra weight loss step in the thermograms of both compared to silica and silica-NH$_2$ NPs which corresponded to the decomposition of the PDA layer at around 310°C.
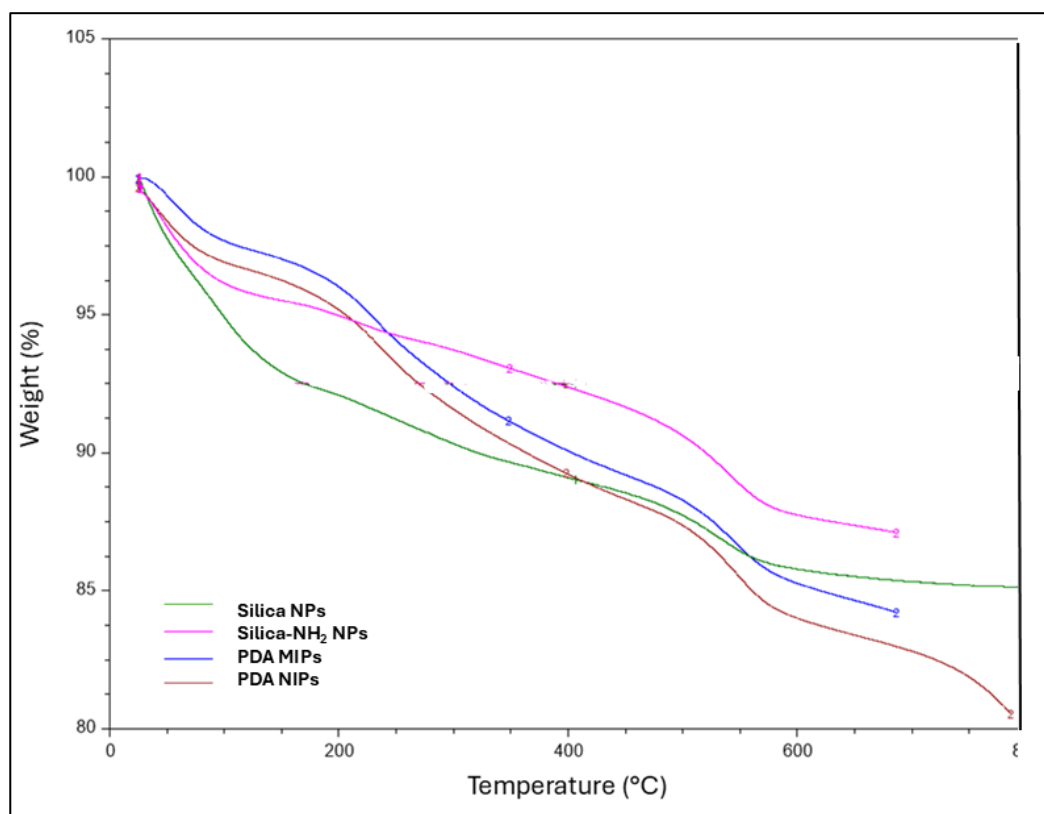
Figure 64. TGA thermograms of silica NPs, silica-NH$_2$ NPs, PDA MIPs, and PDA MIPs.

5.4.6.5. Functional characterisation

In an attempt to understand the binding behaviour of PDA MIPs and comparing it to PDA NIPs, a binding kinetics study was conducted. The resulting curves from plotting time versus binding capacity (Q) are displayed in **Figure 65**. The resulting curves for both PDA MIPs and NIPs are almost identical, showing maximum binding capacity after 2 hours after which the binding reached a plateau.

Therefore, if PDA MIPs did exhibit specific binding sites, it should have shown a different binding kinetics pattern than NIPs. The MIPs developed in the previous chapters and in other reported methods showed faster binding and higher binding capacity than NIPs. This was not the case for PDA MIPs further indicating that binding was governed by nonspecific interactions.
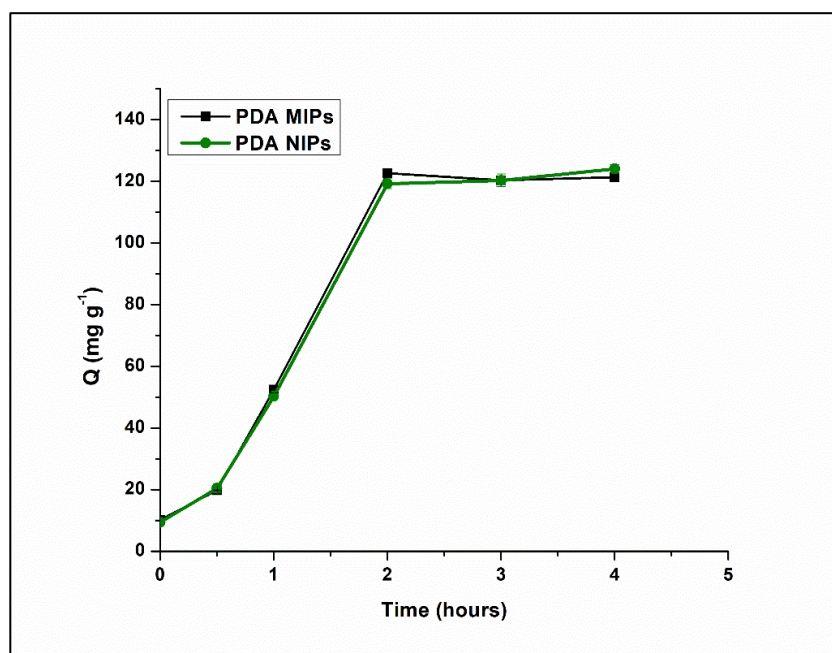
Figure 65. Binding kinetics for PDA MIPs and PDA NIPs (average of triplicate measurements).

The results of the binding isotherm study are shown in **Figure 66.** Again, PDA MIPs and NIPs exhibited similar binding behaviour which is mostly nonspecific towards pepsin with and R^2 values of 0.9791 and 0.9404 for PDA MIPs and NIPs respectively.
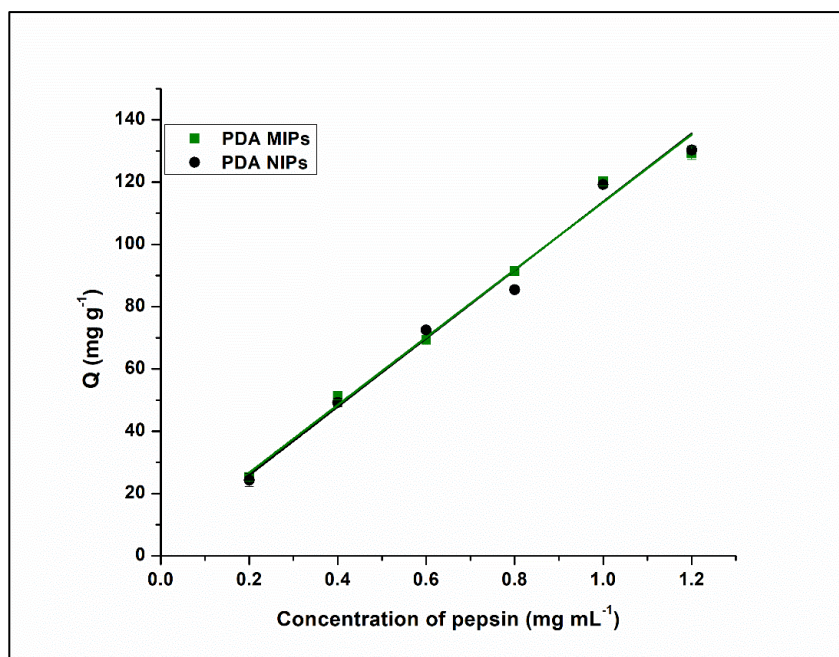
Figure 66. Binding isotherms for PDA MIPs and PDA NIPs (average of triplicate measurements).

5.5. Conclusion and recommendations

In this study, PDA MIPs were synthesised for the selective binding and extraction of pepsin, a biomarker for GERD. Two materials, silica NPs and CDs, were evaluated as core supports for the PDA MIPs. PDA MIPs developed on CDs exhibited a significant reduction in native fluorescence due to adsorption by the black colour of PDA. Consequently, silica NPs proved to be a better alternative as a solid support. To enhance the interaction between pepsin and silica NPs, the latter were functionalised with amino groups via APTES. A series of optimisation experiments were conducted to improve the binding affinity of PDA MIPs to pepsin and increase selectivity compared to NIPs.

However, optimisation had little effect on selectivity, which remained similar to that of the NIPs. Characterisation of both MIPs and NIPs was carried out using techniques such as SEM, FT-IR spectroscopy, DSC, and TGA to investigate the properties of the polymers and determine the cause of the poor selectivity. These analyses confirmed polymerisation, uniform particle size, and the absence of target molecules. Despite this, binding kinetics and isotherm experiments revealed nearly identical behaviour between MIPs and NIPs. A subsequent literature review supported these findings, referencing a 2021 study (318) that explained the apparent selectivity reported for PDA MIPs in previous literature. It was found that the washing step in MIP preparation disrupted the binding cavities and activated the PDA surface, increasing nonspecific binding to the target. Since both MIPs and NIPs were washed using the same solvent and time intervals, the issue became apparent, highlighting the nonspecific binding of PDA MIPs. These conclusions were confirmed through binding experiments and characterisation tests on both PDA MIPs and NIPs. Based on these findings, the following recommendations are proposed:

1. The use of a different monomer which provides multiple points of interaction with the target via different bonds like electrostatic bonds and hydrogen bonds.

2. Washing must be performed on both MIPs and NIPs simultaneously using the same washing solution and same time interval to avoid false high binding results for MIPs resulting from nonspecific binding.

3. The use of different polymerisation systems for carbon dots to avoid physical quenching of fluorescence by the colour of the polymer.

4. To establish a fair comparison between MIPs and NIPs, all the procedures have to be identical including synthesis, washing, binding experiments, and storage.

5. Specific and non-specific binding are very easy to confuse. Therefore, meticulous tests, binding experiments, and validation experiments must be performed to ensure that binding of MIPs is due to the presence of binding sites not due to uncontrolled interaction between random sites of the polymer backbone and the target.

Chapter 6. General Conclusions and Future Work

Chapter 6. General conclusions and future work

Protein biomarkers are a very important class of biomarkers that have captured the attention of many health care professionals in the recent years. Due to their abundance in the body, and their ease of detection without the need for invasive procedures, they have been the focus for the latest research in the field of diagnostics. Herein, the role of analytical chemistry as a science arises to complement the role of diagnostics via providing sensitive, reliable, accurate, and cost-effective methods for detection of different biomarkers.

Pepsin, a digestive enzyme, has been identified recently as a biomarker for gastroesophageal reflux disease. Abnormal concentrations of pepsin in human saliva are indicative of increased reflux resulting in increased stomach contents in the mouth including pepsin. However, a meticulous search showed that only very few analytical methods had been developed for detection and quantitation of pepsin. Consequently, this work took on the burden of developing new, sensitive and applicable methods for the extraction, detection, and quantitation of pepsin that can be applied as effective tools for diagnosis and can actively contribute to patients' welfare.

Molecularly imprinted polymers (MIPs) are a class of synthetic polymers that can be tailor made to bind any target of interest with a selectivity that can match that of antibodies. MIPs presented an attractive solution for the extraction of pepsin from complex matrices such as saliva, where other interfering enzymes and molecules can coexist. In addition, MIPs offer an array of advantages that made them the subject of choice for this work. These advantages included: high selectivity, ease of synthesis, cost effectiveness, reproducibility, long term stability, reusability, and scalability.

The first type of MIPs developed in this work were magnetic MIPs, in which magnetic iron oxide nanoparticles functionalised with amino functional groups were included in the core of MIPs. Different monomers, cross-linkers and different reaction conditions were thoroughly tested to achieve the optimum magnetic MIPs that were capable of binding pepsin with high selectivity. After careful optimisation, magnetic MIPs were found to bind pepsin with a binding capacity (Q) reaching to 190 mg g^{-1} in comparison to their corresponding NIPs. Moreover, the developed MIPs and NIPs were carefully characterised using different analytical methods such as FTIR, TGA, DSC, and SEM to investigate their qualities and prove their validity. Finally, the developed magnetic MIPs were applied successfully for the dispersive solid phase extraction of pepsin from saliva samples. After extraction, only a strong neodymium magnet was used to separate the magnetic MIPs with the bound pepsin without any need for filtration or centrifugation. The bound pepsin could then be released from the MIPs' binding sites using phosphate buffer and became available for further quantitation. The developed magnetic MIPs were also reusable up to three cycles of binding and release of pepsin contributing significantly to their economic value.

For the quantitation of the extracted fragments of pepsin via the developed MIPs, the literature was investigated for simple and sensitive analytical methods that can be applied to the different pepsin samples. Nonetheless, only one LC-MS method was found that was concerned with the analysis of pepsin. Despite the sensitivity of this method, it was very complicated, not-straightforward, and definitely not applicable. As a result, to complement the work and a provide a reliable method for analysis of the extracted pepsin fragments, a new HPLC method was developed for pepsin.

The developed HPLC method utilised a size exclusion chromatography column for effective separation of pepsin. The optimised method applied phosphate buffer (pH 3.0) as a mobile phase, a flow rate of 0.35 mL min^{-1}, and a UV detection at 270 nm. The developed method was validated according to the ICH guidelines regarding accuracy, sensitivity, precision, and robustness. Moreover, the developed method covered a linear range from 0.5 to 150 μg mL^{-1} with an R^2 value of 0.9989. Furthermore, the sensitivity of the developed method was indicated by the measured limit of detection value (LOD) of 0.10 μg mL^{-1} which is ideal for the quantitation of the very low anticipated concentrations of saliva in patients with GERD. Finally, the developed method was successfully applied to human saliva samples spiked with pepsin without any interference from the enzymes coexisting with pepsin in saliva such as amylase or lipase.

Following the development of the magnetic MIPs, efforts were focused on the development of 'an all in one' integrated extraction and analytical tool for pepsin. Therein, the idea of creating new fluorescent MIPs was born as a type of MIPs that could be applied for both the extraction of pepsin and the determination of its concentration via the effect on fluorescence. Consequently, the application of fluorescein as a readily available and relatively cheap fluorescent dye was taken into account. Fluorescein had been employed as a fluorescent dye for many MIPs previously, however, some of the works reported reduced sensitivity and a recommendation for testing another dye. Therefore, rhodamine B was selected to develop another type of fluorescent MIPs and to compare their performance with fluorescein MIPs. The selection of rhodamine B was not random, it was based on a structural feature in rhodamine B which is the two (diethylamino) groups.

226

It was predicted that at the working pH of synthesis, these two groups would carry a positive charge which would enable an electrostatic interaction with the negatively charged pepsin molecule resulting in better binding and high selectivity towards pepsin.

The procedure for making both fluorescein MIPs (FMIPs) and rhodamine B MIPs (RMIPs) was carefully optimised to ensure the highest selectivity and the best possible binding. As predicted, RMIPs exhibited a higher binding capacity value of 256 mg g^{-1} compared to FMIPs at 217 mg g^{-1}, as well as faster binding kinetics where maximum binding occurred after 1 hour compared to FMIPs at 2 hours. In addition, to establishing a complete comparison profile, both FMIPs and RMIPs and their corresponding FNIPs and RNIPs were characterised via SEM, FTIR, TGA and DSC to compare their performance. Finally, it was noted that the binding of pepsin to both FMIPs and RMIPs caused a concentration dependent quenching. Consequently, this quenching was exploited as a quantitation technique for pepsin and therefore achieving the goal of an integrated extraction and analytical tool. RMIPs showed a superior analytical performance covering a linear range from 0.28 to 42.85 μmol L^{-1} compared to FMIPs covering a range from 0.71 to 35.71 μmol L^{-1}. Moreover, the sensitivity of RMIPs was confirmed at a lower limit of detection of 0.11 μmol L^{-1} surpassing the LOD of FMIPs being 0.34 μmol L^{-1}. Both RMIPs and FMIPs were applied effectively for the extraction and quantitation of pepsin from standard solutions and spiked saliva samples proving the achievement of the designated goal of this work.

In an attempt to go beyond the traditional MIPs in powder form, molecularly imprinted membranes (MIMs) were considered for binding of pepsin. MIMs offered a series of advantages that could be useful for binding of pepsin such as the greater surface area, the accessibility to the binding sites, and enhanced mass transfer which were appealing qualities for binding of large targets such as pepsin. In addition, a fluorescent quality was imparted on MIMs via incorporating carbon dots (CDs) in their matrix in order to achieve a visual detection of the binding event. A mixture of hydrophilic monomers was employed in the synthesis of the fluorescent MIM (FMIM) in order to synthesise a hydrophilic FMIM capable of binding pepsin in different aqueous matrices in which it normally existed such as saliva. The procedure was thoroughly optimised to achieve the optimal balance between a reliable binding capacity and a good mechanical stability. The produced membranes were visualised under the fluorescent microscope, which revealed that the CDs were uniformly distributed in the matrix of FMIM and FNIM. Moreover, the developed membranes were also characterised using FTIR, TGA, DSC, and light and fluorescent microscopes to investigate their qualities and applicability. Finally, it was noted that binding of pepsin to the FMIM caused an enhancement in fluorescence under UV light which could be observed with the naked eye. Although the fluorescent signal can be visualised at relatively higher concentrations of pepsin, it is still a very promising diagnostic tool for pepsin via applying spectrofluorimetric analysis using a solid sample holder accessory.

During the literature search for this work, a huge volume of publications that utilised dopamine as a functional monomer for the synthesis of MIPs was noted. As a result, PDA MIPs were considered in this work for the binding and extraction of pepsin.

Dopamine has the ability to self-polymerise at an alkaline pH which was an appealing quality to devise a simple and quick method of synthesis of MIPs for pepsin. To achieve a core shell, imprinting CDs and silica nanoparticles (NPs) were considered for this work. However, after polymerisation the fluorescence of CDs was significantly quenched due to the black colour of PDA MIPs. Therefore, only silica NPs were employed in this work. Functionalisation of silica NPs with amino groups was carried out to enhance the binding with the negatively charged pepsin molecules. During the optimisation phase, it was noted that the binding capacity of PDA MIPs was close to that of PDA NIPs. Despite all efforts made to optimise the procedure to reach high binding capacity and selectivity, PDA NIPs always had similar binding capacity values to that of PDA MIPs reaching to 160 mg g^{-1}. Characterisation of the developed PDA MIPs and NIPs was conducted via FTIR, TGA, DSC, and SEM to ensure complete polymerisation and template removal. Moreover, binding kinetics and binding isotherm studies were carried out to identify the origin of the issue. Various characterisation techniques ensured a complete polymerisation atop silica nanoparticles and complete template removal which ruled out the possibility of errors during synthesis. Nevertheless, the binding kinetics and isotherm studies revealed that PDA MIPs followed a non-specific binding pattern very similar to PDA NIPs.

After a literature search for possible explanations for the root of this problem, a recent study was found that could explain this issue. In this study, the researchers revealed that the high selectivity of PDA MIPs usually reported in different publications can be largely attributed to difference in the washing procedure of the developed MIPs and NIPs. It was noted that in most of these works, only PDA MIPs were washed for target removal while NIPs were only washed with water.

This discrepancy caused the activation of PDA surface and rupture of the imprinted sites resulting in significant non-specific binding. However, PDA MIPs and NIPs washed simultaneously with the same solvent for the same time interval showed similar binding capacity due to non-specific binding which agreed with the findings of this study. Consequently, this work was not taken further for application into extraction of pepsin from different matrices.

In summary, this thesis offers a set of different MIPs each presenting their advantages and potential applications. Magnetic MIPs offered high binding capacity, reusability, easy applicability due to their magnetic quality, and effective extraction and release of pepsin. The fluorescent FMIPs and RMIPs offered an integrated extraction and analysis tool that effectively contributed to the extraction and analysis of pepsin. Meanwhile, RMIPs showed superior binding capacity, linearity and lower limit of detection than FMIPs. In fact, RMIPs showed the highest binding capacity value of all the developed MIPs in this project. The fluorescent MIMs offered a useful binding capacity, applicability and ease of synthesis, and most importantly a visual signal upon binding of pepsin owing to the enhancement of fluorescence after binding pepsin in different samples. If taken further, FMIMs can be a very promising diagnostic and analytical biosensor for pepsin. Finally, PDA MIPs were a promising approach for a simple synthesis route, however, there were significant issues with the selectivity of the developed MIPs in comparison to NIPs that originated from the washing step. Unfortunately, these issues could not be mitigated by careful optimisation or utilisation of different washing solutions, which brought this work to an early end.

The capabilities of MIPs are endless in the field of analytical chemistry and biosensor development. There is always room for more development and applications that can continuously enhance and contribute to human welfare. Future work will focus on the exploration of new types of MIPs for application to other biomarkers or molecules of interest including pharmaceuticals. Greener monomers will be considered as alternatives for the conventional monomers such deep eutectic solvents and chitosan. Higher sensitivity limits will be attempted via using tailor made monomers. Moreover, applications to real patients will be considered to effectively contribute to the field of health care and diagnostics via collaboration with hospitals and health care professionals.

References

1.   Takeuchi T, Sunayama H. Molecularly imprinted polymers. Encycl Polym Nanomater. 2014;126:1–5.

2.   Polyakov MV. Adsorption properties and structure of silica gel. Zh Fiz Khim. 1931;6:799–805.

3.   Pauling LA. Theory of the structure and process of formation of antibodies. J Am Chem Soc. 1940;62:2643–2657.

4.   Wulff G. Molecular imprinting in cross-linked materials with the aid of molecular templates – A way towards artificial antibodies. Angew Chemie Int Ed. 1995;34:1812–1832.

5.   Wulff G, Sarhan A, Zabrocki K. Enzyme-analogue built polymers and their use for the resolution of racemates. Tetrahedron Lett. 1973;14:4329–4332.

6.   Wulff G, Sarhan A. Use of polymers with enzyme-analogous structures for resolution of racemates. Angew Chemie Int Ed. 1972;11:341–344.

7.   Fischer L, Muller R, Ekberg B, Mosbach K. Direct enantioseparation of b-adrenergic blockers using a chiral stationary phase prepared by molecular imprinting. J Am Chem Soc. 1991;113:9358–9360.

8.   Andersson L, Sellergren B, Mosbach K. Imprinting of amino acid derivatives in macroporous polymers. Tetrahedron Lett. 1984;25:5211–5214.

9. Andersson LI, Mosbach K. Molecular imprinting of the coenzyme-substrate analogue N-pyridoxyl-L-phenylalaninanilide. Chem Rapid Commun. 1989;10:491–495.

10. Takano E, Taguchi Y, Ooya T, Takeuchi T. Dummy template-imprinted polymers for Bisphenol A prepared using a Schiff base-type template molecule with post-imprinting oxidation. Anal Lett. 2012;45(10):1204–1213.

11. Shea KJ, Sasaki DY. An analysis of small-molecule binding to functionalized synthetic polymers by 13C CP/MAS NMR and FT-IR spectroscopy. J Am Chem Soc. 1991;113(11):4109–4120.

12. Wulff G, Vesper W, Grobe-Einsler R, Sarhan A. Enzyme-analogue built polymers. On the synthesis of polymers containing chiral cavities and their use for the resolution of racemates. Macromol Chem Phys. 1977;178(10):2799–2816.

13. Komiyama M, Takeuchi T, Mukawa T, Asanuma H. Molecular imprinting-from fundamentals to applications. Vol. 19, IEEE Electrical Insulation Magazine. WILEY-VCH; 2003. 1–174 p.

14. Wright KM, Bowyer MC, McCluskey A, Holdsworth CI. Molecular imprinting of benzylpiperazine: a comparison of the self-assembly and semi-covalent approaches. Int J Mol Sci. 2023;24(6):5117.

15. Spivak DA. Optimization, evaluation, and characterization of molecularly imprinted polymers. Adv Drug Deliv Rev. 2005;57(12):1779–1794.

16. Scorrano S, Mergola L, del Sole R, Vasapollo G. Synthesis of molecularly imprinted polymers for amino acid derivates by using different functional monomers. Int J Mol Sci. 2011;12(3):1735–1743.

17. Athikomrattanakul U, Katterle M, Gajovic-Eichelmann N, Scheller FW. Development of molecularly imprinted polymers for the binding of nitrofurantoin. Biosens Bioelectron. 2009;25(1):82–87.

18. Rostamizadeh K, Abdollahi H, Parsajoo C. Synthesis, optimization, and characterization of molecularly imprinted nanoparticles. Int Nano Lett. 2013;3(1):1–9.

19. Ward MA, Georgiou TK. Thermoresponsive polymers for biomedical applications. Polymers (Basel). 2011;3(3):1215–1242.

20. Fang M, Zhuo K, Chen Y, Zhao Y, Bai G, Wang J. Fluorescent probe based on carbon dots/silica/molecularly imprinted polymer for lysozyme detection and cell imaging. Anal Bioanal Chem. 2019;411(22):5799–5807.

21. Xu R, Tian J, Guan Y, Zhang Y. Peptide-cross-linked protein-imprinted polymers: easy template removal and excellent imprinting effect. CCS Chem. 2019;1(5):544–552.

22. Xu W, Dai Q, Wang Y, Hu X, Xu P, Ni R, et al. Creating magnetic ionic liquid-molecularly imprinted polymers for selective extraction of lysozyme. RSC Adv. 2018;8(39):21850. Available from: http://dx.doi.org/10.1039/C8RA03818J

23. Hansen BB, Spittle S, Chen B, Poe D, Zhang Y, Klein JM, et al. Deep Eutectic Solvents: A Review of Fundamentals and Applications. Chem Rev. 2021;121(3):1232–1285.

24. Abbott A, Capper G, Davies D, Rasheed R, Tambyrajah V. Novel solvent properties of choline chloride/urea. Chem Commun. 2003;8:70–71.

25. Marć M, Jatkowska N, Płotka-Wasylka J, Gallart Mateu D, Esteve Turrillas FA, de la Guardia M. Molecularly imprinted polymers based on deep eutectic solvents as a greenest materials for selective extraction of emerging contaminants from complex samples. TrAC - Trends Anal Chem. 2024;178:117837.

26. Liu Y, Wang Y, Dai Q, Zhou Y. Magnetic deep eutectic solvents molecularly imprinted polymers for the selective recognition and separation of protein. Anal Chim Acta [Internet]. 2016;936:168–178. http://dx.doi.org/10.1016/j.aca.2016.07.003

27. Xu K, Wang Y, Wei X, Chen J, Xu P, Zhou Y. Preparation of magnetic molecularly imprinted polymers based on a deep eutectic solvent as the functional monomer for specific recognition of lysozyme. Microchim Acta. 2018;185(146):1–7.

28. Li X, Row KH. Preparation of deep eutectic solvent-based hexagonal boron nitride-molecularly imprinted polymer nanoparticles for solid phase extraction of flavonoids. Microchim Acta. 2019;186(12):1–10.

29. Tiwari A, Uzun L, editors. Advanced molecularly imprinting materials (advanced material series). 1st ed. Wiley-Scrivener; 2016. 200–230, 432–490, 600–688 p.

30. Yan H, Kyung HR. Characteristic and synthetic approach of molecularly imprinted polymer. Int J Mol Sci. 2006;7(5–6):155–78.

31. Sun Y, Chen J, Li Y, Li H, Zhu X, Hu Y, et al. Bio-inspired magnetic molecularly imprinted polymers based on Pickering emulsions for selective protein recognition. New J Chem. 2016;40(10):8745–8752.

32. Zhai YY, Yun YB, Li CL. Preparation of bovine serum albumin molecularly imprinted polymer by precipitation polymerization. J Dispers Sci Technol 2020;41(9):1371–1380. https://doi.org/10.1080/01932691.2019.1623687

33. Wang X, Dong S, Bai Q. Preparation of lysozyme molecularly imprinted polymers and purification of lysozyme from egg white. Biomed Chromatogr. 2014;28(6):907–912.

34. Zhang X, Yang S, Sun L, Luo A. Surface-imprinted polymer coating l-cysteine-capped ZnS quantum dots for target protein specific recognition. J Mater Sci. 2016;51(12):6075–6085.

35. Komiyama M, Takeuchi T, Mukawa T, Asanuma H. Molecular imprinting: from fundamental to applications. 1st ed. WileyVCH Verlag GmbH & Co. KGaA. 2003. 20–137 p.

36. Chen L, Wang X, Lu W, Wu X, Li J. Molecular imprinting: Perspectives and applications. Chem Soc Rev. 2016;45(8):2137–2211.

37. Yoshimi Y, Katsumata Y, Osawa N, Ogishita N, Kadoya R. Synthesis of fluorescent Molecularly Imprinted Polymer Nanoparticles Sensing Small Neurotransmitters with High Selectivity Using Immobilized Templates with Regulated Surface Density. Nanomaterials. 2023;13(1):212.

38. Zhang Y Da, Huang QW, Ma C, Liu XY, Zhang HX. Magnetic fluorescent molecularly imprinted nanoparticles for detection and separation of transferrin in human serum. Talanta. 2018;188(February):540–545. https://doi.org/10.1016/j.talanta.2018.06.002

39. Lim GW, Lim JK, Ahmad AL, Chan DJC. Fluorescent molecularly imprinted polymer based on Navicula sp. frustules for optical detection of lysozyme. Anal Bioanal Chem. 2016;408(8):2083–2093.

40. Kubo T, Arimura S, Naito T, Sano T, Otsuka K. Competitive ELISA-like label-free detection of lysozyme by using a fluorescent monomer-doped molecularly imprinted hydrogel. Anal Sci. 2017;33(11):1311–1315.

41. Esen C, Canfarotta F. Molecularly imprinted polymer nanoparticles: solid-phase synthesis and molecularly imprinted nanoparticle assay. In: Denizli A, editor. Biophysics At the Nanoscale. 1st ed. Academic Press; 2024. p. 93–106.

42. Włoch M, Datta J. Synthesis and polymerisation techniques of molecularly imprinted polymers. Compr Anal Chem. 2019;86:17–40.

43. Ertürk G, Mattiasson B. Molecular imprinting techniques used for the preparation of biosensors. Sensors. 2017;17(2):1–17.

44. Quinn T. Molecularly imprinted polymers (MIPS) challenges, uses and prospects. 1st ed. Quinn T, editor. Nova Science Publishers, Inc; 2016. 1–45, 50–90 p.

45. Meischl F, Schemeth D, Harder M, Köpfle N, Tessadri R, Rainer M. Synthesis and evaluation of a novel molecularly imprinted polymer for the selective isolation of acetylsalicylic acid from aqueous solutions. J Environ Chem Eng. 2023;4(4):4083–4090.

46. Hou L, Han X, Wang N. High performance of molecularly imprinted polymer for the selective adsorption of erythromycin in water. Colloid Polym Sci. 2020;298(8):1023–1033.

47. Wulandari M, Urraca JL, Descalzo AB, Amran MB, Moreno-Bondi MC. Molecularly imprinted polymers for cleanup and selective extraction of curcuminoids in medicinal herbal extracts. Anal Bioanal Chem. 2015;407(3):803–812.

48. Jin YF, Zhang YJ, Zhang YP, Chen J, Zhou XM, Bai LY. Synthesis and evaluation of molecularly imprinted polymer for the determination of the phthalate esters in the bottled beverages by HPLC. J Chem. 2013;2013:1–9.

49. Boitard C, Rollet AL, Ménager C, Griffete N. Surface-initiated synthesis of bulk-imprinted magnetic polymers for protein recognition. Chem Commun. 2017;53(63):8846–8849.

50. Gomes C, Sadoyan G, Dias RCS, Costa MRPFN. Development of molecularly imprinted polymers to target polyphenols present in plant extracts. Processes. 2017;5(4):1–24.

51. Liu X, Wu F, Au C, Tao Q, Pi M, Zhang W. Synthesis of molecularly imprinted polymer by suspension polymerization for selective extraction of p-hydroxybenzoic acid from water. J Appl Polym Sci. 2019;136(3):1–8.

52. Sun Y, Zhang Y, Ju Z, Niu L, Gong Z, Xu Z. Molecularly imprinted polymers fabricated by Pickering emulsion polymerization for the selective adsorption and separation of quercetin from Spina Gleditsiae. New J Chem. 2019;43(37):14747.

53. Ren Y, Fan Z. Synthesis of molecularly imprinted polymers based on nitrogen-doped carbon dots for specific detection of chlortetracycline by reversed phase microemulsion method. Talanta. 2023;265:124898. https://doi.org/10.1016/j.talanta.2023.124898.

54. Li T, Li X, Liu H, Deng Z, Zhang Y, Zhang Z, et al. Preparation and characterization of molecularly imprinted polymers based on β-cyclodextrin-stabilized Pickering emulsion polymerization for selective recognition of erythromycin from river water and milk. J Sep Sci. 2020;43(18):3683–3690.

55. Zhao G, Liu J, Liu M, Han X, Peng Y, Tian X, et al. Synthesis of molecularly imprinted polymer via emulsion polymerization for application in solanesol separation. Appl Sci. 2020;10(8):3390.

56. Crapnell RD, Hudson A, Foster CW, Eersels K, van Grinsven B, Cleij TJ, et al. Recent advances in electrosynthesized molecularly imprinted polymer sensing platforms for bioanalyte detection. Sensors. 2019;19(5):1–28.

57.	Roland RM, Bhawani SA. Synthesis and characterization of molecular imprinting polymer microspheres of Piperine: extraction of Piperine from spiked urine. J Anal Methods Chem. 2016;2016:1–6.

58.	Dai CM, Zhou XF, Zhang YL, Liu SG, Zhang J. Synthesis by precipitation polymerization of molecularly imprinted polymer for the selective extraction of diclofenac from water samples. J Hazard Mater. 2011;198:175–81. http://dx.doi.org/10.1016/j.jhazmat.2011.10.027

59.	Lu Y, Zhu Y, Zhang Y, Wang K. Synthesizing vitamin E Molecularly Imprinted Polymers via Precipitation Polymerization. J Chem Eng Data. 2019;64(3):1045–1050.

60.	Pardeshi S, Singh SK. Precipitation polymerization: A versatile tool for preparing molecularly imprinted polymer beads for chromatography applications. RSC Adv. 2016;6(28):23525.

61.	Nakamura Y, Masumoto S, Kubo A, Matsunaga H, Haginaka J. Preparation of molecularly imprinted polymers for warfarin and coumachlor by multi-step swelling and polymerization method and their imprinting effects. J Chromatogr. 2017;1516:71–78. http://dx.doi.org/10.1016/j.chroma.2017.08.016

62.	Wu Y, Xiong J, Wei S, Tian L, Shen X, Huang C. Molecularly imprinted polymers by reflux precipitation polymerization for selective solid-phase extraction of quinolone antibiotics from urine. J Chromatogr A. 2024;1714:464550. https://doi.org/10.1016/j.chroma.2023.464550.

63. Eersels K, Lieberzeit P, Wagner P. A Review on synthetic receptors for bioparticle detection created by surface-imprinting techniques - from principles to applications. ACS Sensors. 2016;1(10):1171–1187.

64. Dong C, Shi H, Han Y, Yang Y, Wang R, Men J. Molecularly imprinted polymers by the surface imprinting technique. Eur Polym J. 2021;145(December):110231.https://doi.org/10.1016/j.eurpolymj.2020.110231

65. Bain CD, Whitesides GM. Modeling organic surfaces with self-assembled monolayers. Adv Mater. 1989;1(4):110–116.

66. Whitesides GM, Ostuni E, Jiang X, Ingber DE. Soft lithography in biology and biochemistry. Annu Rev Biomed Eng. 2001;3:335–373. http://www.ncbi.nlm.nih.gov/pubmed/11447067

67. Lalo H, Ayela C, Dague E, Vieu C, Haupt K. Nanopatterning molecularly imprinted polymers by soft lithography: A hierarchical approach. Lab Chip. 2010;10(10):1316–1318.

68. Fernández-Puig S, Lazo-Fraga AR, Korgel BA, Oza G, Dutt A, Vallejo-Becerra V, et al. Molecularly imprinted polymer-silica nanocomposite based potentiometric sensor for early prostate cancer detection. Mater Lett. 2022;309:131324.

69. Miardan LN, Rezaii E, Mahkam M, Khosroshahi HT. Synthesis of mesoporous silica nanoparticles linked by molecularly imprinted polymers and examination of their ability to remove uremic toxins. J Porous Mater. 2023;30(6):1995–2010. https://doi.org/10.1007/s10934-023-01480-w

70.   Yang Y, Meng X, Xiao Z. Synthesis of a surface molecular imprinting polymer based on silica and its application in the identification of nitrocellulose. RSC Adv. 2018;8(18):9802–9811.

71.   Lahcen AA, Surya SG, Beduk T, Vijjapu MT, Lamaoui A, Durmus C, et al. Metal-Organic Frameworks Meet Molecularly Imprinted Polymers: Insights and Prospects for Sensor Applications. ACS Appl Mater Interfaces. 2022;14:49399–424.

72.   Li S, Fang L, Ye M, Zhang Y. Enhanced adsorption of norfloxacin on modified TiO_2 particles prepared via surface molecular imprinting technique. Desalin Water Treat. 2016;57(1):408–418.

73.   Yang Z, Wang H, Sun H, Tang H, Nie G. Preparation of molecular imprinted polymer based on attapulgite and evaluation of its performance for adsorption of benzoic acid in water. Water Sci Technol. 2020;81(10):2176–2188.

74.   Liu H, Zhou Y, Qi Y, Sun Z, Gong B. Preparation of thiamphenicol magnetic surface molecularly imprinted polymers for its selective recognition of thiamphenicol in milk samples. J Liq Chromatogr Relat Technol. 2018;41:868–79.

75.   MIP database [Internet]. 2015 [cited 2024 Aug 10]. Available from: https://www.mipdatabase.com/

76.   Huang S, Xu J, Zheng J, Zhu F, Xie L, Ouyang G. Synthesis and application of magnetic molecularly imprinted polymers in sample preparation. Anal Bioanal Chem. 2018;410(17):3991–4014.

77. Karfa P, Madhuri R, Sharma PK. Development of carbon dots modified fluorescent molecular imprinted Polymer@Ag/AgCl nanoparticle for hepatocellular carcinoma marker. AIP Conf Proc. 2017;1832:1–3.

78. Xu X, Xu G, Wei F, Cen Y, Shi M, Cheng X, et al. Carbon dots coated with molecularly imprinted polymers: A facile bioprobe for fluorescent determination of caffeic acid. J Colloid Interface Sci. 2018;529:568–754.

79. Wu Y, Xiong J, Wei S, Tian L, Shen X, Huang C. Molecularly imprinted polymers by reflux precipitation polymerization for selective solid-phase extraction of quinolone antibiotics from urine. J Chromatogr A. 2024;1714:464550. https://doi.org/10.1016/j.chroma.2023.464550

80. Bhogal S, Kaur K, Maheshwari S, Malik AK. Surface molecularly imprinted carbon dots based core-shell material for selective fluorescence sensing of Ketoprofen. J Fluoresc. 2019;29(1):145–154.

81. Hao T, Wei X, Nie Y, Xu Y, Yan Y, Zhou Z. An eco-friendly molecularly imprinted fluorescence composite material based on carbon dots for fluorescent detection of 4-nitrophenol. Microchim Acta. 2016;183(7):2197–2203. http://dx.doi.org/10.1007/s00604-016-1851-2

82. Nehra M, Rohilla A, Beniwal N, Dilbaghi N, Kumar R, Kumar S. Molecularly Imprinted Polymers/Metal–Organic Framework (MIL-53) for Fluorescent Sensing of Ciprofloxacin in Water. Eng Proc. 2023;35:30.

83.   Wang L, Liang K, Feng W, Chen C, Gong H, Cai C. Molecularly imprinted polymers based on magnetically fluorescent metal–organic frameworks for the selective detection of hepatitis A virus. Microchem J. 2021;164:106047. https://doi.org/10.1016/j.microc.2021.106047

84.   Pal TK. Metal-organic framework (MOF)-based fluorescence "turn-on" sensors. Mater Chem Front. 2022;7(3):405–441.

85.   Liu G, Huang X, Li L, Xu X, Zhang Y, Lv J, et al. Recent advances and perspectives of molecularly imprinted polymer-based fluorescent sensors in food and environment analysis. Nanomaterials. 2019;9(1030):1–19.

86.   Wan W, Wagner S, Rurack K. Fluorescent monomers: "bricks" that make a molecularly imprinted polymer "bright." Vol. 408, Analytical and Bioanalytical Chemistry. Springer Verlag; 2016. p. 1753–1771.

87.   Li Q, Kamra T, Ye L. A modular approach for assembling turn-on fluorescence sensors using molecularly imprinted nanoparticles. Chem Commun. 2016;52(82):12237. http://dx.doi.org/10.1039/C6CC06628C

88.   Lv P, Xie D, Zhang Z. Magnetic carbon dots based molecularly imprinted polymers for fluorescent detection of bovine hemoglobin. Talanta. 2018;188(January):145–151.

89.   Wang M, Fu Q, Zhang K, Wan Y, Wang L, Gao M, et al. A magnetic and carbon dot based molecularly imprinted composite for fluorometric detection of 2,4,6-trinitrophenol. Microchim Acta. 2019;186(86):1–11.

90. Duarte M, Subedi P, Yilmaz E, Marcus K, Laurell T, Ekström S. Molecularly imprinted polymers synthesized via template immobilization on fumed silica nanoparticles for the enrichment of phosphopeptides. J Mol Recognit. 2018;31(3):1–10.

91. Kalecki J, Iskierko Z, Cieplak M, Sharma PS. Oriented Immobilization of Protein Templates: A New Trend in Surface Imprinting. ACS Sensors. 2020;5(12):3710–3720.

92. Chou PC, Rick J, Chou TC. C-reactive protein thin-film molecularly imprinted polymers formed using a micro-contact approach. Anal Chim Acta. 2005;542:20–5.

93. Lin HY, Hsu CY, Thomas JL, Wang SE, Chen HC, Chou TC. The microcontact imprinting of proteins: The effect of cross-linking monomers for lysozyme, ribonuclease A and myoglobin. Biosens Bioelectron. 2006;22(4 SPEC. ISS.):534–543.

94. Ertürk G, Berillo D, Hedström M, Mattiasson B. Microcontact-BSA imprinted capacitive biosensor for real-time, sensitive and selective detection of BSA. Biotechnol Reports. 2014;3:65–72.

95. E.Zeraatkara, M.Javanbakhtb. Protein thin-film molecularly imprinted polymers using a micro-contact approach. In: The 22nd Iranian Seminar of Organic Chemistry. 2014. p. 1.

96.   Wan Q, Liu H, Deng Z, Bu J, Li T, Yang Y, et al. A critical review of molecularly imprinted solid phase extraction technology. J Polym Res. 2021;28(10):401. https://doi.org/10.1007/s10965-021-02744-2

97.   Xu J, Medina-Rangel PX, Haupt K, Tse Sum Bui B. Guide to the preparation of molecularly imprinted polymer nanoparticles for protein recognition by solid-phase synthesis. 1st ed. Vol. 590, Methods in Enzymology. Elsevier Inc.; 2017. 115–141 p. http://dx.doi.org/10.1016/bs.mie.2017.02.004

98.   Cowen T, Stefanucci E, Piletska E, Marrazza G, Canfarotta F, Piletsky SA. Synthetic Mechanism of Molecular Imprinting at the Solid Phase. Macromolecules. 2020;53(4):1435–1442.

99.   Medina Rangel PX, Laclef S, Xu J, Panagiotopoulou M, Kovensky J, Tse Sum Bui B, et al. Solid-phase synthesis of molecularly imprinted polymer nanolabels: Affinity tools for cellular bioimaging of glycans. Sci Rep. 2019;9(1):1–9.

100.   Canfarotta F, Poma A, Guerreiro A, Piletsky S. Solid-phase synthesis of molecularly imprinted nanoparticles. Nat Protoc. 2016;11(3):443–455.

101.   Braunecker WA, Matyjaszewski K. Controlled/living radical polymerization: Features, developments, and perspectives. Prog Polym Sci. 2007;32(1):93–146.

102.   Zhang H. Controlled/"living" radical precipitation polymerization: A versatile polymerization technique for advanced functional polymers. Eur Polym J. 2013;49(3):579–600. http://dx.doi.org/10.1016/j.eurpolymj.2012.12.016.

103. Matyjaszewski K. Fundamentals of controlled/living radical polymerization. Tsarevsky N V, Sumerlin BS, editors. Encyclopedia of Radicals in Chemistry, Biology and Materials. 2012. 1–357 p.

104. Ramakers G, Wackers G, Trouillet V, Welle A, Wagner P, Junkers T. Laser-grafted molecularly imprinted polymers for the detection of Histamine from organocatalyzed atom transfer radical polymerization. Macromolecules. 2019;52(6):2304–2313.

105. Gao SP, Zhang X, Zhang LS, Huang YP, Liu ZS. Molecularly imprinted polymer prepared with polyhedral oligomeric silsesquioxane through reversible addition–fragmentation chain transfer polymerization. Anal Bioanal Chem. 2017;409(15):3741–3748.

106. Boonpangrak S, Whitcombe MJ, Prachayasittikul V, Mosbach K, Ye L. Preparation of molecularly imprinted polymers using nitroxide-mediated living radical polymerization. Biosens Bioelectron. 2006;22(3):349–354.

107. Montagna V, Haupt K, Gonzato C. RAFT coupling chemistry: A general approach for post-functionalizing molecularly imprinted polymers synthesized by radical polymerization. Polym Chem. 2020;11(5):1055–1061.

108. Raziq A, Kidakova A, Boroznjak R, Reut J, Öpik A, Syritski V. Development of a portable MIP-based electrochemical sensor for detection of SARS-CoV-2 antigen. Biosens Bioelectron. 2021;178(January):113029.

109. Moreira Gonçalves L. Electropolymerized molecularly imprinted polymers: perceptions based on recent literature for soon-to-be world-class scientists. Curr Opin Electrochem. 2021;25:100640. https://doi.org/10.1016/j.coelec.2020.09.007

110. Vu OT, Nguyen QH, Nguy Phan T, Luong TT, Eersels K, Wagner P, et al. Highly Sensitive Molecularly Imprinted Polymer-Based Electrochemical Sensors Enhanced by Gold Nanoparticles for Norfloxacin Detection in Aquaculture Water. ACS Omega. 2024;8:2887–2896.

111. Elugoke SE, Adekunle AS, Fayemi OE, Akpan ED, Mamba BB, Sherif ESM, et al. Molecularly imprinted polymers (MIPs) based electrochemical sensors for the determination of catecholamine neurotransmitters – Review. Electrochem Sci Adv. 2021;1(2):1–43.

112. Barcelo D. Comprehensive analytical chemistry: Mip synthesis, characteristics and analytical application. 1st ed. Marc M, editor. Elsevier Science; 2019. 1–392 p.

113. De Middeleer G, Dubruel P, De Saeger S. Characterization of MIP and MIP functionalized surfaces: Current state-of-the-art. Trends Anal Chem. 2016;76:71–85. http://dx.doi.org/10.1016/j.trac.2015.11.007.

114. Gu J, Zhang H, Yuan G, Chen L, Xu X. Surface-initiated molecularly imprinted polymeric column: In situ synthesis and application for semi-preparative separation by high performance liquid chromatography. J Chromatogr A. 2011;1218(45):8150–8155. http://dx.doi.org/10.1016/j.chroma.2011.09.019.

115. Boysen RI. Advances in the development of molecularly imprinted polymers for the separation and analysis of proteins with liquid chromatography. J Sep Sci. 2019;42(1):51–71.

116. Mattiasson B, Ye L. Molecularly imprinted polymers in biotechnology. 1st ed. T.Scheper, editor. Springer International Publishing Switzerland; 2015. 24–231 p.

117. Ning F, Peng H, Dong L, Zhang Z, Li J, Chen L, et al. Preparation and characterization of superparamagnetic molecularly imprinted polymers for selective adsorption and separation of vanillin in food samples. J Agric Food Chem. 2014;62(46):11138–45.

118. López AS, Ramos MP, Herrero R, Vilariño JML. Design, synthesis and HR − MAS NMR characterization of molecular imprinted polymers with emerging contaminants templates. Sep Purif Technol. 2021;257:117860.

119. Abdollah NA, Ahmad A, Omar TFT. Synthesis and characterization of molecular imprinted polymer for the determination of carbonate ion. Biointerface Res Appl Chem. 2020;11(3):10620–10627.

120. Cela-Pérez MC, Lasagabáster-Latorre A, Abad-López MJ, López-Vilariño JM, Gónzalez-Rodríguez M V. A study of competitive molecular interaction effects on imprinting of molecularly imprinted polymers. Vib Spectrosc. 2013;65:74–83.

121. Baggiani C, Giovannoli C, Anfossi L, Passini C, Baravalle P, Giraudi G. A Connection between the binding properties of imprinted and nonimprinted polymers: A change of perspective in molecular imprinting. J Am Chem Soc. 2022;134(3):1513–1518.

122. Pap T, Horvai G. Binding assays with molecularly imprinted polymers - Why do they work? J Chromatogr B Anal Technol Biomed Life Sci. 2014;804(1):167–172.

123. García-Calzón JA, Díaz-García ME. Characterization of binding sites in molecularly imprinted polymers. Sensors Actuators, B Chem. 2007;123(2):1180–1194.

124. Tiller T, editor. Synthetic antibodies: methods and protocols. Springer NewYork; 2017. 350–400 p.

125. Smolinska-kempisty K, Guerreiro A, Canfarotta F, Cáceres C, Whitcombe MJ, Piletsky S. A comparison of the performance of molecularly imprinted polymer nanoparticles for small molecule targets and antibodies in the ELISA format. Sci Rep. 2016;6(May):1–7.

126. Chen L, Xu S, Li J. Recent advances in molecular imprinting technology: Current status, challenges and highlighted applications. Chem Soc Rev. 2011;40(5):2922–2942.

127. Wulff G, Knorr K. Stoichiometric noncovalent interaction in molecular imprinting. Bioseparation. 2001;10(6):257–76.

128. Zimmerman SC, Lemcoff NG. Synthetic hosts via molecular imprinting—are universal synthetic antibodies realistically possible? Chem Commun. 2004;4(1):5–14.

129. Refaat D, Aggour MG, Farghali AA, Mahajan R, Wiklander JG, Nicholls IA, et al. Strategies for molecular imprinting and the evolution of MIP nanoparticles as plastic antibodies—synthesis and applications. Int J Mol Sci. 2019;20(24):1–21.

130. Pirzada M, Altintas Z. Template Removal in Molecular Imprinting: Principles, Strategies, and Challenges. In: Denizli A, editor. Molecular Imprinting for Nanosensors and Other Sensing Applications. 1st ed. Academic Press; 2021. p. 367–406.

131. He X, Wang J, Mei X. Dummy fragment template molecularly imprinted polymers for the selective solid-phase extraction of Gonyautoxins from seawater. Anal Lett. 2017;50(12):1877–1886. https://doi.org/10.1080/00032719.2016.1256408.

132. Marć M, Panuszko A, Namieśnik J, Wieczorek PP. Preparation and characterization of dummy-template molecularly imprinted polymers as potential sorbents for the recognition of selected polybrominated diphenyl ethers. Anal Chim Acta. 2018;1030:77–95.

133. Tokonami S, Shiigi H, Nagaoka T. Review: Micro- and nanosized molecularly imprinted polymers for high-throughput analytical applications. Anal Chim Acta. 2019;641(1–2):7–13.

134. Manesiotis P, Hall AJ, Courtois J, Irgum K, Sellergren B. An artificial riboflavin receptor prepared by a template analogue imprinting strategy. Angew Chemie - Int Ed. 2015;44(25):3902–3906.

135. Li J, Hu X, Guan P, Zhang X, Qian L, Song R, et al. Preparation of molecularly imprinted polymers using ion-pair dummy template imprinting and polymerizable ionic liquids. RSC Adv. 2015;5(77):62697–62705.

136. Hu Y, Liu R, Zhang Y, Li G. Improvement of extraction capability of magnetic molecularly imprinted polymer beads in aqueous media via dual-phase solvent system. Talanta. 2019;79(3):576–582.

137. He Y, Zeng S, Abd El-Aty AM, Hacımüftüoğlu A, Kalekristos Yohannes W, Khan M, et al. Development of water-compatible molecularly imprinted polymers based on functionalized β-cyclodextrin for controlled release of Atropine. Polymers (Basel). 2020;12(1):130.

138. Polyakova I, Borovikova L, Osipenko A, Vlasova E, Volchek B, Pisarev O. Surface molecularly imprinted organic-inorganic polymers having affinity sites for cholesterol. React Funct Polym. 2016;109:88–98. http://dx.doi.org/10.1016/j.reactfunctpolym.2016.10.010

139. Song R, Hu X, Guan P, Li J, Du C, Qian L, et al. Surface modification of imprinted polymer microspheres with ultrathin hydrophilic shells to improve selective recognition of glutathione in aqueous media. Mater Sci Eng C. 2016;60:1–6.

140. Zhou T, Ding L, Che G, Jiang W, Sang L. Recent advances and trends of molecularly imprinted polymers for specific recognition in aqueous matrix: Preparation and application in sample pretreatment. Trends Anal Chem. 2019;114:11–28. https://doi.org/10.1016/j.trac.2019.02.028

141. Xu L, Zhao ZX, Huang YA, Zhu QJ. Preparation of chitosan molecularly imprinted polymers and the recognition mechanism for adsorption of alpha-lipoic acid. Molecules. 2020;25(2):1–15.

142. Sergeyeva T, Piletska O, Piletsky S. Rationally designed molecularly imprinted polymer membranes as antibody and enzyme mimics in analytical biotechnology. BBA Adv. 2023;3:100070. https://doi.org/10.1016/j.bbadva.2022.100070

143. Say R, Gültekin A, Özcan AA, Denizli A, Ersöz A. Preparation of new molecularly imprinted quartz crystal microbalance hybride sensor system for 8-hydroxy-2'-deoxyguanosine determination. Anal Chim Acta. 2009;640(1–2):82–6.

144. El-Schich Z, Zhang Y, Feith M, Beyer S, Sternbæk L, Ohlsson L, et al. Molecularly imprinted polymers in biological applications. Biotechniques. 2020;69(6):407–420.

145. Kalecki J, Iskierko Z, Cieplak M, Sharma PS. Oriented immobilization of protein templates: A new trend in surface imprinting. ACS Sensors. 2020;5(12):3710–3720.

146. Rachkov A, Minoura N. Towards molecularly imprinted polymers selective to peptides and proteins. The epitope approach. Biochim Biophys Acta. 2001;1544(1–2):255–266.

147. Nishino H, Huang CS, Shea KJ. Selective protein capture by epitope imprinting. Angew Chemie - Int Ed. 2006;45(15):2392–2396.

148. Bagán H, Zhou T, Eriksson NL, Bülow L, Ye L. Synthesis and characterization of epitope-imprinted polymers for purification of human hemoglobin. RSC Adv. 2017;7(66):41705.

149. Moczko E, Guerreiro A, Cáceres C, Piletska E, Sellergren B, Piletsky SA. Epitope approach in molecular imprinting of antibodies. J Chromatogr B Anal Technol Biomed Life Sci. 2019;1124(May):1–6. https://doi.org/10.1016/j.jchromb.2019.05.024

150. Bossi AM, Sharma PS, Montana L, Zoccatelli G, Laub O, Levi R. Fingerprint-imprinted polymer: Rational selection of peptide epitope templates for the determination of proteins by molecularly imprinted polymers. Anal Chem. 2022;84(9):4036–4041.

151. Tamahkar E, Denizli A. Metal ion coordination interactions for biomolecule recognition: a review. Hittite J Sci Eng. 2015;1(1):21–26.

152. Kubo T, Arimura S, Tominaga Y, Naito T, Hosoya K, Otsuka K. Molecularly imprinted polymers for selective adsorption of Lysozyme and Cytochrome c using a PEG-based hydrogel: selective recognition for different conformations due to pH conditions. Macromolecules. 2015;48(12):4081–4087.

153. El-Sharif HF, Yapati H, Kalluru S, Reddy SM. Highly selective BSA imprinted polyacrylamide hydrogels facilitated by a metal-coding MIP approach. Acta Biomater. 2015;28:121–127. http://dx.doi.org/10.1016/j.actbio.2015.09.012

154. Ndizeye N, Suriyanarayanan S, Nicholls I. Hierarchical polymeric architectures through molecular imprinting in liquid crystalline environments. Eur Polym J. 2018;106:223–231.

155. Mandal S, Suriyanarayanan S, Nicholls IA, Ramanujam K. Selective sensing of the biotinyl moiety using molecularly imprinted polyaniline nanowires. J Electrochem Soc. 2018;165:B669–B678.

156. Suriyanarayanan S, Mandal S, Ramanujam K, Nicholls IA. Electrochemically synthesized molecularly imprinted polythiophene nanostructures as recognition elements for an aspirin-chemosensor. Sensors Actuators B. 2017;253:428–436.

157. Zaidi SA. Molecular imprinting: A useful approach for drug delivery. Mater Sci Energy Technol. 2024;3:72–77. https://doi.org/10.1016/j.mset.2019.10.012.

158. Bărăian AI, Iacob BC, Bodoki AE, Bodoki E. In vivo applications of molecularly imprinted polymers for drug delivery: a pharmaceutical perspective. Int J Mol Sci. 2022;23(22):14071.

159. Bodoki AE, Iacob BC, Dinte E, Vostinaru O, Samoila O, Bodoki E. Perspectives of molecularly imprinted polymer-based drug delivery systems in ocular therapy. Polymers (Basel). 2021;13(21):3649.

160. Jantarat C, Tangthong N, Songkro S, Martin GP, Suedee R. S-Propranolol imprinted polymer nanoparticle-on-microsphere composite porous cellulose membrane for the enantioselectively controlled delivery of racemic propranolol. Int J Pharm. 2008;349(1–2):212–225.

161. Shadabfar M, Abdouss M, Khonakdar HA. Synthesis, characterization, and evaluation of a magnetic molecular imprinted polymer for 5-fluorouracil as an intelligent drug delivery system for breast cancer treatment. J Mater Sci. 2020;55(26):12287–304. https://doi.org/10.1007/s10853-020-04887-x.

162. Wang P, Zhang A, Jin Y, Zhang Q, Zhang L, Peng Y, et al. Molecularly imprinted layer-coated hollow polysaccharide microcapsules toward gate-controlled release of water-soluble drugs. RSC Adv. 2024;4(50):26063–26073.

163. Luliński P. Molecularly imprinted polymers based drug delivery devices: A way to application in modern pharmacotherapy. A review. Mater Sci Eng C. 2017;76:1344–1353.

164. Vargas-Berrones K, Ocampo-Perez R, Rodríguez-Torres I, Medellín-Castillo NA, Flores-Ramírez R. Molecularly imprinted polymers (MIPs) as efficient catalytic tools for the oxidative degradation of 4-nonylphenol and its by-products. Environ Sci Pollut Res. 2023;30(39):90741–56. https://doi.org/10.1007/s11356-023-28653-z.

165. Li S, Zhu M, Whitcombe MJ, Piletsky SA, Turner APF. Molecularly imprinted polymers for enzyme-like catalysis: principle, design, and applications. principle, design, and applications. Molecularly Imprinted Catalysts. Elsevier Inc.; 2016. 1–17 p.http://dx.doi.org/10.1016/B978-0-12-801301-4.00001-3.

166. Muratsugu S, Shirai S, Tada M. Recent progress in molecularly imprinted approach for catalysis. Tetrahedron Lett. 2020;61(11):151603. https://doi.org/10.1016/j.tetlet.2020.151603.

167. Xiao H, Peng J, Peng H, Bu L, Pan Z, He Y, et al. Preparation and evaluation of surface molecularly imprinted polymers as stationary phase columns for high performance liquid chromatography. Anal Methods. 2016;8(44):7951–7958. http://dx.doi.org/10.1039/C6AY02141G.

168. Hroboňová K, Lomenova A. Molecularly imprinted polymer as stationary phase for HPLC separation of phenylalanine enantiomers. Monatshefte fur Chemie. 2018;149(5):939–946.

169. Walsh R, Osmani Q, Hughes H, Duggan P, McLoughlin P. Synthesis of imprinted beads by aqueous suspension polymerisation for chiral recognition of antihistamines. J Chromatogr B Anal Technol Biomed Life Sci. 2011;879(30):3523–3530. http://dx.doi.org/10.1016/j.jchromb.2011.09.036

170. Yang S, Wang Y, Jiang Y, Li S, Liu W. Molecularly imprinted polymers for the identification and separation of chiral drugs and biomolecules. Polymers (Basel). 2016;8(216):1–16.

171. Moein MM. Advancements of chiral molecularly imprinted polymers in separation and sensor fields: A review of the last decade. Talanta. 2021;224(October2020):121794.https://doi.org/10.1016/j.talanta.2020.121794

172. Malik MI, Shaikh H, Mustafa G, Bhanger MI. Recent applications of molecularly imprinted polymers in analytical chemistry. Sep Purif Rev. 2019;48(3):179–219.https://doi.org/10.1080/15422119.2018.1457541.

173. Vitor RV, Martins MCG, Figueiredo EC, Martins I. Application of molecularly imprinted polymer solid-phase extraction for salivary cotinine. Anal Bioanal Chem. 2011;400(7):2109–2117.

174. Murakami T, Iwamuro Y, Ishimaru R, Chinaka S, Hasegawa H. Molecularly imprinted polymer solid-phase extraction of synthetic cathinones from urine and whole blood samples. J Sep Sci. 2018;41(24):4506–4514.

175. Yang Y, Li Q, Fang G, Wang S. Preparation and evaluation of novel surface molecularly imprinted polymers by sol-gel process for online solid-phase extraction coupled with high performance liquid chromatography to detect trace patulin in fruit derived products. RSC Adv. 2016;6(59):54510. http://dx.doi.org/10.1039/C6RA08736A

176. Bhalla N, Jolly P, Formisano N, Estrela P. Introduction to biosensors. Essays Biochem. 2016;60(1):1–8.

177. Zhou T, Halder A, Sun Y. Fluorescent nanosensor based on molecularly imprinted polymers coated on graphene quantum dots for fast detection of antibiotics. Biosensors. 2022;8(82):4944.

178. Wang L, Wang H, Tang X, Zhao L. Molecularly imprinted polymers-based novel optical biosensor for the detection of cancer marker lysozyme. Sensors Actuators A Phys. 2022;334:113324. https://doi.org/10.1016/j.sna.2021.113324.

179. Liu R, Ko CC. Molecularly Imprinted Polymer-Based Luminescent Chemosensors. Vol. 13, Biosensors. MDPI; 2023. p. 1–24.

180. Garcia-Cruz A, Ahmad OS, Alanazi K, Piletska E, Piletsky SA. Generic sensor platform based on electro-responsive molecularly imprinted polymer nanoparticles (e-NanoMIPs). Microsystems Nanoeng. 2020;6(83):1–9. http://dx.doi.org/10.1038/s41378-020-00193-3.

181. Li Y, Xu W, Zhao X, Huang Y, Kang J, Qi Q, et al. Electrochemical sensors based on molecularly imprinted polymers on Fe_3O_4/graphene modified by gold nanoparticles for highly selective and sensitive detection of trace ractopamine in water. Analyst. 2018;143(21):5094–5102.

182. Wang L, Zhang W. Molecularly imprinted polymer (MIP) based electrochemical sensors and their recent advances in health applications. Sensors and Actuators Reports. 2023;5(February):100153. https://doi.org/10.1016/j.snr.2023.100153.

183. Beloglazova NV., Lenain P, DeRycke E, Goryacheva IY, Knopp D, DeSaeger S. Capacitive sensor for detection of benzo(a)pyrene in water. Talanta. 2018;190(March):219–225. https://doi.org/10.1016/j.talanta.2018.07.084.

184. Kumar PA, Bhand S. Molecularly imprinted polyresorcinol based capacitive sensor for sulphanilamide detection. Electroanalysis. 2019;31(9):1797–1808.

185. Nguyen HH, Park J, Kang S, Kim M. Surface plasmon resonance: A versatile technique for biosensor applications. Sensors (Switzerland). 2015;15(5):10481–10510.

186. Cenci L, Andreetto E, Vestri A, Bovi M, Barozzi M, Iacob E, et al. Surface plasmon resonance based on molecularly imprinted nanoparticles for the picomolar detection of the iron regulating hormone Hepcidin-25. J Nanobiotechnology. 2015;13(1):1–15.

187.	Bereli N, Çimen D, Hüseynli S, Denizli A. Detection of amoxicillin residues in egg extract with a molecularly imprinted polymer on gold microchip using surface plasmon resonance and quartz crystal microbalance methods. J Food Sci. 2020;85(12):4152–4160.

188.	Chiappini A, Pasquardini L, Bossi AM. Molecular imprinted polymers coupled to photonic structures in biosensors: The state of art. Sensors (Switzerland). 2024;20(18):1–23.

189.	Mandal D, Banerjee S. Surface acoustic wave (SAW) sensors: physics, materials, and applications. Sensors. 2022;22:820.

190.	Kartal F, Çimen D, Bereli N, Denizli A. Molecularly imprinted polymer based quartz crystal microbalance sensor for the clinical detection of insulin. Mater Sci Eng C. 2019;97(December 2018):730–737. https://doi.org/10.1016/j.msec.2018.12.086.

191.	Lebal N, Hallil H, Dejous C, Plano B, Krstulja A, Delepée R, et al. Nucleosides analogues recognition by molecularly imprinted polymer-coated Love wave sensor. Micro Nano Lett. 2023;8(10):563–566.

192.	Califf RM. Biomarker definitions and their applications. Exp Biol Med. 2018;243(3):213–221.

193.	Strimbu K, Tavel JA. What are Biomarkers? NIH public access. 2011;5(6):463–466.

194.	Huss R. Biomarkers. In: Atala A, Allickson JG, editors. Translational Regenerative Medicine. Academic Press; 2015. p. 235–241.

195. Puntmann VO. How-to guide on biomarkers: Biomarker definitions, validation and applications with examples from cardiovascular disease. Postgrad Med J. 2009;85(1008):538–545.

196. Lionetto MG, Caricato R, Giordano ME. Pollution biomarkers in environmental and human biomonitoring. Open Biomarkers Journalournal. 2019;9:1–9.

197. Newswire C. PharmiWeb.com Global Pharma News and Resources. 2020 [cited 2024 Feb 13]. https://www.pharmiweb.com/press-release/2020-12-21/biomarker-research-services-market-size-is-expected-to-reach-us-182-billion-by-2026-top-key-play.

198. Mayeux R. Biomarkers: potential uses and limitations. NeuroRx. 2004;1(2):182–8.

199. Gunn GR, Evans C, Yang E. Immunogenicity and biomarkers: Bioanalytical challenges and considerations. Bioanalysis. 2017;9(22):1729–1732.

200. Hosseini S, Vázquez-Villegas P, Rito-Palomares M, Martinez-Chapa SO. Advantages, disadvantages and modifications of conventional ELISA. In: Enzyme-linked Immunosorbent Assay (ELISA) SpringerBriefs in Applied Sciences and Technology. Singapore: Springer; 2018. p. 345–387.

201. Sakamoto S, Putalun W, Vimolmangkang S, Phoolcharoen W, Shoyama Y, Tanaka H, et al. Enzyme-linked immunosorbent assay for the quantitative/qualitative analysis of plant secondary metabolites. J Nat Med. 2018;72(1):32–42. https://doi.org/10.1007/s11418-017-1144-z.

202. Rischke S, Hahnefeld L, Burla B, Behrens F, Gurke R, Garrett TJ. Small molecule biomarker discovery: Proposed workflow for LC-MS-based clinical research projects. J Mass Spectrom Adv Clin Lab. 2023;28(February):47–55. https://doi.org/10.1016/j.jmsacl.2023.02.003

203. Sancho-Albero M, Jarne C, Savirón M, Martín-Duque P, Membrado L, Cebolla VL, et al. Exosomes of Cancer Cells. Int J Mol Sci. 2022;2022:1150.

204. Winnike JH, Wei X, Knagge KJ, Colman SD, Gregory SG, Zhan X. Comparison of GC-MS and GC×GC-MS in the Analysis of Human Serum Samples for Biomarker Discovery. Physiol Behav. 2018;176(5):139–148.

205. Ohtsu Y, Tanaka S, Igarashi H, Kakehi M, Mori T, Nakamura T, et al. Analytical method validation for biomarkers as a drug development tool: Points to consider. Bioanalysis. 2021;13(18):1379–1389.

206. Selvolini G, Marrazza G. MIP-based sensors: Promising new tools for cancer biomarker determination. Sensors (Switzerland). 2017;17(4):718.

207. Zarogoulidis P, Tsakiridis K, Karapantzou C, Lampaki S, Kioumis I, Pitsiou G, et al. Use of proteins as biomarkers and their role in carcinogenesis. J Cancer. 2015;6(1):9–18.

208. Ulaner GA, Riedl CC, Dickler MN, Jhaveri K, Taskar NP, Weber W. Molecular imaging of biomarkers in breast cancer. J Nucl Med. 2016;176(3):139–148.

209. Heikal AA. Intracellular coenzymes as natural biomarkers for metabolic activities and mitochondrial anomalies. Biomark Med. 2010;4(2):241–263.

210. Villalobos P, Wistuba II. Lung cancer biomarkers guideline. Hematol Oncol Clin. 2017;31(1):13–29.

211. Samloff IM, Taggart RT. Pepsinogens, pepsins, and peptic ulcer. Clin Invest Med. 1987 May;10(3):215–221.

212. Boulton KHA, Dettmar PW. A narrative review of the prevalence of gastroesophageal reflux disease (GERD). Vol. 5, Annals of Esophagus. AME Publishing Company; 2022. p. 5–7.

213. Sabry M, Yosef TM, Mahmoud AM, Micheal TMAG. Fasting salivary pepsin level as a reliable non-invasive method of screening for laryngopharyngeal reflux in Egyptian patients. Egypt J Intern Med. 2022 Dec;34(16):1–8.

214. Wang YJ, Lang XQ, Wu D, He YQ, Lan CH, Xiao-Xiao, et al. Salivary pepsin as an intrinsic marker for diagnosis of sub-types of gastroesophageal reflux disease and gastroesophageal reflux disease-related disorders. J Neurogastroenterol Motil. 2020;26(1):74–84.

215. Peptest for diagnosing gastro-oesophageal reflux Medtech innovation briefing [Internet]. 2015. www.nice.org.uk/guidance/mib31

216. Stanforth KJ, Wilcox MD, Chater PI, Brownlee IA, Zakhour MI, Banecki KMRM, et al. Pepsin properties, structure, and its accurate measurement: a narrative review. Ann Esophagus. 2022;5:1–3.

217. Ahn J, Cao MJ, Yu YQ, Engen JR. Accessing the reproducibility and specificity of pepsin and other aspartic proteases. Biochim Biophys Acta. 2013;1834(6):1222–9.https://www.ncbi.nlm.nih.gov/pmc/articles/PMC3624763/pdf/nihms412728.

218. López-Ferrer D, Petritis K, Robinson EW, Hixson KK, Tian Z, Lee JH, et al. Pressurized pepsin digestion in proteomics: An automatable alternative to trypsin for integrated top-down bottom-up proteomics. Mol Cell Proteomics. 2011;10(2):1–11.

219. Neubert H, Gale J, Muirhead D. Online high-flow peptide immunoaffinity enrichment and nanoflow LC-MS/MS: Assay development for total salivary pepsin/pepsinogen. Clin Chem. 2010 Sep;56(9):1413–1423.

220. Piletska E V., Czulak J, Piletsky SS, Guerreiro A, Canfarotta F, Piletsky SA. Novel assay format for proteins based on magnetic molecularly imprinted polymer nanoparticles—detection of pepsin. J Chinese Adv Mater Soc. 2018;6(4):341–351. https://doi.org/10.1080/22243682.2018.1473050.

221. García Y, Czulak J, Pereira ED, Piletsky SA, Piletska E. A magnetic molecularly imprinted nanoparticle assay (MINA) for detection of pepsin. React Funct Polym. 2022 Jan;170:105133. https://linkinghub.elsevier.com/retrieve/pii/S1381514821003254.

222. Pluhar B, Ziener U, Mizaikoff B. Surface imprinting of pepsin via miniemulsion polymerization. J Mater Chem B. 2013;1(40):5489–5495.

223. Dong C, Shi H, Han Y, Yang Y, Wang R, Men J. Molecularly imprinted polymers by the surface imprinting technique. Vol. 145, European Polymer Journal. Elsevier Ltd; 2021. p. 110231.

224. Pluhar B, Ziener U, Mizaikoff B. Binding performance of pepsin surface-imprinted polymer particles in protein mixtures. J Mater Chem B. 2015 Aug 14;3(30):6248–6254.

225. Pichon V, Delaunay N, Combès A. Sample Preparation Using Molecularly Imprinted Polymers. Anal Chem. 2020;92(1):16–33.

226. Ansari S. Application of magnetic molecularly imprinted polymer as a versatile and highly selective tool in food and environmental analysis: Recent developments and trends. Trends Anal Chem. 2017;90:89–106. http://dx.doi.org/10.1016/j.trac.2017.03.001

227. Ansari S, Karimi M. Recent configurations and progressive uses of magnetic molecularly imprinted polymers for drug analysis. Talanta.2017;167(January):470–485.http://dx.doi.org/10.1016/j.talanta.2017.02.049

228. Nursyahera Azreen Ramin, Muggundha Raoov Ramachandran, Noorashikin Md Saleh ZMMA, Asman S. Magnetic nanoparticles molecularly imprinted polymers: a review. Curr Nanosci. 2023;19(3):372–400.

229. Lowdon JW, Dilien H, Singla P, Peeters M, Cleij TJ, Grinsven B Van, et al. MIPs for commercial application in low-cost sensors and assays – An overview of the current status quo. Sensors Actuators B Chem. 2020;325:128973.

230. Sullivan M V., Stockburn WJ, Hawes PC, Mercer T, Reddy SM. Green synthesis as a simple and rapid route to protein modified magnetic nanoparticles for use in the development of a fluorometric molecularly imprinted polymer-based assay for detection of myoglobin. Nanotechnology. 2021;32(9): 1–13.

231. Petcharoen K, Sirivat A. Synthesis and characterization of magnetite nanoparticles via the chemical co-precipitation method. Mater Sci Eng B Solid-State Mater Adv Technol. 2012 Mar 25;177(5):421–427.

232. Hui C, Shen C, Yang T, Bao L, Tian J, Ding H, et al. Large-scale Fe_3O_4 nanoparticles soluble in water synthesized by a facile method. J Phys Chem C. 2008;112(30):11336.

233. Li J, Wang Y, Yu X. Magnetic molecularly imprinted polymers:synthesis and applications in the selective extraction of antibiotics. Front Chem. 2021;9(August):1–17.

234. Medinger J, Nedyalkova M, Lattuada M. Solvothermal synthesis combined with design of experiments—optimization approach for magnetite nanocrystal clusters. Nanomaterials. 2021;11(2):1–19.

235. Kekalo K, Koo K, Zeitchick E, Baker I. Microemulsion synthesis of iron core/iron oxide shell magnetic nanoparticles and their physicochemical properties. J Pediatr. 2013;176(5):139–148.

236. Xu J, Yang H, Fu W, Du K, Sui Y, Chen J, et al. Preparation and magnetic properties of magnetite nanoparticles by sol-gel method. J Magn Magn Mater. 2007;309(2):307–311.

237. Siddiqui MZ. Monoclonal antibodies as diagnostics; An appraisal. Indian J Pharm Sci. 2010;72(1):12–17.

238. Baliga S, Muglikar S, Kale R. Salivary pH: A diagnostic biomarker. J Indian Soc Periodontol. 2023;17(4):461–465.

239. Vasapollo G, Del Sole R, Mergola L, Lazzoi MR, Scardino A, Scorrano S, et al. Molecularly Imprinted Polymers : Present and Future Prospective. Int J Mol Sci. 2011;12:5908–5945.

240. Wang Y, Chai Z, Sun Y, Gao M, Fu G. Preparation of lysozyme imprinted magnetic nanoparticles via surface graft copolymerization. J Biomater Sci Polym Ed. 2015 Jul 24;26(11):644–656.

241. Chen L, Wang X, Lu W, Wu X, Li J. Molecular imprinting: Perspectives and applications. Chem Soc Rev. 2016;45(8):2137–2211.

242. Launer PJ, Arkles B. Infrared analysis of organosilicone compounds: Spectra-structure correlations. In: Silicone compounds: silanes and silicones. 1st ed. Morrisville, PA: Gelest.Inc; 2013. p. 175–8.

243. Fenger F, Andrew RH. on the Isoelectric Precipitation of Pepsin. J Biol Chem [Internet]. 1927;73(2):371–7. Available from: http://dx.doi.org/10.1016/S0021-9258(18)84251-X

244. Boitard C, Michel A, Ménager C, Griffete N. Protein denaturation through the use of magnetic molecularly imprinted polymer nanoparticles. Molecules. 2021 Jul 1;26(13):3980.

245. Pitigoi D. An Overview of High-Performance Liquid Chromatography (HPLC). J

Formul Sci Bioavailab Perspect. 2022;6(1):1–2.

246. Pietri A, Fortunati P, Mulazzi A, Bertuzzi T. Enzyme-assisted extraction for the HPLC determination of aflatoxin M1 in cheese. Food Chem [Internet]. 2016;192:235–41. Available from: http://dx.doi.org/10.1016/j.foodchem.2015.07.006

247. Gallegos Tintoré S, Torres Fuentes C, Solorza Feria J, Alaiz M, Girón Calle J, Martínez Ayala AL, et al. Antioxidant and chelating activity of nontoxic Jatropha curcas L. protein hydrolysates produced by in vitro digestion using pepsin and pancreatin. J Chem. 2015;2015:1–9.

248. Wang J, Chan C, Huang F wen, Xie J feng, Xu H, Ho K wai, et al. Interaction mechanism of pepsin with a natural inhibitor gastrodin studied by spectroscopic methods and molecular docking. Med Chem Res [Internet]. 2017;26(2):405–13. Available from: http://dx.doi.org/10.1007/s00044-016-1760-2

249. Ramm M, Alarcón-Zapata B, Monsalves J, Bustamante L. A Simple Validated Method for the Estimation of Pepsin Activity in Microtiter Array for the INFOGEST Protocol. Foods. 2023;12(20):3851.

250. Mcnay JLM, O'connell JP, Fernandez EJ. Protein unfolding during reversed-phase chromatography: II. role of salt type and ionic strength. Bio-technol Bioeng. 2001;76:233–40.

251. La Verde V, Dominici P, Astegno A. Determination of Hydrodynamic Radius of Proteins by Size Exclusion Chromatography. Bio-Protocol. 2017;7(8):1–14.

252. ICH. Harmonised Tripartite Guideline: Validation of Analytical procedures: Text and Methodology. In: International Conference on Harmonization. Geneva; 2005. p. Q2(R1).

253. Guckeisen T, Hosseinpour S, Peukert W. Effect of pH and urea on the proteins secondary structure at the water/air interface and in solution. J Colloid Interface Sci [Internet]. 2021;590:38–49. Available from: https://doi.org/10.1016/j.jcis.2021.01.015

254. The United States Pharmacopeia 2017. 35th ed. Rockville,MD: United states pharmacoepial convention; 2016. 3179,3180,3181,4806,4807,4808,5490,5491,5492.

255. Gawlitza K, Wan W, Wagner S, Rurack K. Fluorescent Molecularly Imprinted Polymers. In: Tiwari A, Uzun L, editors. Advanced Molecularly Imprinting Materials. 1st ed. Wiley; 2016. p. 189–210.

256. Samarth NB, Kamble V, Mahanwar PA, Rane AV, K. A V. A historical perspective and the development of molecular imprinting polymer-A review. Chem Int. 1AD;4(4):202–10.

257. Guo T, Deng Q, Fang G, Ma L, Wang S. Fluorescence sensor based on molecularly imprinted polymers and core–shell upconversion nanoparticles@metal–organic frameworks for detection of bovine serum albumin. Spectrochim Acta - Part A Mol Biomol Spectrosc. 2022;279(May):121460.

258. Zhang X, Yang S, Jiang R, Sun L, Pang S, Luo A. Fluorescent molecularly

imprinted membranes as biosensor for the detection of target protein. Sensors Actuators, B Chem [Internet]. 2018;254:1078–86. Available from: http://dx.doi.org/10.1016/j.snb.2017.07.205

259. Zhao Y, Chen Y, Fang M, Tian Y, Bai G, Zhuo K. Silanized carbon dot-based thermo-sensitive molecularly imprinted fluorescent sensor for bovine hemoglobin detection. Anal Bioanal Chem. 2020;412(23):5811–7.

260. Piloto AML, Ribeiro DSM, Rodrigues SSM, Santos JLM, Ferreira Sales MG. Label-free quantum dot conjugates for human protein IL-2 based on molecularly imprinted polymers. Sensors Actuators, B Chem. 2020;304(October 2019):127343.

261. Piloto AM, Ribeiro DSM, Rodrigues SSM, Santos C, Santos JLM, Sales MGF. Plastic antibodies tailored on quantum dots for an optical detection of myoglobin down to the femtomolar range. Sci Rep. 2018;8(1):1–11.

262. Zhou T, Halder A, Sun Y. Fluorescent nanosensor based on molecularly imprinted polymers coated on graphene quantum dots for fast detection of antibiotics. Biosensors. 2018;8(3):4944.

263. Wu X, Zhang Z, Li J, You H, Li Y, Chen L. Molecularly imprinted polymers-coated gold nanoclusters for fluorescent detection of bisphenol A. Sensors Actuators, B Chem. 2015;211:507–14.

264. Feng H, Wang N, Tran.t T, Yuan L, Li J, Cai Q. Surface molecular imprinting on dye-(NH2)-SiO2 NPs for specific recognition and direct fluorescent quantification of perfluorooctane sulfonate. Sensors Actuators B Chem. 2014

May;195:266–73.

265. Wan W, Biyikal M, Wagner R, Sellergren B, Rurack K. Fluorescent sensory microparticles that "light-up" consisting of a silica core and a molecularly imprinted polymer (MIP) shell. Angew Chemie - Int Ed. 2013 Jul 1;52(27):7023–7.

266. Xu Z, Deng P, Tang S, Li J. Fluorescent molecularly imprinted polymers based on 1,8-naphthalimide derivatives for efficiently recognition of cholic acid. Mater Sci Eng C. 2016 Jan 1;58:558–67.

267. Sunayama H, Ohta T, Kuwahara A, Takeuchi T. Fluorescence signaling molecularly imprinted polymers for antibiotics prepared via site-directed post-imprinting introduction of plural fluorescent reporters within the recognition cavity. J Mater Chem B. 2016;4(44):7138–45.

268. Wang F, Wang D, Wang T, Jin Y, Ling B, Li Q, et al. A simple approach to prepare fluorescent molecularly imprinted nanoparticles. RSC Adv. 2021 Feb 17;11(13):7732–7.

269. Villacorta A, Cazorla-Ares C, Fuentes-Cebrian V, Valido IH, Vela L, Carrillo-Navarrete F, et al. Fluorescent labeling of micro/nanoplastics for biological applications with a focus on "true-to-life" tracking. J Hazard Mater. 2024;476(March):135134.

270. Benghouzi P, Louadj L, Garnier M, Gonzato C. Epitope-Imprinted Polymer Nanoparticles in Water. Polymers (Basel). 2023;15:1112.

271. Wang S, Yin D, Wang W, Shen X, Zhu JJ, Chen HY, et al. Targeting and Imaging of

Cancer Cells via Monosaccharide-Imprinted Fluorescent Nanoparticles. Sci Rep. 2016 Mar 7;6:22757.

272. Smith BC. Infrared Spectral Interpretation A Systematic Approach. 1st ed. CRC Press; 1998. 200–202 p.

273. Gentleman AS, Lawson T, Ellis MG, Davis M, Turner-Dore J, Ryder ASH, et al. Stern-Volmer analysis of photocatalyst fluorescence quenching within hollow-core photonic crystal fibre microreactors. Chem Commun. 2022;58(75):10548–51.

274. Paterson KA, Arlt J, Jones AC. Dynamic and static quenching of 2-aminopurine fluorescence by the natural DNA nucleotides in solution. Methods Appl Fluoresc. 2020;8(2):25002.

275. Yoshikawa M, Tharpa K, Dima ŞO. Molecularly imprinted membranes: past, present, and future. Chem Rev. 2016;116(19):11500–28.

276. Ratnaningsih E, Kadja GTM, Putri RM, Alni A, Khoiruddin K, Djunaidi MC, et al. Molecularly Imprinted Affinity Membrane: A Review. ACS Omega. 2022;7(27):23009–26.

277. Yang H, Liu HB, Tang ZS, Qiu ZD, Zhu HX, Song ZX, et al. Synthesis, performance, and application of molecularly imprinted membranes: A review. J Environ Chem Eng [Internet]. 2021;9(6):106352. Available from: https://doi.org/10.1016/j.jece.2021.106352

278. Liu J, Li R, Yang B. Carbon dots: a new type of carbon-based nanomaterial with wide applications. ACS Cent Sci. 2020;6(12):2179–95.

279. Liu H, Zhong X, Pan Q, Zhang Y, Deng W, Zou G, et al. A review of carbon dots in synthesis strategy. Coord Chem Rev [Internet]. 2024;498:215468. Available from: https://doi.org/10.1016/j.ccr.2023.215468

280. Ozyurt D, Kobaisi M Al, Hocking RK, Fox B. Properties, synthesis, and applications of carbon dots: A review. Carbon Trends [Internet]. 2023;12(March):100276. Available from: https://doi.org/10.1016/j.cartre.2023.100276

281. Mohiuddin I, Singh R, Kaur V. A review of sensing applications of molecularly imprinted fluorescent carbon dots for food and biological sample analysis. Crit Rev Anal Chem [Internet]. 2023;July:1–22. Available from: https://doi.org/10.1080/10408347.2023.2236215

282. Liu H, Li Z, Sun Y, Geng X, Hu Y, Meng H, et al. Synthesis of Luminescent Carbon Dots with Ultrahigh Quantum Yield and Inherent Folate Receptor-Positive Cancer Cell Targetability. Sci Rep. 2018 Dec 1;8(1):1086.

283. Xie W, Wang H, Tong YW, Sankarakumar N, Yin M, Wu D, et al. Specific purification of a single protein from a cell broth mixture using molecularly imprinted membranes for the biopharmaceutical industry. RSC Adv. 2019;9(41):23425–34.

284. Gheybalizadeh H, Hejazi P. Influence of hydrophilic and hydrophobic functional monomers on the performance of magnetic molecularly imprinted polymers for selective recognition of human insulin. React Funct Polym [Internet]. 2022;171(August 2021):105152. Available from:

https://doi.org/10.1016/j.reactfunctpolym.2021.105152

285. Würth C, Grabolle M, Pauli J, Spieles M, Resch-Genger U. Relative and absolute determination of fluorescence quantum yields of transparent samples. Nat Protoc. 2013;8(8):1535–50.

286. Dimos K. Carbon quantum dots: surface passivation and functionalization. Curr Org Chem. 2016;20(6):1–14.

287. Li H, Kang Z, Liu Y, Lee S. Carbon nanodots: synthesis, properties and applications. J Mater Chem. 2012;22(46):24230–53.

288. Keçili R, Hussain CG, Hussain CM. Fluorescent nanosensors based on green carbon dots (CDs) and molecularly imprinted polymers (MIPs) for environmental pollutants: Emerging trends and future prospects. Trends Environ Anal Chem. 2023;40:213.

289. Yoo D, Park Y, Cheon B, Park MH. Carbon dots as an effective fluorescent sensing platform for metal ion detection. Nanoscale Res Lett. 2019;14(1):272.

290. Juárez Olguín H, Calderón Guzmán D, Hernández García E, Barragán Mejía G. The role of dopamine and its dysfunction as a consequence of oxidative stress. Vol. 2016, Oxidative Medicine and Cellular Longevity. Hindawi Publishing Corporation; 2016. p. 1–13.

291. Ryu JH, Messersmith PB, Lee H. Polydopamine Surface Chemistry: A Decade of Discovery. ACS Appl Mater Interfaces. 2018;10(9):7523–40.

292. Fichman G, Schneider JP. Dopamine self-polymerization as a simple and powerful tool to modulate the viscoelastic mechanical properties of peptide-

based gels. Molecules. 2021 Mar 4;26(5):1363.

293. Zaidi SA. An Account on the Versatility of Dopamine as a Functional Monomer in Molecular Imprinting. Vol. 4, ChemistrySelect. Wiley-Blackwell; 2019. p. 5081–90.

294. Tang M, Wan J, Wang Y, Ye G, Yan Z, Ma Y, et al. Insights into molecular imprinting polydopamine in-situ activating peroxydisulfate for targeted removal of refractory organic pollutants: Overlooked N site. Appl Catal B Environ. 2023 Oct 5;334:122852.

295. Lamaoui A, Lahcen AA, Amine A. Unlocking the Potential of Molecularly Imprinted Polydopamine in Sensing Applications. Polymers (Basel). 2023 Sep 9;15(18):3712.

296. Zhang Z, Liu Y, Huang P, Wu FY, Ma L. Polydopamine molecularly imprinted polymer coated on a biomimetic iron-based metal–organic framework for highly selective fluorescence detection of metronidazole. Talanta. 2021 Sep 1;232:122411.

297. Li C, Han D, Wu Z, Liang Z, Han F, Chen K, et al. Polydopamine-based molecularly imprinted electrochemical sensor for the highly selective determination of ecstasy components. Analyst. 2022 Jun 8;147(14):3291–7.

298. Zalpour N, Roushani M, Hosseini H. Polydopamine imprinted polymer-based tunable electrochemical synthesis of copper benzene-1, 3, 5-tricarboxylate metal-organic framework film as a hybrid dual recognition element for ultra-trace sensing of pregabalin (lyrica). Sensors Actuators B Chem. 2022 Nov

1;370:132418.

299. Zhang YZ, Zhang JW, Wang CZ, Zhou L Di, Zhang QH, Yuan CS. Polydopamine-Coated Magnetic Molecularly Imprinted Polymers with Fragment Template for Identification of Pulsatilla Saponin Metabolites in Rat Feces with UPLC-Q-TOF-MS. J Agric Food Chem. 2018 Jan 24;66(3):653–60.

300. Bhakta S, Mishra P. Molecularly imprinted polymer-based sensors for cancer biomarker detection. Sensors and Actuators Reports. 2021 Nov 1;3:100061.

301. Bhogal S, Mohiuddin I, Kumar S, Malik AK, Kim KH, Kaur K. Self-polymerized polydopamine-imprinted layer-coated carbon dots as a fluorescent sensor for selective and sensitive detection of 17β-oestradiol. Sci Total Environ. 2022 Nov 15;847:157356.

302. Chen W, Fu M, Zhu X, Liu Q. Protein recognition by polydopamine-based molecularly imprinted hollow spheres. Biosens Bioelectron. 2019 Oct 1;142:111492.

303. Zaidi SA. Molecular imprinting: A useful approach for drug delivery. Vol. 3, Materials Science for Energy Technologies. KeAi Communications Co.; 2020. p. 72–7.

304. Li H, Wang X, Wang Z, Wang Y, Dai J, Gao L, et al. A polydopamine-based molecularly imprinted polymer on nanoparticles of type SiO2@rGO@Ag for the detection of λ-cyhalothrin via SERS. Microchim Acta. 2018 Mar 1;185(3):185–93.

305. Gao Z, Shen P, Lan Y, Cui L, Ohm JB, Chen B, et al. Effect of alkaline extraction

pH on structure properties, solubility, and beany flavor of yellow pea protein isolate. Food Res Int. 2020 May 1;131:109045.

306. Liu J, Li R, Yang B. Carbon Dots: A New Type of Carbon-Based Nanomaterial with Wide Applications. ACS Cent Sci. 2020;6(12):2179–95.

307. Lv P, Xie D, Zhang Z. Magnetic carbon dots based molecularly imprinted polymers for fluorescent detection of bovine hemoglobin. Talanta [Internet]. 2018;188(January):145–51. Available from: https://doi.org/10.1016/j.talanta.2018.05.068

308. Akhter F, Rao AA, Abbasi MN, Wahocho SA, Mallah MA, Anees-ur-Rehman H, et al. A Comprehensive Review of Synthesis, Applications and Future Prospects for Silica Nanoparticles (SNPs). Silicon [Internet]. 2022;14(14):8295–310. Available from: https://doi.org/10.1007/s12633-021-01611-5

309. Xia Z, Lin Z, Xiao Y, Wang L, Zheng J, Yang H, et al. Facile synthesis of polydopamine-coated molecularly imprinted silica nanoparticles for protein recognition and separation. Biosens Bioelectron. 2013 Sep 5;47:120–6.

310. Jia X, Xu M, Wang Y, Ran D, Yang S, Zhang M. Polydopamine-based molecular imprinting on silica-modified magnetic nanoparticles for recognition and separation of bovine hemoglobin. Analyst. 2013 Jan 21;138(2):651–8.

311. Roshan S, Mujahid A, Afzal A, Nisar I, Ahmad MN, Hussain T, et al. Molecularly imprinted polymer-silica hybrid particles for biomimetic recognition of target drugs. Adv Polym Technol. 2019;2019:1–7.

312. Lei W, Sun C, Jiang T, Gao Y, Yang Y, Zhao Q, et al. Polydopamine-coated

mesoporous silica nanoparticles for multi-responsive drug delivery and combined chemo-photothermal therapy. Mater Sci Eng C. 2019 Dec 1;105:110103.

313. Zhou L, Qiao M, Zhang L, Sun L, Zhang Y, Liu W. Green and efficient synthesis of carbon quantum dots and their luminescent properties. J Lumin [Internet]. 2019;206(June 2018):158–63. Available from: https://doi.org/10.1016/j.jlumin.2018.10.057

314. Rao KS, El-Hami K, Kodaki T, Matsushige K, Makino K. A novel method for synthesis of silica nanoparticles. J Colloid Interface Sci. 2005;289(1):125–31.

315. Estevão BM, Miletto I, Hioka N, Marchese L, Gianotti E. Mesoporous silica nanoparticles functionalized with amino groups for biomedical applications. ChemistryOpen. 2021;10(12):1251–9.

316. Bhogal S, Mohiuddin I, Kumar S, Malik AK, Kim KH, Kaur K. Self-polymerized polydopamine-imprinted layer-coated carbon dots as a fluorescent sensor for selective and sensitive detection of 17β-oestradiol. Sci Total Environ [Internet]. 2022;847(July):157356. Available from: https://doi.org/10.1016/j.scitotenv.2022.157356

317. Xia Z, Lin Z, Xiao Y, Wang L, Zheng J, Yang H, et al. Facile synthesis of polydopamine-coated molecularly imprinted silica nanoparticles for protein recognition and separation. Biosens Bioelectron [Internet]. 2013;47:120–6. Available from: http://dx.doi.org/10.1016/j.bios.2013.03.024

318. Lamaoui A, Palacios-Santander JM, Amine A, Cubillana-Aguilera L. Molecularly imprinted polymers based on polydopamine: Assessment of non-specific adsorption. Microchem J. 2021;164 (February):106043.